2014-03-28

Identification and Characteristics of Factors Regulating Hepatocellular Carcinoma Progression and Metastasis: A Dissertation

Leanne G. Ahronian
University of Massachusetts Medical School

IDENTIFICATION AND CHARACTERISTICS OF FACTORS REGULATING HEPATOCELLULAR CARCINOMA PROGRESSION AND METASTASIS

A Dissertation Presented

By

LEANNE G. AHRONIAN

Submitted to the Faculty of the
University of Massachusetts Graduate School of Biomedical Sciences, Worcester
in partial fulfillment of the requirements for the degree of

DOCTOR OF PHILOSOPHY

MARCH 28, 2014

CANCER BIOLOGY

IDENTIFICATION AND CHARACTERISTICS OF FACTORS REGULATING HEPATOCELLULAR CARCINOMA PROGRESSION AND METASTASIS

A Dissertation Presented
By

LEANNE G. AHRONIAN

The signatures of the Dissertation Defense Committee signify completion and approval as to the style and content of the Dissertation

_____
Brian C. Lewis, Ph.D., Thesis Advisor

_____
JeanMarie Houghton, M.D., Ph.D., Member of Committee

_____
Alec Kimmelman, M.D., Ph.D., Member of Committee

_____
Karl Simin, Ph.D., Member of Committee

_____
Scot Wolfe, Ph.D., Member of Committee

The signature of the Chair of the Committee signifies that the written dissertation meets the requirements of the Dissertation Committee

_____
Leslie Shaw, Ph.D., Chair of Committee

The signature of the Dean of the Graduate School of Biomedical Sciences signifies that the student has met all graduation requirements of the school.

_____
Anthony Carruthers, Ph.D.,
Dean of the Graduate School of Biomedical Sciences

Cancer Biology

March 28, 2014

Acknowledgements

I would like to thank Brian Lewis for his mentorship during my graduate studies. His encouragement and insights during this journey were indispensable, and I value all of the time he invested in my training. I also appreciate the members of the Lewis Lab, past and present, for their technical support and insights. Particularly, I would like to thank Jiufeng Cai and Victor Adelanwa for their technical assistance.

Experimental contributions from Ya-Wen Chen were critical to the KLF6 project, and I also thank her for taking the time to share her expertise with me after I joined the lab. Lihua (Julie) Zhu provided me with excellent suggestions for experimental design, and I thank her for the bioinformatics analysis and support that she provided.

Leslie Shaw, Karl Simin, and Scot Wolfe provided excellent advice and comments throughout my graduate studies, and I truly appreciate the time they dedicated to considering my work.

I would also like to thank Justine Landis, Brian Quattrochi, and Kirsten Tracy for providing comments on portions of my thesis.

Of course, I must thank my friends and family for the unwavering support they continue to provide.

Abstract

Hepatocellular carcinoma (HCC) is a common malignancy of the liver that is one of the most frequent causes of cancer-related death in the world. Surgical resection and liver transplantation are the only curative options for HCC, and tumor invasion and metastasis render many patients ineligible for these treatments. Identification of the mechanisms that contribute to invasive and metastatic disease may enlighten therapeutic strategies for those not eligible for surgical treatments. In this dissertation, I describe two sets of experiments to elucidate mechanisms underlying HCC dissemination, involving the activities of Krüppel-like factor 6 and a particular p53 point mutation, R172H.

Gene expression profiling of migratory HCC subpopulations demonstrated reduced expression of Krüppel-like factor 6 (KLF6) in invasive HCC cells. Knockdown of KLF6 in HCC cells increased cell transformation and migration. Single-copy deletion of *Klf6* in a HCC mouse model results in increased tumor formation, increased metastasis to the lungs, and decreased survival, indicating that KLF6 suppresses both tumor formation and metastasis in HCC.

To elucidate the mechanism of KLF6-mediated tumor and metastasis suppression, we performed gene expression profiling and ChIP-sequencing to identify direct transcriptional targets of KLF6 in HCC cells. This analysis revealed novel transcriptional targets of KLF6 in HCC including CDC42EP3 and VAV3, both of which are positive regulators of Rho family GTPases. Concordantly, KLF6 knockdown cells demonstrate increased activity of the Rho family GTPases RAC1

and CDC42, and RAC1 is required for migration induced following KLF6 knockdown. Moreover, VAV3 and CDC42EP3 are also required for enhanced cell migration in HCC cells with KLF6 knockdown. Together, this work describes a novel signaling axis through which KLF6-mediated repression of VAV3 and CDC42EP3 inhibits RAC1-mediated HCC cell migration in culture, and potentially HCC metastasis *in vivo*.

TP53 gene mutations are commonly found in HCC and are associated with poor prognosis. Prior studies have suggested that p53 mutants can display gain-of-function properties in other tumor types. Therefore, I sought to determine if a particular hotspot *p53* mutation, $p53^{R172H}$, provided enhanced, gain-of-function properties compared to p53 loss in HCC. *In vitro*, soft agar colony formation and cell migration is reduced upon knockdown of $p53^{R172H}$, indicating that this mutation is required for transformation-associated phenotypes in these cells. However, $p53^{R172H}$-expressing mice did not have enhanced tumor formation or metastasis compared to *p53*-null mice. These data suggest that $p53^{R172H}$ and *p53* deletion are functionally equivalent *in vivo*, and that $p53^{R172H}$ is not a gain-of-function mutant in HCC. Inhibition of the related transcription factors p63 and p73 has been suggested as a potential mechanism by which mutant p53 exerts its gain-of-function effects. Analysis of p63 and p73 target genes demonstrated that they are similarly suppressed in *p53*-null and $p53^{R172H}$-expressing HCC cell lines, suggesting a potential explanation for the phenotypes I observed *in vivo* and *in vitro*.

Together, the studies described in this dissertation increase our understanding of the mechanisms underlying HCC progression and metastasis.

Specifically, we find and characterize KLF6 as a novel suppressor of HCC metastasis, and determine the contribution of a common p53 point mutation in HCC. This work contributes to ongoing efforts to improve treatment options for HCC patients.

Table of Contents

List of Tables

List of Figures

List of Abbreviations

AFB1	Aflatoxin B1
AFP	α-fetoprotein
ChIP	Chromatin Immunoprecipitation
CRIB	Cdc42/Rac interactive binding motif
DEN	Diethylnitrosamine
EMT	Epithelial to mesenchymal transition
GO	Gene ontology
H&E	Hematoxylin and Eosin
HBV	Hepatitis B virus
HBx	Hepatitis B viral protein X
HCC	Hepatocellular carcinoma
HCV	Hepatitis C virus
IGF2	Insulin-like growth factor 2
IHC	Immunohistochemistry
KLF6	Krüppel-like factor 6
LOH	Loss of heterozygosity
NES	Nuclear export signal
NLS	Nuclear localization signal
PyMT	Polyoma middle T-antigen
RCAS	Replication-competent avian sarcoma-leukosis virus with splice acceptor
TMA	Tissue microarray
TSS	Transcriptional start site
TVA	Tumor virus A receptor

CHAPTER I

Introduction

Hepatocellular carcinoma (HCC) is a common malignancy of the liver and is one of the most frequent causes of cancer-related death worldwide. Annually, 800,000 people are diagnosed with liver cancer, contributing to its status as the 2nd leading cause of cancer-related death (Ferlay et al. 2013). The major type of liver cancer is HCC, accounting for 75-80% of liver cancer cases (El-Serag 2011). Despite awareness of many risk factors for HCC, the disease is increasing in incidence both in the United States and worldwide (Davila et al. 2004; Altekruse et al. 2012). Proportionally, liver cancers are more frequent in developing nations, where the incidence risk is more than twice that of a more developed region. Largely, this disparity is due to hepatitis B viral infections, which are significantly less prevalent in developed nations due to vaccination programs (Di Bisceglie 2009).

Despite having a comparably lower risk of HCC in the United States, HCC is still a significant cause of cancer-related death (Jemal et al. 2011). In the U.S., approximately 25,000 new cases of HCC are diagnosed annually. The ratio of men to women diagnosed with HCC in the U.S. is 3:1 (Siegel et al. 2013): a bias which also exists in global statistics. While HCC is not an exceedingly common cancer in the U.S., it is still a significant source of cancer-related death due to poor overall survival. Overall five-year survival for HCC is 16.1%, but this varies greatly by the stage of the cancer at diagnosis. If the tumor is localized at diagnosis, five-year survival is 29.1%. This stands in contrast to HCCs with either regional or distant spread, which have five-year survival rates of 10.2% and 3.0%, respectively (Hayat et al. 2007).

One of the reasons for the dismal survival rates of HCC patients is a limited number of effective treatments. Since HCCs tend to occur in patients with a background of liver disease, many traditional treatments for cancer, such as cytotoxic chemotherapies, generate higher drug toxicity and are not well tolerated (Edeline et al. 2009). In advanced liver disease, there are few opportunities for tumor resection. While patients can be cured by liver transplantation, the paucity of suitable donor livers requires that certain patient eligibility criteria be satisfied. Unfortunately, these criteria exclude many patients, particularly those with invasive or metastatic disease (El-Serag 2011).

Determining the molecular mechanisms that drive cancer has shaped the targeted treatment strategies used in other cancer types. Since many of the mechanisms driving HCC are still unknown, characterization of genes involved in HCC development and progression are essential for discovering new treatment strategies. Studying the mechanisms that lead to invasive or advanced stage HCC are particularly important, since patients at these stages currently have few treatment options.

HCC Etiology and Diagnosis

Virtually all (70-90%) HCC cases develop in the background of chronic liver inflammation and cirrhosis (El-Serag 2011). An inflammatory microenvironment is one of the hallmarks of cancer (Hanahan and Weinberg 2011) contributing to hepatocarcinogenesis through delivery of cytokines and chemokines, increased

hepatocyte turnover, interactions with immune cells, or advantageous interactions with fibrotic stroma (Weber et al. 2011). Common contributors to liver inflammation and eventual cirrhosis include chronic hepatitis B and C infections, and excessive alcohol consumption. Obesity, metabolic syndrome, and smoking are also contributors to liver inflammation and can lead to cell transformation, as depicted in Figure 1.1 (El-Serag and Rudolph 2007).

In East Asia and Africa, regions of high HCC incidence, over 60% of HCCs can be attributed to hepatitis B viral (HBV) infection (Bosch et al. 2004). This stands in contrast to HCC patients in the U.S., of which only 20% are positive for the hepatitis B surface antigen (HBsAg) (Di Bisceglie et al. 2003). Examination of HCC frequencies in HBsAg carriers has found that the relative risk of HCC is 223 times greater than non-carriers (Beasley et al. 1981), providing strong evidence that HBV infection contributes to HCC development. The ability to clear HBV infection increases with age, as viral clearance occurs in 90-95% of adults. However, 25-50% of infected children, and 90% of infants will develop a chronic infection (Alter and Mast 1994). Prevention of HBV transmission in youth is critical to reducing HBV-induced HCC.

Figure 1.1. Development of hepatocellular carcinoma. Several sources of liver injury may result in chronic state of hepatocyte cell death and compensatory proliferation. Chronic liver disease can lead to cirrhosis, which results in the formation of scar tissue. Amidst scar tissue, liver cells become abnormal, and accumulate gene expression changes that can result in progression to carcinoma. (Adapted from (Farazi and DePinho 2006)).

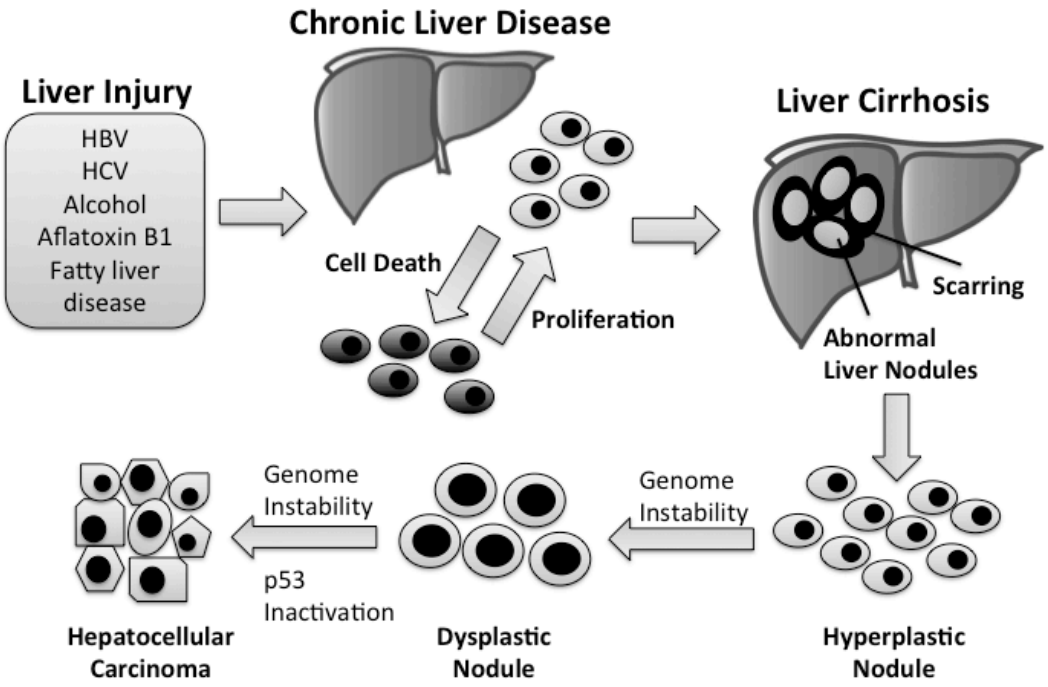

Transmission of HBV can be reduced through a strong hepatitis B vaccination program (Di Bisceglie 2009). As an example, 10% of children in Taiwan were positive for HBsAg in the early 1980s. Following the implementation of a universal infant HBV vaccination program, HBsAG rates decreased to 1.3%. Years later, the incidence of childhood HCC decreased by almost 50%, indicating that vaccination is an effective solution for HCC prevention (Chang et al. 1997). Despite the existence of an effective prevention strategy, over half of HCCs worldwide are still triggered, at least in part, by HBV infection.

HBV can induce the development of HCC through several mechanisms. Firstly, the development of inflammation and increased hepatocyte regeneration in response to HBV infection may provide an environment conducive to cell transformation and tumor growth (Di Bisceglie 2009). In addition to the inflammation caused by chronic viral infection, HBV may accelerate tumor initiation through insertional mutagenesis (Murakami et al. 2005). The HBV genome contains cis-regulatory elements that can result in transcriptional activation of nearby genes. For example, a common site of HBV insertion is near the TERT locus, which can result in telomerase activation (Fujimoto et al. 2012). Lastly, the HBx protein, coded by the HBV genome, is itself an oncogene. Through binding to other transcription factors, HBx activates transcription of both viral and cellular genes. HBx can initiate signaling cascades through activation of kinases such as MAPKs and JNKs (Bouchard and Schneider 2004), and also inactivates the tumor suppressor p53 via direct binding (Wang et al. 1994).

Hepatitis C virus (HCV) infections also contribute to HCC formation, and are responsible for part of the increase in HCC incidence seen in the United States (Davila et al. 2004; Welzel et al. 2013). Unlike HBV, relatively few individuals with acute hepatitis C will clear the infection, and 85-90% develop chronic disease. Of individuals with chronic HCV infection, 50-60% of them will develop liver disease, and up to 20% will develop cirrhosis (Alter and Mast 1994). Of HCV-induced cirrhosis cases, 1-6% per year will develop HCC (Buhler and Bartenschlager 2012). Recent developments in antiviral therapies for hepatitis C can reduce virus below detection levels for two years or more (Lawitz and Gane 2013), so the HCV-induced HCC rate may decrease as these therapies become more commonplace. However, there is no currently available vaccine for hepatitis C (Liang 2013), so worldwide infection rates remain high.

HCV is thought to induce HCC formation through increased cytokine signaling and hepatocyte turnover resulting from chronic liver inflammation and fibrosis (Levrero 2006; Tan et al. 2008). The HCV genome does not integrate into host DNA, so insertional mutagenesis is not a trigger for hepatocyte transformation (Buhler and Bartenschlager 2012). However, HCV-coded proteins, like the HCV core protein, may contribute to cell transformation through interaction with host RNA helicase, DDX3, though its impact on HCC is not known (Owsianka and Patel 1999). Additionally, HCV protein NS5B binds to host Retinoblastoma (Rb) protein. NS5B is thought to downregulate Rb to facilitate viral replication (McGivern et al. 2009). However, no studies have confirmed that these proteins impact hepatocytes *in vivo*

or affect progression to HCC, so the role of viral oncogenes in HCV-induced HCC is unclear.

Another contributor to HCC formation, Aflatoxin B1 (AFB1), is a fungal metabolite that contaminates food products, particularly in tropical regions such as Southeast Asia and Sub-Saharan Africa where the climates are most suitable for growth of the fungi that produce it (Hamid et al. 2013). This toxin is known to induce hepatitis and increase risk of HCC in those who continually ingest it (Alpert and Davidson 1969; Newberne and Butler 1969). AFB1 frequently causes a mutation at $p53^{R249S}$, which is thought to facilitate hepatocarcinogenesis (Bressac et al. 1991; Ozturk 1991; Stern et al. 2001). Unsurprisingly, regions with the highest rates of AFB1 exposure overlap strongly with regions that have the highest rates of HCC (McGlynn and London 2005; Hamid et al. 2013). Food contamination by fungus is rare in developed nations, and is not a major contributor to HCC in these regions.

In regions where HBV infection and aflatoxin exposure are uncommon, a more frequent contributor to HCC is alcohol abuse. Excessive alcohol consumption is known to contribute to hepatic steatosis. A third of such cases will develop fibrosis, which may subsequently lead to HCC (Bellentani et al. 1997). Diabetes and metabolic syndrome are also HCC risk factors more common to Western nations. In these contexts, fatty liver disease is the likely source of increased risk (Davila et al. 2005; Lai et al. 2006).

Like many other cancers, cigarette smoking significantly increases an individual's risk of hepatocellular carcinoma (Jee et al. 2004). Other less frequent

contributors to HCC include autoimmune hepatitis, porphyria, hereditary hemochromatosis, α1-antitrypsin deficiency, and Wilson's disease (El-Serag 2011).

HCCs occurring in a non-damaged liver background account for 10-15% of all cases (Trevisani et al. 2010). These tumors are in patients without viral hepatitis infection, and livers absent of cirrhosis. Typically, these tumors are a single nodule and are well-encapsulated even at sizes greater than 5cm (Cetta et al. 2001).

Early studies attempting to determine genetic components to familial HCC were confounded by the transmission of HBV infection between family members. Recently, family members without viral hepatitis infection were found to share HCC risk, suggesting a genetic predisposition may in fact exist (Turati et al. 2012). The precise genes responsible for this link remain unknown.

Two conventional staging systems are used to classify HCC clinically. One is a modified form of the Tumor-Node-Metastasis (TNM) staging system, which is used to classify many cancers (Vauthey et al. 2002). Another common method for classifying HCC is the Barcelona Clinic Liver Cancer (BCLC) system. BCLC combines features of the tumor(s), such as size, number, and presence of vascular invasion, with the addition of liver function tests. The combination is used to classify tumor stage and patient prognosis (Llovet et al. 1999).

Early HCCs are characterized by their small size, typically less than 2cm, and their well-differentiated cytology. These tumors often display fatty change, but otherwise do not display structural atypia (Takayama et al. 1998; Kondo 2009).

With HCC progression, in addition to a larger cell size, hepatocytes become clearly abnormal and vascularity of the tumor increases (Kojiro 1998).

Molecular Biology of HCC progression

Analyses of gene expression changes in different tumor types have improved classification of patient tumors by providing additional metrics besides histopathology. Copy number analysis of HCCs has revealed that overall, 32% of tumors have focal amplification of chromosomes, while 40% of tumors have homozygous deletions. Tumors with homozygous deletions are associated with the later tumor grades III or IV, and other traits of aggressiveness, such as increased microvascular invasion (Guichard et al. 2012). In combination with copy number analysis, sequence analysis has pointed to five pathways that are frequently disrupted in HCC. Commonly disrupted systems include the p53 pathway, chromatin remodeling enzymes, PI3K/RAS signaling, ER stress, and the Wnt/β-catenin pathway (Aravalli et al. 2008; Fujimoto et al. 2012). However, a clear molecular progression of HCC has not been identified, potentially due to heterogeneity of the disease.

One particular deletion frequently seen by cytogenetic studies in HCC is the recurrent deletion of chromosome 1p. This deletion is common in well-differentiated HCCs, indicating that it may be an early contributor to HCC formation (Chen et al. 1996; Parada et al. 1998). Loss of heterozygosity (LOH) at chromosome

16p is associated with advanced stage or metastatic tumors (Buendia 2000), but which genes are important in either of these regions is unknown.

Allelic deletions at chromosome 17p13 are one of the most common in HCC, and are associated with advanced disease (Buendia 2000). Contained within this region is the tumor suppressor *p53*. LOH of this region has been seen in 25-60% of HCCs, depending on the study (Kusano et al. 1999; Wong et al. 1999b; Buendia 2000). Point mutations in the *p53* sequence are also frequent in HCC (Oda et al. 1992). In HCCs with wild-type p53, inactivation of $p14^{ARF}$ is common, indicating that multiple mechanisms may converge to inactivate the p53 pathway (Tannapfel et al. 2001). Loss of *p53* alone does not induce HCC formation in mice, but HCC mouse models that include *p53* loss generate more aggressive disease that metastasizes to the lung (Lewis et al. 2005). These data indicate that p53 inactivation is a major contributor to HCC progression.

The expression of $p14^{ARF}$/$p16^{INK4A}$ tumor suppressors are often impaired in human HCC. Investigation into this shared promoter region revealed that 60-70% of HCC tissues had hypermethylation of this promoter (Matsuda et al. 1999; Wong et al. 1999a), and deletion of this locus occurs in approximately 10% of cases (Liew et al. 1999). In a *p53*-null HCC mouse model, additional deletion of *Ink4a/Arf* increases tumor formation and lung metastasis (Chen et al. 2007), suggesting that decreased levels of these proteins are important for human HCC development and progression.

The most commonly mutated pathway in HCC is the Wnt/β-catenin pathway. Activating mutations in β-catenin occur in 32.8% of tumors, while inactivating

mutations in *Axin1* or Adenomatous Polyposis coli (APC) occur in 15.2% and 1.6% of tumors, respectively. These mutations are mutually exclusive, resulting in almost half of all HCCs with deregulated Wnt/β-catenin pathway (Guichard et al. 2012). Liver-specific deletion of *APC* in mice generates HCC, while expression of activated β-catenin in mice increases proliferation and hepatomegaly (Cadoret et al. 2001; Colnot et al. 2004). These mouse models indicate that these common mutations are drivers, and not just consequences, of hepatocarcinogenesis.

While Wnt pathway alterations are likely sources of oncogenic activity in many tumors, amplification of *MYC* is also common in HCC. *MYC* amplification is detected in approximately 30% of HCCs (Peng et al. 1993; Kawate et al. 1999; Chan et al. 2004). *MYC* amplification significantly correlates with mutant p53, and is also more frequent in tumors with a higher histologic grade (Kawate et al. 1999). While these data suggest a potential role for MYC in driving tumorigenesis and progression of HCC, others have found no correlation between *MYC* amplification and MYC protein expression, confounding the correlations with *MYC* amplification and HCC (Chan et al. 2004). Yet, mouse models that drive MYC expression in the liver generate HCC, indicating that MYC is sufficient to induce hepatocarcinogenesis (Sandgren et al. 1989; Shachaf et al. 2004; Zender et al. 2006).

Increased PI3K/RAS signaling is common to HCC, even under circumstances where mutations are not detected in pathway components. Direct activation of these pathways through mutation is rare in HCC, where activating KRAS and PIK3CA mutations occur in only 2% of tumors (Guichard et al. 2012). One source of

amplified signaling is thought to be the inflammatory liver microenvironment. In the cirrhotic liver, hepatic stellate cells have been shown to produce TGFβ and PDGF, which activate MAPK and PI3K signaling in hepatocytes (Parsons et al. 2007). Activation of these pathways likely contributes to tumor initiation in the liver in response to liver damage.

While HCC is currently diagnosed using clinical and pathological features, some researchers have pushed to diagnose and characterize HCC by molecular profile. One particular profile of 65 genes is a more accurate prognostic indicator than clinical characteristics alone (Kim et al. 2012). Another study used the expression of only seven proteins to accurately diagnose hepatocellular carcinoma versus normal liver. These critical factors were FOS, ESR1, JUNB, EGFR, SOCS3, FOLH1 and IGF1 (Zhang et al. 2011).

Studies indicate that a combination of current practices and molecular diagnostics could simplify and benefit HCC diagnosis and prognosis. One group combined markers of normal hepatocytes and markers identified from previous HCC prognostic studies in order to assess liver function and tumor stage simultaneously. The markers, assessed by immunohistochemistry, included p53, Ki67, Cyclin D1, β-catenin, CD31, and α-fetoprotein (AFP), among others. The outcomes of these 13 markers can be applied to a model in order to calculate a risk score of the tumor. The score from this risk analysis was found to be a predictor of overall and recurrence-free survival (Srivastava et al. 2012).

Many HCCs display increased expression of insulin-like growth factor II (IGF2), which is negatively correlated with survival (Iizuka et al. 2004). The expression of IGF2 by HCC cells has been found to be critical for HCC metastasis to the lung (Chen et al. 2009). It is no surprise then, that IGF2 is included in lists of prognostic genes for HCC patient outcomes (Kim et al. 2012). IGF2 is even detectable in the serum of some HCC patients (Rehem and El-Shikh 2011) and may be useful to differentiate between liver dysfunction and HCC.

Despite developments in numerous potential diagnostic and prognostic HCC markers, AFP is the only one currently in clinical use. AFP is normally only expressed during liver development and not in healthy adults, but its expression increases in cirrhosis and HCC (Taketa 1990). Since AFP is expressed in advanced liver disease, imaging tests are required to validate an HCC diagnosis (Llovet et al. 1999). Higher levels of AFP are correlated to a decreased survival time in HCC patients (Izumi et al. 1992). While AFP is a marker of poor prognosis in HCC, it is not a driver of tumor formation or progression in HCC (Baig et al. 2009). As more is learned about the molecular drivers and markers of HCC, diagnostic and prognostic methods will likely improve.

HCC Therapeutics

Despite the existence of several treatments for HCC, the only curative options are tumor resection or liver transplant. Some focal tumors may be cured by percutaneous ethanol injection, but liver resection of the tumor area is preferred for

early HCCs (Fortune et al. 2013). For patients with very early, focal HCC, 5-year survival is approximately 90% (El-Serag 2011). However, the average 5-year survival for all HCC patients who undergo resection is only 45-50% (Poon et al. 2000; Lang et al. 2007). Liver resection is not an option for most HCC patients, since those with poor liver function, vascular invasion or extrahepatic spread are typically excluded. Feasibility of tumor resection is also impacted by large tumor size, multiple tumors, or challenging location (Vauthey et al. 2002). Occasionally, resection is performed on tumors with the presence of vascular invasion, but in these instances, 5-year survival post-resection is only 6% due to tumor recurrence (Lang et al. 2007).

Despite careful selection of surgical candidates, many patients still have recurrence of disease following resection (Poon et al. 1999). Of recurrences after resection, 40% occur only in the liver, 33% occur in both the liver and extrahepatic sites, 25% are only in extrahepatic sites, and 2% are of unknown location (Lang et al. 2007). These data indicate that in addition to recurrence at the primary site, tumor cell dissemination to other sites is frequent. Mutational fingerprinting of primary HCCs and secondary HCCs would have to be performed in order to determine if the same primary tumor is recurring, or if there is *de novo* tumor formation. However, the formation of tumors outside the liver post-resection indicates that disseminated cells prior to resection are a major reason for recurrence.

The potential for disease recurrence is one reason why liver transplant is the preferred treatment method, since both the tumor and the tumorigenic environment of the diseased liver are removed (Kakodkar and Soin 2012). The typical requirements for liver transplant are collectively referred to as the Milan Criteria, which restrict patients by tumor size and number of lesions. Using these criteria, 5-year survival is 73.3% post liver transplant, versus 53.6% for patients outside the criteria (Mazzaferro et al. 2009). Patients with liver disease are preferentially selected for liver transplants based on a Model for End-Stage Liver Disease (MELD) score, so that the patients with the greatest need are treated first (Sharma et al. 2004).

Even for HCC patients who undergo liver transplantation, almost 20% of them have recurrence of disease in the five years post-transplantation. The most common site of recurrence is the liver, however the lung and bone are also frequent sites (Roayaie et al. 2004). These data suggest that tumor cell dissemination had already occurred pre-transplant. Relapsed patients require other treatment options, though none are curative at this time.

Several institutions have begun to perform liver transplants on patients whose tumors are outside of the Milan Criteria. Approximately 25% of these patients have comparable overall survival after transplant to those who do fall within the Milan Criteria (Mazzaferro et al. 2009), indicating that these standards do not accurately predict tumor behavior for all patients. Molecular biomarkers of HCC

prognosis may be better predictors of survival outcome post-resection or transplantation (Boyault et al. 2007; Dvorchik et al. 2008; Ji et al. 2009a).

Patients who do not qualify for surgery or have relapsed disease are often treated with radiofrequency ablation or percutaneous ethanol injection. These treatments lead to necrosis of tumor cells and can decrease tumor size (Orlando et al. 2009; Germani et al. 2010). HCCs at an intermediate stage can be treated with transarterial chemoembolization (TACE). In TACE, beads containing doxorubicin are injected, which occlude the feeding arteries of the tumor, and result in tumor cell death. TACE has been shown to extend the survival of patients that are not eligible for surgery (Bruix et al. 1998; Llovet and Bruix 2003).

For advanced patients, treatments are limited to traditional chemotherapy and molecularly-targeted therapy. Chemotherapeutics have had limited efficacy in HCC patients due to high toxicity (Palmer et al. 2004). Only one molecularly targeted therapy, Sorafenib, has been approved for use in HCC thus far. Sorafenib is the only approved systemic treatment for HCC patients that has demonstrated a survival benefit (Gauthier and Ho 2013). Sorafenib was designed to inhibit RAF1, but also inhibits VEGFR1-3, PDGFRβ, FGF1, cKIT, FLT3, and RET (Wilhelm et al. 2004; Carlomagno et al. 2006). In a phase III trial for Sorafenib in HCC patients, survival was significantly extended by a period of three months over those in the placebo arm of the study ($p<0.001$) (Llovet et al. 2008). Additionally, disease was stabilized in a larger proportion of patients taking Sorafenib versus those given placebo (Llovet et al. 2008). While this therapy is beneficial, virtually all HCCs acquire

resistance to Sorafenib (Lencioni et al. 2010) and further study of HCC is required to guide beneficial treatment strategies.

Mouse Models of HCC

Mouse models of HCC take multiple forms. Some are induced with chemical exposure, while others mimic the viral etiologies of the disease. Further, multiple HCC models have been developed using specific oncogenic drivers. Each has been used to parse the molecular changes involved in the formation of HCC.

One chemically induced HCC model utilizes injections of diethylnitrosamine (DEN) to induce liver damage. Treatment with this chemical results in DNA damage and the generation of reactive oxygen species, which leads to HCC formation in 80-100% of male mice (Verna et al. 1996). Unfortunately, DEN can target additional organs in the mouse, including other parts of the gastrointestinal tract, the skin, and hematopoetic cells, where it can also contribute to tumorigenesis (Heindryckx et al. 2009). Despite this downside, DEN treatment generates HCCs that are genetically similar to human HCCs with poor survival (Lee et al. 2004).

Another toxin-induced model mimics human HCC induced by aflatoxin B1 (AFB) ingestion. Consumption of contaminated food has been associated with the formation of hepatocellular carcinoma in both laboratory animals and humans (Alpert and Davidson 1969; Newberne and Butler 1969). While adult mice are resistant to HCC formation when treated with AFB1, when infant mice are injected with three doses of AFB1, 70% form HCC in approximately one year (Vesselinovitch

et al. 1972; McGlynn et al. 2003). Resistance to AFB1-induced HCC in adult mice is due to the high levels of an enzyme that targets the DNA-binding metabolites of AFB1 (Quinn et al. 1990). These mice are valuable for assessing common mutations that occur in response to this toxin in the absence of typical HCC confounders, like hepatitis infection. Additionally, male mice have an increased susceptibility to tumor formation in response to AFB1 treatment, which reflects the male bias of HCC in human disease (Vesselinovitch et al. 1972). These mice may be valuable for determining the causes for increased HCC formation in men.

As described previously, HBV infection is one of the major causes of HCC. To determine if HBx, an oncogene in the HBV genome, was sufficient to induce HCC on its own, transgenic mice were engineered to express the HBx gene (Kim et al. 1991). These mice quickly develop dysplastic hepatocytes, which progress to adenomas by 8-10 months of age. Interestingly, these adenomas progress to carcinoma, but preferentially do so in male mice: 90% of male mice develop HCC, while only 60% of female mice do. Additionally, tumor formation in females has a longer latency than male mice (Kim et al. 1991). Notably, this model demonstrates that the HBx oncogene within HBV is sufficient to induce hepatocarcinogenesis, independent of the inflammation produced by chronic viral infection. Additionally, this model mimics the male bias for HCC formation seen in humans, and may be valuable for determining the mechanisms for this difference.

Another model of HBV-induced HCC uses transgenic mice that express the HBV surface antigen downstream of the Albumin promoter. These mice develop

inflammatory liver disease, and eventually develop HCC (Chisari et al. 1989; Nakamoto et al. 1998). Importantly, this mouse model indicates that the inflammation resulting from HBV infection is sufficient to induce HCC, even without viral genome incorporation or HBx activity.

Another mouse model recapitulates many features of HCCs induced by HBV and HCV without the use of viral components. Previously, it was demonstrated that lymphotoxin signaling was increased in both lymphocytes and hepatocytes of patients with hepatitis or HCC (Haybaeck et al. 2009). Transgenic mice were generated that specifically express lymphotoxin in liver cells, called AlbLTαβ. These mice develop tumors that strongly resemble human HCC induced by chronic viral hepatitis infection. This model has been used to tease apart NF-kb signaling pathways involved in HCC (Ruddell et al. 2009).

Expression of potent oncogenes in the liver can also drive HCC formation. Since alterations to the Wnt/β-Catenin pathway and *c-MYC* amplification are common in human HCC, these pathway alterations have been modeled in mice to determine their roles in HCC formation and progression.

Transgenic mice expressing *c-Myc* under the Albumin promoter develop focal hepatic tumors at approximately 15 months of age (Sandgren et al. 1989). Genetically, these tumors are similar to human HCCs with a good prognostic outcome (Lee et al. 2004). Due to the low penetrance and long latency of tumor formation, these mice were crossed to a transgenic mouse expressing *Tgfα* under the metallothionein1 promoter to co-express TGFα and c-MYC in hepatocytes and

accelerate tumorigenesis (Jhappan et al. 1990). These oncogenes cooperate to produce HCC in 70% of animals by 16 weeks of age. Mice form either single or multifocal tumors that histologically resemble human HCC (Murakami et al. 1993). Their expression patterns bear similarity to human HCC with poor prognosis (Lee et al. 2004). While transgenic c-MYC expression alone resulted in eventual tumor formation in some mice, more robust tumor formation occurs when *c-Myc* is controlled under a liver-specific tetracycline-responsive system. Hepatocyte-specific c-MYC expression induces HCCs that display oncogene addiction to c-MYC, as its withdrawal results in tumor regression (Shachaf et al. 2004). Potentially, the tetracycline-responsive *c-Myc* mouse model results in higher c-MYC expression than the Albumin promoter-driven model, which may account for its enhanced tumor formation.

Several mouse models have been used to recapitulate Wnt/β-catenin pathway alterations seen in human HCCs. Liver-specific deletion of the *Apc* gene in mice leads to nuclear accumulation of β-Catenin and the induction of known downstream target genes. Approximately 70% of these mice develop HCC, which histologically mimics human disease. Interestingly, these tumors show a wide range of aggressiveness, as they possess well, moderate, and poorly differentiated regions (Colnot et al. 2004). Mice expressing a liver-specific, activated form of β-Catenin exhibit hepatomegaly. Hepatocytes have increased proliferative rates in this model, though they do not progress to HCC (Cadoret et al. 2001).

Another HCC model utilizes the RCAS-TVA system to somatically deliver a retrovirus containing the polyoma middle-T oncogene (*PyMT*) to hepatocytes. PyMT expression in these cells induces the formation of HCCs that display histological characteristics reminiscent of human HCC in 50-70% of injected animals (Lewis et al. 2005; Chen et al. 2007). PyMT induces the activity of the RAS and PI3K pathways to drive tumor formation (Schaffhausen and Roberts 2009). These pathways are commonly activated in human HCC (Parsons et al. 2007; Guichard et al. 2012) so use of PyMT provides signaling effects that are relevant to HCC biology. This model forms HCC more rapidly than several other models, as tumors are sometimes detectable as early as four months of age (Lewis et al. 2005). Additionally, these tumors may display metastasis to the lung depending on the tumor suppressor background, so genes modulating HCC progression and metastasis may be studied (Lewis et al. 2005; Chen et al. 2007; Chen et al. 2009).

In addition to viral delivery of oncogenes, hydrodynamic injection has been shown to effectively deliver naked plasmid DNA to hepatocytes. Along with delivery of DNA, the procedure induces some liver inflammation, which may contribute to tumor formation (Sebestyen et al. 2006). As an example, the HBx oncogene was delivered to hepatocytes using this method. The inflammation generated resulted in cycling of affected hepatocytes, which allowed for continued transmission of the HBx gene. HBx was combined with an shRNA to p53 for hydrodynamic delivery in order to mimic gene changes common in HCC (Keng et al. 2011). This method is a fast and effective way to deliver DNA to hepatocytes, and the inflammation induced

may mimic some of what is seen in the human condition, though this state is transitory in the mouse and not sustained in a chronic state like in human disease.

Several studies have found that hepatocytes are particularly sensitive to modulation of the Hippo pathway, as YAP activity is pro-tumorigenic in the liver (Zender et al. 2006). Germline deletions of YAP-repressors *Mst1* and *2* form hepatomegaly and spontaneous HCC due to increased YAP activity (Zhou et al. 2009). Additionally, single-copy germline or liver-specific deletion of *Nf2*, an upstream regulator of the Hippo pathway, results in HCC development (McClatchey et al. 1997; Zhang et al. 2010). Due to these examples, repressors of YAP in the Hippo pathway are considered to be potent tumor suppressors in HCC.

Hepatocytes are highly susceptible to transformation upon deletion of other tumor suppressors as well. Mice with liver-specific deletion of *Nemo* (Luedde et al. 2007), *Dicer* (Sekine et al. 2009), and *Tak1* (Bettermann et al. 2010) all form HCC. Another tumor suppressor characterized in HCC is a transcription factor, Krüppel-like factor 6 (KLF6).

Krüppel-like factor 6

The KLF6 cDNA was originally cloned from a placental cDNA library using a core promoter binding element probe, leading to its original name, core promoter-binding protein (CPBP) (Koritschoner et al. 1997). Almost simultaneously, KLF6 was isolated from a yeast one-hybrid screen using a binding sequence from the HIV-1 core promoter (Suzuki et al. 1998), as well as from injured rat hepatic stellate cells

(Ratziu et al. 1998). By sequence analysis with other known transcription factors, it was determined that KLF6 contained three zinc finger domains in its C-terminus (Koritschoner et al. 1997).

The structure of KLF6 is conserved across many species (Gehrau et al. 2005). In zebrafish, the closest homolog to KLF6 is the gene *copeb*. Upon knockdown of Copeb in embryos, zebrafish development is impaired. Further investigation revealed that liver, pancreas, and intestine are smaller upon Copeb knockdown, suggesting it has an important role in gastrointestinal development (Zhao et al. 2010).

To date, murine germline knockout of any *Klf* gene is lethal, *Klf6* included. *Klf6*$^{-/-}$ mice die by embryonic day 12.5 (Matsumoto et al. 2006). At day 10.5, *Klf6*$^{-/-}$ embryos had no discernable livers, and had a depleted and less organized yolk sac compared to *Klf6*$^{+/-}$, or *Klf6*$^{+/+}$ embryos. Closer analysis of the yolk sacs revealed that the vasculature was not well developed, indicating that KLF6 plays a role in either hematopoiesis or vasculogenesis (Matsumoto et al. 2006). While the impact on organ developmet and size is similar between the zebrafish and mice, vascularity and differentiation of zebrafish liver were not impaired, suggesting the impact on organ size may have been due to parenchymal cell cycle defects (Zhao et al. 2010).

In human cell lines and tissues, KLF6 is localized to both the cytoplasm and nucleus with varying intensity (Slavin et al. 2004). This is due to alternative splicing of the KLF6 gene, particularly full-length *Klf6*, and a small isoform called *Klf6-Sv1*. The localization of KLF6 is regulated by the presence of a nuclear localization signal

(NLS) in the zinc finger domain as well as a nuclear export signal (NES) in the N-terminal region. The NES is common to all KLF6 splice variants, but the NLS is only present in full-length KLF6 and the longest splice variant, SV3 (Figure 1.2). The presence of the NLS is required for nuclear localization and protein stability. Interestingly, KLF6-SV1 lacks the zinc finger domains, and the NLS, leading to its localization to the cytoplasm (Rodriguez et al. 2010). Thus, KLF6-SV1 can act as a dominant negative to full-length KLF6 by directly binding to it and sequestering it from the nucleus. While in the cytoplasm, full-length KLF6 is then preferentially degraded by the proteasome (Vetter et al. 2012).

Alternative splicing of KLF6 is modulated by several mechanisms. Increased PI3K/AKT signaling downstream of RAS increases expression of the dominant negative variant, SV1 (Yea et al. 2008). Additionally, hepatocyte growth factor (HGF) signaling through PI3K/AKT has been shown to favor SV1 splicing (Munoz et al. 2012). Cell proliferation stimulated by HGF was shown to be due, at least in part, to an increase in SV1 levels (Munoz et al. 2012). Splicing of *Klf6* is decreased by TGFβ signaling, resulting in an increase in full-length KLF6 (Botella et al. 2009). Lastly, a single-nucleotide polymorphism (SNP), called IVSdA, was discovered that results in an altered splicing at the *Klf6* locus. In individuals with this SNP, SV1 is expressed at higher levels than in individuals without the SNP (Narla et al. 2005).

Figure 1.2. **The *Klf6* locus is alternatively spliced to generate four known variants.** Full-length KLF6 features an N-terminus (black boxes) that contains both an NES and NLS. Its C-terminus contains three zinc finger binding domains, represented by white boxes. KLF6-SV3 retains the same N-terminal region as full length KLF6, but lacks one zinc finger binding domain. KLF6-SV2 also lacks one DNA binding domain, but additionally lacks the NLS sequence. Lastly, KLF6-SV1 lacks all zinc finger domains, and instead has a novel C-terminus generated by a frame shift, represented by the gray box. SV1 also lacks the NLS sequence.
(Adapted from (Rodriguez et al. 2010).)

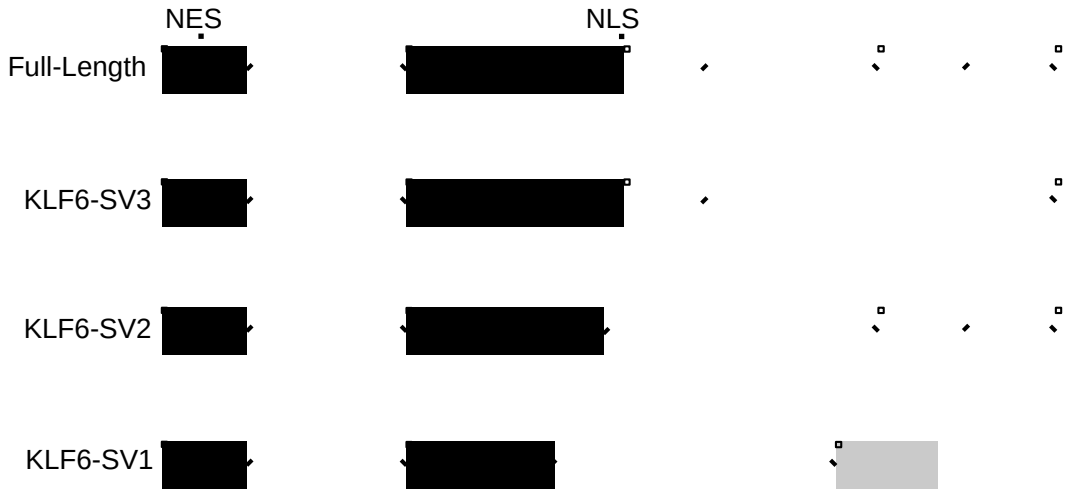

KLF6 Transcriptional Activity

KLF6 is known to behave as both a transcriptional activator and a repressor and has many characterized target genes. It is a direct transcriptional repressor of *Pttg1* (Lee et al. 2010), and *Mdm2* (Tarocchi et al. 2011). It has been shown to be a transcriptional activator of *p21* (Narla et al. 2001; Narla et al. 2007), *Tgfβ1* (Kim et al. 1998), inducible nitric oxide synthase (Warke et al. 2003), urokinase plasminogen activator (Kojima et al. 2000), *Atf3* (Huang et al. 2008), and E-Cadherin (DiFeo et al. 2006). All of these target genes are known to impact human cancer. Intrguingly, KLF6 activates the transcription of genes shown to restrain tumor formation and progression, while it represses the transcription of genes shown to promote tumor formation and progression.

KLF6 may impact gene expression through cooperation with other transcription factors to which it can directly bind, including KLF4. Together, KLF6 and KLF4 transcriptionally activate keratin 4 in esophageal epithelium (Okano et al. 2000). KLF6 interacts with Sp transcription factors as well. For example, KLF6 represses MMP9 in endothelial cells through cooperation with Sp2 (Das et al. 2006). KLF6 was shown to interact with Sp1 to activate transcription of the apoptosis mediator, DAPK2 (Britschgi et al. 2008). Interestingly, Smad3 indirectly interacts with KLF6 via Sp1. This coordinate interaction has been shown to enhance KLF6 transcriptional activity (Botella et al. 2009).

KLF6 and Sp1 were also found to induce expression of IGF1R, but in a p53-dependent manner. In p53-null cells, KLF6-induced transcription from the IGF1R

promoter was reduced when compared to cells that retained wild-type p53. In these cells, KLF6 and p53 physically interact, suggesting KLF6 may be cooperating with p53 to drive gene expression (Rubinstein et al. 2004). In cell lines with functional p53, drug-induced stress reduces KLF6 message levels. Yet, cells with non-functional p53 display increased KLF6 message levels in response to stress agents, implying KLF6 has a role in response to cell stress independent of p53 (Gehrau et al. 2011).

p53 is likely only one of many important components of cell context that can impact KLF6 behavior. Interestingly, this impact may be due to direct interaction between the two proteins. More studies on KLF6 binding partners are required to clarify regulation of this important transcription factor. This is especially the case since many known KLF6 target genes have been implicated in tumorigenesis or tumor progression. Unsurprisingly, studies have found that KLF6 is frequently deregulated in human cancer.

KLF6 in Neoplasms

KLF6 is frequently misexpressed in human cancers, including those of the prostate, lung and breast. This misexpression may occur through a variety of mechanisms, including allelic loss, mutation, or alternative splicing. Chromosome 10p, where *KLF6* is located, is deleted in 55% of prostate cancers. Of prostate tumors with *KLF6* allelic loss, 71% additionally exhibited mutations in an otherwise

intact *KLF6* allele. Due to its frequent loss or mutation, KLF6 was described as a tumor suppressor in prostate cancer (Narla et al. 2001).

KLF6-SV1 is expressed at a higher level in prostate cancers compared to normal tissue. This is especially true for patients that contain the SNP IVSdA, which increases alternative splicing at the KLF6 locus. With IVSdA, increased KLF6-SV1 levels antagonize the function of full-length KLF6. Unfortunately, patients with this SNP have an increased risk of prostate cancer (Narla et al. 2005).

This correlation aside, KLF6 has been shown to directly regulate the formation and progression of prostate cancer. In prostate cancer cells, expression of KLF6 induces apoptosis through transcriptional activation of the pro-apoptotic factor ATF3 (Huang et al. 2008). KLF6-SV1 is highly expressed in metastatic prostate cancer, and is a predictor of poor survival. Forced expression of SV1 increases growth and invasion of prostate cancer cell lines (Narla et al. 2008). When injected into a mouse, these cells show increased dissemination. However, delivery of a siRNA targeting SV1 demonstrated impaired growth of these orthotopic tumors when compared to a control siRNA. Potentially, this variant could be targeted as a therapeutic strategy (Narla et al. 2008).

In non-small cell lung cancer (NSCLC), chromosome 10p15, where *KLF6* is located, is frequently deleted (Girard et al. 2000). 84% of NSCLC samples have decreased KLF6 mRNA when compared to normal lung tissue. LOH analysis of the *KLF6* locus showed that 34% of these tumors had LOH, and 66% of samples had heterozygosity at the *KLF6* locus. In lung cancer cell lines, expression of KLF6

inhibited soft agar colony formation, demonstrating that its expression reduces the transformation status of these cells. Additionally, overexpressing cells displayed higher levels of apoptotic markers, suggesting that loss of KLF6 may enhance transformation and survival of NSCLC (Ito et al. 2004).

In addition to regulating apoptosis in cancer cells, KLF6 has also been shown to inhibit pro-growth mechanisms. In cell lines, KLF6 was shown to directly bind to the oncogene c-JUN, and inhibit its transcriptional activity by facilitating its degradation by the proteasome (Slavin et al. 2004). In cells with decreased KLF6 activity, it is possible that the activity of the c-JUN oncogene is higher, which could facilitate tumor formation or progression in these cells. Another potential mechanism for KLF6 loss to impact tumor formation is its ability to bind directly to Cyclin D1. With this binding, KLF6 inhibits the interaction of Cyclin D1 with CDK4, and thus reduces their phosphorylation of RB, leading to cell cycle inhibition (Benzeno et al. 2004). In a colon cancer cell line, increased KLF6 expression reduces proliferation and promotes growth arrest through this mechanism (Benzeno et al. 2004). This describes another potential mechanism by which KLF6 loss may facilitate tumor formation.

KLF6 expression and localization was also examined in normal and cancerous breast tissues. While normal breast tissue displays a mix between cytoplasmic and nuclear staining, tumor tissues mainly displayed cytoplasmic staining (Gehrau et al. 2010). Of the tumor tissues that had nuclear localization of KLF6, there was a significant correlation with HER2-ERBB2 overexpression. Of stage

I tumors with ERBB2 overexpression, 86% of them exhibited nuclear KLF6, providing a strong association between nuclear KLF6 in breast carcinomas and HER2-ERBB2 positivity. These tumors were also likely to have metastasized to the lymph nodes (Gehrau et al. 2010). While other studies have demonstrated an increase in tumor formation in response to a decrease in KLF6 transcriptional activity, this study finds that the inverse is true for a subset of breast cancers. Potentially, nuclear KLF6 in these cells is accessing a different set of transcriptional targets that allow for KLF6 transcriptional activity to contribute to malignancy instead of repressing it, as has been demonstrated in other tissues.

In a different sampling of breast cancers, tumors with high expression of KLF6-SV1 were associated with an increased risk of forming distant metastasis (Hatami et al. 2013). Ectopic expression of KLF6-SV1 induced a reversible epithelial to mesenchymal transition in breast cancer cells, through the increased expression of TWIST1 in response to SV1 expression. Subcutaneous and orthotopic mouse models demonstrated that increased SV1 levels resulted in greater tumor cell dissemination (Hatami et al. 2013).

KLF6 Status in Hepatocellular Carcinoma

As in many other human cancers, KLF6 expression is also frequently reduced in HCC. However, there is some discrepancy as to the nature of this reduced activity. Studies have connected allelic loss, mutation, or epigenetic alterations to decreased KLF6 activity. The data regarding KLF6 mutation frequency is questionable, since

there are conflicting reports. This conflicting data may be due to the analysis of HCCs of different etiology. However, the consensus of these studies is that KLF6 expression is commonly reduced in human HCC as compared to normal liver.

In one of the first studies of KLF6 in HCC, analysis of microsatellite markers determined that 39% of tumors had single-copy loss at the *KLF6* locus when compared to normal tissue. Also, 15% of tumors had missense mutations in exon 2 of *KLF6* that were not present in matched tissue, but only half of these mutations occurred in a tumor with allelic imbalance (Kremer-Tal et al. 2004). Similarly, another HCC study detected single-copy loss in 52% of tumors, and exon 2 point mutations in 24% of tumors (Wang et al. 2010).

Yet, follow-up studies have not detected mutations at similar frequencies. In one study of 71 HCCs, no mutations in *KLF6* were found (Boyault et al. 2005). In 2006, two additional studies sought to clarify the presence or absence of *KLF6* mutations in HCC. In 21 dysplastic nodules and 85 HCC samples, no mutations in exon 2 of *KLF6* were detected. Allelic loss was not found in any of the dysplastic samples, but was present in 7% of HCCs (Song et al. 2006). In a set of 23 HCCs, only one case was found to have a missense mutation in exon 2. Despite no mutations in the coding sequence, 34.7% of tumors had decreased KLF6 transcript levels as compared to respective normal tissue (Pan et al. 2006). These studies demonstrate that mutation in *KLF6* is a rare event in HCC, or may be strongly dependent on patient selection. Yet, reductions in KLF6 expression can occur in the absence of genetic mutation.

In a set of HCCs from HBV-infected patients, KLF6 was reduced in 57% of tumors compared to control liver. Additionally, this study found that reduced levels of KLF6 are associated with tumors larger than 5cm. In a separate cohort of HCCs from HCV-infected patients, KLF6 was decreased in dysplastic nodules, and further decreased in advanced HCC. Here, a reduction in KLF6 levels correlated with advanced tumor stage (Kremer-Tal et al. 2007). This data suggests that reduced levels of KLF6 may be an early event in hepatocarcinogenesis, but is selected for in later stages as well. Interestingly, frequency or timing of KLF6 deregulation may be dependent on HCC etiology.

In livers with hepatitis C infection displaying a spectrum of disease, decreased levels of KLF6 were associated with more advanced HCC, with the lowest KLF6 levels occurring in very advanced HCCs. In addition to inverse correlation with HCC stage, patients with tumors that had less than 10% of normal KLF6 expression had worse survival and higher tumor recurrence than patients whose tumors had between 10 and 20% of normal KLF6 expression (Tarocchi et al. 2011). These correlations indicate a possible role for decreased KLF6 in HCC progression. Others have found decreased KLF6 in HCC, but in those studies the decrease in KLF6 expression did not correlate with histological grade or stage (Wang et al. 2010).

While the consensus of the literature demonstrates that KLF6 levels are commonly reduced in HCC compared to normal liver, this is not universally the case. In an analysis comparing normal liver, cirrhotic liver, macronodules, and hepatocellular carcinoma, KLF6 expression was decreased in all macronodule

samples as compared to normal liver. However in this study, both cirrohotic livers and HCCs had higher levels of KLF6 expression than the normal livers. Upon sequence analysis, mutations in exon 2 were not found (Bureau et al. 2008).

Several of these studies reveal contradictory information regarding the expression level, mutation, or deletion status of KLF6 in patient samples. This may, in part, be due to the etiological variation in hepatocellular carcinoma patients. It is possible that the form of KLF6 dysfunction is linked to the particular oncogenic stimulus that gives rise to HCC. Yet, with the exception of one study (Bureau et al. 2008), KLF6 levels are decreased in hepatocellular carcinoma compared to normal liver, strongly suggesting a tumor suppressor role for KLF6 in HCC. Some of these studies also show that KLF6 is decreased further in late HCCs versus early HCCs, alluding to a potential role in HCC progression.

In addition to deletion, mutation, and gene expression alterations, increased alternative splicing of the *KLF6* locus is another mechanism of reducing full-length KLF6 activity. Alternative splicing events of *KLF6* have been detected in human prostate cancer (Narla et al. 2005). In HCC, 18% of HBV-derived HCCs had a higher ratio of KLF6-SV1 to full-length KLF6, and no HCV-derived HCCs were found to have an increased splicing ratio (Kremer-Tal et al. 2007). These data indicate that increased splicing of KLF6-SV1 is a less common event in HCC compared to downregulation of total KLF6.

Despite this study suggesting KLF6-SV1 expression in HCC was a rare event, analysis of the ratio of KLF6-SV1 to full length KLF6 in aggressive HCV-induced

HCCs shows that the splicing ratio is higher in HCC versus normal tissue, increases linearly with HCC progression, and is also increased in tumors with vascular invasion (Vetter et al. 2012). Like the mutational analysis of *KLF6*, there is contradictory information regarding the importance of KLF6-SV1 in human HCC. These data suggest that increased splicing of KLF6-SV1 may occur more frequently in later stages than in earlier tumors.

Post-transcriptional regulation of the KLF6 message has recently been described in HCC cells. Decay of KLF6 mRNA was significantly increased in human HCC lines compared to immortalized hepatocytes. The 3' untranslated region (UTR) of KLF6 was subsequently shown to be a negative regulator of mRNA stability using a reporter assay (Diab et al. 2013). This outcome suggests that factors expressed in HCC cells may negatively regulate KLF6 levels through binding to the 3'UTR. This effect is not as strong in normal hepatocytes, and could be one reason why many HCCs have decreased KLF6 levels without the presence of a mutation or allelic loss. At least two microRNAs, miR-122 and miR-181a, are known to negatively regulate KLF6 levels. While not studied in liver cells, miR-181a was found to negatively regulate levels of KLF6 in gastric cancer cells (Zhang et al. 2012a). Mice with deletion of miR-122 display higher KLF6 levels (Tsai et al. 2012). Intriguingly, loss of miR-122 expression in liver cells increases migration and invasion, and correlates with poor HCC prognosis (Coulouarn et al. 2009). These effects upon miR-122 deletion would correlate with an increase in KLF6 expression. This result is inconsistent with other cancer models that have shown that reduced KLF6 levels

lead to increased tumorigenesis and dissemination. Since microRNAs have multiple targets, potentially miR-122 is targeting multiple transcripts in HCC cells that are confounding the correlation between KLF6 and HCC progression.

By Western blot, KLF6 in HCC cells typically appears as multiple species. What was previously thought to represent different splice variants of KLF6 has now been found to be differentially phosphorylated KLF6. A mutant form of KLF6 that could not be phosphorylated lacked the ability to transcribe *p21* (Lang et al. 2013), indicating phosphorylation is required for its activity. N-terminal phosphorylation of the KLF6 transactivation domain is present on about 50% of total KLF6 protein in the fibroblast-like COS7 cells (Slavin et al. 2004). One kinase known to phosphorylate KLF6 is GSK3β (Lang et al. 2013), but there are likely others as well. Regulation of phosphorylation status is yet another mechanism of regulating KLF6 activity.

KLF6 Activity in Hepatocellular Carcinoma

KLF6 was discovered, in part, because of its importance to liver biology. One of the groups that cloned KLF6 identified it in hepatic stellate cells from rats with hepatic fibrosis. KLF6 expression was increased in response to liver injury in these cells, and was localized exclusively to the nucleus, where it increased transcriptional expression of collagen α1, an important component of fibrotic reactions in the liver (Ratziu et al. 1998).

In the human HCC cell line HepG2, forced expression of KLF6 reduces proliferation (Kremer-Tal et al. 2004; Kremer-Tal et al. 2007). However, forced expression of KLF6 mutants fail to reduce proliferation, suggesting the effect is specific to KLF6 activity (Kremer-Tal et al. 2004). These mutants were derived from human HCCs, and their inability to regulate proliferation indicates that their normal transcriptional activation is impaired.

Similarly, *Klf6* was either conditionally deleted, or KLF6-SV1 was overexpressed in primary hepatocytes. In both cases, the rate of proliferation and the ploidy of cells increased. KLF6 expression even regulates proliferation in non-transformed cells, providing evidence that KLF6 functions as a tumor suppressor in hepatocytes (Vetter et al. 2012).

Yet, there is some discrepancy over the role of KLF6 in regulating proliferation. While previously it was shown that KLF6 overexpression reduced proliferation in HepG2 cells, another group demonstrated that KLF6 knockdown by siRNA also decreased proliferation in these cells. Additionally, there was no impact of KLF6 knockdown on growth of immortalized hepatocytes (Sirach et al. 2007), which disagrees with data describing the increased proliferation of primary hepatocytes when *Klf6* is deleted (Vetter et al. 2012). The use of cell lines has resulted in contradictory information regarding the role of KLF6 in HCC, which may be heavily dependent on unknown contextual factors. The use of mouse models can control for some context-dependent factors to potentially clarify the role of KLF6 in HCC.

Klf6 heterozygous mice survive to adulthood with 40-60% of wild-type KLF6 levels, and have increased liver mass compared to wild-type littermates (Narla et al. 2007). After DEN treatment, liver size was increased in *Klf6*$^{+/-}$ mice by 1.5%. Over nine months, these mice have an increase in HCC incidence from 40 to 71%. Additionally, tumor number, and tumor size were increased. Interestingly, since KLF6 is a transcriptional repressor of *Mdm2*, the levels of Mdm2 are increased in mice with reduced KLF6. Higher Mdm2 levels lead to decreased p53 expression in *Klf6*$^{+/-}$ HCCs. Concordantly, the expression signatures of these tumors were similar to HCCs with a deregulated p53 pathway, which is associated with poor survival after tumor resection in human disease. (Tarocchi et al. 2011).

An additional study of KLF6 involvement in hepatocarcinogenesis combined two approaches, liver-specific *Klf6* deletion and increased transgenic expression of human KLF6-SV1. Liver tumor formation was induced by DEN injection. This study found that *Klf6* deletion and KLF6-SV1 both increase HCC tumor formation and tumor size following DEN treatment (Vetter et al. 2012). Together with the germline mouse study, these data demonstrate that a decrease in KLF6 activity increases HCC formation. Interestingly, tumorigenic effects were compounded when *Klf6* conditional deletion and transgenic KLF6-SV1 expression were combined, which suggests that KLF6-SV1 can drive hepatocarcinogenesis, independent of its ability to repress full-length KLF6 (Vetter et al. 2012). Potentially, SV1 may also sequester other transcription factors from the nucleus, thus further deregulating gene expression in HCC.

Previous data has clearly shown that full-length KLF6 expression is commonly decreased in human cancer, including HCC. Importantly, cell line and mouse modeling studies have characterized KLF6 as a regulator of proliferation and cell death, consistent with its status as a tumor suppressor. While studies have found KLF6-SV1 expression increases dissemination and metastasis in prostate and breast cancers, this has not yet been demonstrated in HCC. Several transcriptional targets of KLF6 have been described, but to date, gene expression profiling has not been performed on HCC cells with different KLF6 levels. Therefore, determining KLF6 target genes is important for understanding mechanisms important to the formation and progression of HCC.

p53

The tumor suppressor *p53* is one of the most frequently lost or mutated genes in human cancer, occurring in over 50% of tumors (Hollstein et al. 1994). When active, p53 transcribes DNA as a tetramer (Friedman et al. 1993; Kitayner et al. 2006). While wild-type p53 typically has a short half-life, it is stabilized by cell stressors, such as DNA damage (Vousden and Lu 2002). Once stabilized, p53 tetramers transcribe a host of transcriptional targets that can trigger many cell processes, including cell cycle arrest, apoptosis, or senescence, as seen in Figure 1.3 (Liu et al. 2013a).

The mutant form of p53 is not degraded at the same pace as wild-type p53 and thus has a significantly longer half-life (Hinds et al. 1990). Frequently, tumor

cells are found to have elevated levels of nuclear p53, which is almost always due to accumulated mutant p53 (Bartek et al. 1991). The greatest number of *p53* mutations occur in the DNA binding domain, which ablates normal p53 transcriptional activity (Hollstein et al. 1991).

Despite p53's numerous roles in the cell, mice that possess germline deletions of *p53* are surprisingly developmentally normal, indicating that p53 is not required for normal mouse development. However, over time these mice spontaneously form cancer with high penetrance, indicating p53 is a tumor suppressor (Donehower et al. 1992). While p53 is not required for normal cell development, it is required to effectively mediate responses to cell stress. Without this response, cells are more susceptible to transformation. Concordantly, individuals born with somatic mutations in the *p53* gene suffer from Li-Fraumeni syndrome (Srivastava et al. 1990), and are susceptible to tumor formation. Knock-in mouse models of *p53* mutants that mimic those seen in Li-Fraumeni syndrome also form spontaneous tumors (Lang et al. 2004; Olive et al. 2004).

Figure 1.3. p53 incorporates cellular stress signals and transcribes a myriad of target genes to regulate multiple cell processes. Upon cell stress, p53 is stabilized and no longer targeted for degradation by Mdm2. p53 forms a tetramer to activate transcription, including its negative regulator, Mdm2.
(Adapted from (Liu et al. 2013a))

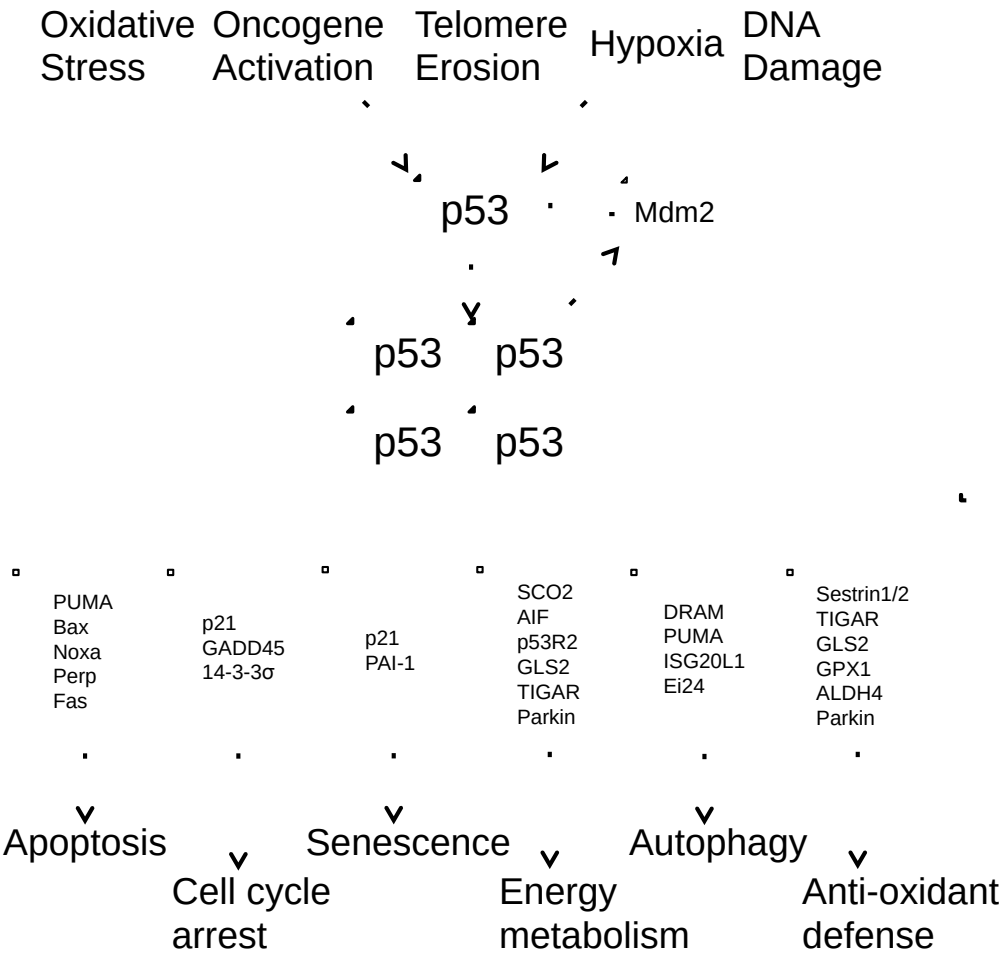

p53 in HCC

Overall, *p53* mutations occur in 33% of HCCs. Of these *p53*-mutated HCCs, 80% of them contain single point mutations, mostly distributed across the DNA binding domain (Oda et al. 1992). HCCs that are poorly differentiated are enriched for *p53* mutations versus those that are well or moderately differentiated, suggesting that aberrations in the *p53* gene are a later event in HCC development. Of HCCs with chromosomal loss at the *p53* locus, 62% have a point mutation on the remaining allele (Oda et al. 1992), which is consistent with its role as a tumor suppressor.

Despite the overall high frequency of *p53* mutations in HCC, the frequency varies depending on HCC etiology. When HBV positive HCCs were examined there was no significant association between HBV positivity and *p53* mutation. Yet, there was a correlation between *p53* mutations and HCV positivity, which occurred in 38.5% of cases (Long et al. 2013).

Another HCC etiology associated with *p53* mutation is the ingestion of AFB1. AFB1 has been shown to induce mutations at codon 249 in p53, and so many HCCs in regions with aflatoxin exposure carry a $p53^{R249S}$ mutation (Bressac et al. 1991; Ozturk 1991; Stern et al. 2001). In a cohort of patients without aflatoxin-induced HCC, the mutation at R249 was shown to be quite rare, and does not occur with a greater frequency in HCC than the general cancer spectrum (Thongbai et al. 2013). This indicates that R249 mutations in HCC are a consequence of AFB1 exposure, and is not otherwise a frequent consequence of HCC progression.

Importantly, *p53* mutations are associated with a poorer prognosis in HCC. In HCC tissue sections that were scored for intensity of nuclear accumulation of p53, tumors that had the highest levels of nuclear p53 had the poorest overall survival. High levels of nuclear p53 in tumor tissue are typically indicative of an accumulation of mutant p53 protein (Bartek et al. 1991). Post-resection, overexpression of p53 was a better predictor of poor overall survival than either tumor size or vascular invasion (Qin et al. 2002).

In addition to impacting HCC tumorigenesis, p53 plays an important role in HCC progression. In an HCC mouse model with intact *p53*, there is little to no metastasis. However, upon deletion of *p53*, the frequency of metastasis increases to 40%. The p53-deficient tumors display a more aggressive morphology and have a gene signature associated with a poorer prognosis (Lewis et al. 2005). It is clear that the loss of wild type p53 function is a frequent and important event in HCC. Yet, it is unclear if p53 mutation may provide an additional advantage to HCC beyond the loss of wild-type p53 tumor suppressor activity.

$p53^{R172H}$ Gain of Function Activity

When the first investigations into p53 function occurred, tumor-derived p53 cDNA was cloned for experimentation. The delivery of the tumor-derived *p53* gene into cell lines increased transformation-related phenotypes, leading to its initial characterization as an oncogene (Eliyahu et al. 1984; Finlay et al. 1988). We now

know this tumor-derived cDNA coded for a mutated *p53* (Hinds et al. 1989), and the transformation advantage it provided was due to the presence of this mutation.

Gain of function mutations in p53 were initially characterized in cell cultures, where cells lacking p53 protein were transfected with common p53 mutants. Upon mutant expression, including hotspot mutation R175H, cell lines displayed increased soft agar colony formation and tumor formation in nude mice (Dittmer et al. 1993). It became clear that the p53 mutant conveyed tumorigenic properties that were independent of wild-type p53 loss.

Most mice with germline *p53* deletion form tumors within six months of age. Largely, these tumors are malignant lymphomas, but sarcomas are common as well (Donehower et al. 1992). In mice heterozygous for *p53*, tumor formation is less frequent, with a longer latency and of a different spectrum than *p53*-null mice. Proportionally, *p53* heterozygous mice generate more sarcomas, and slightly fewer lymphomas. Interestingly, 12% of tumors in *p53* heterozygous mice are carcinomas, since these types of tumors are rare in *p53*-null mice (Lang et al. 2004).

A conditional, single-copy knock-in allele for $p53^{R172H}$ was directly compared to mice with a germline *p53* deletion. In this instance, since no wild-type p53 is present, the p53 mutant is not acting as a dominant negative. When null and mutant mice were compared, the overall survival of mice did not change, but the spectra of tumors differed. Mice with a p53 mutation had an increase in the occurrence of carcinomas, which occurred throughout the mouse in lung, colon, breast, and liver tissue. Interestingly, many of these tumors were invasive or metastatic, which did

not occur in *p53*-null animals. Mutant mice displayed increased tumor formation compared to the *p53*-null mice, and these tumors were more likely to metastasize, suggesting a gain-of-function role for the R172H mutation (Olive et al. 2004).

This $p53^{R172H}$ knock-in allele has been used to characterize p53 gain-of-function globally as well as in tissue-specific contexts. For example, it was found that $p53^{R172H}$ cooperated with activated KRAS to facilitate pancreatic cancer formation and increase metastasis (Morton et al. 2010). Cooperation between oncogenic KRAS and $p53^{R172H}$ also occurs in the skin, where mice with the R172H mutant form more skin tumors than *p53*-null mice. These tumors also progress and become metastatic, while the *p53*-null skin tumors do not (Caulin et al. 2007). When these same proteins are expressed in the oral epithelium, $p53^{R172H}$-expressing mice grew more tumors, which progressed to carcinoma. The *p53*-null animals did generate tumors, but they were fewer, and remained benign (Acin et al. 2011). In a model of breast cancer, $p53^{R172H}$ did not impact the acceleration or metastasis of tumors, but tumor initiation and the number of tumors per mouse were increased compared to *p53*-null animals (Lu et al. 2013). Lastly, a model of colon cancer induced by a pro-inflammatory treatment, dextran sulfate sodium, was used to assess $p53^{R172H}$ gain of function. Mice with $p53^{R172H}$ were more prone to the formation of colon cancer in response to the pro-inflammatory drug than *p53*-null mice (Cooks et al. 2013). Together, these examples demonstrate that $p53^{R172H}$ can produce an array of gain-of-function phenotypes dependent on tissue context.

p53 Gain-of-Function Mechanisms

One well-characterized mechanism by which p53 can acquire gain-of-function abilities is through the inhibition of the transcription factors p63 and p73 (Lang et al. 2004). p63 and p73 are structurally related to p53, particularly in the DNA binding domains (Courtois et al. 2004), and have multiple isoforms and splice variants which play different biological roles (De Laurenzi et al. 1998; Yang et al. 1998; Ueda et al. 1999). Transcriptional targets of p63 and p73 overlap in part with p53 target genes, including *p21*, *Mdm2*, *14-3-3σ*, and *p85* (Jost et al. 1997; Yang et al. 1998; Zhu et al. 1998; Westfall et al. 2003), though each factor also has unique target genes (Dietz et al. 2002).

Like p53, p63 and p73 form tetramers to bind to DNA. These factors do not heterotetramerize with wild-type p53 (Davison et al. 1999; Di Como et al. 1999), yet mutant p53 can heterotetramerize with p63 and p73, and subsequently inhibit their normal transcriptional activity (Di Como et al. 1999; Gaiddon et al. 2001; Strano et al. 2002). In *p53*-null mouse embryonic fibroblasts (MEFs), subsequent knockdown of p63 or p73 increases focus formation. While $p53^{R172H}$-expressing MEFs have a two-fold higher rate of focus formation at baseline, subsequent p63 or p73 knockdown had no impact, suggesting that p63 and p73 activity is already inhibited in p53 mutant cells (Lang et al. 2004).

Unlike *p53*, mice that are deficient for *p63* or *p73* have strong developmental defects (Mills et al. 1999; Yang et al. 1999; Yang et al. 2000). Despite roles that partially overlap wild-type p53 function, *p63* and *p73* are rarely mutated or lost in cancer, suggesting they are not classic tumor suppressor genes (Moll and Slade

2004). However, the inactivation of these transcription factors in the context of mutant p53 seems to exacerbate the loss of p53 tumor suppressive function (Oren and Rotter 2010).

Mutant p53 can also impact the activity of transcription factors other than p63 and p73. Studies have found that mutant p53 can increase transcription of NF-Y target genes via direct binding (Di Agostino et al. 2006). Additionally, mutant p53 directly interacts with SP1 (Chicas et al. 2000) and SREBP (Freed-Pastor et al. 2012) leading to increased transcription of their target genes.

Aside from altering the activity of other transcription factors, mutant p53 can also directly bind DNA and alter gene expression. While p53 DNA binding mutants have lost the ability to bind DNA in a sequence-specific manner, they can still directly bind DNA and impact transcription. Studies have found that mutant p53 binds to DNA in a non-B conformation, independent of the sequence (Gohler et al. 2005). Genes found to be directly transcribed by mutant p53 include *c-MYC* (Frazier et al. 1998), *IGF1R* (Werner et al. 1996), and *IGF2* (Lee et al. 2000), which are known drivers of tumorigenesis and progression in HCC.

Mutant p53 may indirectly impact a large number of genes through the direct regulation of microRNA expression. In particular, mutant p53 was found to repress the expression of miR-130b (Dong et al. 2013) and miR-27a (Wang et al. 2013). Aside from this direct regulation, mutant p53 also inhibits DICER, the microRNA processing enzyme, through inhibition of p63, a transcriptional activator of *Dicer* (Su et al. 2010). Depletion of DICER through this mutant p53-p63 axis has been

shown to promote invasion in cancer cell lines (Muller et al. 2014). Previously, decreased DICER expression has been associated with increased invasion and metastasis (Han et al. 2010; Martello et al. 2010).

p53 Gain-of-Function Activity in HCC

While gain-of-function p53 activity has been characterized for some tissues, the specific impact of p53 mutation is unclear in HCC. A few studies have implicated p53 gain-of-function mutants in HCC cell lines, but results vary by the mutant and cell context used. For example, overexpression of various p53 mutants in a p53-null HCC cell line decreased its apoptotic response. This effect was mediated through the inhibition of p53 family members, p63 and p73 (Schilling et al. 2010). Another study characterized a common p53 mutant, R249S, which occurs in response to aflatoxin exposure. Unlike the previously described study, forced expression of the mutant in *p53*-null HCC cell lines did not confer any proliferation or colony formation benefit. However, p53 knockdown in a cell line with endogenous R249S expression decreased proliferation and increased apoptosis compared to a control infection (Gouas et al. 2010). Though complicated, this suggests that this particular p53 mutant may not confer gain-of-function benefits over p53 loss in HCC cells. Yet, in cells with the endogenous p53 mutant, expression of the mutant is required for its growth and survival phenotypes. This result is in direct contrast with an additional study, which demonstrates impaired cell death in *p53*-null HCC cells ectopically expressing the R249S mutant (Lee et al. 2000). The source of this discrepancy could

be due to artifacts of ectopic expression of the mutant form versus endogenous expression models. Also, unknown differences in cell context may be important for mediating the effects of p53 mutant gain-of-function effects.

Aside from proliferation or survival effects seen with p53 mutant expression, other experiments suggest gain-of-function status through observations of gene expression changes. For example, the expression of Stathmin is decreased upon knockdown of mutant p53, but is not altered upon an increase or decrease in expression of wild-type p53 (Singer et al. 2007). Also, IGF2 expression is increased upon expression of the R249S mutant in a *p53*-null cell line (Lee et al. 2000). Interestingly, increased expression of both of these proteins is associated with HCC progression (Yuan et al. 2006; Chen et al. 2009), so the presence of mutant p53 correlates with the increased expression of these poor-prognosis markers.

Together, these data paint a confusing picture for p53 gain-of-function mutations in HCC, where varied outcomes have been demonstrated depending on the p53 mutation and cell context used. Importantly, none of these studies examine the impact of p53 mutations on HCC *in vivo*. Further study into particular mutations in specific contexts is required to determine if p53 gain-of-function occurs in HCC, and if it is important for HCC progression.

Scope of Thesis

KLF6 has been found to contribute to tumorigenesis in several cancers, including HCC. While it is known that KLF6 is a tumor suppressor for HCC, the

impact of KLF6 loss on HCC progression and metastasis is unknown. The work in Chapter II explores the role of KLF6 in affecting progression-related phenotypes of HCC, particularly migration and metastasis. In Chapter III, I investigate the mechanism of KLF6 function in HCC by elucidating its transcriptional targets. Two target genes, *Vav3* and *Cdc42ep3*, are investigated further for regulation of *in vitro* migration effects downstream of KLF6.

In addition to characterizing the role of KLF6 in HCC progression, I sought to clarify the role of $p53^{R172H}$ in HCC. While several *in vitro* studies point to evidence of gain-of-function p53 activity in HCC, some data is contradictory. As of yet, p53 gain-of-function activity has not been investigated in HCC *in vivo*. Loss of p53 activity has previously been shown to be a crucial driver of HCC progression, and Chapter IV investigates the possibility that the $p53^{R172H}$ mutant has an increased capacity for inducing HCC progression.

Together, this work highlights the activities of two tumor suppressors, KLF6 and p53, and their involvement in the formation and progression of hepatocellular carcinoma.

CHAPTER II

KLF6 is a repressor of HCC cell migration, tumor formation, and metastasis.

Preface

The BL185-M1 and BL185-I1 subpopulations described in Figure 2.1 were isolated by Ya-Wen Chen.

Lihua (Julie) Zhu performed bioinformatics analysis on the gene expression profiling study discussed in this chapter and located in Appendix A.

David Klimstra scored the KLF6 tissue microarray in Figure 2.7 and assessed the histology of the tumors generated during the study. He also kindly took the photographs shown in Figures 2.7A and 2.16.

Introduction

Hepatocellular carcinoma is a common malignancy worldwide that affects over 800,000 people per year, and is the 2nd-leading cause of cancer-related death (Ferlay et al. 2013). Survival for patients with HCC is generally poor, with a 5-year survival rate of 16.1% in the United States. However, patient prognosis is significantly better for patients with localized disease that can be surgically resected, where the survival rate increases to 29% (Hayat et al. 2007). Conversely, treatment options are limited for patients with invasion or metastasis (El-Serag 2011). Despite its potential impact on patient outcome, little is known about the specific genes and pathways involved in HCC progression and dissemination. Given the prevalence of invasive and metastatic disease, studies into these mechanisms may provide opportunities to improve the clinical outcome of a significant fraction of HCC patients.

Metastatic disease occurs through a multistep process by which cancer cells escape the primary tumor and establish one or more secondary tumor sites elsewhere in the body. In solid tumors, this process begins when invasive cells break attachments from the primary tumor. These cells then actively invade through the extracellular matrix, while resisting detachment-induced apoptosis, or anoikis (Liotta and Kohn 2004). These invasive cancer cells then enter lymphatic or blood vessels, a process termed intravasation. Living tumor cells are readily detectable in the circulation of cancer patients, which leave the circulation through a process called extravasation (Chaffer and Weinberg 2011). Cell fate studies have determined

that tumor cell intravasation and extravasation is an efficient process, but only a fraction of these cells will successfully form metastases (Chambers et al. 2002).

Upon leaving the blood or lymph, in the absence of a tumor-supportive environment, many invasive cells will not grow, and become dormant or die (Chambers et al. 2002; Nguyen et al. 2009; Chaffer and Weinberg 2011). An orthotopic cell tracking study found that over 80% of injected cells were able to survive and extravasate from the circulation, yet only 1 in 40 cells were able to form micrometastases. Furthermore, most of these micrometastases did not continue to grow, as only 1 in 100 micrometastases persisted to form a macroscopic tumor (Luzzi et al. 1998). While survival and escape from circulation are efficient processes for tumor cells, most cells are incapable of generating a colony in foreign tissue, and either remain dormant or die.

While inefficient, this process is successful in the approximately 37% of HCC patients who present with extrahepatic metastasis. The most common site of metastasis is the lung, which occurs in 55% of patients with metastatic disease. Second is involvement of the abdominal lymph nodes, which occurs in 41% of these patients (Katyal et al. 2000). Invasion of cells to the portal vein is also a common and deadly occurrence in patients with HCC. Portal vein tumor thrombosis (PVTT) was found to exist in 28% of HCC patients at diagnosis. Patients with PVTT have a median survival of 3.5 months, versus 18.7 months for patients without it (Cheung et al. 2006).

Gene expression profiling studies of HCC have revealed frequent changes to families of genes involved in cell cycle regulation and hepatocyte differentiation (Andrisani et al. 2011). Factors affecting proliferation and differentiation status of hepatocytes are likely important for tumor formation, but few genes are known to correlate with HCC progression. Aberrations that inactivate the p53 pathway are some of the most frequent changes in HCC, and the absence of tumor suppressive p53 activity drives a more invasive phenotype in mice while correlating with poorer survival in human HCC patients (Lewis et al. 2005; Villanueva and Hoshida 2011). In addition to loss of p53, increased IGF2 levels in HCC have been shown to be required for HCC metastasis in mice (Chen et al. 2009), while higher levels of IGF2 correlate with poor survival in humans (Iizuka et al. 2004).

The zinc finger transcription factor KLF6 has been previously shown to be a tumor suppressor in HCC, and low mRNA levels correlate with poor survival in HCC patients (Tarocchi et al. 2011). Heterozygous deletion of *Klf6 in vivo* results in increased hepatocyte proliferation and liver mass, and specific deletion of *Klf6* in primary hepatocytes enhances their proliferation (Tarocchi et al. 2011; Vetter et al. 2012). In mice with liver-specific depletion of *Klf6*, treatment with the carcinogen DEN resulted in increased hepatocarcinogenesis as compared to mice with intact *Klf6* (Vetter et al. 2012). These data confirm a role of KLF6 as a tumor suppressor in HCC, yet data connecting KLF6 to HCC dissemination and metastasis are lacking.

Experiments in other cancers have provided evidence that lower KLF6 activity can drive metastasis. In prostate and breast cancers, increased expression of

the dominant-negative splice variant KLF6-SV1 resulted in decreased survival and increased rates of metastasis (Narla et al. 2008; Hatami et al. 2013). These data suggest that decreased KLF6 activity may be a driver of tumor dissemination in addition to tumor formation.

Here I demonstrate that KLF6 expression is decreased in migratory subpopulations of an HCC cell line. Reduced KLF6 expression correlates with the presence of vascular invasion in HCC patients, and induces cell migration *in vitro*. Moreover, liver-specific deletion of *Klf6* promotes both HCC formation and dissemination to the lungs in mice. This work connects KLF6 and HCC dissemination for the first time.

Results

Subpopulations of an HCC cell line display increased transformation-related phenotypes.

In order to study genes that may impact migration and metastasis in HCC cells, migratory subpopulations of a murine HCC cell line were isolated. BL185 is a heterogeneous, murine HCC line derived from a non-metastatic tumor. This tumor arose in a liver with conditional deletion of *p53* and retroviral delivery of the *PyMT* oncogene (Chen et al. 2007). BL185 displays an intrinsically low level of migration *in vitro*. Migratory subpopulations were isolated by plating BL185 cells into a transwell migration chamber using 10% bovine serum as a chemoattractant. Cells that migrated through the membrane were selected and expanded as separate populations, which were termed BL185-M1 and BL185-I1.

Both M1 and I1 subpopulations display a higher rate of proliferation (Figure 2.1A) and soft agar colony formation (Figure 2.1B) as compared to the parent BL185 cell line. Soft agar colony formation measures the anchorage-independent growth of a cell line, which is used as a method of measuring its transformation status. These higher proliferation and soft agar colony growth rates suggest these subpopulations are more transformed than the parent population of BL185 cells.

Importantly, M1 and I1 also show a ten-fold increase in migration ability over the BL185 parent cell line (Figure 2.1C). Since the *in vitro* migration assay serves as a surrogate for measuring the initial, invasive steps of the metastatic cascade, these

migratory subpopulations may be useful for modeling gene expression changes important for HCC dissemination.

Figure 2.1. Subpopulations of an HCC cell line display increased proliferation, transformation, and migration.

A. Proliferation assay as measured by absorbance with MTS reagent in 24-hour increments. By 48 hours, significant increases in growth are present in M1 and I1 cells (p-values=0.0290 and 0.0047, respectively). These are more exaggerated at 72 hours (p-values=0.0125 and >0.0001). Graph shown is a representative experiment of four replicates.
B. Soft agar colony formation assay, where colonies are counted by size exclusion over 20 fields at 100X magnification. p-values calculated by t-test are 0.0131 and 0.0025 in M1 and I1 cells, respectively. Graph shown is a representative experiment of three replicates.
C. Transwell migration assay, cells that migrated through the membrane were counted per field at 100X magnification. p-values determined by t-test are 0.0012 and >0.0001 in M1 and I1 cells, respectively. Graph shown is an average of three replicate experiments.

A

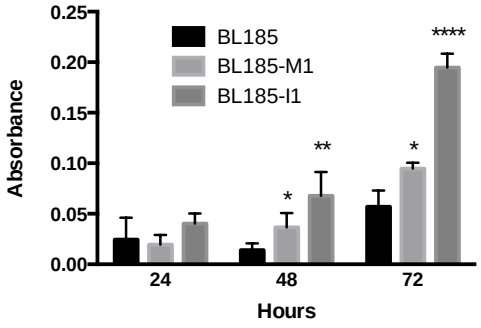

B

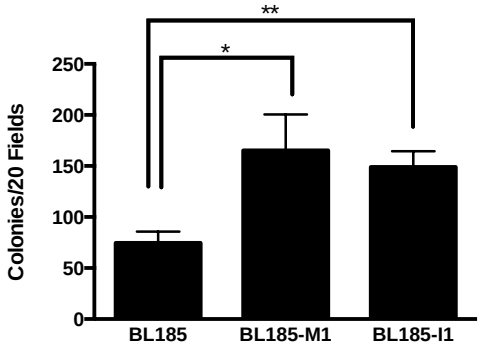

C

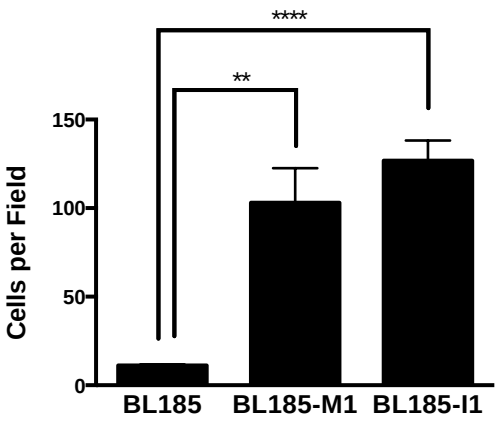

One common mechanism for cells to acquire more migratory characteristics is through epithelial to mesenchymal transition (EMT). EMT is a process whereby epithelial cells lose their epithelial characteristics and enter a more mesenchymal state. This process is thought to commonly occur in cancer cells to allow for increased invasive capacity. Typically, EMT is detected in cell lines through the measurement of decreased epithelial and increased mesenchymal markers. Commonly, E-Cadherin and α-catenin are used as epithelial markers while N-Cadherin and Vimentin are used as mesenchymal markers (Thiery 2002).

To investigate if EMT was responsible for the increased migration capacity of the HCC subpopulations, I assessed common markers for EMT by Western blot (Figure 2.2). None of these markers were differentially expressed in the subpopulations as compared to the parent BL185 cell line, indicating the subpopulations are not more mesenchymal than the parent population. While EMT has been shown to be important for other systems, it is likely not what is driving the phenotypes seen in these cells. Notably, these cells express markers of both epithelial and mesenchymal lineages, suggesting they may exist in an intermediate state. An alternate explanation could be that the populations are heterogeneous for cells expressing either epithelial or mesenchymal markers.

We hypothesized that these subpopulations possessed other gene expression changes that could account for the increased migration they displayed. These expression changes may also be important for HCC progression *in vivo*.

Figure 2.2. Differences in migration of HCC subpopulations are not due to epithelial to mesenchymal transition. Expression of common EMT markers are displayed by Western blot. E-Cadherin and α-Catenin are epithelial markers, while N-Cadherin and Vimentin are mesenchymal markers. β-Actin is used as a loading control. In the Vimentin blot, lysates from 3T3Li cells were included as a positive control sample for Vimentin expression.

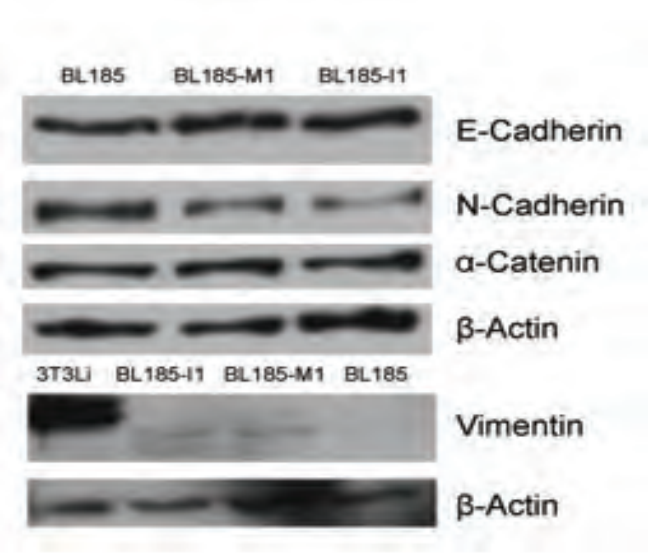

Gene expression profiling of BL185 subpopulations reveals many differentially expressed genes.

In order to find gene expression changes in the migratory subpopulations, whole genome expression analysis was performed on BL185, BL185-M1, and BL185-I1 by microarray. Genes whose expression was in common between M1 and I1, yet significantly changed from the parent BL185 line were selected. This analysis identified 313 genes that were either increased or decreased greater than two-fold in M1 and I1 cells as compared to BL185, with an adjusted p-value less than 0.01 (Appendix A).

Gene Ontology term analysis included categories related to cell cycle, angiogenesis, and migration (Table 2.1). These categories contain several genes that have well-characterized roles in tumor progression and metastasis, such as *Dlc1* and *Hif1α* (Zhou et al. 2008; Lu and Kang 2010; Popescu and Goodison 2014). The detection of genes known to be important for tumor progression within my profiling study demonstrates that my approach is valid for investigating novel genes that may affect these processes.

Several genes that were significantly changed in the microarray study were validated with separate RNA isolations by qRT-PCR (Figure 2.3). Gene expression changes validated by qRT-PCR vary from the microarray by fold change intensity, but largely the changes are consistent.

To prioritize genes for continued study, several criteria were applied. Importantly, the gene could not be previously characterized as a driver of HCC

progression. It was also important that the gene expression change seen in the M1 and I1 cells correlated with human cancer or HCC specifically. Lastly, preference was given to genes whose known or proposed function would influence cell migration or invasion. Several candidate genes that met these criteria were selected for further validation and analysis.

Table 2.1. Gene Ontology terms present in the subpopulation gene expression profiling dataset. GO Term analysis was performed on the gene expression profiling dataset using the GOEAST program (Zheng and Wang 2008). Examples of genes present in the GO term category are provided in addition to p-values calculated with the program.

GO Term	Example Genes	p-value
Cell Cycle	Plk1, Cdk1, Cdc20	1.01×10^{-7}
Cell Migration	Twist2, Cxcl12, Hif1a	0.0349
Angiogenesis	Vegfc, Angptl6, Pdgf	0.00189
Apoptosis	Ank2, Cdkn2c, Casp12	0.0256

Figure 2.3. Fold changes of several differentially expressed genes detected by profiling analysis were validated by qRT-PCR. C_t values for each respective gene were normalized to β-actin as an endogenous reference. These values in the M1 and I1 samples were then normalized to those for the BL185 sample to calculate fold change of a particular message in the subpopulations.

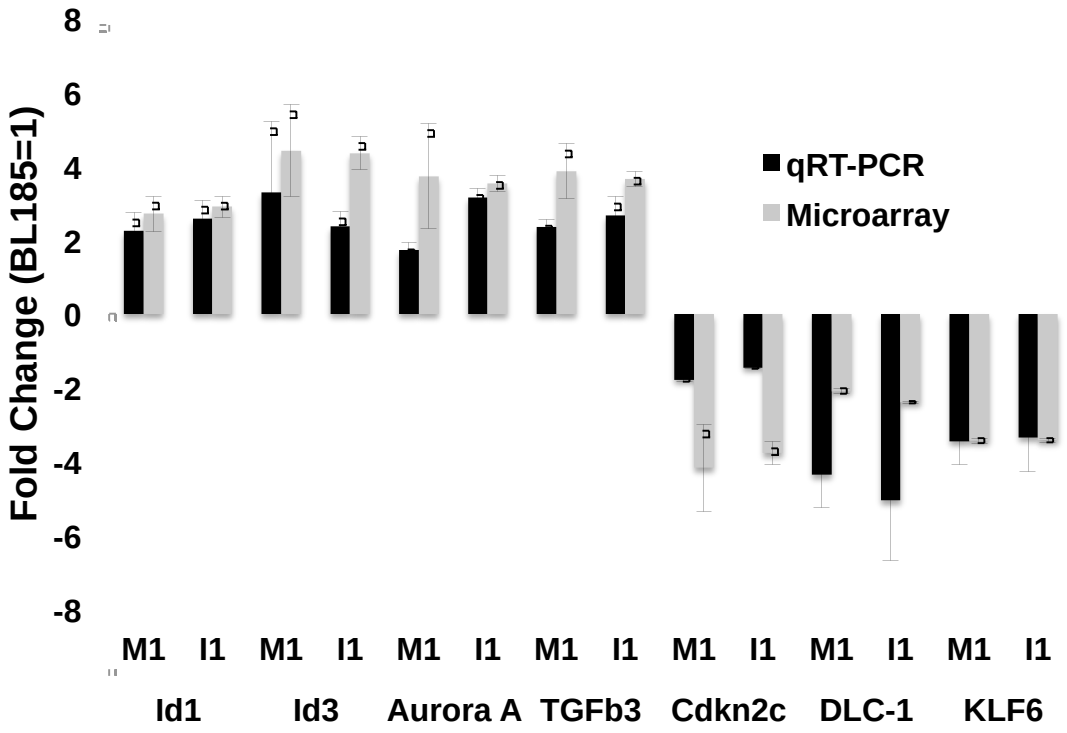

KLF6 is reduced in migratory HCC subpopulations and frequently has reduced activity in HCC.

One gene that exhibited a significant change in expression in the migratory subpopulations was Krüppel-like factor 6 (KLF6). KLF6 has been shown to be decreased at the mRNA level in human HCC (Narla et al. 2001; Ito et al. 2004; Kremer-Tal et al. 2004; Kremer-Tal et al. 2007; Gehrau et al. 2010; Wang et al. 2010; Tarocchi et al. 2011), has tumor suppressor activity in HCC (Tarocchi et al. 2011), and also has target genes including E-Cadherin and MMP9 that are associated with metastasis *in vivo* (DiFeo et al. 2006, Das et al. 2006). Thus, KLF6 satisfied the criteria for further downstream analysis from my expression profiling dataset.

When M1 and I1 HCC cells were compared with their non-migratory BL185 parent population, KLF6 was decreased at the mRNA level (Figure 2.3). In agreement with KLF6 message levels, all species of KLF6 are decreased in M1 and I1 subpopulations when compared to BL185 (Figure 2.4). I hypothesized that decreased levels of KLF6 in these HCC subpopulations was at least partly responsible for their increased growth and migration ability.

Figure 2.4. KLF6 is reduced in migratory subpopulations of HCC. HCC subpopulations were investigated for KLF6 protein levels by Western blot. β-Actin was used as a loading control.

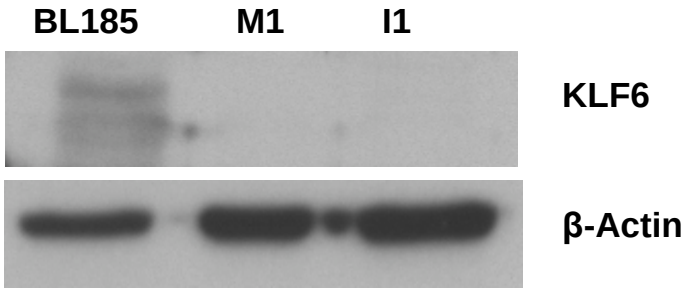

To corroborate the data from my mouse HCC samples, I investigated several sources of human HCC samples to determine KLF6 expression status. Data acquired from the Roessler 2 dataset in Oncomine (Roessler et al. 2010) demonstrates that KLF6 is reduced at the message level in HCC samples as compared to normal liver (Figure 2.5). This result was corroborated in other datasets as well. At the protein level, full-length KLF6 is decreased in human HCC cell lines when compared to an immortalized hepatocyte cell line, Thle2 (Figure 2.6A). KLF6 protein levels are also reduced in 3 out of 4 human tumor samples obtained from the UMMS Cancer Center Tumor Bank versus their matched normal liver samples (Figure 2.6B). Together, these data suggest that KLF6 is commonly reduced in HCC at both the mRNA and protein levels.

Figure 2.5. KLF6 is commonly reduced in human HCC at the message level. KLF6 is reduced at the message level in a profiling study of 225 HCC samples and 220 normal liver samples. These data come from the Roessler 2 profiling study publicly available in Oncomine (Roessler et al. 2010). The p-value, calculated by t-test, is >0.0001.

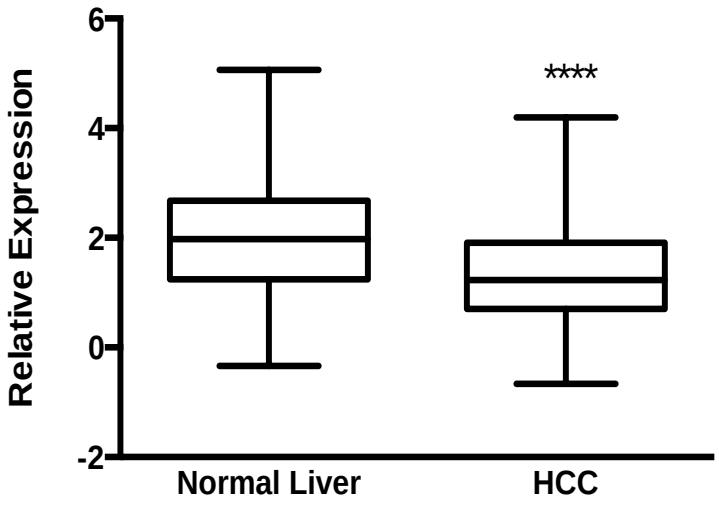

Figure 2.6. KLF6 is commonly reduced in human HCC at the protein level.

A. Western blot displaying KLF6 protein levels in human-derived HCC cell lines as compared to an immortalized hepatocyte cell line, Thle2. β-Actin is used as a loading control. The arrow in the figure indicates full-length KLF6. B. Western blot displaying KLF6 protein levels in human HCC samples. Samples were isolated from normal liver (labeled N) and paired HCC samples (labeled T) resected from human HCC patients. β-Actin is used as a loading control.

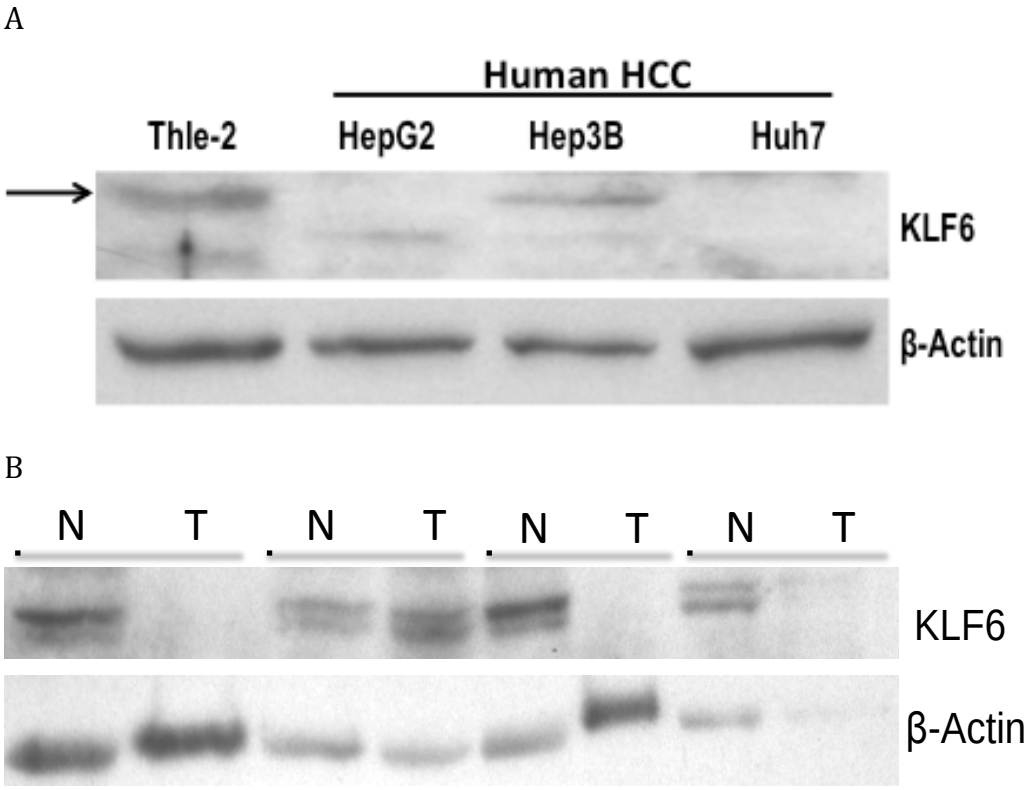

Given that decreased KLF6 levels correlate to increased migration in my HCC subpopulations, I sought to determine if KLF6 could function as a potential prognostic marker for HCC. I performed KLF6 immunohistochemistry (IHC) on a human tissue microarray (TMA) containing 106 human HCCs. Tumor specimens were then scored by an expert pathologist and rated as positive or negative. The staining pattern of positive specimens was then clarified based on predominant localization of KLF6, either cytoplasmic or nuclear (Figure 2.7A). Of 106 HCC samples, 74 were positive for KLF6, and 32 were negative. Of these positive HCCs, 43% had nuclear localization and 57% had cytoplasmic localization (Figure 2.7B). Intriguingly, KLF6 status did not correlate with HCC grade or survival as previous studies using KLF6 mRNA levels have demonstrated (Tarocchi et al. 2011). My TMA data suggests that KLF6 activity is commonly reduced in HCC via decreased expression or mislocalization.

A dataset of HCC surgical specimens available in the Oncomine database scores tumors as having the presence of vascular invasion or not (Wurmbach et al. 2007). The HCC surgical specimens with vascular invasion have less KLF6 expression at the mRNA level than HCCs without vascular invasion (Figure 2.7C). This correlation suggests a potential role for KLF6 in the regulation of HCC progression. Despite no correlation to patient outcomes in my tissue microarray, I sought to determine if decreased KLF6 levels were impacting HCC biology.

Figure 2.7. KLF6 is commonly deregulated in human HCC, but its status does not correlate to tumor grade or overall survival.

A. Examples of KLF6 localization in human tissue microarray HCC samples by IHC. From left to right, these samples were scored as having nuclear expression, cytoplasmic expression, or being negative for KLF6.
B. Distribution of KLF6 status in 106 unique human HCC samples from the tissue microarray after being scored as negative, cytoplasmic, or nuclear.
C. Message levels of KLF6 were accessed from the Wurmbach Liver dataset, in the Oncomine database. The p-value, calculated by Student's t-test, is 0.0038.

A

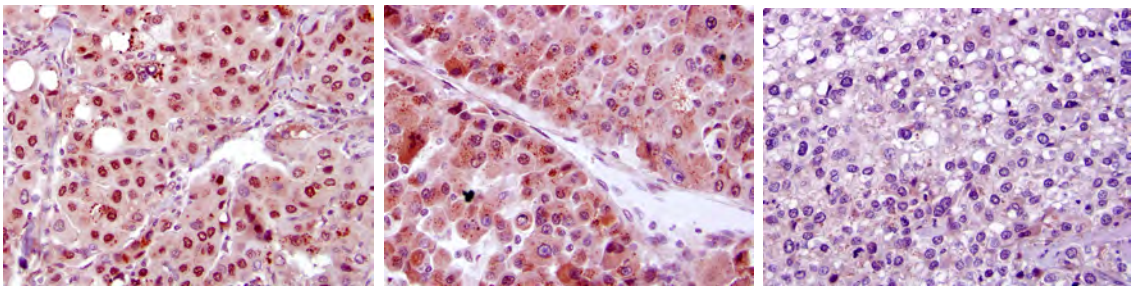

B

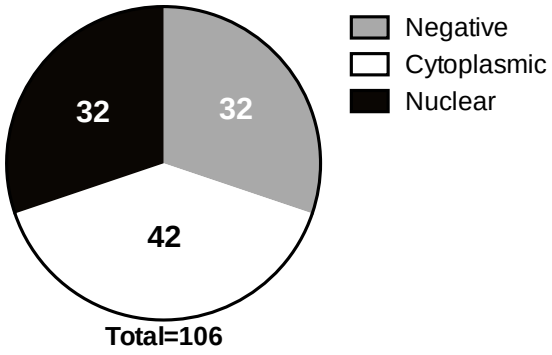

C

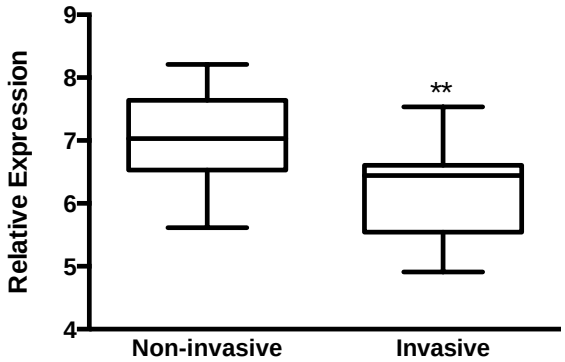

KLF6 suppresses transformation and migration of HCC cells.

Since decreased full-length KLF6 expression and mislocalization of KLF6 are common in HCC, I sought to determine if decreased KLF6 has a direct impact on phenotypes associated with HCC progression. To test this, KLF6 was stably knocked down by two, independent shRNAs in BL185 cells. As a control, BL185 cells were simultaneously infected with a virus containing a GFP-targeting shRNA in place of the KLF6-targeting sequence (Figure 2.8A). Since two shRNA sequences were used to achieve knockdown, this minimizes the chance that cell phenotypes are due to off-target effects of the shRNA. These stable lines were subsequently assayed for soft agar colony growth and migration. Upon KLF6 knockdown, soft agar colony formation increased two-fold (Figure 2.8B) as compared to the GFP control. This result supports this transcription factor's previously known role as a tumor suppressor gene. Yet, KLF6 knockdown also increased the migration ability of these cells two-fold (Figure 2.8C), indicating that KLF6 is a repressor of HCC cell migration, and suggesting that KLF6 may play a role in HCC dissemination.

Figure 2.8. KLF6 suppresses transformation and migration in murine HCC cells.

A. Western blot depicting shRNA-mediated knockdown of KLF6 in BL185 cells, with GFP-targeting shRNA as a control. β-Actin was used as a loading control. Shown is a representative blot of three separate shRNA infections.
B. Soft agar colony formation assay of KLF6 knockdown cells compared to GFP control. p-values, calculated by t-test, are 0.0055 and 0.0342 in KLF6 shA and shB, respectively. Shown is an average of 3 experiments performed in a single shRNA-infected cell line.
C. Transwell migration assay of KLF6 knockdown cells compared to GFP control. p-values, calculated by t-test, are 0.0011 and 0.0013 in KLF6 shA and shB, respectively. Shown is a representative experiment of 4 replicates performed in 2 shRNA-infected lines.

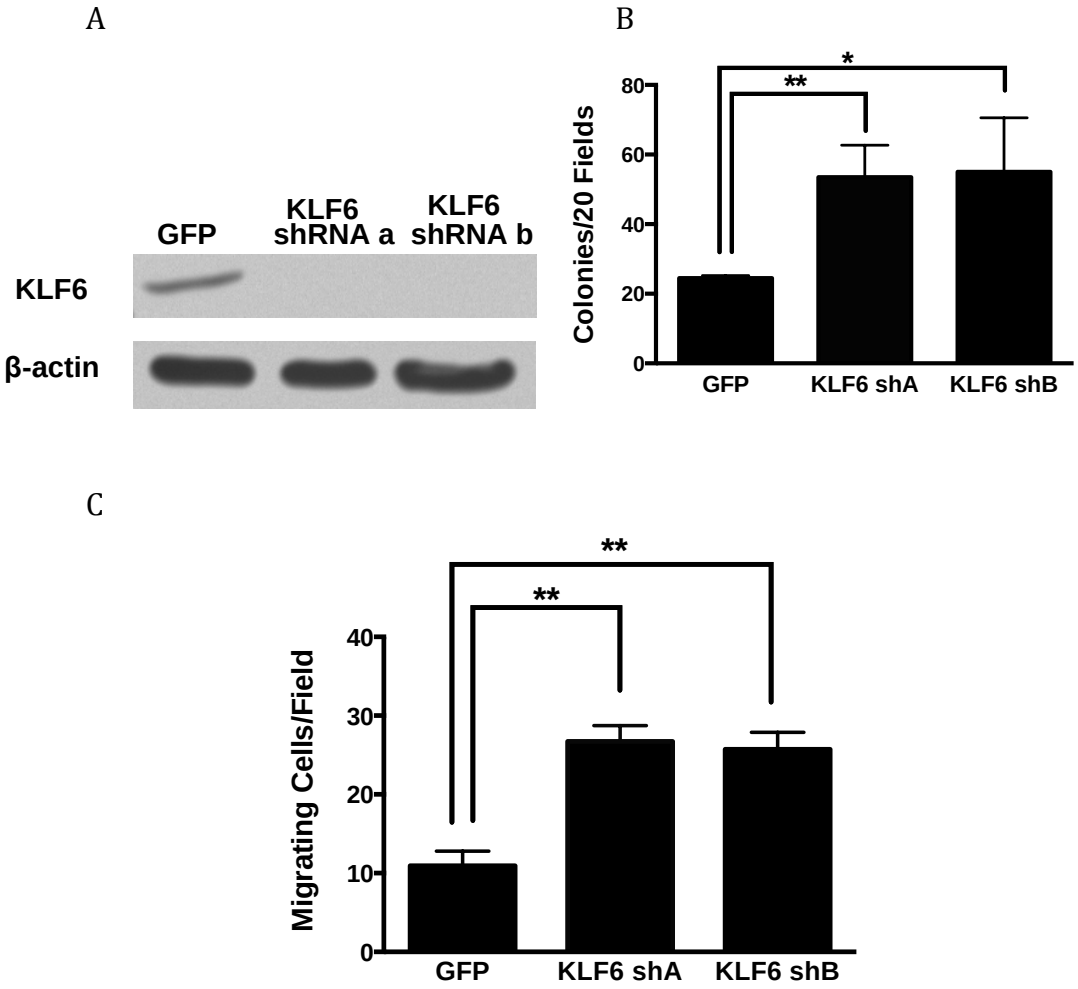

As described earlier, KLF6-SV1 is a splice variant of KLF6 that lacks a nuclear localization site, and is localized in the cytoplasm. KLF6-SV1 functions as a dominant negative for full-length KLF6, and is increased in several tumor types (Vetter et al. 2012). Studies in breast and prostate cancers previously found that increased KLF6-SV1 expression can increase metastasis (Narla et al. 2008; Hatami et al. 2013). To determine if this is similar for HCC, BL185 cells were infected with a retrovirus expressing KLF6-SV1. Control viruses without a gene-coding insert were also delivered to BL185 cells. Levels of KLF6-SV1 were detected using an antibody specific to the splice variant (Figure 2.9A). Ectopic KLF6-SV1 expression in BL185 cells increased cell migration (Figure 2.9B). This result mimics the conclusion found by KLF6 knockdown shown in Figure 2.8, where KLF6 is found to be a suppressor of HCC migration. Importantly, this result also indicates that the migration effect seen in KLF6 knockdown cells is not due to an off-target effect of the shRNAs, but due to decreased KLF6.

Figure 2.9. Expression of KLF6-SV1 increases HCC cell migration.

A. Western blot of KLF6-SV1 with β-Actin as a loading control. Cells were infected with retrovirus containing KLF6-SV1 or a control empty plasmid. B. Transwell migration assay of cells infected with KLF6-SV1 versus empty vector control. p-value by t-test is 0.0188. Shown is a representative experiment of 3 replicates.

A

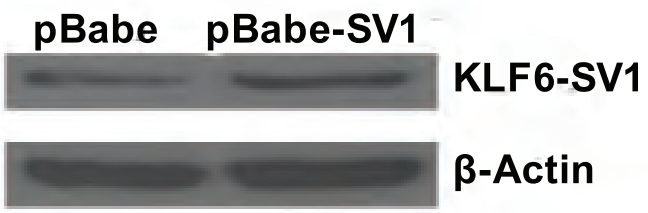

B

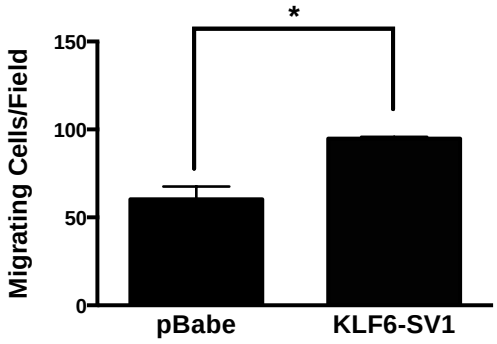

One known transcriptional target of KLF6 is E-Cadherin. Investigation of E-Cadherin levels in KLF6 knockdown cells by Western blot revealed that E-Cadherin levels are decreased in response to KLF6 knockdown (Figure 2.10). Evaluation of other EMT markers revealed that they are not significantly altered upon KLF6 knockdown (Figure 2.10). Similarly to what was seen in the BL185 migratory subpopulations, KLF6 knockdown cells seem to express both epithelial and mesenchymal markers. A previous publication implicated KLF6-SV1 as a positive regulator of EMT (Hatami et al. 2013), but in my HCC cell lines, KLF6 knockdown does not seem to impact the levels of EMT markers other than E-Cadherin. Despite changes in E-Cadherin levels, cell morphology is not altered upon KLF6 knockdown in HCC cells (data not shown).

Together, my data demonstrate that full-length KLF6 functions as a repressor of HCC cell transformation and migration.

Figure 2.10. Some EMT markers are affected in response to KLF6 knockdown. Western blot EMT marker levels in KLF6 knockdown cells compared to GFP control. E-Cadherin and α-catenin are common markers of epithelial cells, while N-Cadherin is a mesenchymal marker. β-Actin serves as a loading control.

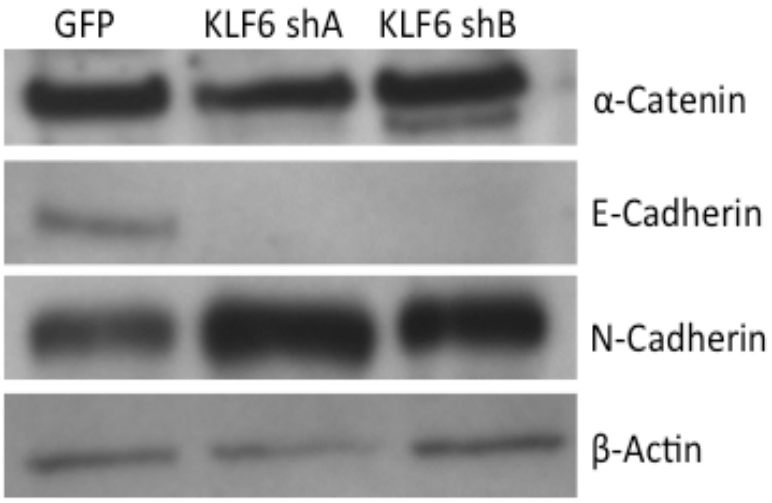

Single-copy loss of *Klf6* in an HCC mouse model increases tumorigenesis and decreases overall survival.

Since KLF6 knockdown resulted in an increase in migration and soft agar colony formation *in vitro*, I sought to determine if decreased KLF6 in an HCC mouse model would increase tumor progression *in vivo*. To model HCC *in vivo*, I utilized the RCAS-TVA system, where liver cells are rendered susceptible to infection by the RCAS retrovirus through expression of the TVA receptor under the Albumin promoter (Lewis et al. 2005). After injection with an RCAS virus containing the *PyMT* oncogene, mice that are Albumin-*tv-a, p53*$^{fl/fl}$, Albumin-*cre* develop HCCs that have the capacity to metastasize to the lung (Lewis et al. 2005; Chen et al. 2007).

We conducted an analysis of the impact of KLF6 on HCC progression by crossing a *Klf6* conditional allele into the mouse model for HCC. The *Klf6* conditional allele was designed with LoxP sites flanking exons 2 and 3 of the *Klf6* gene. By design, deletion of the DNA between these sites would result in a loss of KLF6 message and protein (Leow et al. 2009). However, instead of being a direct repeat, the second LoxP site was inadvertently inverted (Personal communication). As a consequence, *Cre* expression results in an inversion event between exons 2 and 3 instead of a deletion event. Inversion at these sites results in a frame shift that results in non-functional KLF6 message. With sustained *Cre* expression, the inversion can continue, resulting in expression of either wild-type or impaired KLF6 message. This results in the expression or deletion of *Klf6* in a mosaic fashion, instead of a permanent deletion. With this in mind, I crossed Albumin-*tv-a, p53*$^{fl/fl}$,

Albumin-*cre* mice to Albumin-*tv-a, KLF6*$^{fl/wt}$*, p53*$^{fl/fl}$, Albumin-*cre* mice to allow for direct littermate comparison. Approximately half of the mice in each litter have a *Klf6* floxed allele, and half of the mice retained two wild-type *Klf6* alleles.

Over the course of nine months, a cohort of mice was assessed for tumor-free survival. Mice were sacrificed when illness became apparent. If the cause of illness in a sacrificed mouse was not due to the presence of HCC, the mouse was censored from the study. At nine months, all remaining mice in the study were sacrificed and assessed for presence of HCC, providing a total of 16 animals in the *Klf6*$^{wt/wt}$ group, and 23 mice in the *Klf6*$^{fl/wt}$ group. Of five *Klf6*$^{fl/wt}$ mice injected with RCAS-GFP, none formed liver tumors. The study demonstrated that single copy loss of *Klf6* in the liver significantly impairs tumor-free survival as compared to wild type littermates (Figure 2.11A). This reduction in survival is due to an increase in the incidence of HCC in *Klf6* heterozygous mice, as proportionally more mice from the *Klf6*$^{fl/wt}$ group (74%) developed HCC than in the *KLF6* wild-type group (38%) (Figure 2.11B). This increase in tumorigenesis echoes the *in vitro* result of increased soft agar colony formation (Figure 2.8B), and previously published work describing the role of KLF6 as a tumor suppressor in HCC.

Figure 2.11. Single-copy loss of *Klf6* reduces overall survival and increases HCC incidence.

A. Kaplan-Meier curve displaying tumor free survival of GFP-injected *Klf6*$^{fl/wt}$ mice, and *PyMT*-injected *Klf6*$^{fl/wt}$ and *Klf6*$^{wt/wt}$ littermates. Mice were assessed over a period of 9 months and sacrificed when illness was apparent. Only mice whose death was perceived to be due to HCC were included, otherwise the mouse was censored. Censored animals are represented in the figure as tick-marks on the day of death. p-value by Log-rank test between *Klf6*$^{fl/wt}$ and *Klf6*$^{wt/wt}$ *PyMT*-injected mice is 0.0398.
B. Number of mice with gross HCC in *Klf6*$^{fl/wt}$ and *Klf6*$^{wt/wt}$ groups over the course of 9 months. Mice with tumors present upon sacrifice at 9 months are included. p-value by Fisher's exact test is 0.0258.

A

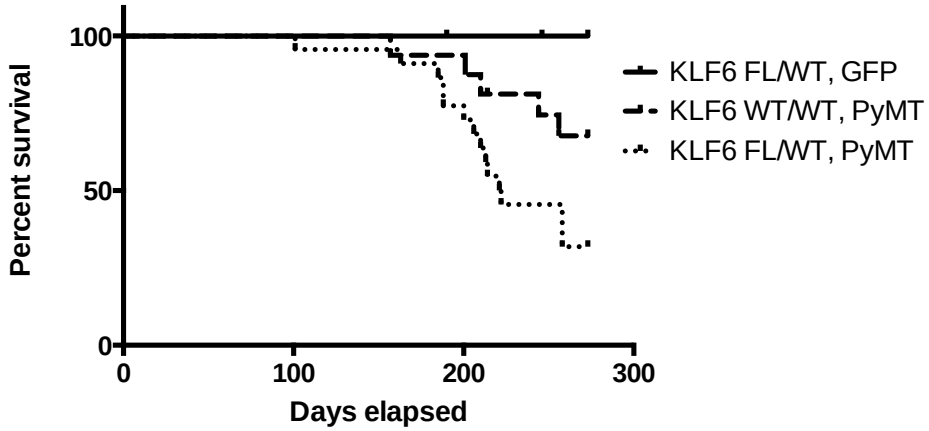

B

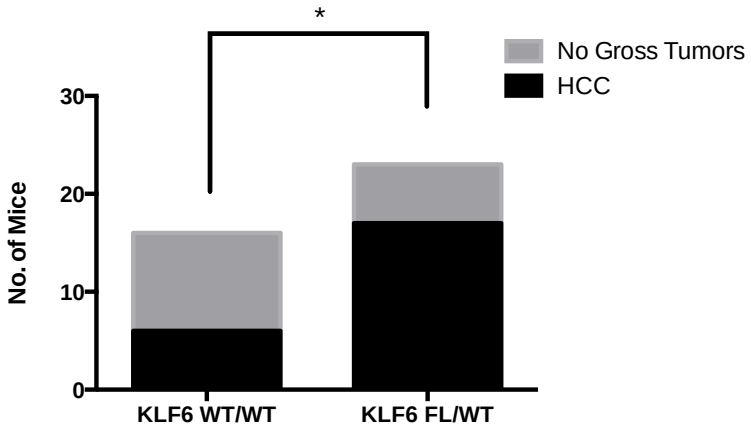

RNA isolated from murine *Klf6*$^{fl/wt}$ HCCs demonstrate that KLF6 is expressed at 50% of *Klf6*$^{wt/wt}$ tumor levels in most cases (Figure 2.12). One *Klf6*$^{fl/wt}$ tumor retained wild-type levels of KLF6 expression, which may be caused by unsuccessful recombination of the conditional *Klf6* allele. An additional tumor lacked detectable KLF6 expression levels, which may indicate loss of the remaining *Klf6* allele.

Figure 2.12. Full-length KLF6 levels are reduced in *Klf6*$^{fl/wt}$ HCC tumors versus *Klf6* wild-type tumors. Full-length KLF6 message was detected by qRT-PCR in RNA derived from murine tumor samples. C_t values for each sample were normalized to β-actin message levels as an endogenous reference. The average C_t values for the *Klf6* wild type tumors were set to 1. All samples were then normalized to this average value in order to obtain a fold change. The p-value, calculated by t-test, is 0.0050.

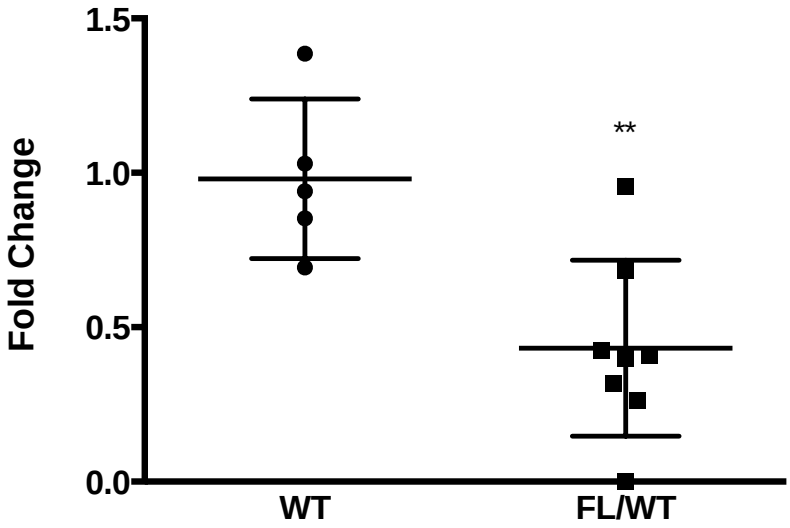

Despite a difference in the incidence of HCC in my mouse model, tumor burden per mouse was not significantly changed between the two groups in the survival cohort (Figure 2.13A). I hypothesized that I was not seeing a difference in tumor burden due to the fact that mice in the survival cohort were only sacrificed when displaying illness or distress. Likely, the tumor burden is normalized to the tumor volume at which mice become ill from HCC. To determine if *Klf6* deletion accelerated HCC development or growth, I generated a separate cohort of mice injected with RCAS-*PyMT*. These mice were sacrificed at 4.5 months of age, prior to displaying symptoms of illness and assayed for tumor size. In this cohort of animals, the tumor burden in $Klf6^{fl/wt}$ mice is significantly greater than tumors formed in the wild-type group (Figure 2.13B).

Figure 2.13. *Klf6*$^{fl/wt}$ HCC tumors are larger at an early study timepoint, but this difference does not persist in the survival cohort. All liver tumors were measured in three dimensions in millimeters. Half of the lengths of each of these axes is represented as variables *a*, *b*, *c* in the following formula. Tumor burden was calculated by using the formula for the volume of an ellipsoid, where V=(4/3)π**abc*. If a mouse had multiple liver tumors, volumes were summed to arrive at total tumor burden per mouse.

A. Tumor burden in the survival cohorts of *Klf6*$^{wt/wt}$ and *Klf6*$^{fl/wt}$ mice.
B. Tumor burden in *Klf6*$^{wt/wt}$ and *Klf6*$^{fl/wt}$ mice at 4.5 months of age. p-value by t-test with Welsh's correction is 0.0212, p-value by F-test is 0.0003.

A

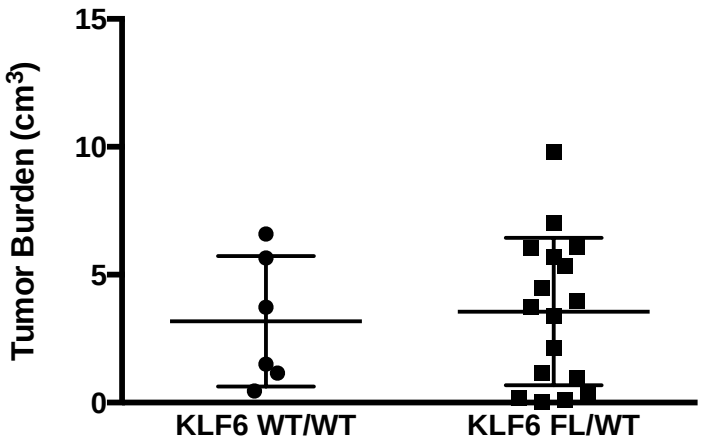

B

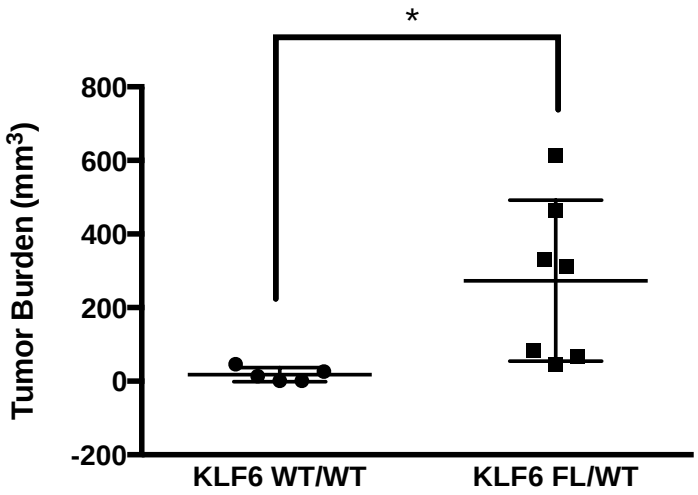

To investigate if *Klf6*$^{fl/wt}$ tumors were proliferating faster or forming earlier, tumors harvested from the 4.5-month cohort of mice were stained for Ki67. Ki67 is a marker of cell proliferation commonly used to detect recent mitoses in tissue sections (Scholzen and Gerdes 2000). Cells with Ki67 positive nuclei were counted in relation to the number of cells that stained negative for Ki67. Tumors from *Klf6*$^{fl/wt}$ mice did not have different rates of proliferation when compared to tumors from *Klf6*$^{wt/wt}$ mice (Figure 2.14). Immunohistochemistry for Cleaved Caspase 3 (CC3) was also performed to detect cells undergoing apoptosis (Persad et al. 2004). Cells positive for CC3 were generally rare, and equal between *Klf6*$^{fl/wt}$ and *Klf6*$^{wt/wt}$ tumors (data not shown). Since rates of proliferation and apoptosis are similar between the tumor types, and *Klf6*$^{fl/wt}$ tumors are larger than *Klf6*$^{wt/wt}$ tumors at 4.5 months (Figure 2.13B), I hypothesized that *Klf6*$^{fl/wt}$ tumors may be initiating earlier than in *Klf6*$^{wt/wt}$ mice.

Although *Klf6*$^{fl/wt}$ mice have a greater incidence of tumor formation than *Klf6*$^{wt/wt}$ mice, these mice have equivalent numbers of liver tumors per mouse (Figure 2.15). One *Klf6* wild-type mouse had as many as 8 separate liver tumors, while one *Klf6*$^{fl/wt}$ mouse had 12 discrete liver tumors, yet most animals had only one grossly visible tumor. The number of gross liver tumors is the same per mouse despite the result that single-copy *Klf6* loss allows for tumors to form earlier than wild-type animals.

Figure 2.14. Proliferation rates in HCCs from 4.5-month old mice do not differ based on *Klf6* status. Sections of HCC from 4.5-month old mice were stained for Ki67 by IHC. Cells with Ki67-positive and negative nuclei were counted in order to obtain the percentage of cells within an HCC section that were Ki67 positive. Five fields in each tumor section were counted to obtain an average, except for one tumor section, which was entirely covered by 3 fields of view (the third tumor in the *Klf6*$^{wt/wt}$ group).

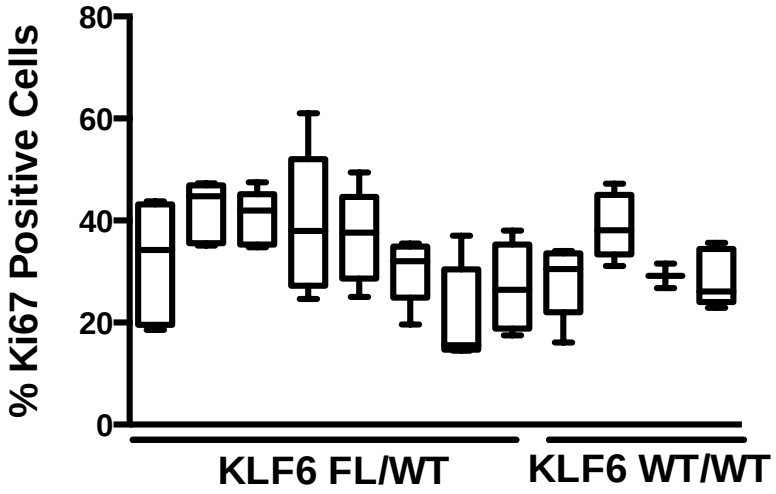

Figure 2.15. The number of liver tumors per mouse does not differ based on *Klf6* status. The number of liver tumors in each mouse was counted based on gross visibility. Best judgment was used to determine which tumor segments were distinct and which were contiguous.

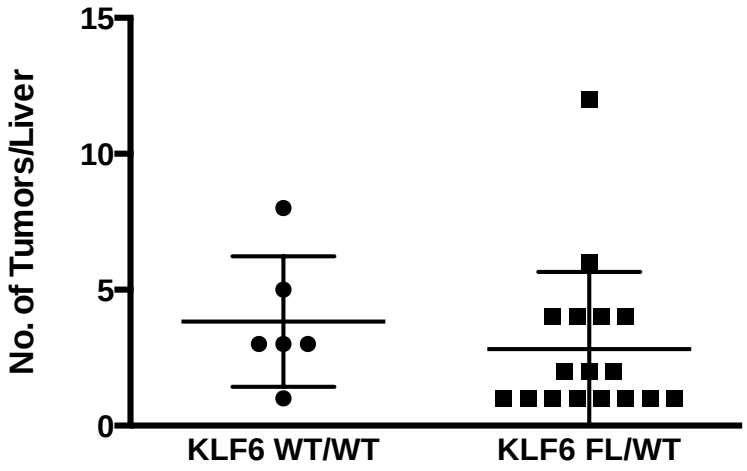

Despite differences in the tumor incidence and the earlier expansion of these tumors, HCCs with single-copy loss of *Klf6* do not display different histology than tumors with wild-type *Klf6* (Figure 2.16). To determine if single-copy deletion of *Klf6* impacts tumor histology, normal livers (A,B) and tumor samples (C-F) from each group of mice were stained with hematoxylin and eosin (H&E) to visualize cell and tissue structure. Livers without tumor appear similarly normal between *Klf6* wild-type and heterozygous mice. The different regions of histology observed in the mouse tumors also commonly occur in human HCC. Among the tumor histology observed is the occurrence of non-invasive tumors composed of large cells with vacuolated cytoplasm (Figure 2.16C,D). Previous studies using this mouse model have associated this vacuolated cytoplasm with the accumulation of fat (Lewis et al. 2005). Also, these tumors display similar frequencies of more cellular, dense, and fibrotic areas (Figure 2.16E,F). Even though single-copy loss of *Klf6* facilitates earlier and more frequent tumor formation, it does not impact the appearance of these HCCs. Pathological analysis determined that neither the grade nor differentiation state of HCCs in our study differed by *Klf6* status.

Figure 2.16. The histological patterns of mouse-derived HCC do not change with *Klf6* status. Panels (A) and (B) are normal liver in mice absent of HCC. Panels (C) and (D) display cells with accumulation of lipid in the cytoplasm. Panels (E) and (F) display regions of necrosis and fibrotic deposition, respectively.

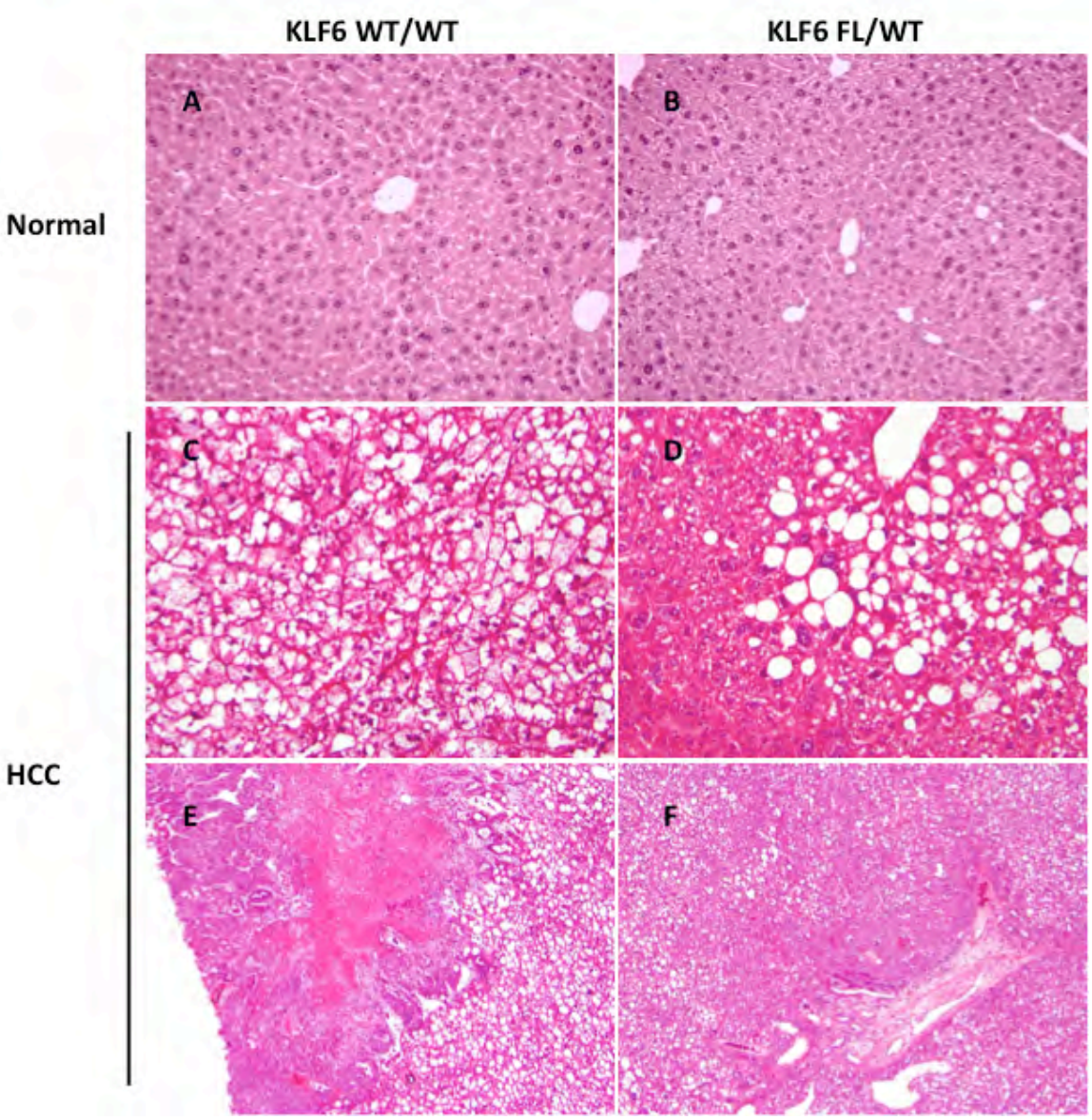

Single-copy loss of *Klf6* increases metastatic burden and affects poor-prognosis genes.

Interestingly, in addition to an increase in tumor formation, proportionally more mice from the *Klf6*$^{fl/wt}$ survival cohort had lung metastases (6/17) than from the KLF6 wild-type group (0/6) (Figure 2.17A). This difference is significant by Chi-Square (p=0.0453), though it is not statistically significant by Fisher's Exact Test, given the relatively small number of mice that developed metastasis, and the small number of tumor-bearing mice in the *Klf6*$^{wt/wt}$ group. Intact lungs from animals in the survival cohort that presented with a grossly visible liver tumor were step sectioned in 200um increments. Each step was stained with H&E and examined for the presence of metastases. A single metastatic lung colony was found in KLF6 wild-type mice with HCC. This single colony was detected microscopically, while several metastases present in the *Klf6*$^{fl/wt}$ cohort were grossly visible (Figure 2.18). Quantified areas of these metastases are shown in (Figure 2.17B). This exciting finding demonstrates that single-copy loss of *Klf6* in HCC increases the metastatic burden to lung.

Figure 2.17. Single-copy loss of *Klf6* increases metastatic burden.

A. Number of mice with lung metastases present in the populations of mice with primary HCC by gross detection.
B. Quantified areas of liver metastases present in the lung. A graticule was used to obtain the lengths of the major and minor axes of lung colonies. Area was calculated using the formula for an ellipse, where A=π*ab*, where *a* and *b* are representative of half the lengths of each the major and minor axes.

A

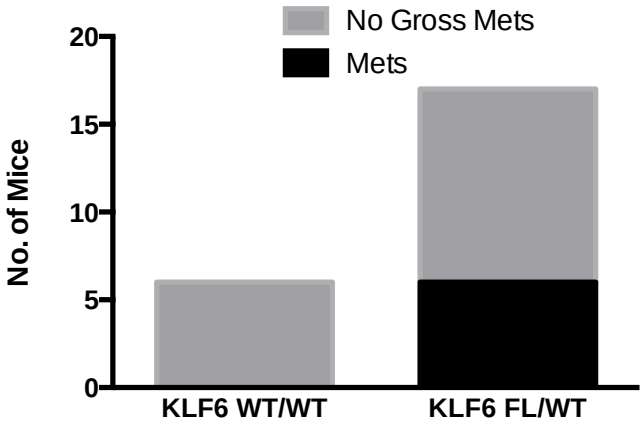

B

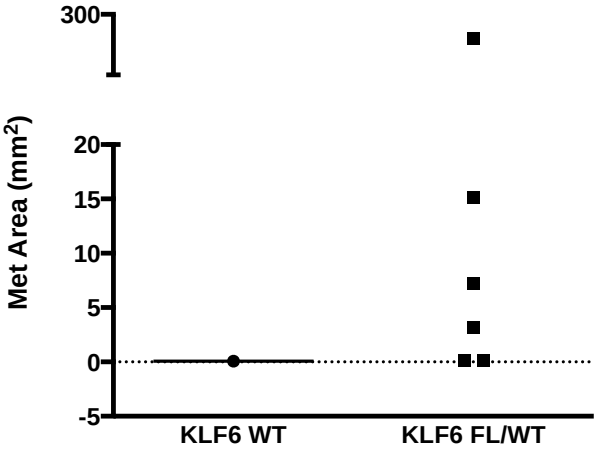

Figure 2.18. Lung metastases present in *Klf6*$^{fl/wt}$ mice are larger than *Klf6*$^{wt/wt}$ mice. H&E stained sections of the lungs were investigated for HCC metastases. Images A, C, E and F were taken at 50X magnification. Images B and D were taken at 200X magnification, of the metastases in A and C respectively. Arrowheads indicate metastatic colonies, while asterisks indicate normal lung.

A. Single metastatic nodule identified in a KLF6 wild-type mouse.
B. Enlarged image of metastatic nodule in A.
C. Metastasis in KLF6 heterozygous mouse.
D. Enlarged image of metastatic nodule in C.
E-F. Example metastasis found in KLF6 heterozygous animals

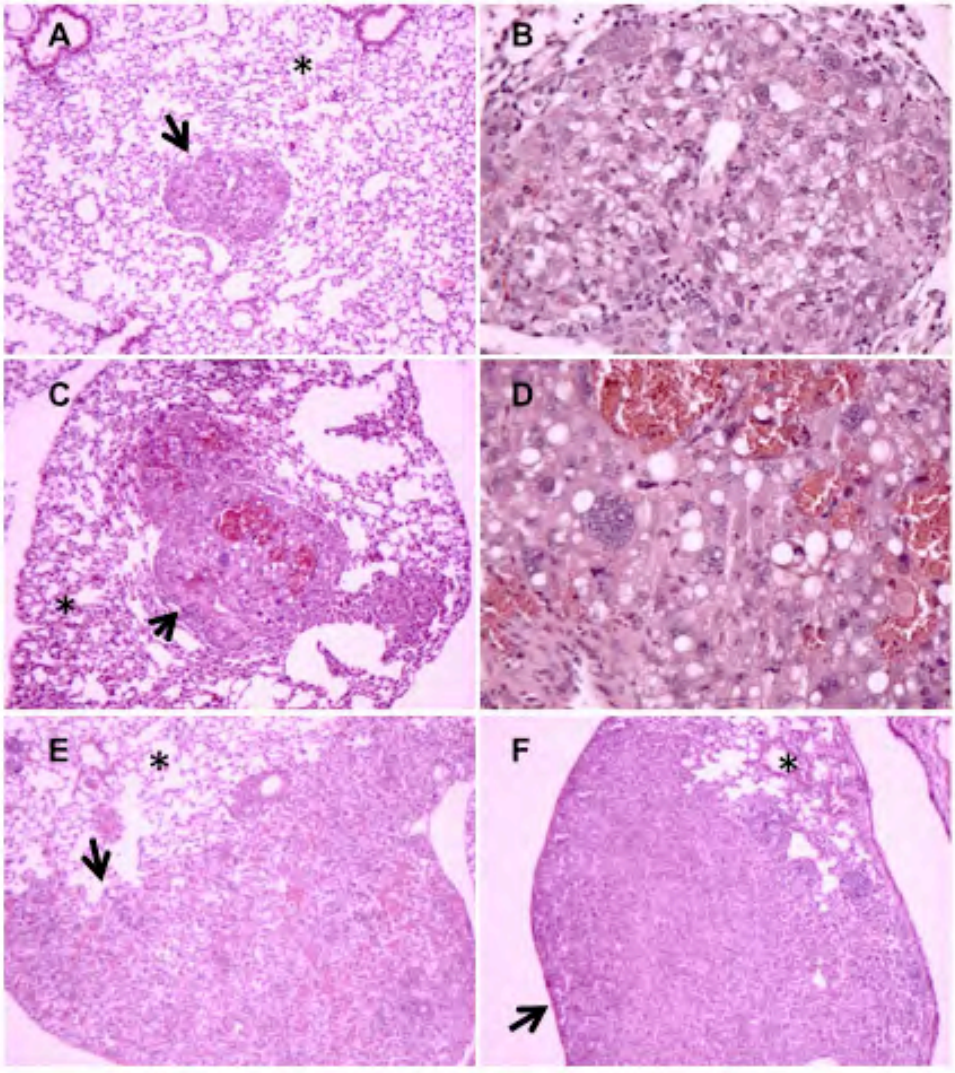

HCCs isolated from the survival cohort of mice were assayed for expression of markers that are associated with poor prognosis of HCC patients. Levels of α-fetoprotein (AFP) and Insulin-like growth factor 2 (IGF2) are elevated in HCC patients and are correlated with poor prognosis (Izumi et al. 1992; Iizuka et al. 2004). mRNA levels of AFP and IGF2 are increased in several of the HCCs from the *Klf6*$^{fl/wt}$ group (Figure 2.19) when compared to the average levels of the *Klf6*$^{wt/wt}$ tumors. The variance in expression in tumors from the KLF6 heterozygous group is significantly different from those in the wild-type group for both poor-prognosis genes (p-value<0.0001 by F-test), indicating the tumor populations are not equal.

Taken together, these data indicate that single-copy loss of *Klf6* results in an increase in HCC development and metastasis, and negatively impacts tumor-free survival. These findings demonstrate a novel consequence of decreased KLF6 activity in promoting HCC progression and lung metastasis.

Figure 2.19. Single-copy loss of *Klf6* results in higher expression of poor-prognosis genes for HCC. α-fetoprotein (AFP) and Insulin-like growth factor 2 (IGF2) levels were assessed by qRT-PCR in RNA derived from mouse HCC tumors. C_t values in each sample were normalized to β-actin as an endogenous reference. To calculate fold change, all samples were normalized to the average C_t value of *Klf6* wild-type tumors. The fold changes are plotted on a log2 scale. p-values for AFP expression is 0.1510 and 0.0883 for IGF2 expression as determined by t-test. p-values for both genes by F-test were <0.0001.

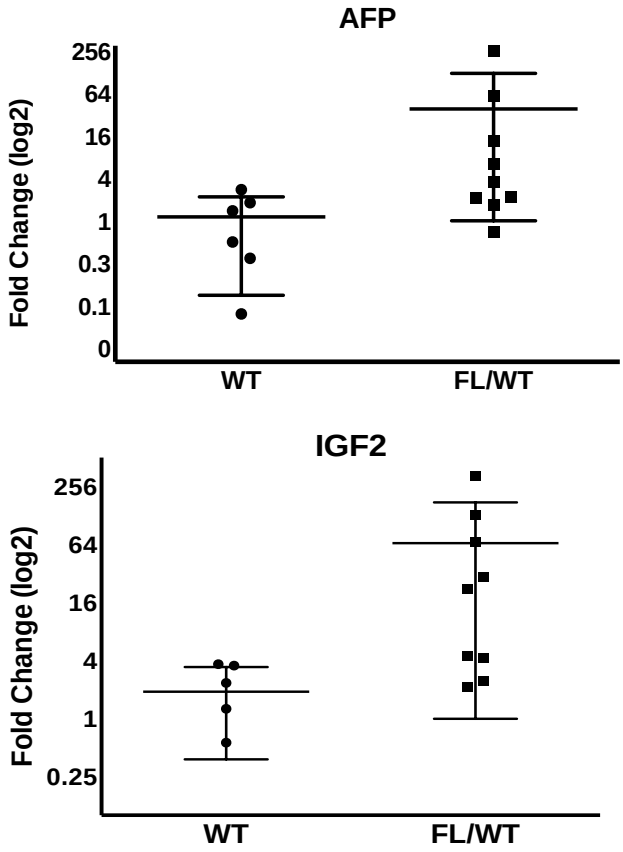

Materials and Methods

Cell culture, isolation of migratory subpopulations.

All mouse HCC cell lines were cultured in high-glucose DMEM (Life Technologies) with 10% FBS and 1% Pen/Strep, termed "Growth Medium." All mammalian cell lines were grown at 37°C. The BL185 cell line was derived from a p53-null mouse HCC (Chen et al. 2007). BL185-M1 and BL185-I1 subpopulations were isolated from BL185 using a transwell migration chamber, or transwell invasion chamber (BD Biosciences 354578; 354480). BL185 cells were plated in the upper levels of each respective chamber in serum-free DMEM. Few cells migrated to 10% serum in the lower chamber, but these were scraped from the membranes and plated in growth medium. BL185-M1 cells came from a migration insert while BL185-I1 cells came from an invasion insert.

DF1 chicken fibroblast cells were cultured in growth medium at 39°C. DF1 cultures in 60mm dishes were transfected with 5ug of RCAS-GFP or RCAS-PyMT using 25uL of Superfect transfection reagent (QIAGEN, 301305). DF1 cells were incubated with transfection complexes for 3 hours at 39°C. Viral titers were calculated using the minimum concentration of serial dilutions of viral supernatant required for naïve DF1 infection. Cells used in mouse experiments required a dilution factor of $2x10^7$ to be suitable for injection. Infections were confirmed by isolating genomic DNA from DF1 cells, and amplifying an RCAS virus sequence by PCR (F: CAG TCT CTC CCT AAC ATT AC; R: CTA CCT TGT GTG CTG TCG ACC).

Infected DF1 cells were only maintained in culture for 1 month before transfections were repeated.

Stable KLF6 knockdown cell lines were generated from lentiviral delivery of pLKO.1 library shRNAs directed to mouse KLF6 (Thermo Scientific; shA: TRCN0000085628, shB: TRCN0000085632). Lentiviruses were produced in 293T cells that were transfected with plasmids containing envelope glycoprotein, required packaging sequences, and pLKO.1 shRNAs. Transfections were performed using Effectene Transfection Reagent (QIAGEN, 301425). HCC target cells were infected with 1 mL of lentiviral supernatant in a well of a 6-well plate using 1ug of polybrene. Cells were subsequently selected in 5ug/mL puromycin prior to experimental analysis.

In vitro migration and soft agar colony analysis

For *in vitro* migration analysis, $2.5x10^4$ cells were plated on a migration insert (BD Biosciences 354578) in serum-free DMEM. Growth Medium was plated into the bottom of the migration chamber. After 20 hours, the cells were fixed with methanol, and stained with Giemsa. Non-migrating cells from the top of the membrane were removed with a cotton swab. Remaining cells were counted in 5 fields per membrane at 100X magnification.

For soft agar colony formation experiments, a 1.4% hard agar solution was combined with 2X DMEM with 20% FBS and 2% Pen/Strep and plated onto 100mm tissue culture plates. After hardening, $1x10^5$ cells were mixed with equal parts of a

0.8% soft agar solution and 2X growth media and added to the top of the hard agar layer. After the soft agar solution hardened, 8mLs of 1X growth media was added to the dishes, which were incubated for 2 weeks at 37°C. Colonies were counted in 20 fields per plate at 100X magnification. Size exclusion was used to ensure that colonies had grown in the dish, and were not just cell clumps.

Proliferation experiments were conducted in 96-well plates. 1000 cells were plated in triplicate wells for each day assayed. Cell Titer 96 MTS reagent (Promega, G3580) was added to wells for 30-minute incubations. Following the incubation, absorbance was read at 490nm using a 96-well plate reader. Empty wells treated with an equal volume of reagent were used as a control absorbance reference. Absorbance values were averaged across the triplicate wells, and the absorbance from the reference was subtracted.

Error bars used for graphical representation of these experiments represent the standard deviation of the dataset. Student's t-tests were used to calculate p-values.

Gene Expression Profiling Analysis of Migratory Subpopulations by Microarray

RNA was isolated from BL185, -M1, and –I1 cells using Trizol reagent (Life Technologies, 10296010). The RNA samples were labeled using the 3' IVT Express Kit (Affymetrix, 901228). Gene Expression profiling was conducted using GeneChip Mouse Genome 430 2.0 arrays (Affymetrix, 900495). Two different RNA isolations

were used as technical replicates. Microarray chip analysis was performed by the UMass Medical School core facility.

To summarize the probe data and normalize the data, the RMA method in the Affymetrix package (Bioconductor) was used. Genes of interest for follow-up study were those whose expression was significantly different in the M1 and I1 cells as compared to the BL185 parent population. Significance was defined as having an adjusted p-value under 0.01 with a fold change greater than 2-fold. Bioinformatics analysis was performed by Lihua (Julie) Zhu (UMMS).

The raw data files in addition to normalized expression data have been deposited in the NCBI GEOArchive under the accession number GSE54757.

Gene Ontology terms were determined through the use of the Gene Ontology Enrichment Analysis Software Toolkit (GOEAST) program (Zheng and Wang 2008).

Western blotting

Protein lysates were generated in RIPA buffer, where concentrations were normalized by Bradford Assay. 20ug of lysate were used for each Western blot sample. 10% acrylamide gels were used for SDS-PAGE, and subsequently blotted onto PVDF membranes. Western blots were blocked for one hour at room temperature in 7.5% nonfat dry milk in TBS. Antibodies for Western blotting were used as described in Table 2.2.

Immunohistochemistry

Portions of each tumor were fixed in formalin and embedded in paraffin. Tissue sections were deparaffinized with heat and rehydrated in decreasing alcohol concentrations. After rehydration, antigen retrieval was performed by microwaving slides in Antigen Unmasking Solution (Vector, H-3300). Endogenous peroxidase activity was inactivated by adding 3% hydrogen peroxide for 10 minutes. Slides were blocked in goat serum in PBS for one hour at room temperature. For KLF6 IHC, biotin blocking was performed prior to adding primary antibody in order to reduce background (Vector, SP-2001).

Primary antibody was added as described in Table 2.2. Biotinylated Rabbit secondary antibody was diluted in goat serum in PBS and added to the slides for one hour at room temperature. Goat serum, secondary antibody, and developing reagents were from Vector ABC kits (PK-4001). Pigment was developed in the tissues using a NovaRed Peroxidase Substrate (Vector, SK-4800). After development, slides were co-stained in hematoxylin, dehydrated, and mounted.

Human HCC tissue microarrays were a kind gift from David Klimstra. Along with human control slides, these were processed and stained for KLF6 in the same method described above. Samples were scored for having either positive or negative staining for KLF6. In samples positive for KLF6, the presence was scored as being primarily cytoplasmic or nuclear.

KLF6 Expression in human HCC datasets

The Oncomine database was used for KLF6 expression data in Figures 2.5A and 2.7. The data in Figure 2.5A was derived from the Roessler Liver-2 dataset, and features 220 normal liver and 225 hepatocellular carcinoma samples (Roessler et al. 2010). Figure 2.7 was derived from the Wurmbach Liver dataset and features 17 non-invasive and 18 invasive hepatocellular cancers (Wurmbach et al. 2007).

Gene Expression qRT-PCR analysis

RNA from cell lines was isolated using Trizol, and converted to cDNA using First-Strand cDNA synthesis kit (Life Technologies, 18080-051). qRT-PCR was performed using SYBR Green (VWR, 95072) in an ABI 7300 machine using 50ng cDNA. Primers used for analysis are listed in Table 2.3.

C_t values for each sample were averaged, and normalized to β-actin C_t values as an endogenous reference. In each case the Comparative C_t Method was used to calculate fold change, where fold change = $2^{-\Delta\Delta CT}$.

Mouse breeding, tumor analysis

Klf6$^{fl/fl}$ mice on a C57/Bl6 background were generously provided by Genentech and obtained from Scott Friedman's laboratory. These mice were crossed with my RCAS-TVA HCC model to obtain Albumin-*tv-a, p53*$^{fl/fl}$, Albumin-*cre, KLF6*$^{fl/wt}$ mice. These mice were crossed with Albumin-*tv-a, p53*$^{fl/fl}$, Albumin-*cre, KLF6*$^{wt/wt}$ mice to obtain littermates that were either heterozygous or wild-type for *Klf6* to be

used for direct comparison. These mice were injected in the liver at 3 days old with $2x10^6$ DF1 cells producing RCAS-GFP or RCAS-PyMT virus (Chen et al. 2007). Mice were assigned to either a survival study or a timepoint study. Mice designated to the timepoint study were sacrificed at 4.5 months of age. Mice in the survival cohorts were sacrificed before suffering was apparent as determined by my mouse protocol, or at 9 months of age, which was the predetermined study endpoint. Kaplan-Meier statistics were performed using the Log-rank test. Tumors found in mice were measured in three dimensions before allocating portions for fixing in formalin or freezing for downstream analysis.

To count and measure lung metastases, FFPE lungs from each mouse with a primary tumor were sectioned in 200um steps. A section from each step was H&E stained and examined for the presence of metastases to lung. Using an eyepiece graticule, lung metastases were measured at their longest and shortest axes. Areas of the metastases were calculated using the formula for area of an ellipse.

Table 2.2. Antibody conditions used for Western blotting and immunohistochemistry.

Target	Manufacturer	ID number	Dilution	Diluent	Condition
KLF6	Santa Cruz	sc-7158	1:1000	5% milk in TBS	Overnight at 4°C
E-Cadherin	BD Biosciences	610181	1:2000	5% milk in TBS	Overnight at 4°C
N-Cadherin	BD Biosciences	610920	1:2000	5% milk in TBS	Overnight at 4°C
Vimentin	Thermo Scientific	MS-129-P0	1:2000	5% milk in TBS	Overnight at 4°C
α-Catenin	BD Biosciences	610193	1:2000	5% milk in TBS	Overnight at 4°C
KLF6-SV1	Life Technologies	39-6900	1:2000	5% milk in TBS	Overnight at 4°C
β-Actin	Santa Cruz	sc-1615-R	1:2000	5% milk in TBS	1 hour at 21°C
KLF6	Santa Cruz	sc-7158	1:250	Goat serum in PBS	Overnight at 4°C
Ki67	Abcam	ab66155	1:500	Goat serum in PBS	Overnight at 4°C

Table 2.3. Primers used for amplification of target genes by qRT-PCR.

Target	F Primer	R Primer
β-Actin	Tcctcctgagcgcaagtactct	cggactcatcgtactcctgctt
KLF6	Cggtatgctttcggaagtg	cgcactcacacaggagaaaa
AFP	Cagcagcctgagagtccata	ggcgatgggtgtttagaaag
IGF2	Tgagaagcaccaacatcgac	cttctcctccgatcctcctg
DLC1	Cggccgagcctcaactc	tatttctgcagcaggttcatctg
AurKA	Gcttctgacctgctccaagtt	tcctgtgtccttctaactcccag
TGFβ3	Tctccactgaggacacattga	attcgacatgatccagggac
ID1	Gagtccatctggtccctcag	gcgagatcagtgccttgg
ID3	Cgctgaccaccctgaacac	tcgacataagctcagaagggaat
Cdkn2c	Ctccggatttccaagtttca	gggggacctagagcaacttac

Discussion

In this work, I sought to uncover additional gene expression changes that are responsible for HCC progression and metastasis. To do this, I used BL185, a low-migrating cell line isolated from a non-metastatic murine HCC, and migratory subpopulations isolated from BL185, termed BL185-M1 and BL185-I1. I employed gene expression profiling of these cell lines to determine expression changes that may be responsible for the increased migration capacity of M1 and I1 cells.

Profiling of these cells revealed several genes already known to participate in tumor progression and metastasis. For example, the expression of known pro-metastatic transcription factor TWIST2 (Fang et al. 2011; Mao et al. 2012) is increased in the migratory subpopulations. Also, transcription factors ID1-3 are increased in the migratory subpopulations as compared to the parent line. Inhibition of ID1 and ID3 has been shown to inhibit metastasis in gastric and pancreatic cancers (Tsuchiya et al. 2005; Shuno et al. 2010), suggesting their expression is important for metastasis. Since these known metastatic drivers were present in our dataset, it suggests that my profiling approach was successful at detecting genes important to migration or metastasis in HCC cells. The profiling dataset likely includes many more genes important to progression or metastasis, and can be interrogated further to characterize novel factors for progression and metastasis in HCC.

In this work, I demonstrate that KLF6 expression is reduced in BL185-M1 and I1, correlating with an increase in cell migration. Expanding on the known role

of KLF6 as a tumor suppressor, I found KLF6 is a suppressor of HCC progression as well. When KLF6 knockdown is performed in the BL185 cell line, both soft agar colony formation and migration are increased. The more transformed phenotypes displayed in response to KLF6 knockdown suggested that a reduction of KLF6 *in vivo* may result in an increase in HCC progression. Indeed, KLF6 is not only commonly decreased in HCC cell lines and tumor samples as compared to normal liver, but is also decreased in HCCs with vascular invasion as compared to non-invasive tumors.

Using the RCAS-TVA model of HCC, mice with single-copy loss of KLF6 displayed phenotypes consistent with the *in vitro* data. $Klf6^{fl/wt}$ mice display increased tumorigenesis, larger metastases, and decreased tumor-free survival compared to $Klf6^{wt/wt}$ mice. Based on these results, a decrease in KLF6 seems to facilitate earlier formation not just of primary HCC tumors, but metastases as well. Notably, only one metastatic focus was found in $Klf6^{wt/wt}$ mice, and it was only visible upon step-sectioning, while many metastases formed in $Klf6^{fl/wt}$ mice were grossly visible.

At this time, the mechanism for the increase in metastasis in $Klf6^{fl/wt}$ mice is not precisely known. In culture, we see an increase in HCC cell migration in response to KLF6 knockdown, so my hypothesis is that HCC cells with reduced KLF6 display increased dissemination *in vivo*. Another possibility is that KLF6 levels do not affect the rate of dissemination from the primary tumor, yet the metastases are more frequent and larger in *Klf6* heterozygous HCC because of an increased capacity

for survival in the bloodstream, or lung colonization. Indeed, the most significant point of disseminated cell attrition occurs after extravasation into new tissue, where most cells remain dormant or die instead of proliferating to form a colony (Luzzi et al. 1998). Lastly, the metastases may be larger because *Klf6* heterozygous tumor cells were able to disseminate earlier compared to *Klf6* wild-type tumor cells. I found that in 4.5 month-old *Klf6* heterozygous mice, primary liver tumors were larger than in wild-type mice. Proliferation rates of these tumors were approximately equal, suggesting that tumor initiation may have occurred earlier in *Klf6* heterozygous animals. This earlier initiation of *Klf6* heterozygous tumors may have allowed for earlier dissemination and initiation of metastasis, which could lead to larger metastatic burden in animals from the survival cohort.

My work is complimentary to studies performed by other groups that have demonstrated KLF6 tumor suppression in HCC. My study corroborates the previous finding that decreased KLF6 levels in hepatocytes results in increased tumor formation (Tarocchi et al. 2011; Vetter et al. 2012). Importantly, the previous approaches used a carcinogen-induced model, while my study validates the finding using a different, oncogene-induced model of HCC.

One major difference between previous studies of KLF6 in HCC and my own, is that my model describes HCC formation in the background of *p53* deletion, while previous HCC studies examined tumor development in a *p53* wild-type background. Inactivation of p53 in combination with *Klf6* heterozygosity may increase or accelerate the effects seen with *Klf6* heterozygosity alone. This difference may

account for why effects on migration or metastasis were not previously detected in studies of KLF6 in HCC. In fact, previous studies have implicated a relationship between p53 and KLF6. KLF6 transcriptional preferences change depending on *p53* status, which may be due to direct interaction between KLF6 and p53 (Rubinstein et al. 2004). Also, regulation of KLF6 levels in response to stress varies depending on the status of *p53* (Gehrau et al. 2011). The role of KLF6 in cancer, particularly HCC, is likely dependent on the status of *p53*.

Together, these results suggest that KLF6 could function as a prognostic marker for HCC patients, where decreased nuclear KLF6 may indicate a poorer prognosis. However, the results from a human HCC tissue microarray for KLF6 demonstrate that while KLF6 was commonly decreased or mislocalized in HCC, this misexpression did not correlate with tumor grade or patient outcomes. This result is in disagreement with previously published results describing a correlation between KLF6 mRNA levels and HCC tumor grade or patient survival (Tarocchi et al. 2011). This discrepancy could be explained by the isoform detection method. While SV1 mRNA can be directly detected by qRT-PCR, our TMA detects all variants, including non-SV1 splice variants that may be contributing to cytoplasmic localization of KLF6. Another possible explanation could reflect the sampling of the tissue microarray. The samples that compose the array are surgically resected samples, which are typically localized and non-metastatic. Thus, the array may be biased against advanced stage disease. My hypothesis is that in a sample set including advanced tumors, KLF6 status may predict invasiveness or survival.

Since the induction of metastasis in our model occurred in combination with *p53* deletion, KLF6 may be a successful prognostic marker when assessed in combination with p53 status. Inactivation of p53 is already known to correlate with poor prognosis in HCC (Woo et al. 2011; Liu et al. 2012), and it would be interesting to investigate if its prognostic accuracy could be improved by including assessment of KLF6 localization. However, based solely on the results of my study, KLF6 localization is not a good candidate for use as a prognostic marker in HCC.

Intriguingly, the major histological appearance of tumors in our study is a vacuolated cytoplasm, which often represents a fatty change in HCC. Previous studies have associated this appearance with less invasive HCC tumors (Lewis et al. 2005). Both $Klf6^{fl/wt}$ and $Klf6^{wt/wt}$ tumors display equal frequencies of this histology, despite $Klf6^{fl/wt}$ tumors generating larger numbers of lung metastases. However in our study, tumors with this histology do form metastases to the lung. Importantly, these vacuolated cells are also present in the lung colonies, indicating these cells are capable of metastasis.

Even though the tumors in *Klf6* heterozygous and wild-type mice are histologically similar, some $Klf6^{fl/wt}$ tumors display increased expression of the poor prognosis markers AFP and IGF2. Increased AFP is detected in the serum of patients for diagnosis of HCC, but it is also increased further in the serum of patients with poor prognosis (Izumi et al. 1992). IGF2 expression is increased in HCCs with poor prognosis as well, and is known to directly participate in HCC metastasis (Iizuka et al. 2004; Chen et al. 2009). While our survival data clearly demonstrate $Klf6^{fl/wt}$ mice

have impaired survival, the increased expression of these poor prognosis markers parallels the expression of these markers in human disease.

Few mechanisms are known which can contribute to the progression of HCC to invasive or metastatic disease. Here, determination of the role of KLF6 as a suppressor of HCC progression is not only important for HCC, but may be important to several other cancers where KLF6 is also misexpressed. Further experimentation regarding the precise activities of KLF6 in HCC progression, such as gene expression profiling and characterization of transcriptional activity, would be an exciting avenue for research.

CHAPTER III

KLF6 suppresses RHO family GTPase activity through transcriptional repression of VAV3 and CDC42EP3

Preface

The RHO family GTPase activity assays shown in Figure 3.2 were performed by Hsiao-Chien Chu and Ya-Wen Chen.

Lihua (Julie) Zhu kindly performed the bioinformatics analysis required for the ChIP-sequencing peak calling and gene expression profiling described throughout this chapter and represented in Figure 3.5, Table 3.1, and Appendix B.

Introduction

In the previous chapter, I characterized KLF6 as a suppressor of HCC cell migration, dissemination and tumor formation. Next, I sought to determine a mechanism by which KLF6 regulates these processes. Here, we find that decreased KLF6 levels impact the activity of RHO family GTPases, particularly CDC42, RAC1, and RHOA, providing a novel function of KLF6 in regulating RHO GTPase activity in HCC.

RHO GTPases belong to the RAS superfamily, and accordingly function as molecular switches that cycle between GDP and GTP-bound states (Hall 1998). The exchange of GDP for GTP is promoted by RHO family guanine nucleotide exchange factors (GEFs) (Rossman et al. 2005). Inversely, hydrolysis of GTP to GDP is facilitated by a group of enzymes called GTPase activating proteins (GAPs) (Bernards 2003). Within Rho family GTPases, proteins are divided into subgroups most homologous to RHOA, most homologous to RAC1 and CDC42, and those that lack GTPase activity (Hall 2012).

When bound to GTP, RHO GTPases are in an active conformation, which renders them capable of signaling to many downstream effectors (Schmidt and Hall 2002). Activation of these effectors impacts a variety of cell processes, including polarity, morphology, motility, gene expression, proliferation, and survival (Hall 2012), as shown in Figure 3.1. Accordingly, increased activity of these GTPases is commonly seen in tumors, particularly those that are invasive and metastatic (Sahai and Marshall 2002; Hall 2012). Interestingly, inhibitory mutations in RAC1 and

CDC42 have been shown to block RAS-mediated transformation in culture (Qiu et al. 1995a; Qiu et al. 1995b; Qiu et al. 1997). Clearly, these proteins play a crucial role in transformation. In addition, RHO GTPases are known to affect the actin cytoskeleton, particularly when inducing cell motility (Hall 1998). CDC42 is required for formation of filopodia, RAC1 for the formation of lamellipodia, and RHOA for cell contractile force (Hall 1998). Together, these proteins allow for directional cell movement, which is the initial step in cancer cell dissemination (Sahai and Marshall 2002; Hall 2012). In this work, we show that decreased KLF6 results in altered GTPase activity in HCC cells. The activity of these GTPases is required for the migration induced by KLF6 knockdown.

KLF6 functions as both a transcriptional activator and repressor. KLF6 is a transcriptional activator of p21 (Narla et al. 2001), TGFβ1 (Kim et al 1998), ATF3 (Huang et al 2008), and E-cadherin (DiFeo et al. 2006). KLF6 is a repressor of targets such as MDM2 (Tarocchi et al. 2011), PTTG1 (Lee et al 2010), and MMP9 (Das et al. 2006). Furthermore, KLF6 has been linked to the regulation of EGFR signaling in lung cancer cells (Sangodkar et al. 2012). Consistent with the common misregulation of KLF6 expression in cancers, these target genes are known to be important for tumor development and progression. Yet, the mechanisms by which KLF6 inactivation contributes to HCC development and progression remain poorly understood.

Figure 3.1. RHO family GTPases are molecular switches which activate downstream effector signaling. RHO GTPases are inactive when bound to GDP. Through interactions with GEFs, GDP is exchanged for GTP, which renders the GTPase active. In this state, the protein can signal to downstream effectors to influence cell processes. GAPs catalyze the hydrolysis of the GTP molecule to a GDP, returning the protein to an inactive state.

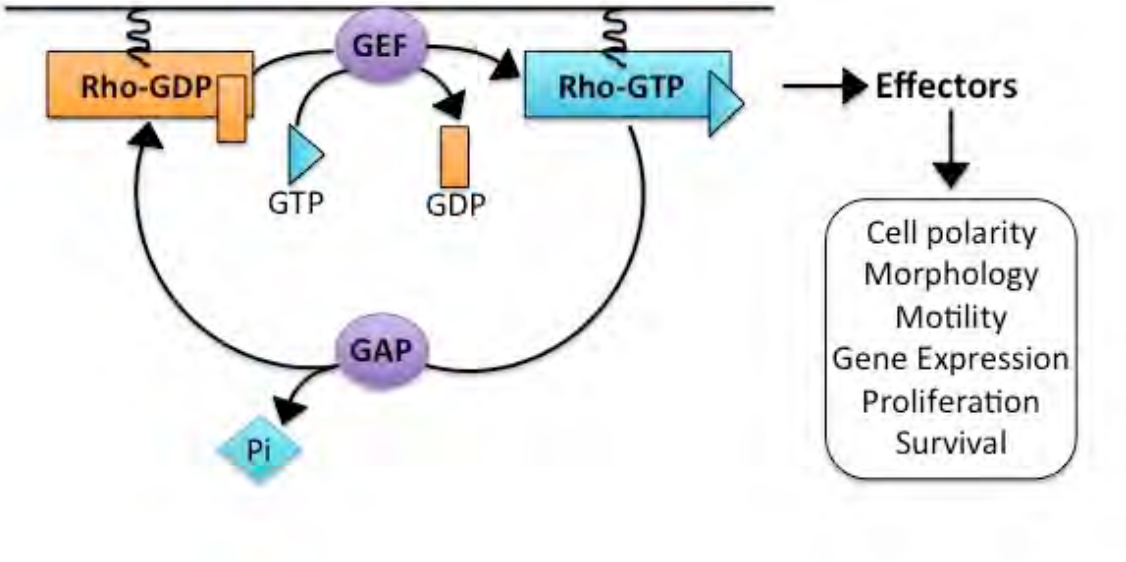

In order to determine the transcriptional targets of KLF6 that could be driving HCC formation and progression, I used two unbiased approaches. KLF6 ChIP-sequencing and gene expression profiling of KLF6 knockdown cells were conducted and combined to create a list of KLF6 transcriptional targets whose expression changed as a result of KLF6 knockdown. Among these are CDC42EP3 and VAV3, known regulators of RHO family GTPase function.

VAV3, a GEF, is responsible for catalyzing the exchange of GDP for GTP on RHO family GTPases, particularly RAC1. In NIH3T3 cells, VAV3 overexpression led to increased focus formation and cell motility (Sachdev et al. 2002). VAV3-mediated focus formation was dependent on RAC1, RHOA, and to a lesser extent, CDC42 activity. However, cell motility was dependent on RAC1 and CDC42, but not RHOA activity (Sachdev et al. 2002). Overexpression of VAV3 has been shown to increase cell migration through RAC1 in lymphoid, fibroblastic, vascular smooth muscle cells, and endothelial cells (Colomba et al. 2008; Brantley-Sieders et al. 2009; Toumaniantz et al. 2010). In addition to driving migration in normal cells, VAV3 has also been implicated in dissemination of cancer cells. VAV3 is overexpressed in 81% of breast cancers, particularly in those that were poorly differentiated (Lee et al. 2008). Similarly, increased VAV3 expression is common in migratory and invasive prostate and gastric cancers. Knockdown of VAV3 in these cancer cell types reduces cell migration and invasion (Lin et al. 2012a; Tan et al. 2013).

CDC42EP3, or CDC42 effector protein 3, is also called BORG2, which stands for Binder of RHO GTPases. CDC423EP3 contains a CDC42/RAC Interactive Binding

(CRIB) domain, through which it binds to TC10 and CDC42 in a GTP-dependent manner (Joberty et al. 1999). Overexpression of CDC42EP3 in NIH3T3 fibroblasts induced pseudopodia formation. Importantly, when the overexpression was performed in combination with a dominant-negative CDC42 or using a CRIB mutant, pseudopodia did not form (Joberty et al. 1999). Similarly, overexpression of CDC42EP family members in keratinocytes resulted in increased stress fiber formation and loss of E-Cadherin from adherens junctions (Hirsch et al. 2001). These data indicate that CDC42EP3 functions downstream of active CDC42 to impact cell shape and motility, though its precise activities are unknown.

I found that HCC cell migration stimulated by KLF6 inactivation is dependent on VAV3 and CDC42EP3 activity. As these proteins are known to mediate the activities of RHO family GTPases, I have found a novel function of KLF6 in regulating RHO GTPase activity in HCC cells.

Results

Knockdown of KLF6 impacts activation of RAC1 and CDC42

I sought to characterize the mechanism of KLF6-mediated suppression of migration and dissemination in HCC. In a previous study on the effects of KLF4 in our HCC cell lines, enhanced migration was dependent on CDC42 activity (Lin et al. 2012b). I hypothesized that KLF6 knockdown was also impacting the activation status of small family GTPases. CDC42, RAC1, and RHOA activity were measured as representatives of their respective GTPase families. Upon KLF6 knockdown in BL185 cells, protein levels of CDC42 and RAC1 were similar between knockdown and control cells. However, levels of RHOA are reduced by almost half in cells with KLF6 knockdown when compared to control cells infected with GFP shRNA (Figure 3.2A). Assessment of the GTP-bound status of these proteins reveals that there is an increase the amount of active CDC42 and RAC1 upon KLF6 knockdown, while there is a slight decrease in RHOA activation (Figure 3.2B).

These data demonstrate that KLF6 is an upstream regulator of RHO family GTPase activity. Based on known roles for RHO GTPases, I hypothesized that the altered activity of these proteins was responsible for the effects seen upon KLF6 knockdown in HCC cells, namely increased migration.

Figure 3.2. KLF6 knockdown results in higher RAC1 and CDC42 activity, and lower RHOA activity.

A. Total protein input of RAC1, CDC42, and RHOA in BL185 cells infected with KLF6 shRNA or GFP shRNA as a control. Graph shown is an average of four experiments.
B. Relative amounts of RAC1, CDC42, and RHOA in the active conformation in KLF6 knockdown and shGFP cells. p-values as determined by t-test are 0.043 for CDC42, 0.062 for RAC1, and 0.020 for RHOA. Graph shown is an average of four experiments.

A

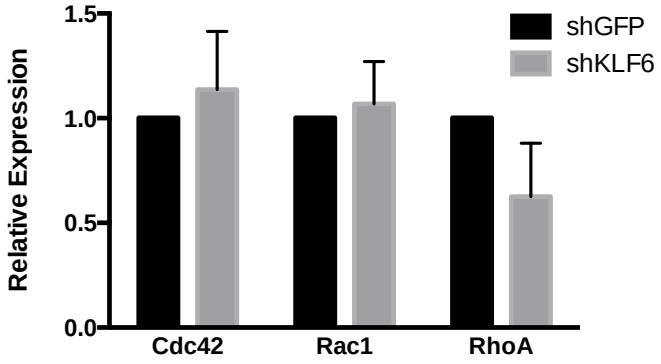

B

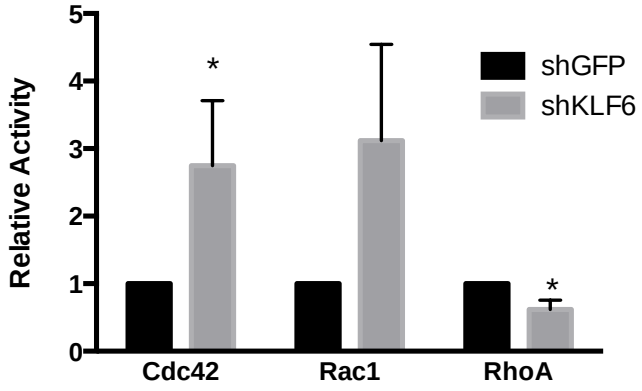

RAC1 activity is required for HCC migration downstream of KLF6 knockdown.

The altered activation of CDC42, RAC1, and RHOA could be responsible for the increase in migration seen in response to KLF6 knockdown. To determine if any of these family members impact HCC cell migration, BL185 cells with KLF6 shRNA were infected with a second shRNA targeting GFP, CDC42, RAC1, or RHOA. These cells were assessed for knockdown of the appropriate protein by Western blot (Figure 3.3A). These cells were subsequently assessed for migration ability. As described previously, addition of KLF6 shRNA to BL185 cells results in increased migration as compared to control cells (Figure 2.8). The additional knockdown of either CDC42 or RHOA did not significantly alter the amount of cell migration. However, RAC1 knockdown in these cells does negatively impact migration (Figure 3.3B). This result suggests that RAC1 is required for KLF6 knockdown-induced migration.

Figure 3.3. Knockdown of RHO GTPases demonstrates that RAC1 is required for mediating migration downstream of KLF6.

A. Western blots of CDC42, RAC1, and RHOA in KLF6 knockdown cells that have been subsequently infected with shRNA targeting GFP, CDC42, RAC1, or RHOA. β-Actin was used as a loading control. shRNA infections were performed twice.
B. Transwell migration assay of BL185 cells infected with shGFP, or shKLF6. Those infected with shKLF6 were also infected with shGFP, shCDC42, shRAC1, or shRHOA and assayed for migration. p-values as determined by t-test are 0.0492 and 0.0008 for the KLF6 and RAC1 knockdown cells, respectively. Shown is the average of four experiments, where the migration activity of shGFP cells is normalized to 100%.

A

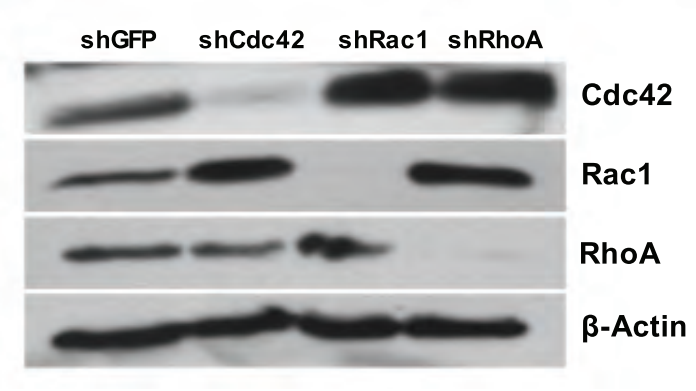

B

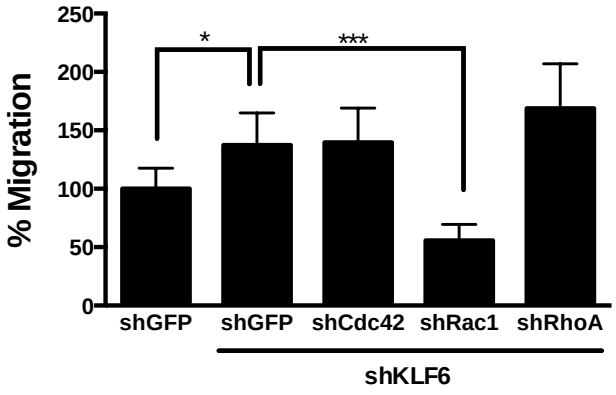

I sought to determine if chemical inhibition of RAC1 would also reduce KLF6 knockdown-induced migration, to validate the effects seen by shRNA infection. To do this, KLF6 knockdown cells were treated with 50uM RAC1 inhibitor, NSC23766. RAC1 inhibition alone in shKLF6, shGFP cells reduced migration by half (Figure 3.4), concordant with the results seen with shRNA-mediated knockdown of RAC1 (Figure 3.3). This result indicates that RAC1 activity is required for the migration that is induced by KLF6 knockdown.

While CDC42 knockdown alone did not have an effect on HCC cell migration, we sought to determine if CDC42 knockdown would cooperate with RAC1 inhibition to reduce HCC cell migration further. We found that in cells with both KLF6 and CDC42 knockdown, RAC1 inhibition resulted in a greater decrease in HCC cell migration (Figure 3.4). While RAC1 inhibition results in more significant effect on HCC cell migration than CDC42 knockdown alone, the combination of RAC1 and CDC42 inhibition has an additive effect to inhibit cell migration, indicating that CDC42 is also contributing to migration regulation in HCC cells.

Figure 3.4. Cells with KLF6 knockdown have impaired migration with RAC inhibition, and this is further decreased with CDC42 knockdown. Cells with KLF6 knockdown were treated with 50uM RAC1 inhibitor NSC23766 upon plating into a transwell migration assay. Cells that migrated through the membrane were counted at 100X magnification. Differences between control and RAC1 inhibitor-treated cells resulted in p-values of 0.028 and 0.0070 in shGFP and shCDC42 cells, respectively. Between RAC1 inhibitor-treated groups, the addition of shCDC42 yields a difference with a p-value of 0.037. Shown is a representative replicate of three experiments.

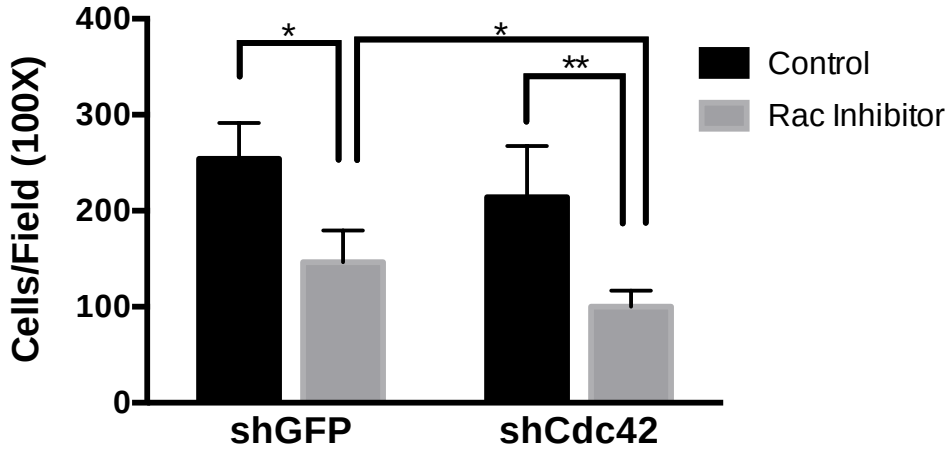

Identification of KLF6 transcriptional targets using a combination of ChIP-sequencing and gene expression profiling

Since KLF6 knockdown results in altered GTP-bound states of CDC42, RAC1, and RHOA, we hypothesized that KLF6 functions as a transcription factor for a regulator of GTPase activity. We therefore sought to determine the transcriptional targets of KLF6 in HCC and which of these targets could be impacting HCC progression and GTPase activity.

To identify transcriptional targets of KLF6 in HCC, we performed two global analyses of KLF6 target genes: gene expression profiling, and Chromatin immunoprecipitation-sequencing (ChIP-seq). Gene expression profiling was performed on cells with KLF6 knockdown compared to cells with a control infection using a GFP-targeting shRNA in order to identify genes whose expression changed upon KLF6 knockdown. ChIP-sequencing determined the binding locations of KLF6 throughout the genome in HCC cells. I hypothesized that establishing the overlap of genes between these datasets would enrich for direct transcriptional KLF6 target genes that may be important for regulating the effects seen in response to KLF6 knockdown.

Gene expression profiling was performed on KLF6 knockdown cells using a whole mouse genome microarray chip. Three sets of infections were performed and analyzed as biological replicates. This analysis resulted in approximately 600 genes with a 1.5-fold or greater fold change and a p-value under 0.01. Target genes from the profiling experiment result in enriched GO terms such as Angiogenesis (p-

value=0.0164), Cell Adhesion (p-value=0.0379), and Cell Proliferation (p-value=$3.54x10^{-4}$). Importantly, KLF6 was detected as being decreased in our microarray analysis, as these cells are infected with KLF6-targeting shRNA. Additional targets of interest include Notch signaling components JAG1 and RBPJ, and VEGFC, all of which are increased upon KLF6 knockdown. The gene expression profiling datasets for the HCC subpopulations and KLF6 knockdown cells share 75 genes in common. Notable genes on the overlap list include *Jag1*, *Dlc1*, *Id2*, and *Twist2*.

To perform ChIP-sequencing, a cDNA encoding a V5 epitope-tagged version of the full-length form of KLF6 was expressed in BL185 cells. Chromatin immunoprecipitation was then performed with a V5-targeting antibody. Two separate libraries were isolated for sequencing, and were compared to input controls. ChIP peaks that were enriched in the KLF6 IP libraries compared to the input libraries were called and annotated to the gene with the nearest transcriptional start site.

The ChIP-seq dataset demonstrated that KLF6 binding is primarily located near transcriptional start sites (TSS) (Figure 3.5A), though binding also occurred at distant sites, both upstream and downstream from a TSS. The location of KLF6 binding did not correlate with whether the target gene had increased or decreased expression in response to KLF6 knockdown. Using a separate ChIP library than was used for deep sequencing, several peaks called in our dataset were validated by ChIP-PCR (Figure 3.5B). The ability to amplify these regions in a separate KLF6 ChIP

indicates that our deep sequencing experiment recognized valid KLF6 binding sites. As a negative control, a gene desert region was amplified, and not detected in our KLF6-IP sample. This indicates that our IP did not enrich for all genomic DNA, and supports the specificity of the identified ChIP peaks.

Figure 3.5. Transcriptional targets of KLF6 were identified by ChIP-sequencing.

A. A density plot shows the number of peaks that fall at noted distances from transcriptional start sites (TSS), which are set to zero.
B. Examples of ChIP peaks identified in the ChIP-seq experiment, validated by ChIP-PCR. The library used for validation was from a separate chromatin isolation and immunoprecipitation experiment than the libraries used for deep sequencing. Here, the IPs performed are listed on the top: V5 IP in cells transfected with either V5-tagged KLF6 or LacZ, or Rabbit IgG IP (Rb IgG). The "No Template" sample served as a PCR negative control. The Input samples are for the V5-tagged KLF6 and LacZ transfected samples, respectively.

A

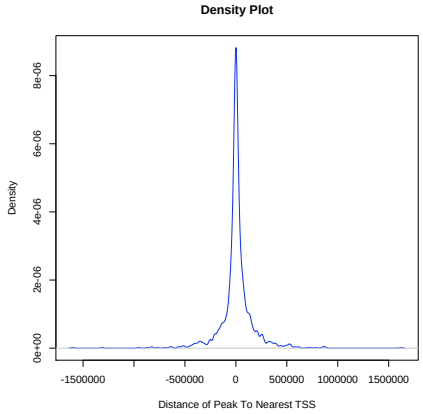

B

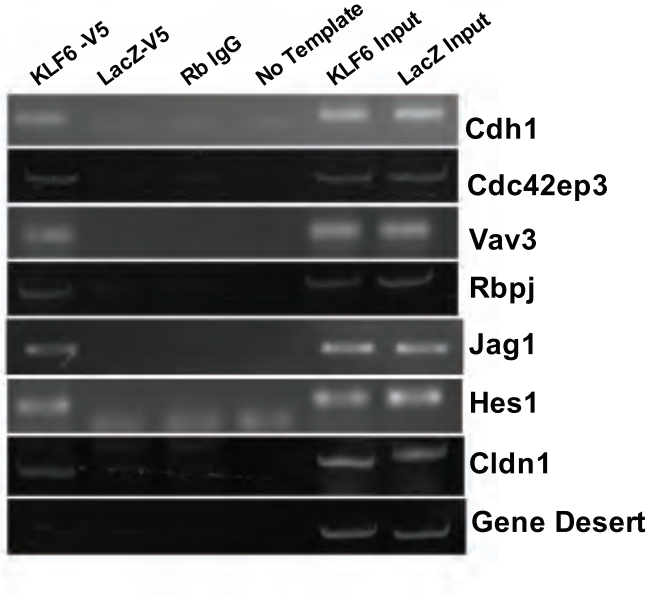

The intersection between the ChIP-seq and profiling experiments was detected to find common targets between both datasets. Performing both of these analyses provided us with a set of genes that are putative direct KLF6 transcriptional targets. Genes whose expression increased or decreased in response to KLF6 knockdown are about equally represented (Table 3.1). Importantly, a published transcriptional target of KLF6, E-Cadherin (CDH1), was detected in our profiling and ChIP-seq studies. The finding that KLF6 directly binds near the E-Cadherin TSS, and that it is decreased in response to KLF6 knockdown serves as an internal validation that our study is detecting genuine KLF6 target genes.

Interestingly, the binding sites for many of the putative KLF6 target genes were not only located proximally to transcriptional start sites, but also within the gene and downstream. This suggests that KLF6 may be regulating gene expression from distant sites, not just from proximal promoters.

Using this list of KLF6 target genes in HCC, we chose to examine which of these expression changes were responsible for the effects that occur downstream of KLF6 knockdown. In particular, given the connection between cell migration and tumor metastasis, we were interested in genes that might mediate KLF6's regulation of HCC cell migration.

Table 3.1. Transcriptional targets of KLF6 as detected by ChIP-sequencing and gene expression profiling of KLF6 knockdown cells.

Gene ID	Chromosome	Peak Start	Peak End	Binding Location	Fold Change (log2)
ENPP2	15	54803450	54803757	upstream	2.072589649
CAR8	4	8145255	8145577	Intron	1.803000883
LILRB4	10	51135250	51135606	upstream	1.530690933
ANK2	3	126876596	126876894	Intron	1.516568098
CLDN1	16	26254098	26254460	downstream	1.334778266
SEMA4A	3	88266618	88266868	upstream	1.113849616
BTBD11	10	84998171	84998559	Intron	1.040213397
GPR116	17	43555305	43555509	Intron	0.981431899
RPS6KA6	X	108530052	108530405	Intron	0.980977038
PTGER4	13	5229494	5230260	upstream	0.973715479
CDC42EP3	17	79694967	79695224	downstream	0.936901219
GFRA1	19	58533225	58533645	upstream	0.932708065
LRCH2	X	144002098	144002543	upstream	0.89374528
HAS2	15	56275124	56275624	downstream	0.874945939
PDZRN3	6	101167668	101167902	Intron	0.864179566
ST3GAL1	15	67284287	67284778	upstream	0.818984451
FLRT2	12	96990500	96990773	Intron	0.767922281
VEGFC	8	55264906	55265248	Intron	0.763817576
SLC4A7	14	15506611	15507331	upstream	0.733950487
VAV3	3	109181903	109182224	Intron	0.714780465
ZFHX4	3	5262877	5263151	Intron	0.707143135
GJA1	10	56115883	56116235	downstream	0.691949349
JAG1	2	136867703	136868005	downstream	0.64423835
MREG	1	72208117	72208319	Intron	0.642418158
PPP3CA	3	136365892	136366269	Intron	0.638465421
OSMR	15	6926550	6926939	upstream	0.634226854
FAM71F1	6	29276886	29277280	Intron/Exon	0.597405284
RBPJ	6	45892447	45892829	downstream	0.585798883
RBPJ	5	54005867	54006240	Intron	0.585798883
MAPRE2	18	23756837	23757250	upstream	-0.586599061
FAM19A5	15	87798350	87798623	downstream	-0.589000873
RHOB	12	8537505	8537813	upstream	-0.591417425
KLF4	4	55550029	55550445	upstream	-0.605786332
EPB4.1L5	1	121619152	121619464	upstream	-0.613637985
CCDC68	18	70026691	70027011	upstream	-0.623281785
DMRT2	19	26016534	26017138	downstream	-0.631332278
ARHGEF16	4	153688134	153688328	upstream	-0.658444838
SPIRE1	18	67785189	67785793	upstream	-0.671742014
HMGCR	13	97486685	97486961	upstream	-0.688581361
B4GALT6	18	20892660	20893030	Intron	-0.703995706
PLOD2	9	92796968	92797282	downstream	-0.732403504
BMP7	2	172665995	172666423	downstream	-0.793876593

EIF4E3	6	99584734	99584987	Intron	-0.799969177
CDH1	8	109126915	109127149	upstream	-0.805352699
IFI204	1	175739583	175739877	upstream	-0.809598051
KLF6	13	5863651	5864920	Intron/Exon	-0.824362282
	13	5860546	5861201	Intron/Exon	-0.824362282
	13	5865504	5866305	Intron/Exon	-0.824362282
	13	5669699	5669426	upstream	-0.824362282
CDKN2D	9	123844234	123844559	downstream	-0.832964627
4631416L12Rik	3	61963003	61963281	upstream	-0.837324781
ITGB6	2	60513302	60513877	Intron	-0.900977262
ANXA10	8	64719939	64720559	upstream	-0.917630286
GGH	4	20110191	20110425	downstream	-0.954220703
MEGF9	4	70179409	70179915	Intron	-0.99976632
RAB28	5	41840319	41840800	downstream	-1.062217563
LYRM2	4	32898800	32899149	downstream	-1.218567249
ALG14	3	121002359	121002723	Intron	-1.660480034

Genome-wide target gene analysis of KLF6 reveals KLF6 is a repressor of CDC42EP3 and VAV3.

Our experiments found that single-copy loss of *Klf6* resulted in HCC progression and dissemination, while KLF6 knockdown resulted in increased *in vitro* migration. This increased migration was dependent on altered GTPase activity, primarily RAC1. We were interested in finding KLF6 transcriptional targets that may impact migration and/or GTPase activity. Two putative KLF6 targets detected in this study were CDC42EP3 and VAV3. CDC42EP3 is known to bind to small GTPases and impact migration in fibroblasts (Joberty et al. 1999; Hirsch et al. 2001). VAV3 is a GEF for several small GTPases, including RAC1, and is known to drive migration in several cell types (Sachdev et al. 2002; Toumaniantz et al. 2010; Lin et al. 2012a; Tan et al. 2013). According to our profiling experiments in KLF6 knockdown cells, CDC42EP3 and VAV3 message levels are increased in cells with KLF6 knockdown (Table 3.1). Indeed, validation of this result by qRT-PCR and Western blot demonstrates that CDC42EP3 and VAV3 expression are increased in KLF6 knockdown cells at both the message level (Figure 3.6A) and the protein level (Figure 3.6B). KLF6 binds directly downstream of CDC42EP3, and within the VAV3 gene, indicating that KLF6 is likely directly repressing transcription of these mRNAs (Figure 3.5B).

Figure 3.6. CDC42EP3 and VAV3 expression is increased in response to KLF6 knockdown.

A. qRT-PCR of CDC42EP3 and VAV3 in cells with KLF6 knockdown. Fold change was calculated by normalizing C_t values of the shKLF6 sample to that of the shGFP sample. β-Actin was used as an endogenous reference for all samples.
B. Western blot of CDC42EP3 and VAV3 in KLF6 knockdown cells as compared to an shGFP control. β-Actin was used as a loading control.

A

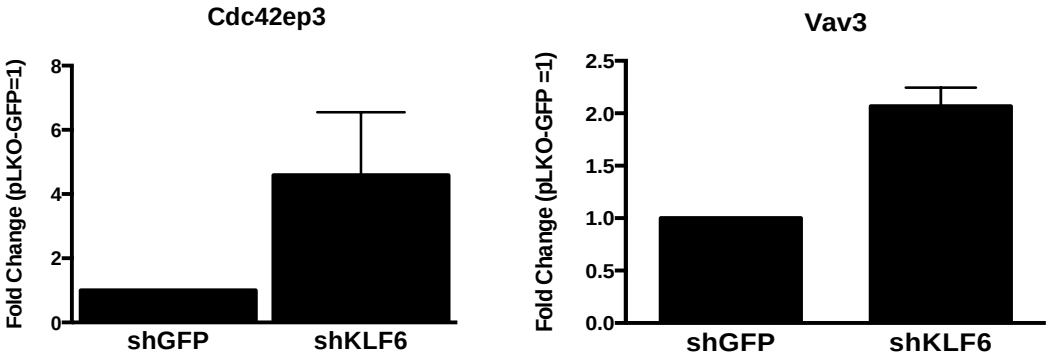

B

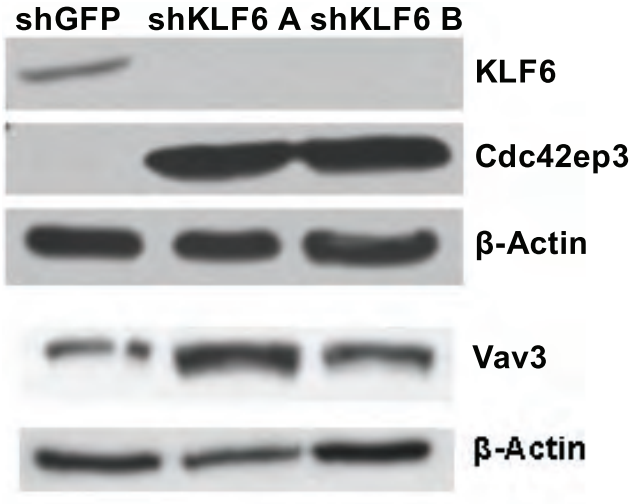

In the previous chapter, human HCC cell lines were shown to have lower levels of KLF6 than an immortalized hepatocyte cell line, Thle2 (Figure 2.6A). In these same cell lines, CDC42EP3 and VAV3 levels are increased as compared to the Thle2 line (Figure 3.7A). In these human HCC cell lines, there is a correlation between reduced KLF6 expression and increased CDC42EP3 and VAV3 expression, which is to be expected based on our finding that KLF6 is a repressor of these genes.

In the tumors generated in our mouse study, VAV3 is increased at the message level in mice with single-copy *Klf6* loss compared to *Klf6* wild-type mice. However, CDC42EP3 expression is not significantly changed at the message level between these tumor groups (Figure 3.7B). It is likely that there are other factors involved in the regulation of these genes that are currently unclear. An additional possibility is that CDC42EP3 levels may only change upon a more complete deletion of *Klf6*.

Figure 3.7. CDC42EP3 and VAV3 are deregulated in HCC.

A. Western blot of CDC42EP3 and VAV3 in human HCC cell lines, with the immortalized hepatocyte cell line Thle2 as a control. β-Actin was used as a loading control.
B. qRT-PCR of CDC42EP3 and VAV3 in HCCs derived from *Klf6*$^{wt/wt}$ or *Klf6*$^{fl/wt}$ mice. C_t values of each gene were averaged and normalized to β-Actin as an endogenous reference. Samples were normalized to the average C_t value from *Klf6*$^{wt/wt}$ tumors in order to calculate fold change.

A

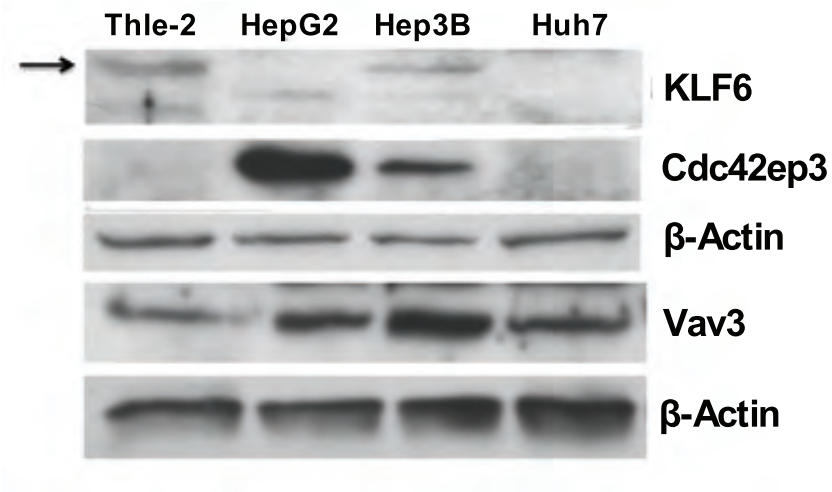

B

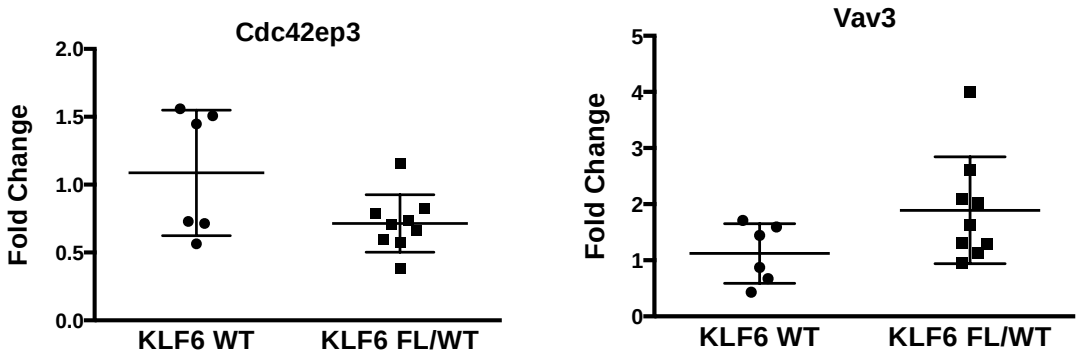

CDC42EP3 and VAV3 impact migration in HCC cells.

Since CDC42EP3 and VAV3 protein levels are increased in response to KLF6 knockdown, we sought to determine if these proteins were responsible for the increase in migration that is seen upon KLF6 knockdown. Two siRNAs targeting CDC42EP3 were transfected into cells infected with either GFP or KLF6-targeting shRNAs, and assayed for CDC42EP3 expression by Western blot (Figure 3.8A).

When a migration assay using these cells was performed, KLF6 knockdown increased the level of migration, as expected. This increase in migration also corresponded to an increase in CDC42EP3 levels (Figure 3.8A). However, when CDC42EP3 and KLF6 knockdown were combined, the level of migration decreased to the same level seen in cells with a control infection (Figure 3.8B). This result indicates that CDC42EP3 is required for KLF6 knockdown-induced migration, and identifies CDC42EP3 as a novel regulator of HCC cell migration.

Figure 3.8. CDC42EP3 is required for migration downstream of KLF6.

A. CDC42EP3 Western blot of cells containing GFP or KLF6-targeting shRNAs with addition of CDC42EP3-targeting siRNAs. β-Actin was used as a loading control. siRNA-mediated knockdown was performed 3 times.
B. Transwell migration assay of cells containing GFP or KLF6-targeting shRNAs with addition of CDC42EP3-targeting siRNAs. Migrating cells were counted at 100X magnification. p-values as calculated by t-test, are 0.0113 for siRNA 1, and 0.0252 for siRNA 2. The p-value between the GFP control and KLF6 knockdown is 0.0184. GFP control cells transfected with CDC42EP3 siRNAs have p-values of 0.1218 and 0.0130, respectively. Shown is a representative experiment of four replicates, with the number of migrating control cells normalized to 100%.

A

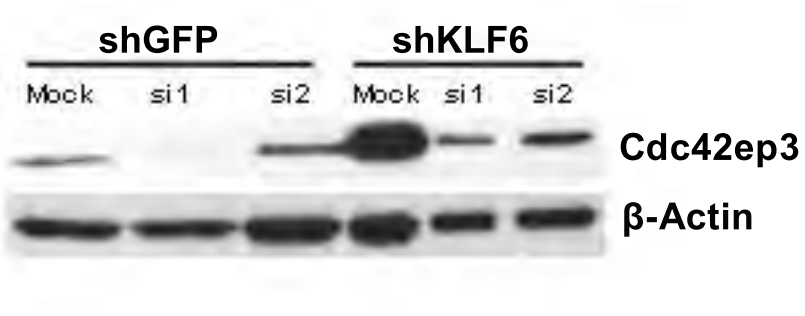

B

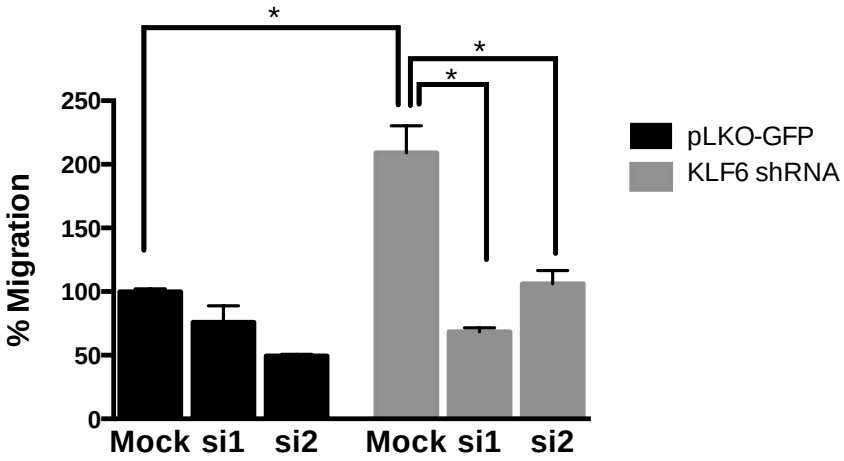

To determine if VAV3 is important for migration downstream of KLF6, VAV3-targeting shRNAs were added to cells with KLF6 knockdown. As a result, VAV3 protein levels are depleted when compared to an empty vector control (Figure 3.9A). Cells with both KLF6 and VAV3 knockdown exhibit reduced levels of migration compared to cells with KLF6 knockdown alone. This suggests that VAV3 activity is required for the migration induced by KLF6 knockdown (Figure 3.9B).

Here, we demonstrate a novel mechanism for increased migration downstream of KLF6 knockdown, detailed in Figure 3.10.

Figure 3.9. VAV3 is required for migration downstream of KLF6.

A. Western blot depicting VAV3 knockdown in KLF6 knockdown cells. β-actin was used as a loading control. pGIPZ represents cells infected with an empty vector control. The arrow denotes VAV3. VAV3 knockdown was performed twice.
B. Transwell migration assay of control cells infected with shGFP and KLF6 knockdown cells that have additionally been infected with an empty vector control, or VAV3-targeting shRNAs. Migrating cells were counted at 100X magnification. p-values, as determined by t-test, are 0.0119 for shVAV3 A, and 0.0204 for shRNA B. Shown is a representative graph of two replicates performed for each set of VAV3 knockdown cell lines.

A

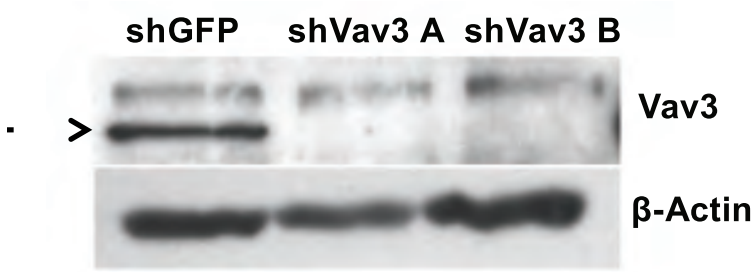

B

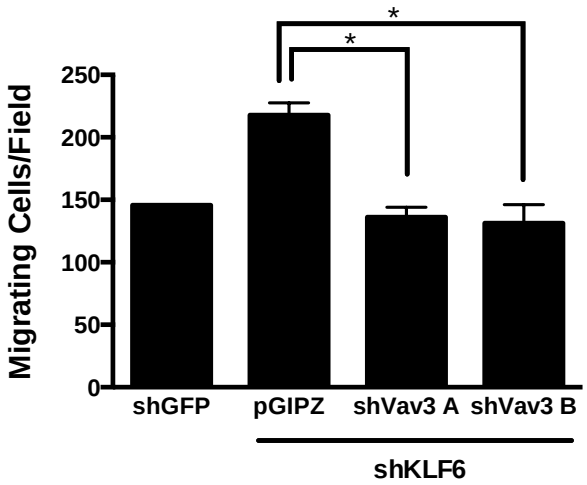

Figure 3.10. A novel KLF6-RHO GTPase axis regulates cell migration and HCC dissemination *in vivo*.

A. KLF6 is a repressor of *Vav3* and *Cdc42ep3* transcription. When KLF6 is expressed, VAV3 and CDC42EP3 levels are low, which results in proportionally higher levels of RAC1 in the GDP-bound, inactive conformation. In this state, cell migration levels are low.
B. When KLF6 expression is decreased, expression of *Vav3* and *Cdc42ep3* is no longer repressed, and their expression level increases. Increased VAV3 expression leads to proportionally higher levels of RAC1-GTP, which is functionally active. RAC1-GTP can then signal to its downstream effectors to influence migration. CDC42EP3 can additionally signal to effectors downstream to increase cell migration.

A

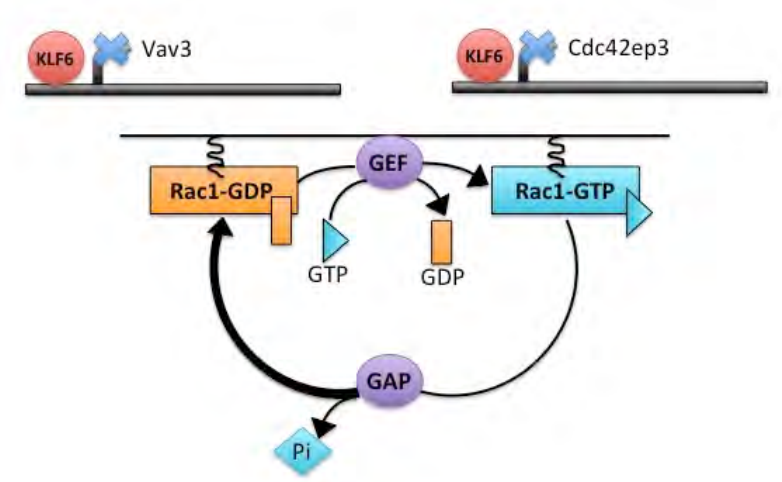

B

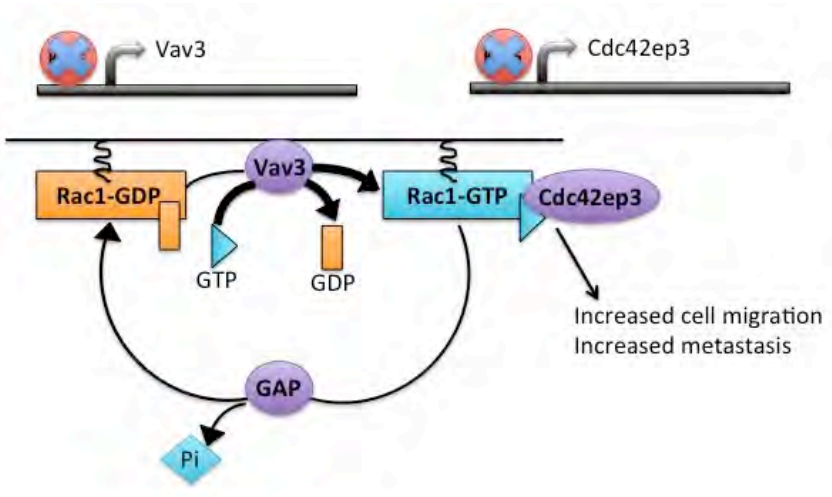

Materials and Methods

Small GTPase Activity Assay

Cell lysates from BL185 cells containing GFP or KLF6-targeting shRNA were incubated with beads conjugated with glutathione S-transferase (GST)-PAK1 or GST-RBD. PAK1 interacts with active CDC42 and RAC1, while RBD interacts with active Rho. Beads were then eluted to obtain the proteins bound to the GST constructs. Bound lysates were analyzed by Western blot for RHOA (Millipore 05-778), CDC42 (Millipore, 07-1466), and RAC1 (Millipore, 05-389). Relative intensity of Western blot bands was calculated using ImageJ.

Cell Culture

Stable knockdown of RAC1, CDC42, and RHOA was established through lentiviral infection of shRNAs from the pLKO.1 library. The shRNAs used to target RAC1, CDC42, and RHOA were TRCN0000310888, TRCN0000331498, and TRCN0000068200, respectively. A plasmid with shRNA targeting GFP was also used as a control. VAV3 knockdown was obtained through lentiviral delivery of shRNA targeting murine VAV3. Plasmids containing shRNAs were obtained from the pGIPZ shRNA library. Clones used for knockdown were V3LMM_425535 and V3LMM_425534. An empty pGIPZ vector was used as a control. Two sets of infections were performed for validation of migration effects. Lentivirus was produced in 293T cells and added to BL185 cells infected with shRNA targeting

KLF6, as described in Chapter II. Since cells were already puromycin resistant at the time of the second infection, there was no drug selection period before cells were assayed for knockdown by Western blot.

The inhibitor to RAC1, NSC23766 (Millipore, 553502) was solubilized in water and filter sterilized. Inhibitor was added to cells as they were plated in a transwell migration chamber to a final concentration of 50uM. The migration assay was then completed as described below.

Knockdown of CDC42EP3 was obtained through transfection of CDC42EP3-targeting siRNA. The siRNAs targeting mouse CDC42EP3 transcript are Mission siRNAs (Sigma) with IDs Mm01_00059270, and Mm01_00059271. Transfections were performed using Lipofectamine 2000 reagent (Life Technologies, 11668027). BL185 cells that were infected with shGFP or shKLF6 were transfected with siRNA at a final concentration of 500pM with 10uL of Lipofectamine 2000 reagent in a 60mm plate. As determined by Western blot, cells transfected with CDC42EP3-targeting siRNA had knockdown at 24 and 48 hours post-transfection, but this knockdown was gone by 72 hours.

In vitro migration analysis

For *in vitro* migration assays, $2.5x10^4$ cells were plated on a migration insert (BD Biosciences 354578) in serum-free DMEM. Growth medium was plated into the bottom of the migration chamber. After 20 hours, the cells were fixed with methanol, and non-migrating cells were removed from the membrane with a cotton

swab. Remaining cells, which had passed through the membrane, were stained with Giemsa. Cells were counted in 5 fields per membrane at 100X magnification.

Error bars used for graphical representation of these experiments represent the standard deviation of the dataset. Student's t-tests were used to calculate p-values.

ChIP-Sequencing

Cells for ChIP were transfected with pcDNA3.1 construct containing KLF6-V5 or LacZ-V5. Cells were fixed in 1% formaldehyde for 10 minutes at room temperature. This crosslinking reaction was inhibited with the addition of glycine. Nuclei were isolated from crosslinked cells per the provided protocol in the SimpleChIP Enzymatic Chromatin IP Kit (Cell Signaling, 9002). Chromatin within intact nuclei was digested with 2.5uL of micrococcal nuclease for 20 minutes at 37°C. Nuclei were lysed by sonication for three 20-second pulses. These chromatin lysates were clarified by centrifugation at 10,000rpm for 10 minutes at 4°C.

35ug of cross-linked chromatin was pre-cleared in protein G beads for one hour at 4°C. After pre-clearing, either 10uL V5 antibody (Abcam, 9116) or Rabbit IgG were added to the pre-cleared chromatin. Antibody-chromatin mixtures were placed on a shaker at 4°C overnight. The next morning, 30uL of protein G beads, premixed with salmon sperm DNA, were added to each chromatin sample. These were returned to the shaker at 4°C for 5 hours.

Beads were then washed in salt buffers included in the SimpleChIP Enzymatic Chromatin IP Kit. Samples were washed four times, three in low-salt buffer, and the last wash in a high-salt buffer. Beads were eluted at 65°C for 30 minutes. Eluent from the beads was digested with proteinase K for 2 hours at 65°C to remove residual protein. DNA remaining in the sample was purified by column.

Following isolation of immunoprecipitated DNA, samples were prepared for deep sequencing on the Illumina platform. Beginning with 50ng of DNA for both input and KLF6 immunoprecipitation samples, fragments were blunt-ended (Epicentre, ER0720). Blunt fragments were cleaned in a column, and A-tails were added using Exo-Minus Klenow Polymerase (Epicentre, KL11250). Illumina Genomic DNA Adapters could then be added to our library DNA. These adapters were ligated to the A-tailed DNA using the Fast-Link Kit (Epicentre, LK11025). These fragments were then isolated and column cleaned using a MinElute Column Kit (QIAGEN, 28004).

Following the ligation of the adapter sequences to the library DNA, libraries were amplified by PCR twice using Solexa Genomic Illumina Primers 1.1 and 1.2, with Stratagene PfuUltra II Fusion HS DNA Polymerase (600670) as described in the manufacturer's protocol. The PCR was performed for 18 cycles. After the first PCR, the PCR product was run on a 2% agarose gel, which was subsequently cut to extract the smear of DNA products from 150-500 basepairs. Gel extraction was performed with the QIAquick Gel Extraction Kit (QIAGEN, 28706), and DNA was eluted into a volume of 30uL of EB buffer for each sample. This size-selected PCR

product was used as the template for the second round of PCR, which was repeated using the same conditions as the first.

Libraries were sequenced on the Illumina platform using a single-end, long 76-basepair read. Sequence reads were mapped to the mm9 genome using the Illumina Genome Analyzer Pipeline. Reads that were uniquely mapped with two or fewer mismatches were retained for peak detection. Peak detection was conducted using the MACS 1.3.6 algorithm. Enriched peaks in the KLF6 IP sample were determined in relation to the total input sample. Peak calling for the ChIP-sequencing experiment was kindly performed by Lihua (Julie) Zhu (UMMS).

ChIP-sequencing raw files and annotated peaks are accessible in the GEOArchive under accession GSE54763.

Gene Expression Profiling

Three sets of KLF6 shRNA and shGFP infections were performed in BL185 cells. RNA was isolated from the three knockdown lines and respective controls using TRIzol reagent (Life Technologies, 10296010). The RNA samples were labeled using the 3' IVT Express Kit (Affymetrix, 901228). Gene Expression profiling was conducted using GeneChip Mouse Genome 430 2.0 arrays (Affymetrix, 900495) at the Memorial Sloan Kettering Cancer Center.

To summarize the probe data and to normalize, the RMA method in the Affymetrix package (Bioconductor) was used. Genes of interest for follow-up study were those whose expression was significantly different in all of the KLF6

knockdown lines when compared to the infection controls. Significance was defined as having an adjusted p-value less than 0.01 with a fold change greater than 1.5. Analysis of the gene expression profiling was performed by Lihua (Julie) Zhu (UMMS).

The raw data files in addition to normalized expression data has been deposited in GEOArchive under the accession number GSE54762.

Gene Expression by qRT-PCR

RNA from cell lines was isolated using TRIzol, and converted to cDNA using First-Strand cDNA synthesis kit (Life Technologies, 18080-051). qRT-PCR was performed using SYBR Green (VWR, 95072) in an ABI 7300 machine using 50ng cDNA per reaction. Amplification of murine VAV3 was performed with forward primer ATT CCA AAG GTA TCG CAG CA, and reverse primer GAA GGA GAT CAA CCT GAG GC. CDC42EP3 was amplified with forward primer CCT TCC ACA GCT CAG AGA AA and reverse primer GCA CCA GCG AGG ACT GTT. β-Actin message was amplified as an endogenous reference using forward primer TCC TCC TGA GCG CAA GTA CTC T and reverse primer CGG ACT CAT CGT ACT CCT GCT T.

C_t values for each sample were averaged and normalized to β-Actin C_t values as an endogenous reference. In each case the Comparative C_t Method was used to calculate fold change, where fold change = $2^{-\Delta\Delta CT}$.

Western blotting

Protein lysates were generated in RIPA buffer and concentrations were determined and normalized by Bradford Assay for loading. 20ug of lysate were used per lane. 10% acrylamide gels were used for SDS-PAGE, and subsequently transferred onto PVDF. Membranes were blocked for one hour at room temperature in 7.5% nonfat dry milk in TBS. Antibodies for Western blotting were used as described in Table 3.2.

Table 3.2. Antibodies and conditions used for Western blotting.

Target	Manufacturer	ID number	Dilution	Diluent	Condition
KLF6	Santa Cruz	sc-7158	1:1000	5% milk in TBS	Overnight at 4°C
RHOA	Santa Cruz	sc-418	1:1000	5% milk in TBS	Overnight at 4°C
RAC1	Upstate	05-389	1:2000	5% milk in TBS	Overnight at 4°C
CDC42	Santa Cruz	sc-8401	1:1000	5% milk in TBS	Overnight at 4°C
VAV3	Bioss	bs-4286R	1:2000	5% milk in TBS	Overnight at 4°C
CDC42EP3	Bethyl	A301-723	1:5000	5% milk in TBS	Overnight at 4°C
β-Actin	Santa Cruz	sc-1615-R	1:2000	5% milk in TBS	1 hour at 21°C

Discussion

We sought to determine the mechanism by which KLF6 knockdown triggered an increase in HCC cell migration, as this mechanism may be crucial to understanding KLF6's impact on tumor formation and metastasis. An investigation into the activation status of RHO family GTPases found that RAC1 and CDC42 activity were increased upon KLF6 knockdown, while RHOA activity was decreased.

Our experiments demonstrate that RAC1 activity is required for the increase in migration seen upon KLF6 knockdown. While RAC1 seems to be the primary mediator of this effect, a combination of CDC42 knockdown and RAC1 inhibitor treatment resulted in greater migration impairment than treating cells with RAC1 inhibitor alone. This result suggests that CDC42 and RAC1 may be cooperating to impact HCC migration downstream of KLF6.

Since KLF6 is a transcription factor, we hypothesized that a transcriptional target of KLF6 was responsible for the altered GTPase activity seen upon KLF6 knockdown. To investigate such targets, we conducted gene expression profiling using KLF6 knockdown cells in order to find gene expression changes that occur upon KLF6 loss. These changes may mimic those that occur upon decreased KLF6 *in vivo*. Since gene expression profiling would likely provide a number of targets that were not due to direct impact of KLF6 knockdown, we also performed ChIP-sequencing using full-length KLF6. Together, these strategies generated a list of genes whose expression is affected by decreased KLF6, yet also have direct KLF6

binding in proximity of the gene's TSS. Our hypothesis was that this strategy would enrich for genes important to mediating the *in vivo* effects of decreased KLF6 activity.

Our strategies revealed that KLF6 was bound to a number of locations on the genome, including the published KLF6 target, E-Cadherin (DiFeo et al. 2006). The effects we see *in vitro* and *in vivo* in response to decreased KLF6 levels are due, at least in part, to the misexpression of these target genes. Two such genes are *Cdc42ep3* and *Vav3*. Expression of these genes is increased in response to KLF6 knockdown, suggesting that KLF6 normally acts to repress their expression. Indeed, KLF6 was found to bind to the genomic loci of *Cdc42ep3* and *Vav3*, indicating their repression by KLF6 is direct. While increased expression of VAV3 has previously been shown to drive cell migration and metastasis (Sachdev et al. 2002; Lin et al. 2012a; Tan et al. 2013), our study is the first to describe its increased activity in HCC. CDC42EP3 has also been shown to drive cell migration, yet it has never been associated with cancer cell migration. Here, we show that these two proteins are required for mediating migration downstream of KLF6 knockdown, as diagrammed in Figure 3.10.

What role CDC42EP3 is playing in the cell is still unclear, but based on its known role in binding to active GTPases, it may be mediating the effects of increased RAC1 or CDC42 activity. The increase in VAV3 expression in response to KLF6 knockdown is a likely contributor to the increase in GTP-bound RAC1 and CDC42 that occurs upon KLF6 knockdown. Thus, KLF6 suppresses migration via the

repression of a RHO GTPase signaling axis, which is mediated in part through a RHO GEF, VAV3, and a GTPase effector protein, CDC42EP3.

While our experiments demonstrate that RAC1 is the primary mediator of KLF6 knockdown-induced migration, we have not ruled out the potential importance of decreased RHOA activity in these cells. Aside from decreased RHOA activity, RHOA is also decreased at the protein level upon KLF6 knockdown. While RHOA was not detected in my transcriptional profiling analyses, these experiments did determine that KLF6 is a direct transcriptional repressor of RHOB. While knockdown of RHOA or RHOB did not affect HCC cell migration, this does not rule out their importance downstream of KLF6 in HCC.

Impaired KLF6 activity is important to cancers other than HCC, including breast and prostate (Narla et al. 2001; Ito et al. 2004; Hatami et al. 2013). In these cancers, KLF6 has been shown to impact a host of cell processes, including proliferation, apoptosis, survival, and migration (DiFeo et al. 2009). Here, we show that decreased KLF6 results in an increase of active RAC1 and CDC42, which impact many cellular processes themselves (Sahai and Marshall 2002; Hall 2012). Potentially, the effects seen upon KLF6 knockdown in other cancers are also mediated through increased activity of RHO family GTPases. Investigating this possibility may be an interesting avenue for research, and could provide more insights into the mechanism of KLF6-mediated tumor and metastasis suppression. Additionally, such work could reveal new opportunities for drug targeting downstream of KLF6 inactivation.

Our studies implicate RAC1 as a primary driver of HCC cell migration downstream of KLF6 knockdown. Excitingly, there are several chemical inhibitors of RAC1 that impair its activity. Inhibition of RAC1 may be a potential therapeutic strategy for tumors with low KLF6 activity, as this may inhibit invasion and metastasis in these tumors. In fact, several early studies of RAC1 inhibition in cell lines and mouse models suggest a potential benefit. RAC1 inhibition prevented growth of prostate cancer xenografts (Zins et al. 2013), reduced breast cancer cell growth and metastasis (Rosenblatt et al. 2011; Bid et al. 2013), reduced proliferation and migration of non-small cell lung cancer (Akunuru et al. 2011; Gastonguay et al. 2012), and suppressed motility in HCC cells (Liu et al. 2008). Inhibition of RAC1 activity may have clinical benefit in a variety of human cancers and further study is certainly warranted.

Few mechanisms are known which contribute to the invasive progression of HCC. Here, we find that decreased KLF6 expression leads to increased RAC1 activity, which is required for increased HCC cell migration. In addition to the potential importance of this signaling activity to HCC, this mechanism may also occur in other human cancers that see frequent misregulation of KLF6. Inhibition of RHO family GTPases, particularly RAC1, may be a potential therapeutic strategy for invasive cancers with low KLF6 levels.

CHAPTER IV

The $p53^{R172H}$ mutant does not enhance hepatocellular carcinoma development and progression.

Preface

David Klimstra analyzed the histology of murine tumors isolated during this study. His photographs are shown in Figure 4.3.

Introduction

Hepatocellular carcinoma is a common and highly deadly malignancy worldwide. At present, there are no curative options for patients with unresectable disease, and the current treatment, Sorafenib, extends survival by only 2.8 months (Llovet et al. 2008). Therefore, understanding the molecular mechanisms underlying HCC dissemination is of great importance for improving the prognosis for HCC patients.

One mechanism known to be important for HCC progression is inactivation of the tumor suppressor TP53, which often occurs through missense point mutation (Hollstein et al. 1991). In HCC, *TP53* gene mutation is observed in over 30% of cases (Liu et al. 2012). Loss of heterozygosity in this region occurs in 25-60% of cases, depending on the study (Kusano et al. 1999; Wong et al. 1999b; Buendia 2000). Interestingly, *TP53* mutations are absent in hepatic adenomas, while the frequency of *TP53* mutation increases with tumor grade and differentiation status, occurring in 54% of poorly differentiated HCCs (Oda et al. 1992; Buendia 2000). This suggests that mutations in the *TP53* gene occur later in HCC development, and potentially are selected for over time.

Indeed, *TP53* mutations are associated with a higher rate of relapse and decreased overall survival in HCC (Woo et al. 2011; Liu et al. 2012). Furthermore, in a non-metastatic HCC mouse model, deletion of *Trp53* resulted in tumors with more aggressive histology and increased metastasis to the lungs (Lewis et al. 2005).

Together, these findings suggest a specific role for p53 inactivation in promoting HCC progression and metastasis.

In addition to inactivating wild-type p53, some *p53* missense point mutations have been found to exert both dominant negative and gain-of-function effects (Sigal and Rotter 2000). One particular mutation, $p53^{R172H}$, which corresponds to human *p53* hotspot R175H, has been shown to inhibit wild-type p53 function (Kern et al. 1992; Unger et al. 1992; de Vries et al. 2002), thus functioning as a dominant negative. However, in the absence of wild-type p53, mutant p53 can contribute oncogenic effects. Mice with a single-copy of a knock-in *LSL-*$p53^{R172H}$ allele were compared to *p53*-null mice. These mice had comparable survival rates, but the types of tumors that formed differed. *Trp53* mutant mice had an increase in the number of carcinomas, which formed throughout the mouse (Olive et al. 2004). Interestingly, many of these carcinomas were invasive or metastatic, which rarely occurred in *p53*-null animals. This change in tumor formation and increase in metastasis suggested a gain-of-function role for $p53^{R172H}$ in cancer (Olive et al. 2004).

Subsequently, p53 gain-of-function activity was also characterized in tissue-specific contexts. In both the pancreas and skin, $p53^{R172H}$ expression was found to cooperate with oncogenic KRAS to increase tumor formation and metastasis as compared to oncogenic KRAS and *p53* nullizygosity (Caulin et al. 2007; Morton et al. 2010). $p53^{R172H}$ and oncogenic KRAS were also found to cooperate in the oral epithelium. In this tissue, the presence of the p53 mutant increased tumor formation and progression to carcinoma, while the *p53*-null tumors remained benign (Acin et

al. 2011). Lastly, mice with $p53^{R172H}$ were found have an increased rate of tumor formation in models of breast and colon cancer as compared to *p53*-null mice (Cooks et al. 2013; Lu et al. 2013). In these tissue contexts, $p53^{R172H}$ contributed to both increased tumor formation and increased metastasis *in vivo*.

Yet, p53 mutants do not display gain-of-function properties in every context. In a UV-induced skin cancer mouse model, $p53^{R270H}$ exerted dominant negative effects against wild-type p53 that resulted in increased tumor formation and decreased survival as compared to *p53* heterozygous mice. But when mice with a single copy of $p53^{R270H}$ were compared to $p53^{fl/fl}$ mice, there was no change in tumor formation or survival, indicating that the p53 mutant did not exert gain-of-function effects in this skin cancer model (Wijnhoven et al. 2007).

The role of p53 gain-of-function activity in liver cancer is unclear, as previous studies have only been performed using ectopic expression of mutants in HCC cell lines. One study found that overexpression of several p53 mutants in HCC cell lines decreased apoptosis in response to stress (Schilling et al. 2010). Another study, using the aflatoxin-induced $p53^{R249S}$ mutant, found that ectopic expression did not confer any growth benefit to an HCC cell line. However, in an HCC cell line with endogenous expression of $p53^{R249S}$, p53 knockdown decreased proliferation and increased cell death (Gouas et al. 2010). These data demonstrate that phenotypes of cell lines may vary depending on endogenous or exogenous expression of these mutants. Additionally, cell context and the type of p53 mutant may also be important factors dictating p53 gain-of-function activity in HCC.

One mechanism for $p53^{R172H}$ gain-of-function activity is through inhibition of the p53-related transcription factors p63 and p73, (Lang et al. 2004; Li and Prives 2007). The *p63* and *p73* genes each encode multiple protein products. Expression of *p63* and *p73* can occur from two distinct promoters, resulting in TA or ΔN isoforms. Additionally, several splice sites result in multiple protein products from each of the TA and ΔN promoters (Benard et al. 2003). Importantly, the transcriptional targets of p63 and p73 vary depending on which particular isoform and splice variant is expressed. In general, TA variants are thought to transcribe similar targets as p53, while ΔN variants can behave as dominant negatives to other p53 family members. However, ΔN isoforms also have additional transcriptional targets unique from the TA isoforms (Murray-Zmijewski et al. 2006). Based on these roles, TA isoforms are characterized as tumor suppressors, while ΔN isoforms have oncogenic behavior.

Mice with heterozygous deletion of *p63* or *p73* develop spontaneous tumors with accompanying loss of heterozygosity, indicating that these transcription factors act as tumor suppressors (Flores et al. 2005). Moreover, inhibition of p63 or p73 exacerbates tumor development and progression in p53-deficient animals, suggesting that they have non-overlapping tumor suppressor functions with p53 (Flores et al. 2005; Oren and Rotter 2010).

However, unlike the pattern of p53 inactivation seen in HCC patient specimens, *p63* and *p73* mutations and allelic loss have not been detected (Pan et al. 2002; Petitjean et al. 2005). Interestingly, p63 and p73 expression from the TA promoter is increased in HCCs as compared to normal liver (Stiewe et al. 2004;

Petitjean et al. 2005). In the case of p73, higher expression levels are correlated with p53 inactivation (Herath et al. 2000; Sayan et al. 2001) and poorer prognosis (Tannapfel et al. 1999). Yet, mice with single-copy loss of both *p53* and *p73* develop spontaneous HCC, and many of these tumors lose the remaining *p73* allele (Flores et al. 2005).

Given the absence of homozygous *TP53* deletion in human HCCs, and because $p53^{R172H}$ has been shown to contribute to metastasis in other mouse models, I sought to determine whether $p53^{R172H}$ enhances HCC progression relative to *p53* nullizygosity. To approach this question, I utilized the RCAS-TVA mouse model for HCC (Lewis et al. 2005; Chen et al. 2007) in conjunction with a conditional $p53^{R172H}$ knock-in allele (Olive et al. 2004).

Results

$p53^{R172H}$ does not promote HCC development, progression, and metastasis *in vivo*.

To determine if $p53^{R172H}$ exhibits gain-of-function properties in HCC, I generated Albumin-*tv-a, Trp53*$^{LSL\text{-}R172H/flox}$, Albumin-*cre* mice and Albumin-*tv-a, Trp53*$^{flox/flox}$, Albumin-*cre* littermates (Figure 4.1). The *Trp53*$^{LSL\text{-}R172H}$ allele expresses $p53^{R172H}$ under the endogenous *p53* promoter upon *Cre* expression, when its stop cassette is excised (Olive et al. 2004). The *Trp53*^{flox} allele results in excision of exons 2-10 at the *p53* locus upon *Cre* expression (Jonkers et al. 2001). These mice were injected with DF1 cells producing RCAS-PyMT to induce HCC, as done previously (Lewis et al. 2005; Chen et al. 2007). In this model, loss of p53 function is required for metastasis, which can be enhanced through concomitant deletion of *Ink4a/Arf* (Lewis et al. 2005; Chen et al. 2007). Therefore, if $p53^{R172H}$ has gain-of-function properties, these should be observed in this model. I found that the presence of the mutated *p53* allele did not impact tumor-free survival (Figure 4.2A). In addition, mice with the *p53*^{R172H} mutant did not have significantly different rates of metastasis as compared to *p53*-deleted littermates, with 17% of *p53*-deleted, and 25% of *p53*^{R172H} mice displaying metastasis to the lungs (Figure 4.2B). One mouse with metastasis to the ovary was the only instance of metastasis detected in an organ other than the lung.

In addition to these characteristics, I assessed whether tumor burden or tumor histology differed between tumors induced in *p53* mutant and nullizygous

mice. I found that the total tumor burden for each mouse in the survival study was not statistically different between the two groups (Figure 4.2C). Moreover, the tumors induced in the two groups appeared to be histologically similar. Evaluation of H&E stained tissue sections demonstrated that regions of unique HCC histology appear at similar frequencies in both groups (Figure 4.3). The most common appearance of HCCs in the PyMT-driven model is the presence of very large cells with vacuolated cytoplasm, often indicative of the accumulation of fat, represented in the middle panel. Another histology frequently seen includes dense regions of less-differentiated cells, as shown in the bottom panel. The cells in these areas have abnormal nuclei, and have lost the normal trabecular architecture typical of normal liver. Both of these tumor morphologies also commonly occur in human HCC.

To determine if proliferation rates were different between tumor groups, Ki67, a marker of proliferation, was evaluated in mouse tissue sections. Quantification of Ki67 staining revealed that the proliferation rates are similar between tumors with or without the p53 mutant (Figure 4.4). Indeed, variation between tumors within the same group was greater than variation between the two groups.

Figure 4.1. Schematic diagram of p53^{R172H} mouse study approach.

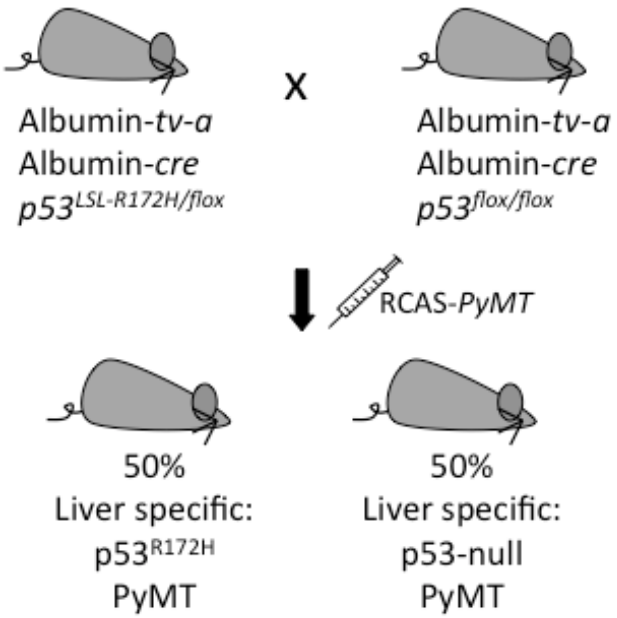

Figure 4.2. The *p53^{R172H}* mutation does not decrease survival or enhance metastasis in an HCC mouse model as compared to *p53* deletion.

A. Kaplan-Meier curve displaying tumor free survival of *p53$^{fl/fl}$* and *p53$^{R172H/fl}$* littermates. Mice were assessed over a period of 9 months and sacrificed when illness was apparent. Only mice whose death was perceived to be due to HCC were included, otherwise the mouse was censored. Censored animals are represented in the figure as tick-marks on the day of death. Survival statistics were calculated by the log-rank test.
B. Number of mice with gross metastasis in the survival cohort, as measured over a period of 9 months.
C. Total tumor burden in survival cohort mice. Individual tumor volume was calculated using the formula for an ellipsoid. All of the tumor volumes for a given mouse were summed to arrive at the tumor burden per animal.

A

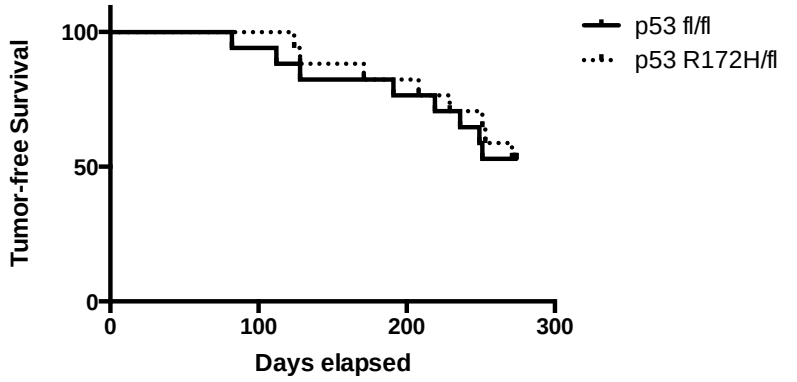

B

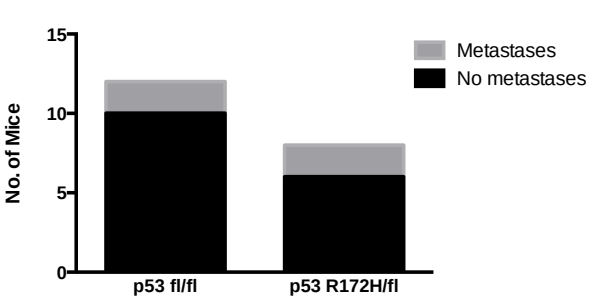

C

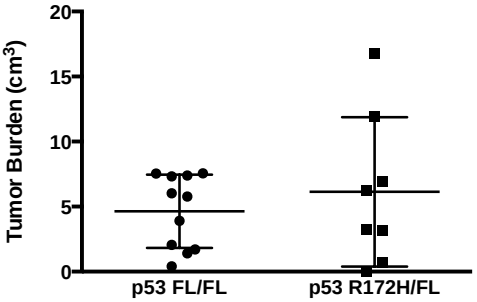

Figure 4.3. H&E staining depicting common architectural morphologies in *p53*$^{R172H/fl}$ and *p53*$^{fl/fl}$ HCCs.

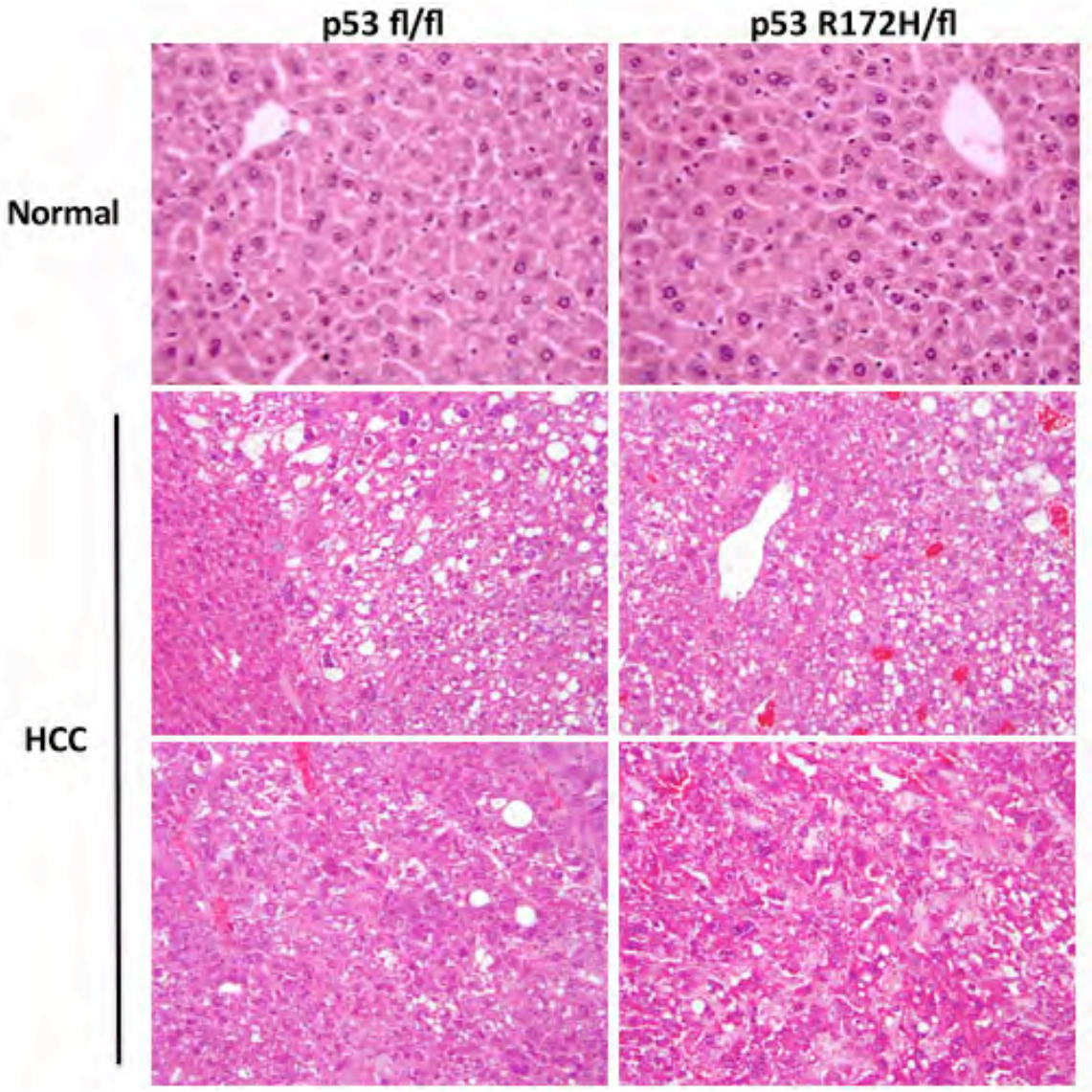

Figure 4.4. *p53*$^{R172H/fl}$ and *p53*$^{fl/fl}$ HCCs do not have different rates of proliferation.

A. Representative images of Ki67 IHC in normal mouse liver and HCC from *p53*$^{fl/fl}$ and *p53*$^{R172H/fl}$ mice from the survival cohort. Arrows in the images indicate examples of positive nuclei.
B. Cells with Ki67-positive and negative nuclei were counted to obtain the percentage of cells within an HCC section that were Ki67 positive. Five fields in each tumor section were counted to obtain an average. In each cluster of bars, the first bar is the quantification of Ki67 staining in a liver without the presence of gross HCC.

A

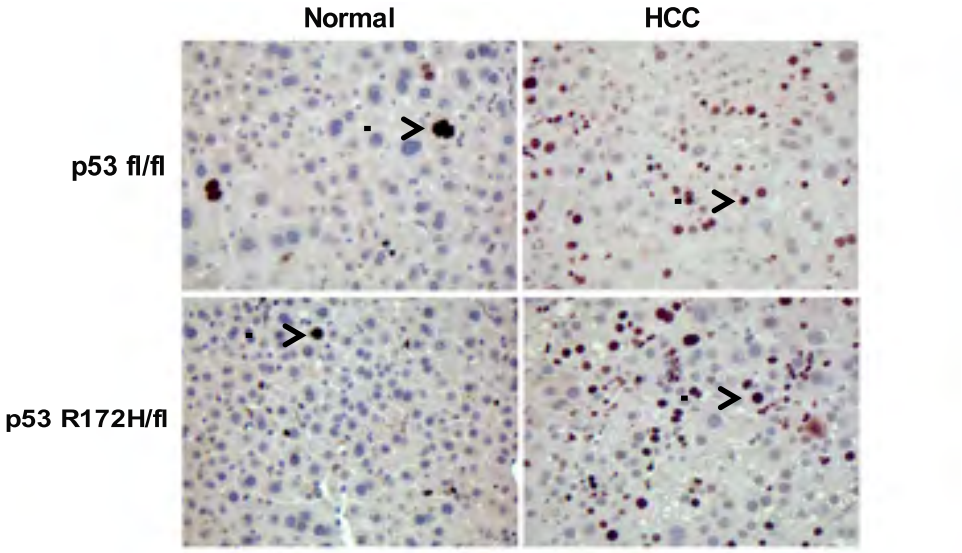

B

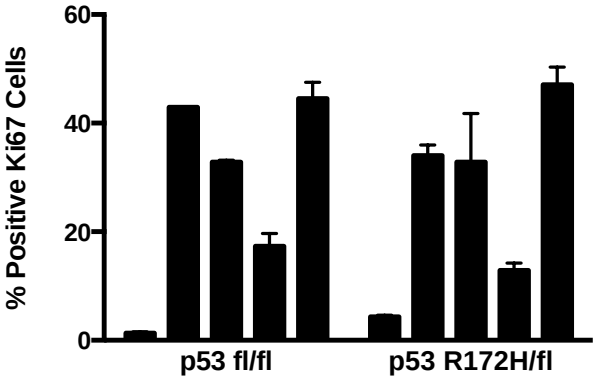

p53^{R172H} does not accelerate tumor onset or metastasis *in vivo*.

Since p53 gain-of-function properties were not seen in a cohort of animals assessed over nine months, I sought to determine if the p53 mutant could exact gain-of-function effects at different steps in tumorigenesis. For example, tumor initiation or time to metastasis may differ between groups of mice. To ascertain if p53^{R172H} accelerated tumor formation or metastatic progression in this model, a separate cohort of animals was sacrificed at timepoints of three, six, or eight months, unless the mouse displayed signs of high tumor burden and had to be euthanized in accordance with the approved animal protocol.

Because of illness, several mice were sacrificed prior to their designated timepoints. Due to the variation in age, mice are represented in groups of 12-16, 17-24, and 25-35 weeks (Table 4.1). At each of these timepoints, the incidence of HCC is similar between *p53^{R172H}* and *p53*-null groups. Additionally, the proportion of mice with primary tumors that progressed to metastatic disease is almost equal at each range of time assessed. These results indicate that there is no acceleration of HCC formation or progression when p53^{R172H} is expressed in the liver.

When all of these ranges of time are combined, the proportion of mice that developed primary HCC and progressed to metastasis is almost identical between p53-null and p53-mutant groups, which reflects the result found in the survival study.

Table 4.1. The incidence of HCC or gross metastases is not different at any period of time in HCC development.

p53 fl/fl

Weeks	Tumors/Mouse (%)	Metastases (%)
12-16	9/16 (56)	3/9 (33)
17-24	6/8 (75)	1/6 (17)
25-35	9/16 (56)	1/9 (11)
Total	24/40 (60)	5/24 (21)

p53 R172H/fl

Weeks	Tumors/Mouse (%)	Metastases (%)
12-16	4/13 (31)	2/4 (50)
17-24	6/8 (75)	1/6 (17)
25-35	8/12 (67)	1/8 (13)
Total	18/33 (54)	4/18 (22)

Analysis of genomic DNA isolated from a selection of mouse tumors confirmed recombination of the LSL cassette in the *p53*^{R172H} tumors. Additionally, recombination of the appropriate sites in the *p53* floxed allele was confirmed (Figure 4.5).

Figure 4.5. Recombination of the *p53*$^{LSL\text{-}R172H}$ cassette and the floxed *p53* allele occurred as predicted. Genomic DNA isolated from representative mouse liver tumors were examined by PCR for allelic recombination. In the top gel, the band representing 1 LoxP site demonstrates that recombination occurred at the LSL cassette in the *p53*$^{LSL\text{-}R172H}$ allele. The lower band, labeled "wild-type" represents the *p53* allele that does not contain an LSL cassette. The band on the lower gel represents recombination of the *p53*^{fl} allele, demonstrating that deletion of exons 2 through 10 occurred.

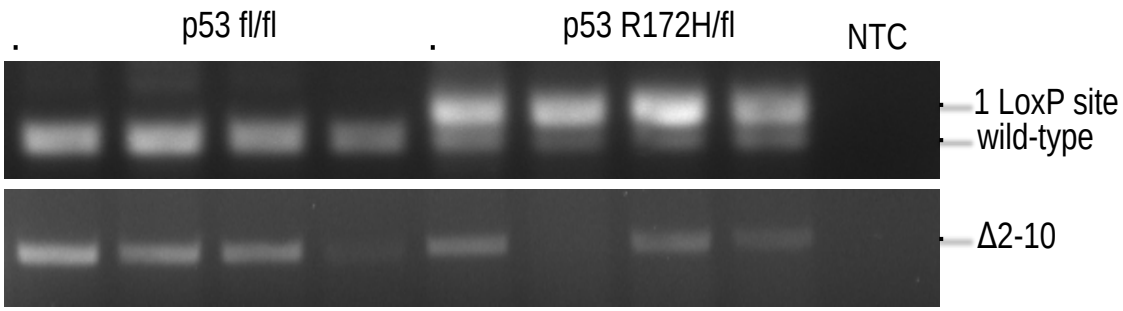

Tumor-derived cell lines from *p53^{R172H}*-containing HCCs do not display enhanced properties relative to *p53*-null cell lines.

To investigate potential gain of function properties *in vitro*, I generated a collection of HCC cell lines isolated from tumors induced in p53 null and p53 mutant livers. Eight tumor cell lines, four from each group, were compared to determine whether the presence of p53^{R172H} enhanced cell transformation or migration *in vitro*. Tumor-derived cell lines from mutant animals expressed p53 as expected, while nullizygous cell lines had no detectable p53 (Figure 4.6A). Importantly, expression of the p53 target p21 was not induced in mutant cell lines relative to null lines following Gemcitabine treatment, consistent with the absence of functional p53 protein (Figure 4.6A).

To ascertain whether p53^{R172H} enhances HCC cell migration, a phenotype that serves as an *in vitro* surrogate for metastatic capability, I performed transwell migration assays. I found that p53 null cell lines migrated as well as p53 mutant lines (Figure 4.6B). Thus, the presence of mutant p53 does not enhance this property, an outcome consistent with the similar rates of metastasis observed *in vivo*. Similarly, I found that p53^{R172H} does not enhance anchorage-independent growth, relative to p53 nullizygosity, as measured by a soft agar colony formation assay (Figure 4.6C). These data are consistent with the similar rates of tumor incidence and tumor size found in the mouse study. Thus, in combination with the *in vivo* results, my *in vitro* data suggest that the p53^{R172H} mutant does not promote an enhanced tumor phenotype in HCC.

Figure 4.6. Cell lines derived from p53^{R172H}-containing HCCs do not display enhanced properties when compared to p53-null HCCs.

A. Western blots demonstrating expression of p53 and p21 in selected mouse tumor-derived cell lines. β-Actin was used as a loading control.
B. Transwell migration assay of HCC cell lines derived from *p53$^{fl/fl}$* and *p53$^{R172H/fl}$* tumors. Graph shown is a representative experiment performed 4 times.
C. Soft agar colony formation assay of HCC cell lines derived from *p53$^{fl/fl}$* and *p53$^{R172H/fl}$* tumors. Graph shown is a representative experiment performed 3 times.

A

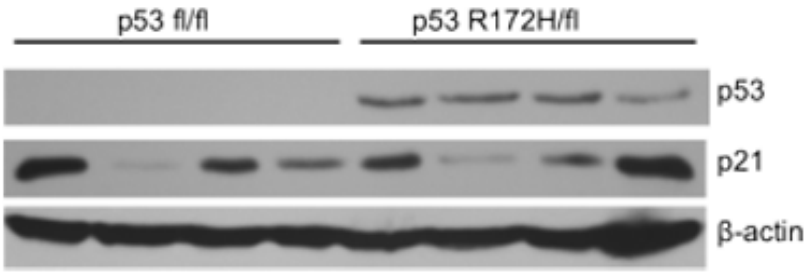

B

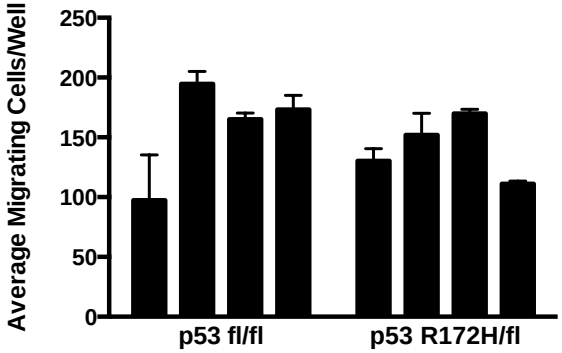

C

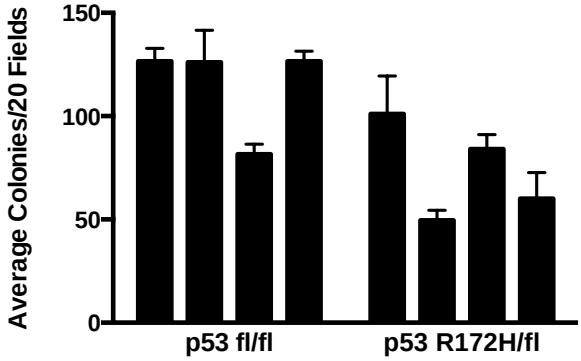

$p53^{R172H}$ is required for HCC cell transformation-related phenotypes with endogenous mutant expression.

In previous studies analyzing the gain-of-function properties of mutant p53 proteins, a hallmark experiment was the demonstration that knockdown of mutant p53 abrogated the transformed phenotype (Olive et al. 2004). I therefore determined whether depletion of mutant p53 similarly impacted $p53^{R172H}$-containing HCC cell lines. I knocked down $p53^{R172H}$ in two cell lines derived from murine mutant tumors. As a control for potential off-target effects, I introduced the p53-targeting shRNA into a *p53*-null cell line. Knockdown of p53 was confirmed by immunoblotting (Figure 4.7A). I observed that p53 knockdown impaired cell migration (Figure 4.7B) and soft agar colony formation (Figure 4.7C) relative to controls. Interestingly, this result suggests that mutant p53 is required for these phenotypes in $p53^{R172H}$-expressing HCC cell lines. Importantly, expression of the p53-targeting shRNA in p53 null cell lines did not impact cell migration or soft agar colony formation, confirming that these effects result from suppression of mutant p53 and not off-target effects.

Figure 4.7. $p53^{R172H}$ is required for transformation-related phenotypes in HCC cell lines.

A. Western blot of p53 depicting 3 HCC cell lines infected with shRNA as compared to an empty vector control labeled pGIPZ. β-Actin was used as a loading control.
B. Transwell migration assay of p53 shRNA-infected HCC cell lines. A p53-null cell line was used as an experimental control p-values, calculated by Student's t-test are 0.020 and 0.022 for R172H lines 1 and 2, respectively. Shown is the average of 2 experiments, with the number of migrating cells in each pGIPZ control infection set to 100%.
C. Soft agar colony formation assay of p53 shRNA-infected HCC cell lines. A p53-null cell line was used as an experimental control. p-values, calculated by Student's t-test are 0.044 and 0.004 for R172H lines 1 and 2, respectively. Shown is the average of 2 experiments, with the number of colonies for each pGIPZ control infection set to 100%.

A

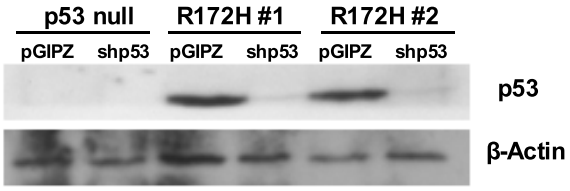

B

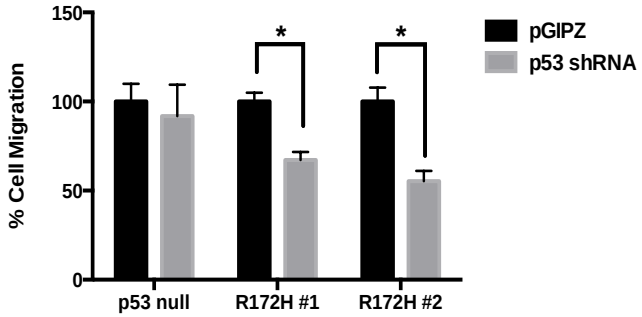

C

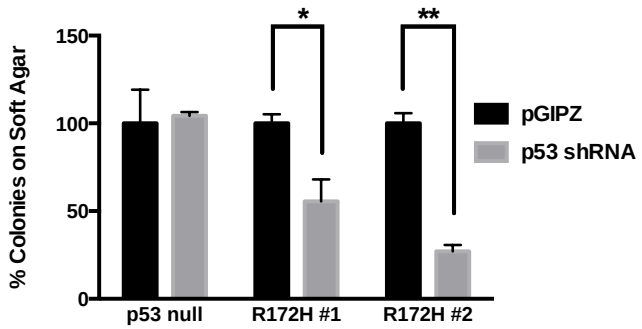

p53 family transcriptional activity is similar in p53 null and p53^{R172H}-expressing HCC lines.

The above data reveal that p53^{R172H} is required for transformation-associated phenotypes in HCC cells that express the mutant, but the presence of mutant p53 does not enhance these properties beyond what is observed in p53 null lines. This suggests, potentially, that similar pathways are impacted in both contexts. Since p53^{R172H} is known to bind to, and inhibit, other p53 family transcription factors as a gain-of-function mechanism, I examined the mRNA levels of a collection of genes known to be regulated by the related p63 and p73 proteins. I found that the mRNA levels of p53 family target genes involved in cell signaling (Figure 4.8A), DNA damage (Figure 4.8B), and cellular processes (Figure 4.8C), are unchanged between *p53* mutant and nullizygous cell lines.

Figure 4.8. *p53* mutant and *p53*-null HCC cell lines do not display differential expression of p53 family transcriptional targets. p53 family transcriptional target levels were assessed by qRT-PCR in RNA derived from mouse HCC cell lines. C_t values in each sample were normalized to β-actin as an endogenous reference. To calculate fold change, all samples were normalized to the average C_t value of $p53^{fl/fl}$ cell lines, so the average of the $p53^{fl/fl}$ cell lines is set to 1. The Comparative C_t method was used to calculate fold change. Dark circles indicate $p53^{fl/fl}$ cell lines, while open circles are $p53^{R172H/fl}$ cell lines

A. qRT-PCR of DNA damage-related targets of p53 family transcription factors.
B. qRT-PCR analysis of p53 family targets related to cell signaling.
C. qRT-PCR analsysis of p53 family targets related to other cell processes.

A

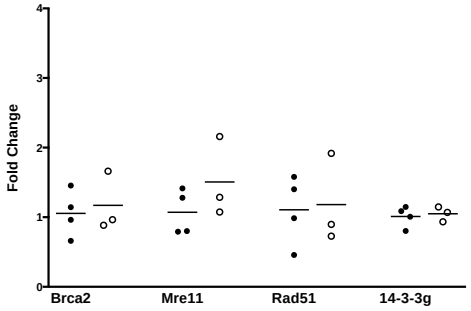

B

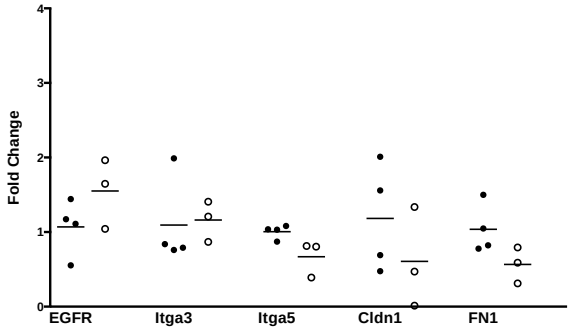

C

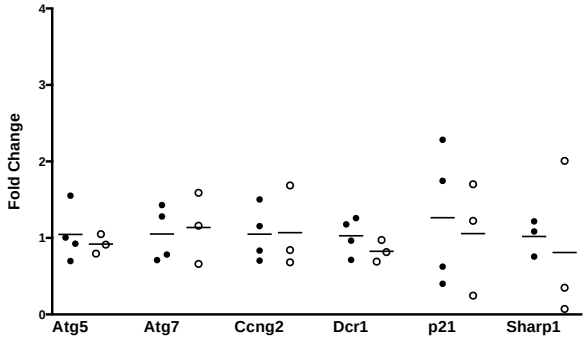

p53 family target gene expression is increased upon knockdown of mutant p53.

Tumor-derived cell lines containing $p53^{R172H}$ do not have enhanced *in vitro* properties as compared to p53 null cell lines. This could in part be attributed to similar levels of p53 family transcriptional activity as shown in Figure 4.8. However, upon knockdown of $p53^{R172H}$, transformation-related properties decrease, indicating that mutant p53 is required for the phenotypes displayed in these cells (Figure 4.7).

We therefore evaluated a subset of the target genes analyzed in Figure 4.8 to determine whether their mRNA levels increased upon knockdown of $p53^{R172H}$. p53 shRNA was added to two additional $p53^{R172H}$ tumor-derived cell lines and knockdown was confirmed by immunoblot (Figure 4.9A). When combined with the two knockdown lines previously generated (Figure 4.7), this generated a panel of four knockdown cell lines, and paired controls, for analysis. I found that the levels of the p63 and p73-regulated genes, *p21*, *Cldn1*, and *Rad51* were consistently increased in knockdown cells relative to paired control cells (Figure 4.9B). This suggests that mutant p53 suppressed their expression, potentially by functionally interfering with p63 and p73.

Figure 4.9. Knockdown of p53^{R172H} in *p53* mutant HCC cell lines results in increased expression of several p53 family transcriptional targets.

A. Western blot demonstrating knockdown of p53 from cell lines derived from *LSL-p53$^{R172H/fl}$* mouse HCCs as compared to pGIPZ empty vector control infections. β-Actin was used as a loading control.
B. Quantitative RT-PCR analysis of p53 family transcriptional targets in four mouse HCC cell lines with knockdown of p53^{R172H}. C_t values in each sample were normalized to β-Actin as an endogenous reference. Fold changes were calculated by normalizing all samples to the average C_t value of the cell line's pGIPZ control. The Comparative C_t method was used for fold change calculation.

A

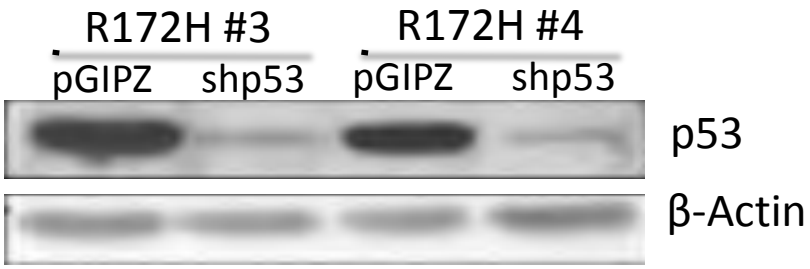

B

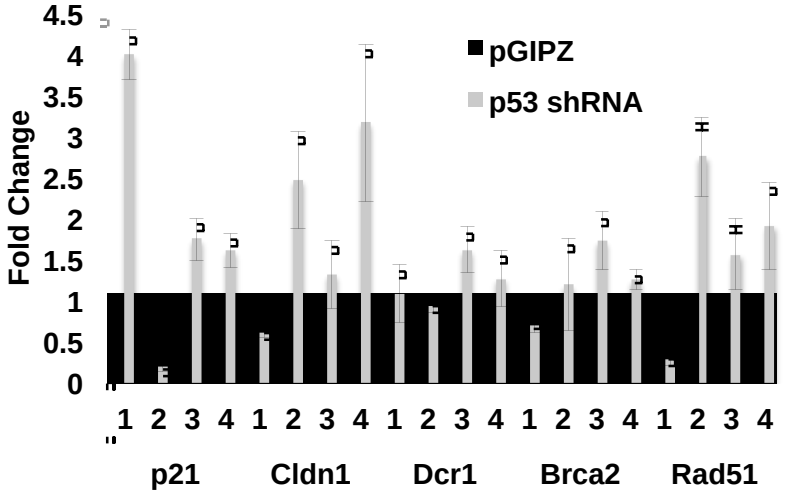

Materials and Methods

Animal Studies

Trp53 LSL-R172H mice (Olive et al. 2004) were obtained and crossed with *Albumin-tva, p53 flox/flox, Albumin-cre* mice (Chen et al. 2007). *Albumin-tva, Trp53 LSL-R172H/flox, Albumin-cre* mice were crossed to *Albumin-tva, Trp53 flox/flox, Albumin-cre* mice in order to obtain littermates for direct comparison. Three day-old pups were injected in the liver with $2x10^6$ DF1 cells producing RCAS-PyMT in 5uL of serum free DMEM (Chen et al. 2007). Mice in the tumor study were divided into either a survival or timepoint cohort. 30 injected mice were enrolled in a survival study. In the survival study, mice were sacrificed when distress was apparent as defined by my mouse protocol, or at the age of 9 months, whichever came first. Mice whose cause of death was likely due to tumor burden or metastatic disease were counted in the Kaplan-Meier curve. Mice that died without primary HCC were censored. Kaplan-meier statistics were calculated using the Log-rank test. An additional cohort of mice was assigned to timepoint groups of 3, 6, or 8 months as they were enrolled in the study. Mice were sacrificed at these timepoints, or when distress was apparent. For both the timepoint and survival studies, liver and lung tissues from each mouse were harvested. Individual tumors were counted and measured in three dimensions. Portions of fresh HCC were excised from harvested tissue in order to establish cell lines. Additionally, portions of tumor were flash frozen in liquid nitrogen for later isolation of nucleic acids and protein. Remaining

liver and lung tissue from each animal were formalin-fixed and paraffin-embedded for further analysis.

Cell Culture

Tumor-derived cell lines were isolated by mincing mouse tumor tissue and culturing in high-glucose DMEM with 10% FBS and 1% Pen/Strep. Appropriate p53 expression was confirmed by Western blot.

Stable p53 knockdown was performed using pGIPZ library shRNA directed to mouse Trp53 (Thermo Scientific, V3LHS_646511). An empty pGIPZ plasmid was used as a control. Lentiviruses were produced in 293T cells that were transfected with plasmids containing envelope glycoprotein, required packaging sequences, and pGIPZ plasmid. Transfections were performed using Effectene Transfection Reagent (QIAGEN, 301425). HCC target cells were infected with 1 mL of lentiviral supernatant in a well of a 6-well plate using 1ug of polybrene. Following infection, cells were selected in 6ug/mL puromycin before experimental analysis. To induce cell stress and p53 expression, 50nM Gemcitabine was added to growth media for 24 hours before generating protein lysates.

Transwell migration assay

Migration of cell lines was assessed by plating $2.5x10^4$ cells on a migration insert (BD Biosciences, 354578) in serum-free DMEM. DMEM containing 10% FBS was placed in the lower chamber as a chemoattractant. After 20 hours, non-

migrating cells were removed from the upper membrane, and migrating cells were stained with Giemsa. The migrating cells per well were determined by averaging the cell numbers across 5 fields at 100X magnification. Error bars on migration assay graphs are representative of standard deviation. p-values were calculated by Student's t-test.

Soft agar colony assay

For soft agar colony formation experiments, a 1.4% hard agar solution was combined with 2X DMEM with 20% FBS and 2% Pen/Strep and plated onto 100mm tissue culture plates. After hardening, 1x10^5 cells were mixed with equal parts of a 0.8% soft agar solution and 2X growth media. After the soft agar solution hardened, 8mLs of 1X growth media was added to the dishes, which were incubated for 2 weeks at 37°C. Colonies were counted in 20 fields per plate at 100X magnification. Size exclusion was used to ensure that colonies had grown in the dish, and were not just cell clumps. Error bars on migration and soft agar colony experiments are representative of standard deviation. p-values were calculated by Student's T-test.

Western blotting

Protein lysates from cell lines were generated in RIPA buffer, where concentrations were normalized by Bradford Assay. 20ug of lysate were used for each Western blot sample. 10% acrylamide gels were used for SDS-PAGE, and subsequently blotted onto PVDF. Western blots were blocked for one hour at room

temperature in 7.5% nonfat dry milk in TBS. Antibodies for Western blotting were used as described in Table 4.2.

Immunohistochemistry

Portions of each tumor were fixed in formalin and embedded in paraffin. Tissue sections were deparaffiniized with heat and rehydrated in decreasing alcohol concentrations. After rehydration, Antigen retrieval was performed by microwaving slides in Antigen Unmasking Solution (Vector, H-3300). After cooling, endogenous peroxides were invactivated by adding 3% hydrogen peroxide for 10 minutes. Slides were blocked in goat serum in PBS for one hour at room temperature. Primary antibody was added as described in Table 4.2. Biotinylated Rabbit secondary antibody was diluted in goat serum in PBS and added to the slides for one hour at room temperature. Goat serum, secondary antibody, and developing reagents were from Vector ABC kits (PK-4001). Pigment was developed in the tissues using a NovaRed Peroxidase Substrate (Vector, SK-4800). After development, slides were co-stained in hematoxylin, dehydrated, and mounted.

p53 family target gene analysis

RNA from cell lines was isolated using Trizol, and converted to cDNA using First-Strand cDNA synthesis kit (Invitrogen, 18080-051). qRT-PCR was performed using Quanta Perfecta SYBR Green (VWR, 95072) in an ABI 7300 machine using 50ng cDNA. p63 targets were amplified using the primers listed in Table 4.3.

For qPCR studies on the tumor-derived cell line panel, average C_t values for each cell line were determined for both the target gene and β-actin endogenous control. C_t values for each individual cell line were normalized to the average C_t value for the p53-null cell lines, so that each cell line fold change is calculated in relationship to the average of four p53 fl/fl cell lines. All individual lines were normalized to β-actin as an endogenous reference.

For assaying p53 knockdown cell lines, each shRNA-infected line was normalized to its respective pGIPZ-infected control, after normalizing to an endogenous reference. In each case the Comparative C_t Method was used to calculate fold change, where fold change = $2^{-\Delta\Delta CT}$.

Table 4.2. Antibodies and conditions used for Western blotting and immunohistochemistry.

Target	Manufacturer	ID number	Dilution	Diluent	Condition
p53	Cell Signaling	1C12	1:2000	5% milk in TBS	Overnight at 4°C
p21	Santa Cruz	Sc-6246	1:1000	5% milk in TBS	Overnight at 4°C
β-Actin	Santa Cruz	Sc-1615-R	1:2000	5% milk in TBS	Overnight at 4°C
Ki67	Abcam	Ab66155	1:500	Goat serum in PBS	Overnight at 4°C

Table 4.3. Primer sequences used for detection of transcripts by qRT-PCR.

Target Gene	F Primer	R Primer
β-Actin	tcctcctgagcgcaagtactct	cggactcatcgtactcctgctt
Brca2	ggatggctcttcaggatcattcg	gtgcttttgaagtaccattgaccttta
Mre11	cgaagaacgttgaaaggttcaaagc	gggaacgactggggaatcctca
Rad51	tgggaagctcaaaaccatctcttaac	gtgtgtttctgtgaatgtatgcctaat
14-3-3g	ttggacagtggttcgttcag	agcaactggtgcagaaagc
EGFR	ctgcaggctcagaaagtggt	acactgctggtgttgctgac
Itga3	tgaggggacacaggtacaca	agactgagcgacaacagcg
Itga5	gacagcaccaccttgcagta	ttctccgtggagttttaccg
Cldn1	ctgcacagagagcaagggta	agtggcagatgcagaaagtg
FN1	actggatggggtgggaat	ggagtggcactgtcaacctc
Atg5	aagtctgtccttccgcagtc	tgaagaaagttatctgggtagctca
Atg7	atgccaggacaccctgtgaacttc	acatcattgcagaagtagcagcca
Ccng2	ctgagaaatgccaaagtgga	gggccaagaatctatccaaa
Dcr1	tgatgggaacgctaacacat	tctgctcagagtccatcctg
p21	atcaccaggattggacatgg	cggtgtcagagtctagggga
Sharp1	gacagccattgaacatggac	cttggtatcgtctcgcttca

Discussion

p53 inactivation is an important step in HCC tumorigenesis that is associated with increased dissemination and poor prognosis (Lewis et al. 2005; Woo et al. 2011; Liu et al. 2012). Point mutations in the *p53* gene are prevalent in human HCC, and occur more frequently in advanced disease (Oda et al. 1992; Buendia 2000). Previous work has demonstrated that a common mutation, $p53^{R172H}$, can contribute to enhanced tumorigenesis and metastasis in other tumor types, including breast, skin, colon, pancreas, and the oral epithelium (Olive et al. 2004; Caulin et al. 2007; Morton et al. 2010; Acin et al. 2011; Lu et al. 2012; Cooks et al. 2013). Taken together, I hypothesized that the $p53^{R172H}$ mutation would enhance HCC progression through gain-of-function properties.

Using the RCAS-TVA model of HCC, I found that $p53^{fl/fl}$ and $p53^{R172H/fl}$ mice display equal tumorigenic properties. Mice with *p53* deletion and mutation had similar rates of tumor formation and metastasis at every time point examined. Also, tumor-free survival was virtually identical between $p53^{fl/fl}$ and $p53^{R172H/fl}$ mice. Lastly, cell lines derived from tumors in each of these groups display similar rates of soft agar colony formation and migration *in vitro*. These data indicate that for HCC, this particular *p53* mutation does not contribute oncogenic effects that are worse than *p53* loss.

Yet in Figure 4.7, I demonstrate that the migration and transformation characteristics of tumor-derived cell lines containing the $p53^{R172H/fl}$ mutation are dependent on the p53 mutant protein. Knockdown of the mutant in two R172H-

containing HCC cell lines decreases migration and transformation levels. While confusing, this piece of data suggests that the $p53^{R172H}$ mutant is contributing to cell phenotypes, despite the lack of enhancement in progression when compared to the $p53^{fl/fl}$ tumors. The HCCs formed in $p53^{fl/fl}$ animals can achieve the same levels of tumor formation and progression as in $p53^{R172H/fl}$ mice, just via a different mechanism than $p53^{R172H}$ gain-of-function activities.

Concordant with my findings, a previous study indicated that forced-expression of p53 mutants in HCC lines did not affect proliferation or soft agar colony formation. Yet, upon knockdown of p53 in HCC cells with endogenous *p53* mutations, proliferation decreased while apoptosis increased (Gouas et al. 2010). This outcome is similar to my study, where endogenous *p53* mutations are required for cell phenotypes, however do not necessarily enhance tumorigenic phenotypes when compared to *p53*-null lines.

My data suggest that a possible mechanism for HCC progression in the absence of functional p53 is through regulation of p63/p73 activity. Since studies have demonstrated that one $p53^{R172H}$ gain-of-function mechanism is through inactivation of the p63/p73 transcription factors (Lang et al. 2004; Li and Prives 2007), I sought to determine if tumors with the $p53^{R172H}$ mutant and the $p53^{fl/fl}$ alleles had similar levels of p63/p73 activity. HCCs from $p53^{fl/fl}$ tumors display similar p63/p73 transcriptional activity as tumors from $p53^{R172H/fl}$ mice, as seen in Figure 4.8.

Since it appears that $p53^{R172H}$ is suppressing activity of p63/p73, p53-family transcriptional activity was measured in cells with $p53^{R172H}$ knockdown. Upon knockdown of the p53 mutant, several p53 family transcriptional targets were increased (Figure 4.9), reflecting a release of the suppression by $p53^{R172H}$. This data suggests an importance for p53 family transcriptional activity in HCC as a whole, which may be more important than *p53* status alone.

Where a *p53* mutation may inhibit p53 family transcriptional activity in other tumor contexts, in HCC there is no significant difference in p53 family activity when $p53^{R172H/fl}$ and $p53^{fl/fl}$ tumors are compared. This indicates a potential explanation for $p53^{R172H}$ not displaying enhanced oncogenic properties in HCC. Potentially, p53 family activity in $p53^{fl/fl}$ tumors is reduced, resulting in an outcome similar to the inhibition provided by $p53^{R172H}$.

Previous work by Schilling et al. described the expression of tumor-associated *p53* mutants in Hep3B cells and demonstrated that apoptosis is reduced when these mutants are expressed. Further, co-transfection experiments with p63/p73 and the p53 mutants demonstrate that the p53 gain-of-function mutants can inhibit p63 and p73 transcriptional activity in HCC (Schilling et al. 2010). This work supports my finding, in that the $p53^{R172H}$ mutant inhibits p53 family transcriptional activity in HCC cells. However, my *in vivo* study demonstrates that the gain-of-function traits of $p53^{R172H}$ do not enhance HCC progression when compared to p53 null tumors.

My results suggest that the *p53*$^{fl/fl}$ tumors have reduced p63/p73 transcriptional activity by another mechanism. It is possible that *p53* status is less important for HCC progression and metastasis than p53 family transcriptional activity as a whole. Detection of TAp73 and TAp63 in HCC reveals their expression is increased (Stiewe et al. 2004; Petitjean et al. 2005). In the case of p73, this upregulation has been associated with inactivation of p53 (Herath et al. 2000; Sayan et al. 2001; Stiewe et al. 2004). It is possible that the regulation of other p53 family members differs in the context of *p53* loss versus *p53* mutation. Changes in the expression pattern or levels of p63 and p73 may account for the reason why p53-family target genes are unchanged between *p53*$^{fl/fl}$ and *p53*$^{R172H/fl}$ tumors.

This outcome places a large importance on reduced p63/p73 function in the context of p53 inactivation in order for HCC progression to occur. Further experimentation must be done in order to adequately demonstrate that p63/p73 inhibition is responsible for HCC progression in the absence of functional p53.

CHAPTER V

Discussion

KLF6 and HCC dissemination

Hepatocellular carcinoma is a highly deadly malignancy due to its capacity for dissemination and recurrence (Hayat et al. 2007; Jemal et al. 2011). Unfortunately, little is known about the precise molecular mechanisms driving the progression and dissemination of the disease. Determining the important drivers of HCC progression is critical to informing treatment strategies for patients who are not eligible for curative surgery. In this work, I characterized the impact of impaired KLF6 activity in HCC progression.

I began investigating genes involved in HCC migration through gene expression profiling of migratory subpopulations of an HCC cell line, BL185. In this profiling study, KLF6 was decreased in migratory subpopulations compared to the less migratory parent cell line. Further analysis into human HCC cell lines and HCC tumor samples confirmed that KLF6 was not only commonly decreased in human HCC when compared to normal liver, but was also decreased in HCCs with vascular invasion compared to non-invasive HCCs.

We do not know the mechanism by which KLF6 expression is reduced in our migratory HCC subpopulations. In these lines, KLF6 is reduced at both the message and protein levels, indicating regulation is happening, at least in part, at the transcript level. One possible mechanism for this change is an altered KLF6 splicing ratio. KLF6-SV1 is a splice variant of KLF6 that functions as a dominant negative to the full-length form (Narla et al. 2005; Vetter et al. 2012). Importantly, increased KLF6-SV1 has been found to be oncogenic and a metastatic driver in breast and

prostate cancers (Narla et al. 2008; Hatami et al. 2013). Examination of our HCC cell lines indicates there is no increase in expression of other variants, suggesting that the decrease in full-length KLF6 is not due to a change in the splicing ratios between full-length and KLF6-SV1. Several other possibilities could account for these differences in expression. One is that the KLF6 promoter may have increased methylation in the subpopulations, which could result in decreased KLF6 transcription. KLF6 promoter methylation has been demonstrated in esophageal cancer, and is responsible for reduced KLF6 levels in that tumor type (Yamashita et al. 2002).

Another possibility for reduced KLF6 expression is that a transcription factor required for KLF6 transcription has altered expression in our subpopulations. In the absence of a transcriptional activator, or overexpression of a repressor, KLF6 transcript levels may be reduced. Transcriptional regulators of KLF6 have not been characterized and may be an interesting area for future research.

A recently characterized source of KLF6 regulation is through its 3' UTR. Interestingly, the full-length KLF6 message has decreased stability in HCC cells when compared with immortalized hepatocytes (Diab et al. 2013). The decrease in KLF6 mRNA stability in cancer cells suggests that a protein or microRNA is binding to the message and impacting its stability. Potentially, the KLF6 message is less stable in our HCC subpopulations, and this is the cause of the expression decrease that I detected. If this is indeed the case, an interesting experiment would be to perform a screen for proteins which bind to the KLF6 3'UTR. A yeast three-hybrid

approach can be used to detect the RNA binding proteins that interact with this segment of the KLF6 message (SenGupta et al. 1996). Once these RNA-binding proteins are identified, they can be individually validated using RNA cross-linking and immunoprecipitation (CLIP) (Ule et al. 2003).

In addition to RNA binding proteins, KLF6 message levels may also be targeted by a microRNA that is differentially expressed between our BL185 cells and migratory subpopulations. Increased expression of a KLF6-targeting microRNA in the subpopulations would result in increased decay or reduced translation of the KLF6 transcript. Previous studies have shown that KLF6 is targeted by miR-122 and miR-181a (Tsai et al. 2012; Zhang et al. 2012a). Potentially, increased expression of one of these microRNAs is responsible for the decrease of KLF6 message in the migratory subpopulations. Yet, miR-122 is often decreased in HCC compared to normal liver (Coulouarn et al. 2009; Koberle et al. 2013; Nakao et al. 2014), which is inconsistent with the decreased KLF6 levels frequently encountered in HCC (Kremer-Tal et al. 2004; Kremer-Tal et al. 2007; Wang et al. 2010; Tarocchi et al. 2011). This disparity is likely due to the fact that miR-122 is a regulator of hepatocyte differentiation and maintenance (Chang et al. 2004; Deng et al. 2014), and additionally targets AKT3 (Nassirpour et al. 2013). Upon its loss, strong signals of de-differentiation and increased AKT signaling may be more important to hepatocyte transformation than the impact of miR-122 on KLF6.

To find other microRNAs that are impacting KLF6, algorithms, such as miRanda, can predict possible KLF6-targeting microRNAs (Betel et al. 2008). This

algorithm reveals that miR-181, miR-21, and several members of the miR-17-92 family putatively target KLF6. Interestingly, these microRNAs are often elevated in human cancers, including HCC (Cho 2007; Connolly et al. 2008; Ji et al. 2009b; Olive et al. 2010), which suggests they may be responsible for decreased KLF6 levels in human cancer. qRT-PCR could be employed to determine if the expression of one or more of these particular microRNAs is increased in the HCC subpopulations as compared to the BL185 parent line.

In addition to being the causes of decreased KLF6 in our migratory subpopulations, these mechanisms may also contribute to decreased KLF6 levels in HCC specimens. Since *Klf6* mutations and allelic changes are rare events in human HCC (Boyault et al. 2005; Pan et al. 2006; Song et al. 2006), it is likely that these other mechanisms contribute to decreased KLF6 expression. While KLF6 is commonly decreased, its transcript and protein are typically detectable (Kremer-Tal et al. 2007; Wang et al. 2010; Tarocchi et al. 2011), which is unusual for a tumor suppressor. This suggests that KLF6 dosage is important, consistent with my finding that *Klf6* heterozygous mice have increased tumor formation and metastasis.

KLF6 was previously described as a tumor suppressor in HCC when KLF6-depleted livers had greater tumor formation upon DEN treatment (Tarocchi et al. 2011; Vetter et al. 2012). Our data describe an additional role for decreased KLF6 levels in HCC: an increase in HCC cell migration. Concordantly, tumors with single-copy loss of *Klf6* generate greater metastatic burden to the lungs than those with wild-type *Klf6*.

In our study, single-copy loss of *Klf6* increases metastasis compared to wild-type mice, where only one metastatic colony was detected upon microscopic examination. Several possible mechanisms could account for the increased metastatic burden in these mice, including enhanced tumor cell invasion and dissemination, survival in the bloodstream, or ability to establish colonies in the lungs. Lastly, another possibility could be that metastasis initiates earlier in these mice, and thus colonies have more time to expand in the lung.

Since *in vitro* migration is increased upon KLF6 knockdown in our HCC cell lines, these cells may have increased invasion and dissemination *in vivo*, which could result in increased metastasis. To determine if more cells are disseminating in *Klf6* heterozygous mice, the number of circulating tumor cells (CTCs) could be examined in *Klf6* heterozygous versus wild-type mice. It may be possible to detect that a larger number of disseminating cells are present in *Klf6* heterozygous mice. Various methods of detecting CTCs based on expression of epithelial markers are available, including the EPISPOT assay, and several CTC-chips (Alix-Panabieres 2012; Zhang et al. 2012b).

To test if KLF6-depleted cells have improved survival in the bloodstream, and colonization ability, comparing these cells by tail vein injection may be valuable. While not a measure of metastasis, it could determine if *Klf6* heterozygous cells are better able to survive in circulation and subsequently establish lung colonies compared to wild-type mice.

Previous tracking studies of metastatic cells have demonstrated that the greatest limiting step in the metastatic process is the formation of a colony after extravasation into new tissue (Luzzi et al. 1998). *Klf6* heterozygous tumors may disseminate earlier than in wild-type, providing more time for cells to escape dormancy and proliferate in the lungs. This is a possibility, because my study provides evidence that HCCs are forming earlier in *Klf6* heterozygous mice. In mice sacrificed at 4.5 months, liver tumors from $Klf6^{fl/wt}$ animals were larger than in wild-type. Since proliferation rates in these tumors were similar, and apoptosis rates in these tumors are very low, I hypothesized that *Klf6* heterozygous tumors were forming earlier. This may coincide with earlier dissemination of tumor cells as well. To test this, it would be necessary to perform an analysis of tumor and metastasis formation in these mice at multiple, early time points. Here, detection of CTCs may again be valuable to determine when dissemination is occurring in these animals.

Surprisingly, single-copy loss of *Klf6* was sufficient to drive HCC progression and metastasis in our model, as tumor suppressor genes are traditionally thought to require biallelic inactivation (Berger et al. 2011). However, this is not completely unusual for KLF6 expression in the liver. Mice that have a single-copy germline deletion of *Klf6* are phenotypically normal. However, upon treatment with a hepatotoxin, hepatocytes in *Klf6* heterozygous mice have increased proliferation, (Tarocchi et al. 2011), resulting in enlarged livers that are more susceptible to HCC formation (Narla et al. 2007). These previous experiments demonstrate that hepatocytes are sensitive to single-copy *Klf6* loss, and so it is not entirely surprising

that we were able to see effects on tumorigenesis and metastasis with single-copy loss in the liver. Clearly, KLF6 levels are important for maintenance of hepatocyte stasis.

Notably, our KLF6 studies were performed in mice with liver-specific *p53* deletion. Additionally, our mouse-derived HCC cell lines also lacked p53 expression. This is important, since *p53* deletion was previously shown to be sufficient to induce HCC metastasis in our PyMT-driven mouse model (Lewis et al. 2005). Our data suggest that KLF6 may be involved in increasing metastasis that is already facilitated by *p53* nullizygosity. The absence of p53 expression may be another contributor to why single-copy loss of *Klf6* was sufficient to increase tumor formation and metastasis. Previous experiments that described KLF6 as a tumor suppressor in HCC were performed in a *p53* wild-type background (Tarocchi et al. 2011; Vetter et al. 2012), which may explain why metastasis was not noted to have occurred in these studies.

In addition to facilitating metastasis in our model, *p53* loss may have additional importance for KLF6 activity, as previous studies have indicated there is a relationship between the two proteins (Gehrau et al. 2011). In the absence of p53, the target genes transcribed by KLF6 vary, as demonstrated with IGF1R transcription (Rubinstein et al. 2004). Since KLF6 transcriptional activity is different with impaired p53, it is possible that this different set of KLF6 target genes may be responsible for the metastasis that occurred in our mouse model, and could account for why metastasis was not detected in other HCC studies on KLF6.

Differences in the mouse model used could also account for the absence of metastasis in earlier studies. Previous work used the carcinogen DEN to induce HCC formation in mice (Tarocchi et al. 2011; Vetter et al. 2012). HCCs from this mouse model are capable of generating lung metastases, though they mostly occur between 80 and 90 weeks of age (Vesselinovitch et al. 1978). Indeed, DEN-treated mice analyzed in these *Klf6* studies were sacrificed at nine months of age (Tarocchi et al. 2011; Vetter et al. 2012). In our mouse model, grossly visible lung metastases can be detected as early as four to six months of age (Lewis et al. 2005; Chen et al. 2007), which may explain why I was able to detect an increase in metastatic burden.

It would be interesting to determine if *Klf6* loss alone is sufficient for driving metastasis in our model, independent of p53 inactivation. However, a previous study found that KLF6 is a direct transcriptional repressor of MDM2 (Tarocchi et al. 2011). Therefore, even if the *p53* locus were intact, decreased KLF6 expression would increase transcription of MDM2, subsequently leading to the degradation of p53. Due to their linked expression, it would be challenging to determine the role of KLF6 in the context of normal, wild-type p53 expression. In this study, I show that KLF6 can function as a tumor suppressor for HCC, even in the absence of the KLF6-MDM2-p53 axis.

Since my study examined the impact of single-copy loss of *Klf6* on HCC progression and dissemination, it may be valuable to also determine the impact of losing both *Klf6* copies. My hypothesis is that loss of both copies would increase and accelerate tumor formation, while also further increasing metastatic burden. What

would be very interesting to determine, is if complete *Klf6* knockout in the liver would be sufficient to drive HCC progression and metastasis in the absence of *p53* deletion. Based on the known KLF6-MDM2-p53 axis (Tarocchi et al. 2011), the levels of active p53 would be relatively low in a *Klf6*-null hepatocyte, potentially resulting in a similar effect to compound *Klf6* and *p53* deletion.

We performed a HCC tissue microarray to determine if KLF6 localization could be used as a prognostic indicator for HCC. We found that over a third of HCCs display cytoplasmic KLF6, which has previously been described the presence of KLF6-SV1 or SV2 (Narla et al. 2005; Vetter et al. 2012). KLF6-SV1 was found to be rare in HCCs induced by HBV or HCV infection (Kremer-Tal et al. 2007), but other studies found that splicing of KLF6-SV1 was increased in advanced HCCs (Vetter et al. 2012). Since KLF6-SV1 has been found to be a dominant negative variant of full-length KLF6, cytoplasmic KLF6 often occurs in the absence of nuclear KLF6 (Narla et al. 2005; Vetter et al. 2012). In our study, the presence of cytoplasmic KLF6 was more frequent than was found in HBV and HCV-induced HCCs, yet it did not correlate to tumor stage or decreased patient survival.

Another interesting finding in the HCC tissue microarray was that approximately a third of HCCs were largely negative for KLF6. Most previous studies indicate that transcript levels of KLF6 are decreased in HCC as compared to normal liver, but transcripts are still detectable (Kremer-Tal et al. 2007; Wang et al. 2010; Tarocchi et al. 2011). Considering this information, the occurrence of so many tumors that appeared negative for KLF6 protein was surprising, and suggests that

perhaps post-transcriptional regulation of KLF6 results in a further decrease in protein expression despite the presence of transcript.

Previous studies have described stepwise decreases in KLF6 transcript with increasing HCC stage (Tarocchi et al. 2011). By performing a tissue microarray for HCC, I was expecting to find a similar correlation, where HCCs with nuclear KLF6 would have a better prognosis than those with cytoplasmic or negative KLF6 staining. However, I did not find any correlation to KLF6 localization and patient outcome. There are several possible reasons for our TMA results disagreeing with the published transcript data. One is that post-transcriptional regulation of KLF6 may lead to a disparity between mRNA and protein expression. Also, tumors selected in the previous study were from HCCs driven by HCV infection (Tarocchi et al. 2011), while the TMA was assembled from patients with mixed etiology. Different HCC etiologies may account for differences in KLF6 expression. Another possibility is related to the selection of HCC samples for the tissue microarray. The samples included in the TMA were from patients who were eligible for surgical resection or liver transplant. By nature of patient eligibility for surgical treatment, tumors included in the HCC TMA tend to be at an earlier, less invasive stage. My hypothesis is that a bias toward HCCs of good prognosis in the TMA is the reason why we did not see a correlation between KLF6 expression and prognosis.

Potentially, p53 and KLF6 status could be combined to improve prognostic value. p53 is already used as a prognostic marker in HCC, where its inactivation is associated with poor prognosis in HCC (Woo et al. 2011; Liu et al. 2012). Since the

increased metastasis and decreased survival observed in our model occurred in the background of a *p53* deletion, the prognostic value of KLF6 might rely on inactivation of p53. If patients were first stratified between those with intact or inactivated p53, it would be interesting to determine if subsequent assessment of KLF6 status could improve prognostic predictions.

In this study, I did not thoroughly investigate *Klf6* loss of heterozygosity (LOH) in the primary tumor or the lung metastases. By qRT-PCR, all except one of the primary HCCs in $Klf6^{fl/wt}$ mice retained expression of the full-length KLF6 transcript. KLF6 levels in most of the heterozygous tumors were reduced by half of what was present in *Klf6* wild-type tumors. As is common in other metastasis suppressors, it would be interesting to find if KLF6 expression was further reduced in the metastases as compared to the primary tumors. Also, it would be interesting if the KLF6 levels in the single *Klf6* wild-type lung metastasis found during the study were reduced as compared to its primary liver tumor. While only a single sample, this result would suggest that a reduction in KLF6 levels is required for HCC metastasis.

Studies of breast and prostate cancers found that an increase in the dominant negative KLF6-SV1 variant increased metastasis (Narla et al. 2008; Hatami et al. 2013). Of note, migration and metastasis in our model was not driven by an increase in KLF6-SV1, but by a decrease in total KLF6 levels. The importance of KLF6-SV1 in human HCC is unclear (Kremer-Tal et al. 2007; Vetter et al. 2012), but my data

indicates that alternative splicing of KLF6 may be more common to human HCC than previously described.

While KLF6-SV1 has been well described as a dominant negative to full-length KLF6 (Narla et al. 2005; Vetter et al. 2012), KLF6-SV1 may have other roles in the cell as well. In an HCC study, mice with liver-specific KLF6 depletion were combined with transgenic mice expressing *Klf6-SV1*. Mice with both SV1 expression and *Klf6* deletion had increased tumor formation compared to mice with *Klf6* deletion alone (Vetter et al. 2012). If the only role for KLF6-SV1 were to inhibit full-length KLF6, then these two models would be functionally equivalent. The fact that the combination of SV1 expression and *Klf6* deletion forms more tumors suggests that KLF6-SV1 has roles outside of inhibiting full-length KLF6. KLF6-SV1 may have additional oncogenic functions, including inhibition of transcription factors other than KLF6. Impacting the activity of several transcription factors would greatly alter gene expression and could potentially drive tumorigenesis and dissemination. Since SV1 expression has been shown to induce HCC formation (Vetter et al. 2012), it would be interesting to find if transgenic expression of KLF6-SV1 would also increase metastasis in our HCC model.

After finding that decreased levels of KLF6 were important not just for driving HCC formation but dissemination as well, I sought to determine the mechanism by which KLF6 was regulating these processes. In breast cancer, increased KLF6-SV1 was found to drive EMT through increased expression of Twist1 (Hatami et al. 2013). The role of KLF6-SV1 as an EMT regulator makes sense

in the context of the previously described role for KLF6 as a transcriptional activator of E-Cadherin (DiFeo et al. 2006). However, I did not find evidence that an EMT was induced in our HCC cell lines. The migratory subpopulations did not have altered expression of epithelial or mesenchymal markers, providing no evidence that an EMT had occurred. Also, while KLF6 knockdown resulted in decreased E-Cadherin expression, there was not a significant change in other markers. Of note, our murine HCC cell lines express both epithelial and mesenchymal markers simultaneously, indicating that our mouse HCC tumors exist in a state between these two lineages. Of course, this study does not rule out the possibility that EMT is occurring transiently during periods of migration, but I have no evidence that this is the case. While EMT is a common mechanism in human cancer for increasing invasion and metastasis (Kalluri and Weinberg 2009), this study does not suggest it is a primary cause of HCC dissemination in our model.

To explore the mechanism of increased migration and metastasis in response to decreased KLF6, I investigated the status of RHO family GTPases, particularly RAC1, CDC42, and RHOA. As a result of these studies, I found that increased RAC1 activity was required for the migration induced by KLF6 knockdown. My data suggest that the use of a RAC1-targeting inhibitor may help to prevent the migration of HCC cells in cancer therapy. Of course, RAC1 activity has also been shown to impact cell proliferation and survival (Bustelo et al. 2007), so therapeutic doses may have a greater impact on a tumor cell beyond inhibition of motility. Several studies have found that RAC1 activity is critical for mediating effects related to

tumorigenesis, angiogenesis and metastasis, and have theorized the use of RAC1 inhibition as a cancer therapeutic (Liu et al. 2008; Akunuru et al. 2011; Rosenblatt et al. 2011; Bid et al. 2013).

To determine if RAC1 inhibition would be a useful therapy for HCC, it would be interesting to compare survival of *Klf6* heterozygous mice with and without RAC1-targeting treatment. A different approach would be to combine our *Klf6* heterozygous HCC mouse model with a liver-specific deletion of *Rac1* (Glogauer et al. 2003). If RAC1 activity is required for the metastasis that occurred in *Klf6* heterozygous mice, its inhibition would decrease metastasis in these animals. These studies would be additionally informative regarding the response of primary HCC to RAC1 inhibition or loss. As RAC1 has been associated with cell growth and angiogenesis (Bustelo et al. 2007; Bid et al. 2013) the formation of primary tumors in mice with impaired RAC1 may also be negatively affected.

After this finding, I sought to determine what transcriptional targets of KLF6 were responsible for mediating the migration and metastasis effects seen in response to decreased KLF6. Prior to this study, one gene expression profiling analysis that compared *Klf6* heterozygous to *Klf6* wild-type livers had been performed (Tarocchi et al. 2011). However, the analysis examined mouse livers that had been treated with DEN before progression to HCC. Here, I used two global approaches: gene expression profiling of KLF6 knockdown cells, and ChIP-sequencing, in order to determine new transcriptional targets of KLF6 in HCC cells. Previous analyses of KLF6 binding sites have only examined the promoter regions of

specific target genes through ChIP-PCR (DiFeo et al. 2006; Lee et al. 2010; Tarocchi et al. 2011). Notably, we found that while KLF6 binds to promoter regions proximal to transcriptional start sites, KLF6 also binds to sites distant from known transcriptional start sequences. Of target genes that were found in both the expression profiling and ChIP-sequencing datasets, KLF6 was more likely to be bound at locations distal from the transcriptional start site. One identified target in particular, E-Cadherin, was previously identified as a KLF6 transcriptional target (DiFeo et al. 2006), suggesting that my approaches are detecting genuine KLF6 target genes. My study also uncovered several novel target genes that may be important for tumor formation and metastasis. Two such target genes include *Vav3* and *Cdc42ep3*.

In this study, I found that KLF6 is a repressor of VAV3 and CDC42EP3 transcription. Upon KLF6 knockdown, expression levels of these genes increase, and their expression is required for the increase in migration induced upon KLF6 knockdown. I hypothesize, that through its known role as a GEF for RAC1 (Sachdev et al. 2002), VAV3 increases RAC1 activity and subsequently increases cell migration. While its precise role is unknown, CDC42EP3 is likely mediating signaling downstream of the active GTPases to regulate migration (Hirsch et al. 2001). Together, these proteins are responsible for mediating a GTPase cascade that induces HCC cell migration.

However in its current state, the evidence connecting increased levels of RAC1 and CDC42 activity with VAV3 and CDC42EP3 is circumstantial. To confirm

this hypothesis, it would be necessary to demonstrate that upon VAV3 knockdown, the activity levels of RAC1 and/or CDC42 decrease. Also, a downstream readout for CDC42 activity would need to be measured in order to determine that CDC42EP3 was indeed mediating effects downstream of active CDC42. While this is my hypothesis based on the known functions of these proteins, it has not been proven to be the mechanism by which VAV3 or CDC42EP3 knockdown regulates migration in our HCC cells. Indeed, they may have separate roles in the cell through which they are driving migration.

To further explore the potential relationship between KLF6 and CDC42EP3 or VAV3 on migration and metastasis, it would be interesting to perform mouse experiments with compound deletions. Similar to our *in vitro* study, I hypothesize that *Klf6* heterozygous mice with additional *Cdc42ep3* or *Vav3* deletion would have fewer HCC metastases than mice with *Klf6* deletion alone. In this study, I did not explore the impact of VAV3 or CDC42EP3 on cell proliferation or survival, but it is possible that these proteins may also have an impact on tumor formation in addition to metastasis. VAV3 has previously been characterized as a proto-oncogene, and has been shown to increase cell proliferation (Sachdev et al. 2002; Toumaniantz et al. 2010; Tan et al. 2013). If this were also the case in HCC, a mouse with both *Klf6* and *Vav3* deletion may also have decreased tumor formation compared to mice with deletion of *Klf6* only. *Vav3* knockout mice are viable (Faccio et al. 2005; Sauzeau et al. 2006), so this knockout allele could be combined with our HCC model to explore this possibility. If true, VAV3 would be implicated as a therapeutic target in HCC.

While the function of CDC42EP3 is not well characterized, if it is mediating signaling effects downstream of CDC42 as described (Joberty et al. 1999; Hirsch et al. 2001), it may not be restricted to only affecting cell migration. CDC42 activity has been shown to also affect cell cycle (Qiu et al. 1997), so CDC42EP3 may also be responsible for mediating this effect. No current mouse models for CDC42EP members exist, but *Cdc42ep3* deletion in the liver may also impact tumorigenesis as well as metastasis in our HCC model.

My data demonstrate that CDC42EP3 is required for migration induced by knockdown of KLF6 in HCC. While it was previously demonstrated that increased CDC42EP3 expression increases migration of fibroblasts in culture (Hirsch et al. 2001), it is unclear what precise role CDC42EP3 has in the cell. CDC42EP3 has been shown to bind to CDC42 in a GTP-dependent manner (Joberty et al. 1999), but its downstream activities are not characterized. I have hypothesized that CDC42EP3 is binding to CDC42-GTP, which is increased upon KLF6 knockdown cells, but this interaction has not been validated. What also remains to be characterized is what pathways CDC42EP3 is affecting. Unlike some GTPase effectors, CDC42EP3 does not have a kinase domain (Joberty et al. 1999), so it is unlikely to be directly impacting signaling. While the formation of pseudopodia and changes in keratinocyte morphology are dependent on an intact CRIB domain (Hirsch et al. 2001), additional CRIB mutant studies of CDC42EP family members demonstrated it could still induce cell shape changes in the absence of an interaction with CDC42 (Joberty et al. 1999). These data suggest that CDC42EP family members may have CDC42-dependent and

independent functions. My hypothesis is that CDC42EP3 is behaving as a scaffolding protein for active CDC42 and other effectors that may directly impact signaling and downstream functions of CDC42. An interesting experiment would be to immunoprecipitate CDC42EP3 and perform mass spectrometry to identify its interacting proteins in HCC cells. This approach could potentially enlighten the mechanism through which CDC42EP3 is impacting migration.

While we have shown that VAV3 and CDC42EP3 are important for migration downstream of KLF6, other interesting genes were also found in our KLF6 target analysis. Some of these other targets include components of the Notch signaling pathway, such as JAG1 and RBPJ. Expression of both of these Notch pathway components is increased in response to KLF6 knockdown. Additionally, KLF6 was found to bind near the *Hes1* gene, though differential expression was not detected in our gene expression profiling analysis. Potentially, KLF6 may mediate its tumor suppressor activity in part via inhibition of multiple Notch pathway signaling components. However, the role of Notch signaling in HCC is complicated. In some studies, increased Notch signaling is tumor suppressive (Qi et al. 2003; Viatour et al. 2011), while it is pro-tumorigenic in other cases (Lobry et al. 2011; Villanueva et al. 2012). Notably, JAG1 expression in breast cancer cells was shown to facilitate the formation of metastases (Sethi et al. 2011), so increased JAG1 expression may facilitate metastasis in HCC as well. If Notch signaling is pro-tumorigenic or pro-metastatic in HCC, inhibiting the transcription of pathway components may be one mechanism through which KLF6 functions as a tumor and metastasis suppressor.

To determine if Notch signaling is important downstream of KLF6 in HCC, our *Klf6* heterozygous model could be combined with one of the several models available that impact Notch signaling. Based on the enriched Notch signaling upon KLF6 knockdown, my hypothesis is that Notch inhibition would reduce tumor formation and metastasis in this model. However, since some studies describe a tumor suppressive role for Notch signaling in HCCs (Qi et al. 2003; Viatour et al. 2011), this effect may be strongly dependent on cell context. It would be interesting to combine our KLF6 mouse model with conditional deletion of *Notch1* (Yang et al. 2004), or *Jag1* (Loomes et al. 2007), to determine the pathway's impact on HCC formation and metastasis. An additional approach could be to treat *Klf6* heterozygous mice with γ-secretase inhibitors to block Notch signaling (Shih Ie and Wang 2007). This method may demonstrate a reduction in tumor formation or metastasis as compared to a placebo treated cohort.

Another interesting target found in our study is KLF4. Known for being a transcriptional regulator of "stemness" genes (Takahashi and Yamanaka 2006; Nakagawa et al. 2008), KLF4 has also been shown to physically interact with KLF6 to affect transcription, particularly of Keratin 4 (Okano et al. 2000). My study found that KLF4 is directly targeted by KLF6 transcription. Importantly, KLF4 has been shown to be a suppressor of proliferation and migration in HCC cell lines in addition to repressing subcutaneous tumor formation and metastasis (Li et al. 2012; Lin et al. 2012b). As KLF6 and KLF4 can co-activate transcription, depletion of KLF4 in cells with reduced KLF6 may impact a large number of target genes. It would be

interesting to determine if effects seen in response to KLF6 loss were in part mediated through a reduction in KLF4 activity, which could be performed through the use of a mouse with conditional deletion of *Klf4* (Katz et al. 2002).

Another intriguing target found in our analysis is KLF6 itself. It is unsurprising to find that the gene expression profiling experiment detected KLF6 transcript levels were reduced, as the cells were treated with KLF6 shRNA. However, it was interesting to find that the *Klf6* gene was directly bound by KLF6 through the ChIP-sequencing study. This finding suggests that KLF6 may participate in a feedback loop regulating its own expression. As little is known about the transcriptional regulation of KLF6, this finding provides insight for one new mechanism.

I selected KLF6 from our gene expression profiling dataset of migratory subpopulations for further study. Yet, the profiling study provided several potentially interesting targets that may be important for HCC progression and metastasis. For example, ID proteins 1-3 have increased expression in our HCC subpopulations. Increased ID1 and ID3 have been associated with increased metastasis in gastric, pancreas, and breast cancer (Tsuchiya et al. 2005; Gupta et al. 2007; Shuno et al. 2010). Potentially, the increased ID protein expression may be important for HCC progression in addition to impacting migration in our HCC cell lines. Also, several chromatin regulators appear in this dataset, including HMGA1 and 2. Altered expression of these regulators have been demonstrated in several human cancers (Fusco and Fedele 2007), and may result in a host of gene

expression changes that could increase migration and metastasis in HCC cells. Previous studies have demonstrated promotion of metastasis as a result of chromatin remodeling (Gupta et al. 2010). KLF6 was an excellent candidate for further study from the HCC subpopulation profiling study due to its expression pattern in human cancer, and its known role as a tumor suppressor in HCC. Yet, deeper interrogation of this dataset may reveal additional factors important to HCC metastasis.

$p53^{R172H}$ gain-of-function properties in HCC

Previous reports have found that some common p53 mutants have gain-of-function properties in cancer cells. These gain-of-function effects occur in the context of *p53* deletion, so they are not simply due to loss of tumor suppressor activity. Examples of this gain-of-function behavior include increased tumorigenesis, decreased survival, and increased tumor cell dissemination in mice with a p53 mutant compared to tumors without p53 (Olive et al. 2004; Caulin et al. 2007; Morton et al. 2010; Acin et al. 2011; Cooks et al. 2013; Lu et al. 2013).

Previously it was shown that p53 loss drives progression and metastasis of HCC (Lewis et al. 2005). Also, p53 mutation is associated with a higher rate of HCC relapse and poorer survival (Woo et al. 2011; Liu et al. 2012). Since p53 mutations are enriched in late stage HCCs (Oda et al. 1992; Buendia 2000), I hypothesized that one of these mutants, $p53^{R172H}$, resulted in gain-of-function properties in HCC.

Instead of finding that $p53^{R172H}$ enhanced properties of tumorigenesis, we found no differences between *p53*$^{R172H/fl}$ and *p53*-null tumors or tumor-derived cell lines. The results of these experiments indicate that $p53^{R172H}$ does not enhance tumor-associated properties of HCC compared to p53 loss. Interestingly though, I found that $p53^{R172H}$ is required for the phenotypes of HCC cell lines that endogenously express the mutant.

If inhibitors to p53 mutant gain-of-function activities become available, my results show that patients with p53-mutant HCCs may still benefit from this treatment, despite no measureable differences between tumor types. Reduction of this activity, as shown in our cell lines with p53 knockdown, may impair growth and migration of these tumors. An approach to test this possibility would be to use an inducible $p53^{R172H}$ mouse, where expression of the mutant could be reversed after tumor formation. Despite not displaying enhanced properties when compared to the *p53*-null tumors, deleting the *p53* mutant in tumors that have grown dependent on it may reveal "oncogene addiction" to the p53 mutant. While no inhibitor exists for R172H, a compound has been developed which stabilizes a different structural mutant, resulting in reactivation of wild-type p53 function (Liu et al. 2013b), so R172H may eventually become a druggable target.

Exploration of p63/p73 target genes in our tumor-derived cell lines, and those with p53 knockdown, revealed that p63/p73 activity was repressed in both $p53^{R172H}$ and *p53*-null cell lines. My hypothesis is that p63/p73 deregulation is

crucial for HCC formation or progression. Investigating this possibility would be an exciting avenue for HCC research.

Modulation of the levels of these transcription factors in mice and HCC cell lines is an interesting approach to determine if p63 or p73 are important for HCC. Interestingly, mice with heterozygous deletion of both *p53* and *p73* form spontaneous HCC (Flores et al. 2005), suggesting that there may be synergistic tumor suppression in hepatocytes between these two proteins. In these tumors, the remaining copy of *p73* is lost. However, mice with *p63* and *p53* heterozygosity do not form HCC (Flores et al. 2005), indicating that *p73* loss alone may cooperate with p53 inactivation for HCC development. Yet, p63 and p73 expression is increased in HCC compared to normal liver (Stiewe et al. 2004; Petitjean et al. 2005). In fact, increased p73 levels are correlated with poor prognosis (Tannapfel et al. 1999), suggesting that further experimentation needs to be done to determine in which contexts p63 or p73 inactivation occurs, and which particular isoforms of these proteins are being expressed.

p63/p73 are expressed from two different promoters, TA and ΔN, from which each message can be alternatively spliced (Benard et al. 2003). The ΔN isoforms are thought to function as dominant negative transcription factors, yet they also have unique transcriptional targets as well. The TA isoforms generally have similar behavior to p53, and regulate many cell cycle-related genes (Courtois et al. 2004; Murray-Zmijewski et al. 2006). It would be interesting to determine if the spectrum of p63/p73 isoform expression changed upon HCC formation or p53

inactivation. During the course of my studies, I attempted to identify the expression levels of specific p63 and p73 isoforms in p53 null and $p53^{R172H}$-expressing HCC cells, but these attempts were unsuccessful. Based on my studies of p53-family target gene expression, many of the targets affected by mutant p53 knockdown were those that were targeted by the TA isoforms. However, expression of the genes associated with the TA isoforms can also be impacted by the ΔN isoform's dominant negative activity (Murray-Zmijewski et al. 2006). Since previously used mouse models delete all isoforms of *p63* and *p73* (Flores et al. 2005), it is difficult to interpret how the balance of these isoforms impacts HCC *in vivo*. Instead, examination of HCC development and progression through the use of TA or ΔN-specific *p63/p73* knockouts (Tomasini et al. 2008; Su et al. 2009; Wilhelm et al. 2010; Romano et al. 2012) may prove more valuable. In addition to exploring the impact of isoform-specific *p63/p73* loss in HCC, it would also be interesting to determine how increased expression of particular p63/p73 isoforms would impact HCC cell phenotypes *in vitro*.

The only mechanism for gain-of-function I investigated is inactivation of p63 and p73. Of course, other mechanisms of p53 gain-of-function activity may also be occurring in the *p53* mutant and *p53*-null HCC cell lines. For example, p53 mutants have been shown to bind to and inactivate other transcription factors (Chicas et al. 2000; Di Agostino et al. 2006; Freed-Pastor et al. 2012). Similarly to what I have shown with p63/p73 activity, the activities of these other transcription factors may be reduced in *p53*-null cells.

In this study, I only examined a small number of p63/p73 target genes. Further analysis of p63/p73 transcriptional targets in HCC may be valuable for determining if the effects seen upon decreased p63/p73 activity are due to target genes that overlap with wild-type p53, or are unique to the other family members. It may be informative to modulate the expression levels of p63 and p73 in HCC cells and subsequently perform gene expression profiling in order to determine transcriptional target genes of these factors specific to HCC.

One potentially important factor deregulated in our *p53* mutant and null cells is Dicer. Dicer is a transcriptional target of p63, and upon mutant p53 expression, its transcription is inhibited via p63 (Su et al. 2010). I showed that the $p53^{R172H}$ mutant repressed Dicer expression in HCC cell lines, since its expression increased in response to p53 knockdown. Regulation of Dicer has been shown in many contexts to be important in cancer. In particular, decreased Dicer expression has been shown to induce metastasis (Han et al. 2010; Su et al. 2010; Muller et al. 2014). In tumors with nonfunctional p53, Dicer may be one of the important mediators of tumor progression and metastasis.

Previous studies of p53 mutants in HCC used ectopic expression of the mutants in *p53* null cells to test for gain-of-function activity (Gouas et al. 2010; Schilling et al. 2010). I did not perform a similar experiment in this study. However, if my hypothesis is true, expression of $p53^{R172H}$ in *p53*-null cells would have no effect, since p63/p73 activity is already inhibited in *p53*-null HCC. Also, ectopic expression of p53 mutants may provide artifactual results. Since the mutant forms

of p53 are not efficiently degraded, the mutant protein accumulates (Bartek et al. 1991). However, its transcription is still regulated by endogenous conditions. Forced overexpression of these mutants may result in a larger accumulation than would typically occur. Since mutant p53 binds to many transcription factors to alter their behavior, ectopic amounts of mutant p53 may result in greater transcriptional inhibition that may not otherwise occur. In my studies described in this dissertation, the use of an *in vivo* knock-in construct likely resulted in lower levels of p53 mutant expression than ectopic expression systems.

In this study, I only examined the potential effects of the $p53^{R172H}$ mutant. This structural hotspot mutation, correlating to human R175H, occurs frequently in HCC (Olivier et al. 2010), however, the most frequent mutations occur in the DNA binding domain (Oda et al. 1992). While $p53^{R172H}$ did not provide enhanced tumor properties as compared to p53 loss, other p53 mutants, specifically those in the DNA binding region, may provide enhanced tumor properties. Similar to the R172H allele used in our study, a conditional knock-in allele exists for the DNA binding domain mutant R270H (Olive et al. 2004). Perhaps in combination with our HCC model, this DNA binding mutant would provide enhanced gain-of-function characteristics.

It would also be interesting to perform a similar experiment using the $p53^{R249S}$ mutant, which is associated with exposure to AFB1 (Bressac et al. 1991; Ozturk 1991; Stern et al. 2001). Since this mutation is enriched in HCC specifically (Thongbai et al. 2013), this mutation may provide advantages to the formation and progression of HCC. *In vitro* studies of the R249S mutant demonstrated that cells

that endogenously express the mutant rely on its expression for proliferation (Gouas et al. 2010). However, ectopic expression of this mutant in *p53*-null cells did not provide a proliferation advantage (Gouas et al. 2010), reflecting a similar outcome to my R172H data.

While $p53^{R172H}$ did not enhance phenotypes in our PyMT-driven HCC model, the use of another HCC mouse model may provide a different outcome. A similar observation has been made in models of skin carcinogenesis. In two mouse models of skin cancer, one demonstrated gain-of-function properties with p53 mutation versus p53 nullizygosity (Caulin et al. 2007), while a different mouse model showed no gain-of-function activity upon mutant expression (Wijnhoven et al. 2007). Clearly, the context in which these tumors are formed is important for dictating p53 gain-of-function properties. PyMT is a very potent oncogene that results in relatively fast HCC formation and metastasis, which can be detected beginning at 4 months of age (Lewis et al. 2005). HCC mouse models induced by DEN or transgenic c-MYC develop tumors with a longer latency of approximately nine months to one year (Vesselinovitch et al. 1978; Sandgren et al. 1989). Rates of metastasis are also low in these models (Heindryckx et al. 2009) relative to the RCAS-TVA system. Perhaps in a tumor environment with a weaker oncogenic stimulus, p53 mutants would have the opportunity to display enhanced gain-of-function properties compared to *p53*-null HCCs.

Our study of $p53^{R172H}$ in HCC explains that the p53 mutant is acting in a gain-of-function manner through inhibiting p63 and p73 target genes. However, p63 and

p73 transcription factors are also inhibited in *p53*-null cells, suggesting that multiple pathways converge on inhibition of p63 and p73 in HCC cells. This result indicates that inhibition or loss of these factors is likely important for HCC development or progression. While KLF6 loss results in an increase in progression, $p53^{R172H}$ does not enhance HCC progression beyond loss of wild-type p53 function.

Factors regulating HCC progression and metastasis

Together, the data in this dissertation describe the roles of two transcription factors in the progression of hepatocellular carcinoma. Both *p53* mutations and decreased KLF6 levels are common alterations in HCC. Interestingly, these alterations occur most frequently in advanced HCCs (Oda et al. 1992; Tarocchi et al. 2011), providing a correlation with *p53* mutation or *Klf6* loss and poor prognosis. While there is a correlation between each of these changes and progression of HCC, the direct impact of these factors on disease progression and metastasis had not been experimentally demonstrated *in vivo*.

As *p53* deletion has previously been shown to drive HCC progression (Lewis et al. 2005), I chose to determine if the addition of $p53^{R172H}$ or impairment of KLF6 in a *p53*-deleted background would contribute further to HCC formation and dissemination. In the case of KLF6, reduced levels increased tumor formation and metastasis in an HCC mouse model, indicating that the decreased KLF6 levels in human HCC are driving tumor progression, and are not simply correlative. Conversely, despite the correlation of *p53* mutations with advanced HCC, $p53^{R172H}$

did not increase HCC formation or metastasis compared with *p53*-deleted HCCs. Since $p53^{R172H}$ is not significantly different from *p53* deletion in HCC, the enrichment of p53 mutations in advanced HCCs may be more important for the inactivation of wild-type p53, not necessarily for p53 gain-of-function mutant effects.

Many gene expression changes have been found which correlate with HCC formation and progression, but few of these have been experimentally validated (Buendia 2000; Guichard et al. 2012). As many of these gene expression changes or mutations are likely passenger alterations, and not drivers of disease formation and progression (Stratton et al. 2009), it is of great importance to determine the impact of such changes on tumor biology *in vivo*. Here, my work clarifies the roles of two factors that correlate with disease progression, but had not yet been experimentally validated.

In both cases, my studies revealed deeper mechanisms of HCC progression. The $p53^{R172H}$ study highlighted the important role of deregulation of all p53 family transcription factors in the development and progression of HCC, while the KLF6 study demonstrated that modulation of RHO GTPase activity, particularly RAC1, was critical for HCC progression. In addition to describing the impact of these transcription factors, my work raises additional questions regarding the precise roles of p53 family transcription factors and RHO family GTPases in HCC. Further inquiries into these mechanisms of action may provide valuable insights into the molecular biology of HCC progression and metastasis.

APPENDIX A

Gene Expression Profiling of BL185, BL185-M1, and BL185-I1

Gene Symbol	p-value	BL185 vs M1 Fold Change	BL185 vs I1 Fold Change
Mycn	2.39E-05	18.6375787	21.92951528
Dmrta1	3.20E-05	13.43135873	13.79859477
Krt14	5.45E-05	0.405941934	0.100849029
Clca6	7.88E-05	49.46753717	48.73798558
Hpgd	0.000129027	2.70054023	0.345928549
Ly6c	0.000129027	0.376424315	0.249573755
Krt14	0.000129027	0.335509077	0.051971174
Ndg2	0.000143443	13.91304206	7.244953207
Mgam	0.000184463	5.366939524	5.286514101
Gzme	0.000184463	0.455505339	0.250239357
Mcm5	0.000185127	0.159742875	0.209918025
Gdf15	0.000229696	24.76443866	19.77608647
Gm566	0.000229696	12.74775397	9.999858263
Trim15	0.000229696	11.50037045	9.865779468
Stmn2	0.000229696	4.342090262	0.118859642
Prom1	0.000260977	7.598896642	6.666250826
Birc5	0.000267867	0.132577809	0.154837931
Col5a1	0.000312657	0.130465841	0.173618314
Tuba1a	0.00033154	0.246154762	0.223663286
Rrm2	0.000339447	0.259549069	0.212695281
2810417H13Rik	0.000408539	0.109033935	0.124625055
Mki67	0.000512992	0.096584723	0.134327603
Hmgn2	0.000573548	0.072591042	0.078038154
Rhox5	0.000575766	9.51929988	6.648035149
Cd68	0.000575766	9.241268579	8.284852645
Kif22	0.000609119	0.291821874	0.277267085
Gsta2	0.000681866	1.672830462	0.461679204
B4galnt2	0.000681971	31.00832904	5.398460685
Aldh1a3	0.00078359	13.57021799	11.74228475
Ccna2	0.00078359	0.160327391	0.210230541
Kif23	0.000821484	0.206486363	0.229328161
Shcbp1	0.000821484	0.132108326	0.117017508
Birc1a	0.000831581	7.397381319	6.451565196
Ccna2	0.000831581	0.207521022	0.209499818
B4galnt2	0.000858941	13.43900288	6.905011745
Fxyd5	0.000858941	0.549493176	0.500280512
S100g	0.000938233	0.203420138	0.133831786

Rrm2	0.001001502	0.309522535	0.273187889
Col6a2	0.001001502	0.228811206	0.178982549
Cxcl12	0.001065678	0.379581912	0.331175989
Ccl2	0.001150694	0.0587104	0.141226559
Sprr2a	0.001167813	0.461653513	0.186225514
H2-Q10	0.001188912	5.196063734	4.502334444
Ceacam18	0.001188912	3.85500891	2.573901319
S100a4	0.001188912	0.192772807	0.093405326
Crip1	0.001188912	0.155366895	0.165823822
Vip	0.001388077	42.96012439	10.19985173
Car2	0.001388077	3.703279751	2.935311531
Nat8l	0.001479271	8.50595813	3.701949288
Slc25a30	0.001485264	4.757805021	4.645708015
Cdca3	0.001506506	0.102361965	0.102684126
Gtpbp2	0.001565198	5.784610987	5.793257624
Rnf125	0.001565198	5.364633199	4.1211531
2310042E22Rik	0.001565198	4.507976615	2.021794581
C2	0.001565198	2.748384477	2.118224761
Tmem150	0.001565198	2.639858073	2.891269735
Fabp5	0.001565198	0.261182698	0.352207506
Kif2c	0.00164263	0.164520983	0.147895914
Lgals2	0.001679597	0.45963143	0.29286788
Pbk	0.001679597	0.233091385	0.22720511
Ndg2	0.00168768	11.09178021	6.366892347
1500012F01Rik	0.00168768	3.048062774	2.92992758
Scn5a	0.00168768	0.357007272	0.432910309
Tk1	0.00168768	0.13246388	0.154810843
Rrm2	0.001710233	0.250778068	0.231417167
Cln8	0.001795062	3.235371296	3.010591634
Cdc2a	0.001795113	0.301991565	0.342410119
Itm2a	0.001863812	8.113299015	6.417352279
Col6a1	0.001863812	0.302883597	0.232177251
Cdc20	0.001863812	0.239972407	0.223270708
Tcf19	0.001988745	0.246090294	0.236449549
Gjb2	0.002025843	4.089875847	2.765315961
Gnas	0.002025843	2.668365898	2.712254741
Pbp2	0.002074216	4.597375368	3.149178861
Ttc7b	0.002074216	3.993139349	4.384765123
Slc43a3	0.002092196	8.539500955	3.740860053

Col6a2	0.002111372	0.152533389	0.104357651
Ddit3	0.00225376	7.674901119	5.462215623
Cdc42ep2	0.00225376	0.314670964	0.250770079
Tanc2	0.002276568	8.353457533	7.519863658
Car8	0.002277827	13.40770237	9.669765711
Satb1	0.002277827	9.980816392	2.998524811
H2afj	0.002277827	0.288601132	0.308472515
Satb1	0.002305913	7.387540883	4.123368563
Aldh1l1	0.002315686	1.850749281	1.62166328
Serac1	0.002319768	2.129592902	2.630595998
Akr1b7	0.002347205	10.00415576	9.023839623
Tmem56	0.002404173	4.265227354	4.287337653
Car6	0.002407202	11.76049839	10.67819155
9130404D08Rik	0.002421784	2.456459733	2.5650147
AI427515	0.002421784	0.133804922	0.245275532
5430416N02Rik	0.002428494	6.521265278	5.847574995
Lpl	0.002428494	4.995256933	4.179503256
Larp7	0.002428494	0.485891191	0.44865231
Heph	0.002448915	1.97756035	1.785323755
0610040J01Rik	0.002609922	3.170831449	2.212745637
Maoa	0.002628791	6.200781364	6.392601621
Sh3kbp1	0.002628791	2.945509819	3.146046524
Cnp1	0.002628791	0.6148689	0.56719914
Havcr2	0.002660547	2.789643321	2.49425754
Tuba3a	0.002660547	0.266672981	0.278331475
BC049816	0.002762239	0.076571467	0.09472858
Sacs	0.002800323	1.978546638	2.790111466
Ube2c	0.002800323	0.356289528	0.391130866
Mga	0.002807775	2.067792488	2.37923582
Myd116	0.002863067	11.0015357	8.389082981
Scn8a	0.00289813	1.682878867	1.493569168
Ccnb2	0.002910421	0.203910928	0.195201907
Dsc2	0.002915285	5.089732546	3.884417611
Anapc13	0.002915285	0.448165939	0.411443085
Fstl1	0.002915285	0.080751652	0.057807969
Sprr2a	0.002923687	0.427996513	0.198106631
Reep6	0.002946149	4.308801874	3.64443214
Wnt4	0.002946149	0.137831842	0.184229124
Cdca8	0.002956814	0.371015488	0.354524363

2310005L22Rik	0.003005639	7.071257653	6.977522197
Raet1a	0.003005639	2.951882895	2.482828103
Cdca5	0.003053732	0.208856415	0.253185529
Plf	0.003160388	16.87659228	2.864550974
Slc43a2	0.003160388	0.413383025	0.4108956
D17H6S56E-5	0.003160388	0.231502028	0.150070873
Avil	0.003231914	10.86951594	9.710844132
Hmga1	0.003276515	2.174638153	2.808999473
Tnfaip8l1	0.003316898	0.617146926	0.428423737
Stbd1	0.003343569	9.424871693	6.97270258
Nupr1	0.003343569	7.030942443	2.802195248
Cenpa	0.003343569	0.326684987	0.31820146
9830002I17Rik	0.003345046	0.320290408	0.509076082
Aqp9	0.003346091	9.725736834	4.471851405
Aqp9	0.003355926	5.061157756	5.119970407
Lztr2	0.003370842	8.110647202	7.690225763
Pgf	0.003370842	6.068129433	1.986675282
Lig1	0.003370842	0.289228131	0.318503238
Jag1	0.003380836	8.441030547	7.609053136
Ctsb	0.003380836	5.762991784	4.697654329
Huwe1	0.003380836	3.230397832	3.780980187
Ddi2	0.003380836	2.535337211	2.634034996
Otop1	0.003380836	2.386642494	2.341595805
Epas1	0.003380836	2.184525182	1.892805152
Smc2	0.003380836	0.267271479	0.309817248
Angptl6	0.003387493	6.379059112	6.176217693
Akap8l	0.003413976	2.469212931	2.426041069
Rest	0.003418441	1.767371977	1.65779857
Ncapd2	0.003418441	0.22014273	0.218884139
BC049816	0.003418441	0.135254683	0.187225885
Hgfac	0.00342034	3.418429355	1.898945349
Lsm3	0.003429556	0.27056332	0.318569166
2210401J11Rik	0.003545207	4.471608043	2.475072819
Cep55	0.003584969	0.199142696	0.202241445
1810032O08Rik	0.00370203	6.386847794	5.639073389
Tgfb3	0.003736714	0.259113616	0.274210174
Mfap3l	0.003761304	2.408058941	2.311745334
Fstl1	0.003761304	0.062336499	0.038959192
Cd53	0.003765784	3.155197537	2.7467338

Cxcl5	0.003769452	0.077580132	0.046876531
Huwe1	0.003964862	3.142123289	3.719125522
Ank2	0.003964862	3.068432553	3.539632603
Trib3	0.003998194	6.131089217	4.436612157
Cyp3a13	0.004015636	11.07515808	3.562844286
Twist2	0.004160686	0.312499903	0.489143177
Pole	0.004257385	0.322122536	0.460566342
Cxxc5	0.004261471	0.375735093	0.353465612
Grpel2	0.004296769	2.865441868	3.026812365
Pbxip1	0.004296769	2.181578256	1.71670266
Tuba4a	0.004296769	0.4770419	0.418422345
Timp1	0.004296769	0.281109068	0.237884929
Spbc24	0.004296769	0.21058255	0.226910994
Crisp1	0.004296769	0.047731174	0.245570826
D730039F16Rik	0.004335042	1.762606882	1.535282971
Ptprn	0.004335042	0.643962612	0.543054104
Id1	0.004335042	0.369807147	0.344101804
D1Ertd471e	0.004335042	0.290024105	0.290143477
Spbc25	0.004335042	0.237648931	0.209267228
Cdkn3	0.004335042	0.216093608	0.222060151
Pmm1	0.004380462	3.854389798	5.244775151
Eomes	0.004427627	2.263818863	2.540458063
B230342M21Rik	0.004444724	5.169177764	5.626542628
Cd55	0.004499567	2.650051684	2.817223611
BC046404	0.004525636	3.354977946	1.729799874
Ank2	0.004525636	3.079181469	3.091242588
B4galnt2	0.004537752	4.287928948	4.688302614
Slu7	0.004537752	2.000053604	2.329546268
Tm4sf1	0.004562696	2.464366268	2.747697856
Acot2	0.004660806	5.037065763	4.150102355
Jmjd3	0.004672581	3.336412631	3.071116775
Tuba3a	0.004672581	0.466450303	0.515030789
Pcp2	0.004672581	0.400490811	0.290675938
Mst1	0.00468969	3.12507587	2.648749214
Lphn2	0.00468969	2.754194166	2.545547858
Ak5	0.004716756	1.834402562	1.992410279
Cd55	0.004779253	2.982454609	3.347356478
Bre	0.004779253	1.785713869	2.01396938
Tubb2c	0.004839628	0.298692208	0.309187368

Uhrf1	0.005012925	0.218668144	0.268281785
Ces2	0.005068817	2.990894277	2.67604044
Cp	0.005123234	0.26846989	0.20060232
Nid1	0.005156882	3.899856036	3.299288401
Gm440	0.005281574	4.315897494	2.326937588
Cdca2	0.005290859	0.336689025	0.349005791
Atf6	0.005298598	2.640694983	2.511624153
D2Ertd750e	0.005298598	0.275068403	0.264191367
Bub1b	0.005299275	0.209473312	0.186626628
Ahcyl1	0.005304355	3.008933793	3.308694694
Snai2	0.005360215	1.660494723	1.712081211
Fkbp11	0.005404579	6.551865835	3.124299458
Sparc	0.005453296	0.165383853	0.159509936
AI788777	0.005538418	0.362509817	0.290067576
Rrm1	0.00555708	0.321307301	0.323304876
Sqstm1	0.005610451	3.894036414	3.448486413
Opa3	0.00574786	0.635147915	0.52200986
Pttg1	0.005765046	0.327759801	0.346709267
Btbd11	0.005776891	7.052830376	3.212251214
Tacc3	0.005776891	0.235314541	0.202752938
Nup98	0.0058216	2.424878723	2.818199664
D17H6S56E-5	0.005914234	0.251538051	0.151888159
Nrip1	0.006055285	6.105619172	6.545867466
Mxra7	0.006055285	0.459141196	0.634460063
Rbbp6	0.006190431	2.641662691	2.898644339
Ndrg1	0.006272831	6.191152368	4.35462388
Col27a1	0.006272831	0.334014453	0.396889817
Btbd11	0.006311773	5.429511859	3.670597348
Cul2	0.006311773	3.13900827	3.866685054
Ogt	0.006311773	2.365527919	2.628122714
Dlc1	0.006311773	2.105636175	2.402184807
Pcolce	0.006311773	0.269214586	0.209143523
Sparc	0.006323938	0.22004752	0.224062226
Soat2	0.006376737	7.084411896	3.798369162
Ppp1r3b	0.006386857	10.58282098	3.378103779
Cdkn2c	0.006420512	0.239964022	0.264767418
Gpt2	0.006430655	3.826563971	3.972113943
Napb	0.00644782	2.729279802	2.198240615
Cd38	0.006460134	1.606239004	1.571578078

Rps25	0.006460134	0.317540211	0.345471896
Abcc2	0.006558454	2.50420391	2.636925648
Zfp397	0.006657147	2.339503569	3.386951791
Ereg	0.006700752	17.15577855	8.59044318
Cxcl1	0.006700752	0.246422779	0.220447473
Tyms	0.006722994	0.248980217	0.244217182
Zfand2a	0.006742236	4.277176127	4.093326388
Nr4a1	0.006746412	2.553788111	2.522113538
Sh3bgrl2	0.006828712	3.206613344	2.767700949
1200009I06Rik	0.006847792	0.147158072	0.194759019
Trim35	0.00686979	4.997793564	4.045270863
Ppp1r2	0.00686979	2.295819596	2.107389121
Aurka	0.006883334	0.269317248	0.28400712
Hist1h2ao	0.006883334	0.260059986	0.30599703
Spns2	0.006883334	0.220127279	0.244512902
Fgb	0.006897418	3.440699749	3.821076678
Obfc2a	0.006918388	5.336790648	5.362519937
Ddit4l	0.007019898	0.495832534	0.356366039
Pvr	0.007025532	6.071980281	7.379161519
Glrb	0.007093003	2.938551132	3.039268773
4930402H24Rik	0.007132943	3.042041509	1.893389324
B230112P13Rik	0.007158195	5.046418004	3.97071133
Adar	0.007158195	2.022404273	2.107131558
Cp	0.007205511	0.348095145	0.272988514
Tmem140	0.007263509	4.24390777	3.124400018
Clybl	0.007300366	4.04136411	2.677648644
Etv5	0.007300366	1.976105101	2.302483
Klf6	0.007304121	3.448900107	3.433727988
2410014A08Rik	0.007456514	0.249784684	0.204646276
Col27a1	0.007492421	0.326163463	0.472722706
9430098F02Rik	0.007646717	1.995878058	2.347690936
Plk1	0.007646717	0.200046085	0.202035917
Pitpnb	0.00776292	2.097710663	2.984063107
Ptprt	0.007766094	5.719380232	5.884702622
Msn	0.007766094	4.448308361	5.625372626
Tiparp	0.007766094	3.902708192	3.950750787
Zfand2a	0.007766094	3.691311831	5.035703903
Stom	0.007766094	3.417598009	3.716305706
Ankrd11	0.007766094	2.975994968	2.79775562

Cdr2l	0.007766094	2.948897314	3.532654819
B3gnt2	0.007766094	2.841474759	3.194691351
Pcdh19	0.007766094	0.408328151	0.411071256
AW552393	0.00777326	2.169005285	2.43482012
Igf2r	0.007822466	1.878529116	2.076339412
Lhfpl2	0.007948874	6.346813839	5.902136867
Hmmr	0.008042175	0.250816633	0.210438821
Ccnb1	0.008046787	0.318796849	0.313160084
Cxadr	0.008068775	3.927920599	4.549661769
Lrrc14	0.008068775	2.615768667	2.823374088
Cela1	0.008093119	4.362505475	4.922844857
H2afx	0.008108546	0.320313556	0.495122063
D10627	0.008205985	2.800107958	3.32109035
Dnaja3	0.008207976	2.900585138	3.064245352
Lmna	0.008304088	0.299720215	0.239380289
Tspyl1	0.008313343	1.651126984	2.080666997
Efemp2	0.008313343	0.268142172	0.303809938
D430039N05Rik	0.008328109	5.037348891	6.41977022
Ptpn22	0.008328109	3.048130019	3.498230938
Bub1b	0.008328109	0.245386719	0.247852777
Zfp655	0.008342735	2.354780819	3.027205273
Ocln	0.008419169	3.340707802	2.215239498
Napb	0.008438884	3.065011026	2.815338161
D1Ertd448e	0.008664401	4.083053616	5.651186879
Itpk1	0.008707775	4.652633434	2.366706372
Rfc5	0.008707775	0.33189261	0.395448626
6720460F02Rik	0.008758216	0.239979922	0.281063629
Plxna2	0.008995637	0.537509571	0.537032246
Tnrc15	0.009079687	2.960500154	3.1737458
Uqcrh	0.009079687	0.54532322	0.492810174
Ncapg	0.009079687	0.23704754	0.231459724
Cldn23	0.00911783	2.589381383	2.626006565
5730410E15Rik	0.009177103	2.588479403	3.165095723
Cenpf	0.009369253	0.185049472	0.254900737
Pmm1	0.009503746	4.211083819	3.794669233
Acsl1	0.009618901	1.89648253	2.20310998
0610012G03Rik	0.009732567	20.83775615	11.46154
Bmp1	0.009775294	0.404826029	0.374812676
Casp4	0.009916431	1.696185077	1.801113569

Slc43a2	0.009920598	0.484457602	0.511793495
H2-Q8	0.009954765	2.337085793	2.557542925
Mbnl2	0.009976159	2.709514363	2.832646077
Hif1a	0.01001529	3.656682431	4.102682672
Tmed5	0.010021225	3.149186124	3.340402744
Arhgap5	0.010021225	2.863143686	2.299248759

APPENDIX B

Gene Expression Profiling of HCC Cells with KLF6 knockdown

Gene Symbol	p-value	Fold Change (log2) Knockdown v. Control	Gene Symbol	p-value	Fold Change (log2) Knockdown v. Control
Plau	3.85E-06	1.762227291	Spata6	0.002453886	-0.593753526
Uap1	1.35E-05	-1.458238381	Gstm2	0.002467081	0.984571765
Uap1	2.37E-05	-1.595251461	Epcam	0.002472838	1.709331708
Dlc1	2.46E-05	1.860343451	Lrrfip1	0.002490078	-0.600132767
Mycl1	3.07E-05	1.187973114	Tgfbi	0.002501542	2.082084519
Smpdl3b	3.28E-05	1.393190011	Gm11818	0.002508045	-0.74861109
Ppm1a	3.42E-05	-1.235872998	Pabpc4	0.002523909	-0.620052197
Fam107a	3.81E-05	1.603192983	Mtm1	0.002526668	0.5885022
Dlc1	3.87E-05	1.649607222	Enpp1	0.002530293	0.832551137
Prkaa2	4.15E-05	-1.228875689	Leprot	0.002546544	-0.649815254
Ctnnal1	4.88E-05	1.091069077	N4bp2l1	0.002610284	1.664306702
1200002N14Rik	5.64E-05	1.153656265	Smpd3	0.002623292	-0.742017872
Lamb1-1	8.06E-05	1.37449819	Skp2	0.002631105	0.641314392
Crip1	8.46E-05	-1.444911446	Twist2	0.002641133	-0.902721013
Prom1	9.48E-05	1.064690626	Hoxb5	0.002641651	0.686547268
A030004J04Rik	9.64E-05	2.240787245	Ddhd1	0.002649767	0.743719439
Gpr116	9.70E-05	0.981431899	Ly6c1	0.002659032	1.407139429
Fbln1	9.71E-05	1.944755032	Wiz	0.002668493	0.66522312
Tor1b	0.000104083	-1.06211018	Bicd1	0.002677934	-0.748573055
Avpr1a	0.000106961	1.293061077	Ston2	0.002706969	-0.638325833
Car12	0.000116075	1.051635899	Leprot	0.002720669	-0.793291941
Flrt2	0.000127149	1.069131875	Id2	0.002726102	-1.240178267
Macc1	0.000140945	1.80713777	Nudt6	0.002727083	0.691211849
Cmtm3	0.000141562	1.307394006	Sema3d	0.002736656	0.78781102
Plau	0.000144508	0.898393979	Cdca7	0.002746019	0.638588898
Pno1	0.000175537	-1.108917851	Gpbp1	0.002763384	0.606273759
1810055E12Rik	0.000185123	-1.211232778	Adamts1	0.002773951	0.920852928
Uap1	0.000185349	-1.397032621	Mettl1	0.002779502	-0.696047218
Lrch2	0.000193094	0.89374528	2010003O02Rik	0.00278764	-0.72021946
Enpp1	0.000193738	0.91516716	D13Ertd608e	0.002841484	-0.703509474
Zdhhc2	0.000202895	-1.033982934	Stard5	0.002846852	0.626408274
Ubxn2a	0.000205648	-1.93552093	Fam107a	0.002851129	0.670444996
Ube2w	0.000206028	-1.016143921	Lhfpl2	0.002869439	0.641930757
Gzme	0.000218115	1.728697861	Sall1	0.002881167	-0.641365883
Pkdcc	0.000235341	0.976024437	Adcy9	0.002883211	-0.646212959

Tgfbi	0.000235721	2.432722606	Spire1	0.002905422	-0.671742014
Serpinb8	0.000236422	-0.892405159	Slc37a3	0.00291557	-0.881818225
Gzme	0.000245797	1.213091255	Ndrg4	0.002927438	-0.607961889
Ptgds	0.000257894	0.915802085	Hmgcr	0.002976248	-0.688581361
Slain1	0.000258932	-0.864212256	Sprr1b	0.003018385	0.833404305
Tor1b	0.000272519	-0.85966816	Krt80	0.003018871	0.723031504
Hnmt	0.000272607	0.990894098	Lactb2	0.003036363	-0.613108731
Cxxc4	0.000277449	-0.827243541	Cep97	0.003047418	0.610562712
Cxcl16	0.000281491	1.329128217	AI467606	0.003063955	0.842655771
Slc24a3	0.000285904	1.04927184	Fam57a	0.003076916	-0.651060824
Fbln1	0.000289824	1.944486384	Krt39	0.003096599	1.210944376
Plekha7	0.000293592	-1.08035233	Hpdl	0.003097405	-0.586945416
Eif4e3	0.000305286	-0.799969177	Fmn1	0.003099178	1.245452029
LOC100048050	0.000312838	1.510576777	Cyp4a10	0.003107953	-0.915239301
Cpt1a	0.000318386	-1.06928744	1436240_at	0.003109123	0.597759426
Adamts4	0.000327324	0.820603936	Suv420h1	0.003113982	-0.656433231
Sfmbt2	0.000333262	-1.036548793	Smpd3	0.003166642	-0.724985306
Nipa1	0.000343719	-0.794493839	Rhob	0.003169701	-0.591417425
Camk2d	0.000377908	-1.260358184	2310057J16Rik	0.00317018	-0.989643753
Sult4a1	0.00038701	-0.853113356	Has2	0.003181107	0.874945939
Zdhhc2	0.000388686	-0.925556158	Tspan17	0.003191299	-0.817715937
Arhgap29	0.000394635	0.753213937	Athl1	0.003193568	-0.648430875
Pja1	0.000401214	-0.767175476	Zfhx4	0.003197246	0.749487626
Sod2	0.000404688	-0.837673732	Ephx2	0.003210472	-0.684959306
Dsp	0.000407098	-0.751876163	Eif4e3	0.003216935	-0.663110312
Ubxn2a	0.000413005	-0.965959667	Metrnl	0.00321999	1.456363807
Ggh	0.000416947	-0.954220703	Spata6	0.003222242	-0.634014329
Cdc42ep3	0.000425647	1.26131205	Uap1	0.003243502	-0.599655866
Tanc2	0.000428004	1.157550031	Pgpep1	0.003261603	0.736779744
Serpine2	0.000431931	1.349082382	Tbc1d16	0.003262343	0.662670059
Ndst1	0.000441671	-0.790198948	Il1rn	0.00328888	0.765477963
Vsig1	0.000442809	-1.456836034	Adk	0.003290401	0.863637351
Ly6e	0.000442959	2.340338496	Gm1157	0.003292821	-1.037569456
2410076I21Rik	0.000449637	0.787459016	S100a3	0.003340096	-0.748867406
Cdc2l6	0.00045074	-1.508232133	Slc9a3r2	0.003341955	-0.83881258
Lamb1-1	0.000451749	1.17073545	Mmp3	0.003351317	1.032870846
Hspb8	0.00045521	-0.924313309	Sult1c2	0.003395405	0.833270127
Dnajc5	0.000459038	-0.750030372	Gdf15	0.003406838	2.319866057
A930035D04Rik	0.000472892	-0.916035222	Zdhhc6	0.003413213	-0.735314581

Bmp2	0.000481307	-0.914708689	Fam71f1	0.003417808	0.597405284
Hnrnpa3	0.000484357	0.738080121	Cldn1	0.003418355	1.334778266
Krtap16-7	0.000499333	-0.840030483	D730040F13Rik	0.003434316	-0.657039962
Zdhhc2	0.000500021	-0.756281451	Tln1	0.003455799	-0.753093218
Tanc2	0.000507302	1.327487172	Myo5b	0.003468442	-0.594849499
Kif23	0.000508846	-0.929172366	Fst	0.003499528	1.297545537
Cpne8	0.000515687	0.961393908	Prss23	0.003511766	1.363822334
Cpt1a	0.00051947	-1.319330216	Tom1l1	0.003541248	-0.600576648
B4galt6	0.000530262	-0.74804846	Chfr	0.003564194	-0.818534345
Aebp1	0.000530874	0.751007381	Ccbe1	0.003572192	1.067156342
Tpcn1	0.000534639	-1.093585369	Cpsf6	0.003606607	0.827469476
Prl6a1	0.000545961	1.134763655	Rps6ka6	0.003677601	0.980977038
Fam43a	0.000552051	0.721591372	Rbpms2	0.003693628	0.66468463
Rab27b	0.000561191	-0.793890464	Clmn	0.00371989	-0.596699734
Glt8d1	0.000562084	-0.819438728	Id2	0.003720923	-1.187599805
Kazald1	0.000571528	-0.81445701	BC016423	0.003722627	0.596626571
Dnajc5	0.000573002	-0.770015247	Itgb6	0.003734725	-0.900977262
Fgf1	0.0005815	-0.763496089	Ppl	0.003739264	-1.151328866
Dsp	0.000589639	-0.707657417	Kif1b	0.003761936	-0.661465698
Ptprd	0.000600743	0.69479981	Stc2	0.003819068	1.672313729
Gfra1	0.000611461	0.932708065	Tmem179b	0.003836678	-0.673865409
Epb4.1l1	0.000617977	-1.009455234	Gusb	0.003845331	0.71018386
LOC100048050	0.000618302	1.528132882	Lyrm2	0.003847246	-0.834024091
Nup50	0.000619507	-0.712909922	Cep97	0.003863294	0.625539176
Abcb7	0.00062169	-0.713172899	Ndufaf1	0.003867201	-0.796370982
Slc15a4	0.000627969	-0.769417161	Nudt19	0.003872934	-0.798582358
Tubb4	0.000628561	-0.853091152	1441020_at	0.003874182	0.635962493
Gnb4	0.000628739	-0.794626052	Id2	0.003874369	-1.211432958
Gata5	0.000638358	-0.707068056	Tmtc2	0.003909816	0.974676814
Lrrfip1	0.000641478	-0.751479748	Amot	0.003924561	-0.869329599
Ecscr	0.000650762	1.755329747	Pear1	0.003929477	-0.789815381
Plod2	0.000653801	-0.732403504	Gm16367	0.003948616	-0.710751714
D4Ertd22e	0.000656892	-0.786955765	Rgs3	0.003957554	0.70064593
Mfsd6	0.000660258	-0.952576887	Mest	0.003965405	0.780497753
Prkaa2	0.000665939	-1.239663201	Rnf157	0.003967367	0.654215347
LOC639910	0.000667632	-0.946096466	Igsf9	0.003973862	0.749251878
Tgfbi	0.000670379	1.986956398	Hltf	0.003974471	0.84665315
Flrt2	0.00068395	0.767922281	H2afz	0.004012187	-0.58885814
Serpinb8	0.000686434	-0.794526646	Lbh	0.004020555	0.725499543

Satb1	0.000688306	2.126210827	March2	0.004025173	-0.585214774
B4galt6	0.000694966	-0.703995706	Col1a1	0.004108703	0.710404915
Dctd	0.000705637	0.844990613	Trpt1	0.004111949	-0.585804457
Unc119	0.000708597	0.737088544	C76336	0.004114743	-0.908872103
C1galt1	0.000711502	0.901050835	Fam171a1	0.004117391	-0.610020099
Tm4sf1	0.000722311	1.833066055	Tgfa	0.004131855	-0.7583242
Arrdc4	0.00073047	0.864959032	Lpar2	0.004138072	0.822360831
1600021P15Rik	0.000731694	-0.988247795	EG628475	0.004143728	-0.756922855
Cdc2l6	0.000745553	-0.945297279	Fndc4	0.004171172	0.952767546
Mtap4	0.000746506	-0.953982527	Gja1	0.004187191	0.691949349
Pax8	0.000747102	0.791061267	Churc1	0.004189274	-0.598606281
Tomm22	0.000748676	-0.75407341	Gda	0.004193156	0.895138024
Tcf4	0.000749703	0.950342423	Oxct1	0.004200482	0.676369259
Ccnc	0.000751712	-1.091947263	Nsbp1	0.004216033	-0.9631205
Il18rap	0.000755237	1.110989678	Cldn2	0.00422295	-0.599372628
Tspan2	0.000763194	0.823272404	Hipk3	0.00422589	-0.67116717
Fam65b	0.000764592	-0.820728254	Cdc26	0.004235394	-0.769368366
Cdca7l	0.000766815	0.715442007	Slc6a6	0.004240301	-0.812236392
Avpr1a	0.000776655	0.765794262	Gm14226	0.004253985	-1.080773942
Sema6a	0.000777131	1.311924262	Lilrb4	0.004259722	1.530690933
Enpp2	0.000777721	2.072589649	Aqp9	0.004273167	0.775469669
Mpp7	0.000779598	-0.733020774	Ccdc47	0.004285701	0.721848567
Vegfc	0.00077984	0.763817576	Tmem9b	0.004295504	-0.764093001
Rb1	0.000788477	-0.729810168	Ddx26b	0.004302591	0.7181883
Evc2	0.000791109	0.665675092	Tmem9b	0.004316337	-0.609473416
Alg14	0.00082697	-1.660480034	B4galnt4	0.004331409	0.701997302
Celsr1	0.0008495	0.713041834	9030025P20Rik	0.004354905	-0.67796281
Slc9a3r2	0.000856241	-0.99464123	Tor1aip2	0.00437073	-0.647925401
Anxa4	0.0008586	-0.674168306	Bbs4	0.004382594	-0.802197169
Lrrc8a	0.000864924	-0.801752352	Cpne8	0.00439809	0.839913857
Crip2	0.00086891	-1.315816099	Als2cr12	0.004438836	0.763678937
Cxcl16	0.000872106	0.748746608	1500003O03Rik	0.004439212	-0.624291879
Ifitm1	0.000873457	1.366565507	Cttnbp2	0.004447476	1.540655614
Dnajc5	0.000883076	-0.755696168	Ccnc	0.004448667	-0.668396802
Ogg1	0.000884096	-0.715638391	Adam12	0.004453543	0.927438658
Chfr	0.000893155	-1.124291176	S100g	0.004490665	1.537318257
Vcan	0.000902955	0.815642225	Prdx3	0.004493067	-0.625485094
Orm1	0.000908582	1.15723001	Plce1	0.004501079	-0.671011402
Ly6e	0.000912903	1.388800574	Lnpep	0.004526912	-0.619288296

Krt14	0.000913932	0.681479786	Nicn1	0.004540724	-0.592376523
Glt8d1	0.000916887	-0.807648208	Tnfaip1	0.004543775	-0.722686191
Cpt1a	0.00094163	-1.046024127	Dok1	0.004546766	0.82042274
Ano1	0.00094195	-0.71618039	Cdc42ep3	0.004561712	0.936901219
Sytl2	0.000944993	-0.744073822	Tmem69	0.004651925	-0.759619203
Chml	0.000945396	-0.716788746	Ddx26b	0.004677127	0.672887455
Ptger4	0.000959148	0.973715479	Ccdc68	0.004678017	-0.623281785
Rab27b	0.000966924	-1.098534567	2310005N03Rik	0.00468583	-1.484375898
Sema4a	0.000974266	1.113849616	Enpp1	0.004689716	0.717067714
Ahnak2	0.000981767	-0.661147291	Sema3b	0.004713403	0.636689122
Spa17	0.000991928	-1.470909362	Zdhhc3	0.004727269	-0.781158033
Htra1	0.000998495	1.288632361	Rnf11	0.004728855	-0.611606453
Prss23	0.001019158	1.318452404	Klf6	0.004729363	-0.61287183
Ank2	0.001031298	1.516568098	Ccl9	0.004740001	1.473055745
2810022L02Rik	0.001034596	-1.069171058	Pde7a	0.004753294	0.742251548
Skp2	0.001046376	0.760906037	Ndrg3	0.004762166	-0.705574158
Gtf2b	0.001052163	-0.748248981	Cars2	0.004765604	-0.625158968
Tinagl1	0.001057266	-0.947175225	Tcf4	0.004772639	0.826453996
2610002J02Rik	0.001072638	-0.646086179	Grasp	0.004817902	0.824364434
Zfpm1	0.001086201	-0.673449658	Pde7a	0.004822081	0.705983839
1500003O03Rik	0.001090246	-0.648346372	Cdh1	0.004832479	-0.805352699
Rab27b	0.001094988	-0.742339669	Ptprf	0.004835692	-0.880288406
Rab3gap2	0.001103693	-0.620077358	Jag1	0.004855883	0.82447283
Satb1	0.001111253	2.146846888	Bmp7	0.004871938	-0.793876593
Megf9	0.001112211	-0.99976632	Sertad4	0.004881019	1.199148249
Aplp1	0.001131337	-1.336740824	Edn1	0.004890304	1.047249779
Tspan2	0.001133831	0.670025782	Osmr	0.004910909	0.634226854
Zfp618	0.00115386	0.73585893	4932441K18Rik	0.004918897	0.587691815
Stc2	0.001178737	1.180840161	Cachd1	0.004931001	-0.718242963
F2rl1	0.001187387	0.798507096	Bbs10	0.004932327	-0.839255079
Pde7a	0.001189456	0.853495983	Slc37a3	0.004947824	-0.730342649
Arhgef16	0.001195155	-0.658444838	Kcnab1	0.004955651	-0.668750035
1600029D21Rik	0.001195898	1.233002961	Vcl	0.004958123	0.60850883
Qsox2	0.00120096	-0.650671615	Slco2a1	0.004969889	-0.61204628
Adcy9	0.001203247	-0.74149866	2810410D24Rik	0.005004148	-0.640332353
Lpl	0.001218325	1.109337689	Renbp	0.005024122	0.678220295
Cd276	0.001224574	0.699645924	Micalcl	0.005035739	-0.618487316
Cep290	0.001228892	-0.828117697	Tcf4	0.005056212	0.832527615
Sytl2	0.001228893	-0.876867375	Grasp	0.005152902	1.188151169

Lmna	0.001228965	-0.665163284	A630095E13Rik	0.005195836	0.878692585
S100a13	0.001231299	-1.088122583	Adora2b	0.005214136	0.708232254
Ifi204	0.001232211	-0.809598051	Fam19a5	0.005215129	-0.881604816
Rab28	0.001236985	-1.062217563	6720475J19Rik	0.005224547	0.952917606
Car8	0.001240084	1.803000883	Wasl	0.00523539	0.641257048
B230120H23Rik	0.001242771	0.716060251	Jag1	0.005243397	0.64423835
Pkdcc	0.001243073	0.99770131	St3gal5	0.005243929	-0.683748385
Gja1	0.001252941	0.899967973	Nbl1	0.005258454	-0.593857485
Nfic	0.001255649	-0.67773405	Igsf11	0.005274541	-0.742715019
D16H22S680E	0.001257756	-0.785768857	Ela1	0.005315403	0.623065944
Flywch2	0.00125856	0.868425869	Mylk	0.005340125	0.857035294
Adamts6	0.001261445	1.04304323	Ngef	0.005350864	0.716281413
Csnk1a1	0.001281757	-0.617043272	Nbeal2	0.005359723	-0.614795087
Slc27a1	0.001287696	0.691482654	A230067G21Rik	0.005368959	-0.591187066
Ktelc1	0.001312578	0.706351899	Parp3	0.005398508	-0.646879201
Pdzrn3	0.001313139	0.864179566	Ptplad2	0.00544809	0.639728076
Npc1	0.001315801	-0.768084508	5730410E15Rik	0.005471505	0.705164341
Gja1	0.001317548	0.815952903	Ccnyl1	0.005526123	-0.602362479
Mcpt8	0.001318603	1.432686544	Mfsd6	0.005526964	-0.673366317
Akt3	0.001322057	-0.667794778	Rbpj	0.005576877	0.959160671
Dmrt2	0.001334632	-0.631332278	Rhox5	0.00561405	1.667155822
Anxa10	0.001334872	-0.917630286	Fut10	0.005615972	0.634041131
Casp12	0.001354926	1.064271491	Faah	0.005662243	-0.609753333
Kif23	0.001367347	-0.733829366	Atl3	0.005728075	-0.917466379
Maf	0.001370739	0.627384024	Serpinb1a	0.005755068	0.966003947
Slc25a12	0.001381082	-0.668043867	Maf	0.005786715	0.706309932
Fst	0.001381959	2.164641799	1810032O08Rik	0.005822576	0.588783492
Gstt1	0.001396486	1.128958226	Epb4.1l5	0.005827623	-0.613637985
1110007A13Rik	0.001397025	-0.765563981	2010011I20Rik	0.005892763	-0.774185635
Gm9971	0.001411885	-0.612527585	Car2	0.005901111	0.688075037
Kif1b	0.001415802	-0.610963744	Malat1	0.005919577	-0.744111719
Aplp1	0.001418147	-0.631992482	Ung	0.005933682	0.638463522
Vegfc	0.00141903	0.809319721	B230380D07Rik	0.005967118	-0.74961381
Tcf4	0.001425156	1.065834841	Rabl4	0.005983069	-0.66760294
E430016P22Rik	0.001432043	0.908168894	1190007F08Rik	0.006000901	-0.64535038
Lyrm2	0.001433856	-1.218567249	5330431N19Rik	0.006068229	-0.703712553
Gjb4	0.00143487	-0.651959318	Hoxa1	0.006164709	-1.28909575
Nfic	0.00144847	-1.077814818	Gabarapl2	0.006168816	-0.601301836
Tgfbi	0.001452591	2.083734424	Abhd2	0.006247226	-0.749958174

6030426L16Rik	0.001453339	-0.937498442	Kbtbd7	0.006307958	-1.00393646
Gja1	0.001462264	0.831213957	Tcf4	0.006322314	0.866832731
Ppp1r7	0.001465692	-1.25487732	Nid1	0.006334857	0.678737528
Ano1	0.001480204	-0.636865246	Cdkn2d	0.006387225	-0.832964627
H60a	0.001499201	1.573678416	Tgif2	0.006405291	0.762525825
Smap1	0.001525737	-0.596148213	Ptgds	0.00642541	1.129059934
Greb1	0.00153139	1.015254213	Cybasc3	0.006438208	-0.66865316
Pcnx	0.001536248	-0.586721122	Mctp1	0.006493057	0.704028206
1810048J11Rik	0.00153722	-0.680938079	Ccbe1	0.006497449	1.156955636
Fam19a5	0.001540936	-0.589000873	Cdyl2	0.006550749	-1.027711301
Tomm22	0.001545759	-0.718785569	2610034B18Rik	0.006616051	-0.626275369
Hist2h2aa1	0.001547579	-0.613903782	Rshl2a	0.006640076	1.082073283
Klf6	0.001554328	-0.77001268	Traf3ip1	0.006655917	-0.809717598
Abhd2	0.001554507	-0.672339411	Prkar2a	0.006735434	-0.700063142
Abhd2	0.001559487	-0.65838517	9130219A07Rik	0.006778388	-0.700840576
Wdr90	0.001561199	-0.59204578	Ralgps1	0.006790885	-0.616706501
Slco2a1	0.001580312	-0.666408337	Dll1	0.006798618	1.19034083
Klf4	0.001594087	-0.605786332	Eif5a2	0.006832626	-0.647458244
Nras	0.001594308	-0.586234907	LOC100046012	0.006836442	0.60095445
Smad6	0.001595912	-0.682124161	Mreg	0.006864439	0.642418158
Cltb	0.001599812	-0.632888132	Chrna1	0.00687285	-1.129281869
Efna5	0.001605106	0.585551826	Tlcd2	0.006888723	1.132391361
Srgap3	0.001626443	0.72685787	Osbpl2	0.006901172	-0.693548201
Mcart6	0.001633225	-0.633697731	Tcstv1	0.006956239	-0.899163299
Gm13043	0.001647176	-0.610205428	Itm2a	0.006963889	1.711218168
Ror1	0.00165188	-2.169639027	Mfsd4	0.006994472	-0.68474979
4930504B16Rik	0.001660563	0.631686269	Ddr2	0.007061434	0.814425004
Suds3	0.001662515	-0.758481423	Oxct1	0.007071156	0.645728665
Casp12	0.001669105	0.996259045	Unc13b	0.007075966	-0.596016313
Mylk	0.001686029	0.80125245	Pik3r5	0.007076805	0.596500587
Lad1	0.001686291	-0.672811107	Ppnr	0.007111736	-0.58871335
Tex264	0.001686492	-0.651448511	LysA	0.00711733	-0.688109964
4631416L12Rik	0.001694661	-0.837324781	Flt3l	0.007124815	-0.596787395
Ifna7	0.00171645	-0.779899969	Flt1	0.007149789	-0.73333226
Abcb7	0.001723168	-0.94101719	Serpinb7	0.007194049	-1.019517682
2010011I20Rik	0.001725308	-0.742339977	Tst	0.007203125	-0.832501806
Xdh	0.00175243	1.118397988	Mrps6	0.007247694	0.591810801
Nol7	0.001759719	-0.624680547	Wdr78	0.007265546	-0.720338799
Slc33a1	0.00176062	-0.762009371	Rps24	0.007268758	1.154906103

Gnb4	0.001771923	-0.611845963	Snx24	0.007328167	0.713283814
Tspan7	0.001778696	0.860456227	Slc39a4	0.007347198	1.730183414
B4galnt2	0.001781799	0.70471415	2310009A05Rik	0.007362112	-0.716023729
Ado	0.00178241	-0.589077207	Ablim3	0.007367664	-1.474274234
Klf6	0.001787759	-0.696443823	Slc25a16	0.007396142	-0.599039084
Mtm1	0.00179735	0.670452894	S100a1	0.007471308	-0.67730295
Cxxc4	0.001800005	-0.804025029	Sh3kbp1	0.007473351	0.679375923
Id4	0.001812886	-0.653357498	Mpped2	0.007499244	-0.70019001
Slco2a1	0.001819738	-0.811785881	Rangap1	0.00754191	0.678241266
Rnf11	0.001827166	-0.588679225	Rnf157	0.007566952	0.91022584
Gpr161	0.001829287	0.611641084	Rbpj	0.007580781	0.585798883
Sh3bp2	0.001850542	0.684218795	Mlph	0.007586609	-1.020780111
Tmem65	0.001855729	-0.603219797	Ccnc	0.007654383	-0.593283649
Vegfc	0.001859962	0.805760347	5133401H06Rik	0.007701805	-1.072684608
Bmp7	0.001861009	-0.683730227	Havcr2	0.007843037	1.54679209
Kras	0.001878822	-0.640713665	Ptprf	0.007863623	-0.936179187
F13a1	0.001889884	2.671442527	Slc43a3	0.007878318	1.80075045
Tmem86a	0.001893484	0.992222932	Slc4a7	0.00788119	0.733950487
Ckb	0.001898274	-0.809266723	St3gal1	0.007912608	0.818984451
Lhfpl2	0.001898309	0.745981826	Isyna1	0.007958061	0.991279272
Atp10a	0.001907485	-0.625268396	Mmd	0.008028152	0.603653596
Trfr2	0.001912894	0.662932109	Nphp3	0.008032451	-0.617213869
Mpped2	0.001913574	-0.621277247	Slc36a1	0.008035479	-0.597480663
Sec16b	0.001915339	1.3704358	Il1rn	0.00812388	0.76819484
Enpp2	0.001923853	0.700178823	Zdhhc2	0.008178043	-0.864465773
2010300C02Rik	0.001937402	1.34617287	4933407K13Rik	0.008179036	0.747300979
9030622O22Rik	0.001939794	-0.74449225	Hnf4g	0.008207643	0.687810762
Klf6	0.001951907	-0.824362282	Tmem218	0.008239935	-0.799594439
Mapre2	0.001951968	-0.586599061	Dnajb14	0.008252578	-0.603785832
Gabarapl2	0.001963173	-0.713404755	Zfhx4	0.008260313	0.707143135
Klhl22	0.00196454	0.595332938	Asrgl1	0.008324136	0.605742829
D8Ertd82e	0.001971591	0.686988552	Mki67	0.00843237	-0.791671778
Pabpc4	0.001975151	-0.653687764	Ctnnal1	0.008461623	0.623586104
Hoxb8	0.001984113	1.47929964	A630038E17Rik	0.008493903	0.614595679
Ndst1	0.002008746	-0.704798641	Phtf1	0.008673962	0.604339711
Ripk3	0.002011709	0.874948097	Spry3	0.008681241	0.660361783
Neto2	0.002023777	0.773071356	Cdkl2	0.0086939	-0.647276147
Slc9a3r2	0.002030875	-0.75392176	Fam117a	0.008714481	0.739142171
Tmbim4	0.002049613	-0.70273702	Enpp4	0.008765466	-0.693871716

2010107G23Rik	0.00206265	-0.598826433	Atp8a1	0.008766505	0.697023214
Ube2w	0.002063697	-0.76560239	Nbr1	0.00879876	-0.676697483
Leprot	0.002064864	-0.656933473	Ccl9	0.008878713	1.213162161
1810044D09Rik	0.00206568	-0.775906383	Btbd11	0.008885198	1.040213397
Vav3	0.002073646	0.714780465	Itgb8	0.008902296	1.288206616
Fgfr4	0.002081706	1.021058271	Mtmr9	0.008914516	-0.910948016
Trim24	0.002086905	0.631543707	Yif1a	0.009030848	-0.623328555
Tor3a	0.002088831	-0.814523243	Spo0B	0.009034428	-0.717814606
Mtap4	0.002096772	-0.624212975	Nme5	0.009048164	-0.796723111
Nat8l	0.002107018	1.106153044	Av336852	0.009072036	-0.731475696
Rab28	0.002108387	-0.911863545	Rasl11b	0.00908389	0.690455179
Smap1	0.002122533	-0.644882977	2700023E23Rik	0.009151307	0.659867411
Ppp3ca	0.002123854	0.638465421	Nudt18	0.009160089	-0.617133928
Htra1	0.002133383	1.142136004	Pcyt1b	0.009190708	0.851080568
Kat2a	0.002147061	0.586243811	Gm5909	0.00919109	0.590944286
Syk	0.002150994	1.063855581	Atoh8	0.009310657	-0.992028861
4930562D19Rik	0.002188115	-0.641327358	Itgb7	0.009338489	0.778809068
2210008F06Rik	0.002200967	-0.6229643	Esco2	0.009357422	-0.664167809
Slc7a4	0.00221159	-0.75902829	Fkrp	0.009434719	-0.598399547
Vcan	0.002244263	0.669919613	Ildr2	0.009477763	-1.071173029
2810022L02Rik	0.002245143	-1.233421552	Lbh	0.009481658	0.627587606
Rab11fip5	0.002276501	0.726797859	Sept6	0.009486128	0.665448444
Gusb	0.002278325	0.739788187	Tpm3	0.009496658	-0.630672198
Tspan15	0.002285516	-0.699401569	Rbm26	0.009509285	0.607537203
Hspb11	0.002287859	-0.600448992	EG434402	0.009536923	-0.611955808
Pla1a	0.002292985	0.690349514	Slco4a1	0.009587095	0.72795444
Smpd3	0.002340221	-0.592351869	Tmem168	0.009603835	-0.712682555
Plekha5	0.002348979	0.612589025	Ugp2	0.00961702	-0.805818694
Vat1l	0.002357099	-1.559152399	Nucks1	0.009691974	-0.761569059
Slfn2	0.002390086	1.184898546	Mapk11	0.009733833	-0.625831409
Gda	0.002396194	0.935013244	Slc7a2	0.009910713	0.704317457
AU020206	0.002403585	0.595745529	Apob	0.009986501	-0.587603738
Yif1a	0.002442222	-0.682509116	Scrn3	0.009990957	-0.85441688

Bibliography

Acin S, Li Z, Mejia O, Roop DR, El-Naggar AK, Caulin C. 2011. Gain-of-function mutant p53 but not p53 deletion promotes head and neck cancer progression in response to oncogenic K-ras. *The Journal of pathology* **225**: 479-489.

Akunuru S, Palumbo J, Zhai QJ, Zheng Y. 2011. Rac1 targeting suppresses human non-small cell lung adenocarcinoma cancer stem cell activity. *PloS one* **6**: e16951.

Alix-Panabieres C. 2012. EPISPOT assay: detection of viable DTCs/CTCs in solid tumor patients. *Recent results in cancer research Fortschritte der Krebsforschung Progres dans les recherches sur le cancer* **195**: 69-76.

Alpert ME, Davidson CS. 1969. Mycotoxins. A possible cause of primary carcinoma of the liver. *The American journal of medicine* **46**: 325-329.

Altekruse SF, McGlynn KA, Dickie LA, Kleiner DE. 2012. Hepatocellular carcinoma confirmation, treatment, and survival in surveillance, epidemiology, and end results registries, 1992-2008. *Hepatology* **55**: 476-482.

Alter MJ, Mast EE. 1994. The epidemiology of viral hepatitis in the United States. *Gastroenterology clinics of North America* **23**: 437-455.

Andrisani OM, Studach L, Merle P. 2011. Gene signatures in hepatocellular carcinoma (HCC). *Seminars in cancer biology* **21**: 4-9.

Aravalli RN, Steer CJ, Cressman EN. 2008. Molecular mechanisms of hepatocellular carcinoma. *Hepatology* **48**: 2047-2063.

Baig JA, Alam JM, Mahmood SR, Baig M, Shaheen R, Sultana I, Waheed A. 2009. Hepatocellular carcinoma (HCC) and diagnostic significance of A-fetoprotein (AFP). *Journal of Ayub Medical College, Abbottabad : JAMC* **21**: 72-75.

Bartek J, Bartkova J, Vojtesek B, Staskova Z, Lukas J, Rejthar A, Kovarik J, Midgley CA, Gannon JV, Lane DP. 1991. Aberrant expression of the p53 oncoprotein is a common feature of a wide spectrum of human malignancies. *Oncogene* **6**: 1699-1703.

Beasley RP, Hwang LY, Lin CC, Chien CS. 1981. Hepatocellular carcinoma and hepatitis B virus. A prospective study of 22 707 men in Taiwan. *Lancet* **2**: 1129-1133.

Bellentani S, Saccoccio G, Costa G, Tiribelli C, Manenti F, Sodde M, Saveria Croce L, Sasso F, Pozzato G, Cristianini G et al. 1997. Drinking habits as cofactors of risk for alcohol induced liver damage. The Dionysos Study Group. *Gut* **41**: 845-850.

Benard J, Douc-Rasy S, Ahomadegbe JC. 2003. TP53 family members and human cancers. *Human mutation* **21**: 182-191.

Benzeno S, Narla G, Allina J, Cheng GZ, Reeves HL, Banck MS, Odin JA, Diehl JA, Germain D, Friedman SL. 2004. Cyclin-dependent kinase inhibition by the KLF6 tumor suppressor protein through interaction with cyclin D1. *Cancer research* **64**: 3885-3891.

Berger AH, Knudson AG, Pandolfi PP. 2011. A continuum model for tumour suppression. *Nature* **476**: 163-169.

Bernards A. 2003. GAPs galore! A survey of putative Ras superfamily GTPase activating proteins in man and Drosophila. *Biochimica et biophysica acta* **1603**: 47-82.

Betel D, Wilson M, Gabow A, Marks DS, Sander C. 2008. The microRNA.org resource: targets and expression. *Nucleic acids research* **36**: D149-153.

Bettermann K, Vucur M, Haybaeck J, Koppe C, Janssen J, Heymann F, Weber A, Weiskirchen R, Liedtke C, Gassler N et al. 2010. TAK1 suppresses a NEMO-dependent but NF-kappaB-independent pathway to liver cancer. *Cancer cell* **17**: 481-496.

Bid HK, Roberts RD, Manchanda PK, Houghton PJ. 2013. RAC1: an emerging therapeutic option for targeting cancer angiogenesis and metastasis. *Molecular cancer therapeutics* **12**: 1925-1934.

Bosch FX, Ribes J, Diaz M, Cleries R. 2004. Primary liver cancer: worldwide incidence and trends. *Gastroenterology* **127**: S5-S16.

Botella LM, Sanz-Rodriguez F, Komi Y, Fernandez LA, Varela E, Garrido-Martin EM, Narla G, Friedman SL, Kojima S. 2009. TGF-beta regulates the expression of transcription factor KLF6 and its splice variants and promotes co-operative transactivation of common target genes through a Smad3-Sp1-KLF6 interaction. *The Biochemical journal* **419**: 485-495.

Bouchard MJ, Schneider RJ. 2004. The enigmatic X gene of hepatitis B virus. *Journal of virology* **78**: 12725-12734.

Boyault S, Herault A, Balabaud C, Zucman-Rossi J. 2005. Absence of KLF6 gene mutation in 71 hepatocellular carcinomas. *Hepatology* **41**: 681-682; author reply 682-683.

Boyault S, Rickman DS, de Reynies A, Balabaud C, Rebouissou S, Jeannot E, Herault A, Saric J, Belghiti J, Franco D et al. 2007. Transcriptome classification of HCC is related to gene alterations and to new therapeutic targets. *Hepatology* **45**: 42-52.

Brantley-Sieders DM, Zhuang G, Vaught D, Freeman T, Hwang Y, Hicks D, Chen J. 2009. Host deficiency in Vav2/3 guanine nucleotide exchange factors impairs tumor growth, survival, and angiogenesis in vivo. *Molecular cancer research : MCR* **7**: 615-623.

Bressac B, Kew M, Wands J, Ozturk M. 1991. Selective G to T mutations of p53 gene in hepatocellular carcinoma from southern Africa. *Nature* **350**: 429-431.

Britschgi A, Trinh E, Rizzi M, Jenal M, Ress A, Tobler A, Fey MF, Helin K, Tschan MP. 2008. DAPK2 is a novel E2F1/KLF6 target gene involved in their proapoptotic function. *Oncogene* **27**: 5706-5716.

Bruix J, Llovet JM, Castells A, Montana X, Bru C, Ayuso MC, Vilana R, Rodes J. 1998. Transarterial embolization versus symptomatic treatment in patients with advanced hepatocellular carcinoma: results of a randomized, controlled trial in a single institution. *Hepatology* **27**: 1578-1583.

Buendia MA. 2000. Genetics of hepatocellular carcinoma. *Seminars in cancer biology* **10**: 185-200.

Buhler S, Bartenschlager R. 2012. Promotion of hepatocellular carcinoma by hepatitis C virus. *Digestive diseases* **30**: 445-452.

Bureau C, Peron JM, Bouisson M, Danjoux M, Selves J, Bioulac-Sage P, Balabaud C, Torrisani J, Cordelier P, Buscail L et al. 2008. Expression of the transcription factor Klf6 in cirrhosis, macronodules, and hepatocellular carcinoma. *Journal of gastroenterology and hepatology* **23**: 78-86.

Bustelo XR, Sauzeau V, Berenjeno IM. 2007. GTP-binding proteins of the Rho/Rac family: regulation, effectors and functions in vivo. *BioEssays : news and reviews in molecular, cellular and developmental biology* **29**: 356-370.

Cadoret A, Ovejero C, Saadi-Kheddouci S, Souil E, Fabre M, Romagnolo B, Kahn A, Perret C. 2001. Hepatomegaly in transgenic mice expressing an oncogenic form of beta-catenin. *Cancer research* **61**: 3245-3249.

Carlomagno F, Anaganti S, Guida T, Salvatore G, Troncone G, Wilhelm SM, Santoro M. 2006. BAY 43-9006 inhibition of oncogenic RET mutants. *Journal of the National Cancer Institute* **98**: 326-334.

Caulin C, Nguyen T, Lang GA, Goepfert TM, Brinkley BR, Cai WW, Lozano G, Roop DR. 2007. An inducible mouse model for skin cancer reveals distinct roles for gain- and loss-of-function p53 mutations. *The Journal of clinical investigation* **117**: 1893-1901.

Cetta F, Zuckermann M, del Vecchio MT, Ercolani G, Mazziotti A. 2001. Histological and genetic heterogeneity in synchronous hepatocellular carcinoma. *Gut* **49**: 155-156.

Chaffer CL, Weinberg RA. 2011. A perspective on cancer cell metastasis. *Science* **331**: 1559-1564.

Chambers AF, Groom AC, MacDonald IC. 2002. Dissemination and growth of cancer cells in metastatic sites. *Nature reviews Cancer* **2**: 563-572.

Chan KL, Guan XY, Ng IO. 2004. High-throughput tissue microarray analysis of c-myc activation in chronic liver diseases and hepatocellular carcinoma. *Human pathology* **35**: 1324-1331.

Chang J, Nicolas E, Marks D, Sander C, Lerro A, Buendia MA, Xu C, Mason WS, Moloshok T, Bort R et al. 2004. miR-122, a mammalian liver-specific microRNA, is processed from hcr mRNA and may downregulate the high affinity cationic amino acid transporter CAT-1. *RNA biology* **1**: 106-113.

Chang MH, Chen CJ, Lai MS, Hsu HM, Wu TC, Kong MS, Liang DC, Shau WY, Chen DS. 1997. Universal hepatitis B vaccination in Taiwan and the incidence of hepatocellular carcinoma in children. Taiwan Childhood Hepatoma Study Group. *The New England journal of medicine* **336**: 1855-1859.

Chen HL, Chen YC, Chen DS. 1996. Chromosome 1p aberrations are frequent in human primary hepatocellular carcinoma. *Cancer genetics and cytogenetics* **86**: 102-106.

Chen YW, Boyartchuk V, Lewis BC. 2009. Differential roles of insulin-like growth factor receptor- and insulin receptor-mediated signaling in the phenotypes of hepatocellular carcinoma cells. *Neoplasia* **11**: 835-845.

Chen YW, Klimstra DS, Mongeau ME, Tatem JL, Boyartchuk V, Lewis BC. 2007. Loss of p53 and Ink4a/Arf cooperate in a cell autonomous fashion to induce metastasis of hepatocellular carcinoma cells. *Cancer research* **67**: 7589-7596.

Cheung TK, Lai CL, Wong BC, Fung J, Yuen MF. 2006. Clinical features, biochemical parameters, and virological profiles of patients with hepatocellular carcinoma in Hong Kong. *Alimentary pharmacology & therapeutics* **24**: 573-583.

Chicas A, Molina P, Bargonetti J. 2000. Mutant p53 forms a complex with Sp1 on HIV-LTR DNA. *Biochemical and biophysical research communications* **279**: 383-390.

Chisari FV, Klopchin K, Moriyama T, Pasquinelli C, Dunsford HA, Sell S, Pinkert CA, Brinster RL, Palmiter RD. 1989. Molecular pathogenesis of hepatocellular carcinoma in hepatitis B virus transgenic mice. *Cell* **59**: 1145-1156.

Cho WC. 2007. OncomiRs: the discovery and progress of microRNAs in cancers. *Molecular cancer* **6**: 60.

Colnot S, Decaens T, Niwa-Kawakita M, Godard C, Hamard G, Kahn A, Giovannini M, Perret C. 2004. Liver-targeted disruption of Apc in mice activates beta-catenin signaling and leads to hepatocellular carcinomas. *Proceedings of the National Academy of Sciences of the United States of America* **101**: 17216-17221.

Colomba A, Courilleau D, Ramel D, Billadeau DD, Espinos E, Delsol G, Payrastre B, Gaits-Iacovoni F. 2008. Activation of Rac1 and the exchange factor Vav3 are involved in NPM-ALK signaling in anaplastic large cell lymphomas. *Oncogene* **27**: 2728-2736.

Connolly E, Melegari M, Landgraf P, Tchaikovskaya T, Tennant BC, Slagle BL, Rogler LE, Zavolan M, Tuschl T, Rogler CE. 2008. Elevated expression of the miR-17-92 polycistron and miR-21 in hepadnavirus-associated hepatocellular carcinoma contributes to the malignant phenotype. *The American journal of pathology* **173**: 856-864.

Cooks T, Pateras IS, Tarcic O, Solomon H, Schetter AJ, Wilder S, Lozano G, Pikarsky E, Forshew T, Rosenfeld N et al. 2013. Mutant p53 prolongs NF-kappaB activation and promotes chronic inflammation and inflammation-associated colorectal cancer. *Cancer cell* **23**: 634-646.

Coulouarn C, Factor VM, Andersen JB, Durkin ME, Thorgeirsson SS. 2009. Loss of miR-122 expression in liver cancer correlates with suppression of the hepatic phenotype and gain of metastatic properties. *Oncogene* **28**: 3526-3536.

Courtois S, Caron de Fromentel C, Hainaut P. 2004. p53 protein variants: structural and functional similarities with p63 and p73 isoforms. *Oncogene* **23**: 631-638.

Das A, Fernandez-Zapico ME, Cao S, Yao J, Fiorucci S, Hebbel RP, Urrutia R, Shah VH. 2006. Disruption of an SP2/KLF6 repression complex by SHP is required for farnesoid X receptor-induced endothelial cell migration. *The Journal of biological chemistry* **281**: 39105-39113.

Davila JA, Morgan RO, Shaib Y, McGlynn KA, El-Serag HB. 2004. Hepatitis C infection and the increasing incidence of hepatocellular carcinoma: a population-based study. *Gastroenterology* **127**: 1372-1380.

-. 2005. Diabetes increases the risk of hepatocellular carcinoma in the United States: a population based case control study. *Gut* **54**: 533-539.

Davison TS, Vagner C, Kaghad M, Ayed A, Caput D, Arrowsmith CH. 1999. p73 and p63 are homotetramers capable of weak heterotypic interactions with each other but not with p53. *The Journal of biological chemistry* **274**: 18709-18714.

De Laurenzi V, Costanzo A, Barcaroli D, Terrinoni A, Falco M, Annicchiarico-Petruzzelli M, Levrero M, Melino G. 1998. Two new p73 splice variants, gamma and delta, with different transcriptional activity. *The Journal of experimental medicine* **188**: 1763-1768.

de Vries A, Flores ER, Miranda B, Hsieh HM, van Oostrom CT, Sage J, Jacks T. 2002. Targeted point mutations of p53 lead to dominant-negative inhibition of wild-type p53 function. *Proceedings of the National Academy of Sciences of the United States of America* **99**: 2948-2953.

Deng XG, Qiu RL, Wu YH, Li ZX, Xie P, Zhang J, Zhou JJ, Zeng LX, Tang J, Maharjan A et al. 2014. Overexpression of miR-122 promotes the hepatic differentiation and maturation of mouse ESCs through a miR-122/FoxA1/HNF4a-positive feedback loop. *Liver international : official journal of the International Association for the Study of the Liver* **34**: 281-295.

Di Agostino S, Strano S, Emiliozzi V, Zerbini V, Mottolese M, Sacchi A, Blandino G, Piaggio G. 2006. Gain of function of mutant p53: the mutant p53/NF-Y protein complex reveals an aberrant transcriptional mechanism of cell cycle regulation. *Cancer cell* **10**: 191-202.

Di Bisceglie AM. 2009. Hepatitis B and hepatocellular carcinoma. *Hepatology* **49**: S56-60.

Di Bisceglie AM, Lyra AC, Schwartz M, Reddy RK, Martin P, Gores G, Lok AS, Hussain KB, Gish R, Van Thiel DH et al. 2003. Hepatitis C-related hepatocellular carcinoma in the United States: influence of ethnic status. *The American journal of gastroenterology* **98**: 2060-2063.

Di Como CJ, Gaiddon C, Prives C. 1999. p73 function is inhibited by tumor-derived p53 mutants in mammalian cells. *Molecular and cellular biology* **19**: 1438-1449.

Diab T, Hanoun N, Bureau C, Christol C, Buscail L, Cordelier P, Torrisani J. 2013. The Role of the 3' Untranslated Region in the Post-Transcriptional Regulation of KLF6 Gene Expression in Hepatocellular Carcinoma. *Cancers* **6**: 28-41.

Dietz S, Rother K, Bamberger C, Schmale H, Mossner J, Engeland K. 2002. Differential regulation of transcription and induction of programmed cell death by human p53-family members p63 and p73. *FEBS letters* **525**: 93-99.

DiFeo A, Martignetti JA, Narla G. 2009. The role of KLF6 and its splice variants in cancer therapy. *Drug resistance updates : reviews and commentaries in antimicrobial and anticancer chemotherapy* **12**: 1-7.

DiFeo A, Narla G, Camacho-Vanegas O, Nishio H, Rose SL, Buller RE, Friedman SL, Walsh MJ, Martignetti JA. 2006. E-cadherin is a novel transcriptional target of the KLF6 tumor suppressor. *Oncogene* **25**: 6026-6031.

Dittmer D, Pati S, Zambetti G, Chu S, Teresky AK, Moore M, Finlay C, Levine AJ. 1993. Gain of function mutations in p53. *Nature genetics* **4**: 42-46.

Donehower LA, Harvey M, Slagle BL, McArthur MJ, Montgomery CA, Jr., Butel JS, Bradley A. 1992. Mice deficient for p53 are developmentally normal but susceptible to spontaneous tumours. *Nature* **356**: 215-221.

Dong P, Karaayvaz M, Jia N, Kaneuchi M, Hamada J, Watari H, Sudo S, Ju J, Sakuragi N. 2013. Mutant p53 gain-of-function induces epithelial-mesenchymal transition through modulation of the miR-130b-ZEB1 axis. *Oncogene* **32**: 3286-3295.

Dvorchik I, Schwartz M, Fiel MI, Finkelstein SD, Marsh JW. 2008. Fractional allelic imbalance could allow for the development of an equitable transplant selection policy for patients with hepatocellular carcinoma. *Liver transplantation : official publication of the American Association for the Study of Liver Diseases and the International Liver Transplantation Society* **14**: 443-450.

Edeline J, Raoul JL, Vauleon E, Guillygomac'h A, Boudjema K, Boucher E. 2009. Systemic chemotherapy for hepatocellular carcinoma in non-cirrhotic liver: a retrospective study. *World journal of gastroenterology : WJG* **15**: 713-716.

El-Serag HB. 2011. Hepatocellular carcinoma. *The New England journal of medicine* **365**: 1118-1127.

El-Serag HB, Rudolph KL. 2007. Hepatocellular carcinoma: epidemiology and molecular carcinogenesis. *Gastroenterology* **132**: 2557-2576.

Eliyahu D, Raz A, Gruss P, Givol D, Oren M. 1984. Participation of p53 cellular tumour antigen in transformation of normal embryonic cells. *Nature* **312**: 646-649.

Faccio R, Teitelbaum SL, Fujikawa K, Chappel J, Zallone A, Tybulewicz VL, Ross FP, Swat W. 2005. Vav3 regulates osteoclast function and bone mass. *Nature medicine* **11**: 284-290.

Fang X, Cai Y, Liu J, Wang Z, Wu Q, Zhang Z, Yang CJ, Yuan L, Ouyang G. 2011. Twist2 contributes to breast cancer progression by promoting an epithelial-mesenchymal transition and cancer stem-like cell self-renewal. *Oncogene* **30**: 4707-4720.

Farazi PA, DePinho RA. 2006. Hepatocellular carcinoma pathogenesis: from genes to environment. *Nature reviews Cancer* **6**: 674-687.

Finlay CA, Hinds PW, Tan TH, Eliyahu D, Oren M, Levine AJ. 1988. Activating mutations for transformation by p53 produce a gene product that forms an hsc70-p53 complex with an altered half-life. *Molecular and cellular biology* **8**: 531-539.

Flores ER, Sengupta S, Miller JB, Newman JJ, Bronson R, Crowley D, Yang A, McKeon F, Jacks T. 2005. Tumor predisposition in mice mutant for p63 and p73: evidence for broader tumor suppressor functions for the p53 family. *Cancer cell* **7**: 363-373.

Fortune BE, Umman V, Gilliland T, Emre S. 2013. Liver Transplantation for Hepatocellular Carcinoma: A Surgical Perspective. *Journal of clinical gastroenterology*.

Frazier MW, He X, Wang J, Gu Z, Cleveland JL, Zambetti GP. 1998. Activation of c-myc gene expression by tumor-derived p53 mutants requires a discrete C-terminal domain. *Molecular and cellular biology* **18**: 3735-3743.

Freed-Pastor WA, Mizuno H, Zhao X, Langerod A, Moon SH, Rodriguez-Barrueco R, Barsotti A, Chicas A, Li W, Polotskaia A et al. 2012. Mutant p53 disrupts mammary tissue architecture via the mevalonate pathway. *Cell* **148**: 244-258.

Friedman PN, Chen X, Bargonetti J, Prives C. 1993. The p53 protein is an unusually shaped tetramer that binds directly to DNA. *Proceedings of the National Academy of Sciences of the United States of America* **90**: 3319-3323.

Fujimoto A, Totoki Y, Abe T, Boroevich KA, Hosoda F, Nguyen HH, Aoki M, Hosono N, Kubo M, Miya F et al. 2012. Whole-genome sequencing of liver cancers identifies etiological influences on mutation patterns and recurrent mutations in chromatin regulators. *Nature genetics* **44**: 760-764.

Fusco A, Fedele M. 2007. Roles of HMGA proteins in cancer. *Nature reviews Cancer* **7**: 899-910.

Gaiddon C, Lokshin M, Ahn J, Zhang T, Prives C. 2001. A subset of tumor-derived mutant forms of p53 down-regulate p63 and p73 through a direct interaction with the p53 core domain. *Molecular and cellular biology* **21**: 1874-1887.

Gastonguay A, Berg T, Hauser AD, Schuld N, Lorimer E, Williams CL. 2012. The role of Rac1 in the regulation of NF-kappaB activity, cell proliferation, and cell migration in non-small cell lung carcinoma. *Cancer biology & therapy* **13**: 647-656.

Gauthier A, Ho M. 2013. Role of sorafenib in the treatment of advanced hepatocellular carcinoma: An update. *Hepatology research : the official journal of the Japan Society of Hepatology* **43**: 147-154.

Gehrau RC, D'Astolfo DS, Andreoli V, Bocco JL, Koritschoner NP. 2011. Differential expression of the klf6 tumor suppressor gene upon cell damaging treatments in cancer cells. *Mutation research* **707**: 15-23.

Gehrau RC, D'Astolfo DS, Dumur CI, Bocco JL, Koritschoner NP. 2010. Nuclear expression of KLF6 tumor suppressor factor is highly associated with

overexpression of ERBB2 oncoprotein in ductal breast carcinomas. *PloS one* **5**: e8929.

Gehrau RC, D'Astolfo DS, Prieto C, Bocco JL, Koritschoner NP. 2005. Genomic organization and functional analysis of the gene encoding the Kruppel-like transcription factor KLF6. *Biochimica et biophysica acta* **1730**: 137-146.

Germani G, Pleguezuelo M, Gurusamy K, Meyer T, Isgro G, Burroughs AK. 2010. Clinical outcomes of radiofrequency ablation, percutaneous alcohol and acetic acid injection for hepatocelullar carcinoma: a meta-analysis. *Journal of hepatology* **52**: 380-388.

Girard L, Zochbauer-Muller S, Virmani AK, Gazdar AF, Minna JD. 2000. Genome-wide allelotyping of lung cancer identifies new regions of allelic loss, differences between small cell lung cancer and non-small cell lung cancer, and loci clustering. *Cancer research* **60**: 4894-4906.

Glogauer M, Marchal CC, Zhu F, Worku A, Clausen BE, Foerster I, Marks P, Downey GP, Dinauer M, Kwiatkowski DJ. 2003. Rac1 deletion in mouse neutrophils has selective effects on neutrophil functions. *Journal of immunology* **170**: 5652-5657.

Gohler T, Jager S, Warnecke G, Yasuda H, Kim E, Deppert W. 2005. Mutant p53 proteins bind DNA in a DNA structure-selective mode. *Nucleic acids research* **33**: 1087-1100.

Gouas DA, Shi H, Hautefeuille AH, Ortiz-Cuaran SL, Legros PC, Szymanska KJ, Galy O, Egevad LA, Abedi-Ardekani B, Wiman KG et al. 2010. Effects of the TP53 p.R249S mutant on proliferation and clonogenic properties in human hepatocellular carcinoma cell lines: interaction with hepatitis B virus X protein. *Carcinogenesis* **31**: 1475-1482.

Guichard C, Amaddeo G, Imbeaud S, Ladeiro Y, Pelletier L, Maad IB, Calderaro J, Bioulac-Sage P, Letexier M, Degos F et al. 2012. Integrated analysis of somatic mutations and focal copy-number changes identifies key genes and pathways in hepatocellular carcinoma. *Nature genetics* **44**: 694-698.

Gupta GP, Perk J, Acharyya S, de Candia P, Mittal V, Todorova-Manova K, Gerald WL, Brogi E, Benezra R, Massague J. 2007. ID genes mediate tumor reinitiation during breast cancer lung metastasis. *Proceedings of the National Academy of Sciences of the United States of America* **104**: 19506-19511.

Gupta RA, Shah N, Wang KC, Kim J, Horlings HM, Wong DJ, Tsai MC, Hung T, Argani P, Rinn JL et al. 2010. Long non-coding RNA HOTAIR reprograms chromatin state to promote cancer metastasis. *Nature* **464**: 1071-1076.

Hall A. 1998. Rho GTPases and the actin cytoskeleton. *Science* **279**: 509-514.

-. 2012. Rho family GTPases. *Biochemical Society transactions* **40**: 1378-1382.

Hamid AS, Tesfamariam IG, Zhang Y, Zhang ZG. 2013. Aflatoxin B1-induced hepatocellular carcinoma in developing countries: Geographical distribution, mechanism of action and prevention. *Oncology letters* **5**: 1087-1092.

Han L, Zhang A, Zhou X, Xu P, Wang GX, Pu PY, Kang CS. 2010. Downregulation of Dicer enhances tumor cell proliferation and invasion. *International journal of oncology* **37**: 299-305.

Hanahan D, Weinberg RA. 2011. Hallmarks of cancer: the next generation. *Cell* **144**: 646-674.

Hatami R, Sieuwerts AM, Izadmehr S, Yao Z, Qiao RF, Papa L, Look MP, Smid M, Ohlssen J, Levine AC et al. 2013. KLF6-SV1 drives breast cancer metastasis and is associated with poor survival. *Science translational medicine* **5**: 169ra112.

Hayat MJ, Howlader N, Reichman ME, Edwards BK. 2007. Cancer statistics, trends, and multiple primary cancer analyses from the Surveillance, Epidemiology, and End Results (SEER) Program. *The oncologist* **12**: 20-37.

Haybaeck J, Zeller N, Wolf MJ, Weber A, Wagner U, Kurrer MO, Bremer J, Iezzi G, Graf R, Clavien PA et al. 2009. A lymphotoxin-driven pathway to hepatocellular carcinoma. *Cancer cell* **16**: 295-308.

Heindryckx F, Colle I, Van Vlierberghe H. 2009. Experimental mouse models for hepatocellular carcinoma research. *International journal of experimental pathology* **90**: 367-386.

Herath NI, Kew MC, Whitehall VL, Walsh MD, Jass JR, Khanna KK, Young J, Powell LW, Leggett BA, Macdonald GA. 2000. p73 is up-regulated in a subset of hepatocellular carcinomas. *Hepatology* **31**: 601-605.

Hinds P, Finlay C, Levine AJ. 1989. Mutation is required to activate the p53 gene for cooperation with the ras oncogene and transformation. *Journal of virology* **63**: 739-746.

Hinds PW, Finlay CA, Quartin RS, Baker SJ, Fearon ER, Vogelstein B, Levine AJ. 1990. Mutant p53 DNA clones from human colon carcinomas cooperate with ras in transforming primary rat cells: a comparison of the "hot spot" mutant phenotypes. *Cell growth & differentiation : the molecular biology journal of the American Association for Cancer Research* **1**: 571-580.

Hirsch DS, Pirone DM, Burbelo PD. 2001. A new family of Cdc42 effector proteins, CEPs, function in fibroblast and epithelial cell shape changes. *The Journal of biological chemistry* **276**: 875-883.

Hollstein M, Rice K, Greenblatt MS, Soussi T, Fuchs R, Sorlie T, Hovig E, Smith-Sorensen B, Montesano R, Harris CC. 1994. Database of p53 gene somatic mutations in human tumors and cell lines. *Nucleic acids research* **22**: 3551-3555.

Hollstein M, Sidransky D, Vogelstein B, Harris CC. 1991. p53 mutations in human cancers. *Science* **253**: 49-53.

Huang X, Li X, Guo B. 2008. KLF6 induces apoptosis in prostate cancer cells through up-regulation of ATF3. *The Journal of biological chemistry* **283**: 29795-29801.

Iizuka N, Oka M, Tamesa T, Hamamoto Y, Yamada-Okabe H. 2004. Imbalance in expression levels of insulin-like growth factor 2 and H19 transcripts linked to progression of hepatocellular carcinoma. *Anticancer research* **24**: 4085-4089.

Ito G, Uchiyama M, Kondo M, Mori S, Usami N, Maeda O, Kawabe T, Hasegawa Y, Shimokata K, Sekido Y. 2004. Kruppel-like factor 6 is frequently down-regulated and induces apoptosis in non-small cell lung cancer cells. *Cancer research* **64**: 3838-3843.

Izumi R, Shimizu K, Kiriyama M, Hashimoto T, Urade M, Yagi M, Mizukami Y, Nonomura A, Miyazaki I. 1992. Alpha-fetoprotein production by hepatocellular carcinoma is prognostic of poor patient survival. *Journal of surgical oncology* **49**: 151-155.

Jee SH, Ohrr H, Sull JW, Samet JM. 2004. Cigarette smoking, alcohol drinking, hepatitis B, and risk for hepatocellular carcinoma in Korea. *Journal of the National Cancer Institute* **96**: 1851-1856.

Jemal A, Bray F, Center MM, Ferlay J, Ward E, Forman D. 2011. Global cancer statistics. *CA: a cancer journal for clinicians* **61**: 69-90.

Jhappan C, Stahle C, Harkins RN, Fausto N, Smith GH, Merlino GT. 1990. TGF alpha overexpression in transgenic mice induces liver neoplasia and abnormal development of the mammary gland and pancreas. *Cell* **61**: 1137-1146.

Ji J, Shi J, Budhu A, Yu Z, Forgues M, Roessler S, Ambs S, Chen Y, Meltzer PS, Croce CM et al. 2009a. MicroRNA expression, survival, and response to interferon in liver cancer. *The New England journal of medicine* **361**: 1437-1447.

Ji J, Yamashita T, Budhu A, Forgues M, Jia HL, Li C, Deng C, Wauthier E, Reid LM, Ye QH et al. 2009b. Identification of microRNA-181 by genome-wide screening as a critical player in EpCAM-positive hepatic cancer stem cells. *Hepatology* **50**: 472-480.

Joberty G, Perlungher RR, Macara IG. 1999. The Borgs, a new family of Cdc42 and TC10 GTPase-interacting proteins. *Molecular and cellular biology* **19**: 6585-6597.

Jonkers J, Meuwissen R, van der Gulden H, Peterse H, van der Valk M, Berns A. 2001. Synergistic tumor suppressor activity of BRCA2 and p53 in a conditional mouse model for breast cancer. *Nature genetics* **29**: 418-425.

Jost CA, Marin MC, Kaelin WG, Jr. 1997. p73 is a simian [correction of human] p53-related protein that can induce apoptosis. *Nature* **389**: 191-194.

Kakodkar R, Soin AS. 2012. Liver Transplantation for HCC: A Review. *The Indian journal of surgery* **74**: 100-117.

Kalluri R, Weinberg RA. 2009. The basics of epithelial-mesenchymal transition. *The Journal of clinical investigation* **119**: 1420-1428.

Katyal S, Oliver JH, 3rd, Peterson MS, Ferris JV, Carr BS, Baron RL. 2000. Extrahepatic metastases of hepatocellular carcinoma. *Radiology* **216**: 698-703.

Katz JP, Perreault N, Goldstein BG, Lee CS, Labosky PA, Yang VW, Kaestner KH. 2002. The zinc-finger transcription factor Klf4 is required for terminal differentiation of goblet cells in the colon. *Development* **129**: 2619-2628.

Kawate S, Fukusato T, Ohwada S, Watanuki A, Morishita Y. 1999. Amplification of c-myc in hepatocellular carcinoma: correlation with clinicopathologic features, proliferative activity and p53 overexpression. *Oncology* **57**: 157-163.

Keng VW, Tschida BR, Bell JB, Largaespada DA. 2011. Modeling hepatitis B virus X-induced hepatocellular carcinoma in mice with the Sleeping Beauty transposon system. *Hepatology* **53**: 781-790.

Kern SE, Pietenpol JA, Thiagalingam S, Seymour A, Kinzler KW, Vogelstein B. 1992. Oncogenic forms of p53 inhibit p53-regulated gene expression. *Science* **256**: 827-830.

Kim CM, Koike K, Saito I, Miyamura T, Jay G. 1991. HBx gene of hepatitis B virus induces liver cancer in transgenic mice. *Nature* **351**: 317-320.

Kim SM, Leem SH, Chu IS, Park YY, Kim SC, Kim SB, Park ES, Lim JY, Heo J, Kim YJ et al. 2012. Sixty-five gene-based risk score classifier predicts overall survival in hepatocellular carcinoma. *Hepatology* **55**: 1443-1452.

Kim Y, Ratziu V, Choi SG, Lalazar A, Theiss G, Dang Q, Kim SJ, Friedman SL. 1998. Transcriptional activation of transforming growth factor beta1 and its receptors by the Kruppel-like factor Zf9/core promoter-binding protein and Sp1. Potential mechanisms for autocrine fibrogenesis in response to injury. *The Journal of biological chemistry* **273**: 33750-33758.

Kitayner M, Rozenberg H, Kessler N, Rabinovich D, Shaulov L, Haran TE, Shakked Z. 2006. Structural basis of DNA recognition by p53 tetramers. *Molecular cell* **22**: 741-753.

Koberle V, Kronenberger B, Pleli T, Trojan J, Imelmann E, Peveling-Oberhag J, Welker MW, Elhendawy M, Zeuzem S, Piiper A et al. 2013. Serum microRNA-1 and microRNA-122 are prognostic markers in patients with hepatocellular carcinoma. *European journal of cancer* **49**: 3442-3449.

Kojima S, Hayashi S, Shimokado K, Suzuki Y, Shimada J, Crippa MP, Friedman SL. 2000. Transcriptional activation of urokinase by the Kruppel-like factor Zf9/COPEB activates latent TGF-beta1 in vascular endothelial cells. *Blood* **95**: 1309-1316.

Kojiro M. 1998. Pathology of early hepatocellular carcinoma: progression from early to advanced. *Hepato-gastroenterology* **45 Suppl 3**: 1203-1205.

Kondo F. 2009. Histological features of early hepatocellular carcinomas and their developmental process: for daily practical clinical application : Hepatocellular carcinoma. *Hepatology international* **3**: 283-293.

Koritschoner NP, Bocco JL, Panzetta-Dutari GM, Dumur CI, Flury A, Patrito LC. 1997. A novel human zinc finger protein that interacts with the core promoter element of a TATA box-less gene. *The Journal of biological chemistry* **272**: 9573-9580.

Kremer-Tal S, Narla G, Chen Y, Hod E, DiFeo A, Yea S, Lee JS, Schwartz M, Thung SN, Fiel IM et al. 2007. Downregulation of KLF6 is an early event in hepatocarcinogenesis, and stimulates proliferation while reducing differentiation. *Journal of hepatology* **46**: 645-654.

Kremer-Tal S, Reeves HL, Narla G, Thung SN, Schwartz M, Difeo A, Katz A, Bruix J, Bioulac-Sage P, Martignetti JA et al. 2004. Frequent inactivation of the tumor suppressor Kruppel-like factor 6 (KLF6) in hepatocellular carcinoma. *Hepatology* **40**: 1047-1052.

Kusano N, Shiraishi K, Kubo K, Oga A, Okita K, Sasaki K. 1999. Genetic aberrations detected by comparative genomic hybridization in hepatocellular carcinomas: their relationship to clinicopathological features. *Hepatology* **29**: 1858-1862.

Lai MS, Hsieh MS, Chiu YH, Chen TH. 2006. Type 2 diabetes and hepatocellular carcinoma: A cohort study in high prevalence area of hepatitis virus infection. *Hepatology* **43**: 1295-1302.

Lang GA, Iwakuma T, Suh YA, Liu G, Rao VA, Parant JM, Valentin-Vega YA, Terzian T, Caldwell LC, Strong LC et al. 2004. Gain of function of a p53 hot spot mutation in a mouse model of Li-Fraumeni syndrome. *Cell* **119**: 861-872.

Lang H, Sotiropoulos GC, Brokalaki EI, Schmitz KJ, Bertona C, Meyer G, Frilling A, Paul A, Malago M, Broelsch CE. 2007. Survival and recurrence rates after resection for hepatocellular carcinoma in noncirrhotic livers. *Journal of the American College of Surgeons* **205**: 27-36.

Lang UE, Kocabayoglu P, Cheng GZ, Ghiassi-Nejad Z, Munoz U, Vetter D, Eckstein DA, Hannivoort RA, Walsh MJ, Friedman SL. 2013. GSK3beta phosphorylation of the KLF6 tumor suppressor promotes its transactivation of p21. *Oncogene* **32**: 4557-4564.

Lawitz E, Gane EJ. 2013. Sofosbuvir for previously untreated chronic hepatitis C infection. *The New England journal of medicine* **369**: 678-679.

Lee JS, Chu IS, Mikaelyan A, Calvisi DF, Heo J, Reddy JK, Thorgeirsson SS. 2004. Application of comparative functional genomics to identify best-fit mouse models to study human cancer. *Nature genetics* **36**: 1306-1311.

Lee K, Liu Y, Mo JQ, Zhang J, Dong Z, Lu S. 2008. Vav3 oncogene activates estrogen receptor and its overexpression may be involved in human breast cancer. *BMC cancer* **8**: 158.

Lee UE, Ghiassi-Nejad Z, Paris AJ, Yea S, Narla G, Walsh M, Friedman SL. 2010. Tumor suppressor activity of KLF6 mediated by downregulation of the PTTG1 oncogene. *FEBS letters* **584**: 1006-1010.

Lee YI, Lee S, Das GC, Park US, Park SM, Lee YI. 2000. Activation of the insulin-like growth factor II transcription by aflatoxin B1 induced p53 mutant 249 is caused by activation of transcription complexes; implications for a gain-of-function during the formation of hepatocellular carcinoma. *Oncogene* **19**: 3717-3726.

Lencioni R, Marrero J, Venook A, Ye SL, Kudo M. 2010. Design and rationale for the non-interventional Global Investigation of Therapeutic DEcisions in Hepatocellular Carcinoma and Of its Treatment with Sorafenib (GIDEON) study. *International journal of clinical practice* **64**: 1034-1041.

Leow CC, Wang BE, Ross J, Chan SM, Zha J, Carano RA, Frantz G, Shen MM, de Sauvage FJ, Gao WQ. 2009. Prostate-specific Klf6 inactivation impairs anterior prostate branching morphogenesis through increased activation of the Shh pathway. *The Journal of biological chemistry* **284**: 21057-21065.

Levrero M. 2006. Viral hepatitis and liver cancer: the case of hepatitis C. *Oncogene* **25**: 3834-3847.

Lewis BC, Klimstra DS, Socci ND, Xu S, Koutcher JA, Varmus HE. 2005. The absence of p53 promotes metastasis in a novel somatic mouse model for hepatocellular carcinoma. *Molecular and cellular biology* **25**: 1228-1237.

Li Q, Gao Y, Jia Z, Mishra L, Guo K, Li Z, Le X, Wei D, Huang S, Xie K. 2012. Dysregulated Kruppel-like factor 4 and vitamin D receptor signaling contribute to progression of hepatocellular carcinoma. *Gastroenterology* **143**: 799-810 e791-792.

Li Y, Prives C. 2007. Are interactions with p63 and p73 involved in mutant p53 gain of oncogenic function? *Oncogene* **26**: 2220-2225.

Liang TJ. 2013. Current progress in development of hepatitis C virus vaccines. *Nature medicine* **19**: 869-878.

Liew CT, Li HM, Lo KW, Leow CK, Chan JY, Hin LY, Lau WY, Lai PB, Lim BK, Huang J et al. 1999. High frequency of p16INK4A gene alterations in hepatocellular carcinoma. *Oncogene* **18**: 789-795.

Lin KT, Gong J, Li CF, Jang TH, Chen WL, Chen HJ, Wang LH. 2012a. Vav3-rac1 signaling regulates prostate cancer metastasis with elevated Vav3 expression correlating with prostate cancer progression and posttreatment recurrence. *Cancer research* **72**: 3000-3009.

Lin ZS, Chu HC, Yen YC, Lewis BC, Chen YW. 2012b. Kruppel-like factor 4, a tumor suppressor in hepatocellular carcinoma cells reverts epithelial mesenchymal transition by suppressing slug expression. *PloS one* **7**: e43593.

Liotta LA, Kohn E. 2004. Anoikis: cancer and the homeless cell. *Nature* **430**: 973-974.

Liu J, Ma Q, Zhang M, Wang X, Zhang D, Li W, Wang F, Wu E. 2012. Alterations of TP53 are associated with a poor outcome for patients with hepatocellular carcinoma: evidence from a systematic review and meta-analysis. *European journal of cancer* **48**: 2328-2338.

Liu J, Zhang C, Feng Z. 2013a. Tumor suppressor p53 and its gain-of-function mutants in cancer. *Acta biochimica et biophysica Sinica*.

Liu S, Yu M, He Y, Xiao L, Wang F, Song C, Sun S, Ling C, Xu Z. 2008. Melittin prevents liver cancer cell metastasis through inhibition of the Rac1-dependent pathway. *Hepatology* **47**: 1964-1973.

Liu X, Wilcken R, Joerger AC, Chuckowree IS, Amin J, Spencer J, Fersht AR. 2013b. Small molecule induced reactivation of mutant p53 in cancer cells. *Nucleic acids research* **41**: 6034-6044.

Llovet JM, Bru C, Bruix J. 1999. Prognosis of hepatocellular carcinoma: the BCLC staging classification. *Seminars in liver disease* **19**: 329-338.

Llovet JM, Bruix J. 2003. Systematic review of randomized trials for unresectable hepatocellular carcinoma: Chemoembolization improves survival. *Hepatology* **37**: 429-442.

Llovet JM, Ricci S, Mazzaferro V, Hilgard P, Gane E, Blanc JF, de Oliveira AC, Santoro A, Raoul JL, Forner A et al. 2008. Sorafenib in advanced hepatocellular carcinoma. *The New England journal of medicine* **359**: 378-390.

Lobry C, Oh P, Aifantis I. 2011. Oncogenic and tumor suppressor functions of Notch in cancer: it's NOTCH what you think. *The Journal of experimental medicine* **208**: 1931-1935.

Long J, Wang Y, Li M, Tong WM, Jia JD, Huang J. 2013. Correlation of TP53 mutations with HCV positivity in hepatocarcinogenesis: identification of a novel TP53 microindel in hepatocellular carcinoma with HCV infection. *Oncology reports* **30**: 119-124.

Loomes KM, Russo P, Ryan M, Nelson A, Underkoffler L, Glover C, Fu H, Gridley T, Kaestner KH, Oakey RJ. 2007. Bile duct proliferation in liver-specific Jag1 conditional knockout mice: effects of gene dosage. *Hepatology* **45**: 323-330.

Lu X, Kang Y. 2010. Hypoxia and hypoxia-inducible factors: master regulators of metastasis. *Clinical cancer research : an official journal of the American Association for Cancer Research* **16**: 5928-5935.

Lu X, Liu DP, Xu Y. 2012. The gain of function of p53 cancer mutant in promoting mammary tumorigenesis. *Oncogene*.

-. 2013. The gain of function of p53 cancer mutant in promoting mammary tumorigenesis. *Oncogene* **32**: 2900-2906.

Luedde T, Beraza N, Kotsikoris V, van Loo G, Nenci A, De Vos R, Roskams T, Trautwein C, Pasparakis M. 2007. Deletion of NEMO/IKKgamma in liver parenchymal cells causes steatohepatitis and hepatocellular carcinoma. *Cancer cell* **11**: 119-132.

Luzzi KJ, MacDonald IC, Schmidt EE, Kerkvliet N, Morris VL, Chambers AF, Groom AC. 1998. Multistep nature of metastatic inefficiency: dormancy of solitary cells after successful extravasation and limited survival of early micrometastases. *The American journal of pathology* **153**: 865-873.

Mao Y, Zhang N, Xu J, Ding Z, Zong R, Liu Z. 2012. Significance of heterogeneous Twist2 expression in human breast cancers. *PloS one* **7**: e48178.

Martello G, Rosato A, Ferrari F, Manfrin A, Cordenonsi M, Dupont S, Enzo E, Guzzardo V, Rondina M, Spruce T et al. 2010. A MicroRNA targeting dicer for metastasis control. *Cell* **141**: 1195-1207.

Matsuda Y, Ichida T, Matsuzawa J, Sugimura K, Asakura H. 1999. p16(INK4) is inactivated by extensive CpG methylation in human hepatocellular carcinoma. *Gastroenterology* **116**: 394-400.

Matsumoto N, Kubo A, Liu H, Akita K, Laub F, Ramirez F, Keller G, Friedman SL. 2006. Developmental regulation of yolk sac hematopoiesis by Kruppel-like factor 6. *Blood* **107**: 1357-1365.

Mazzaferro V, Llovet JM, Miceli R, Bhoori S, Schiavo M, Mariani L, Camerini T, Roayaie S, Schwartz ME, Grazi GL et al. 2009. Predicting survival after liver transplantation in patients with hepatocellular carcinoma beyond the Milan criteria: a retrospective, exploratory analysis. *The lancet oncology* **10**: 35-43.

McClatchey AI, Saotome I, Ramesh V, Gusella JF, Jacks T. 1997. The Nf2 tumor suppressor gene product is essential for extraembryonic development immediately prior to gastrulation. *Genes & development* **11**: 1253-1265.

McGivern DR, Villanueva RA, Chinnaswamy S, Kao CC, Lemon SM. 2009. Impaired replication of hepatitis C virus containing mutations in a conserved NS5B retinoblastoma protein-binding motif. *Journal of virology* **83**: 7422-7433.

McGlynn KA, Hunter K, LeVoyer T, Roush J, Wise P, Michielli RA, Shen FM, Evans AA, London WT, Buetow KH. 2003. Susceptibility to aflatoxin B1-related primary hepatocellular carcinoma in mice and humans. *Cancer research* **63**: 4594-4601.

McGlynn KA, London WT. 2005. Epidemiology and natural history of hepatocellular carcinoma. *Best practice & research Clinical gastroenterology* **19**: 3-23.

Mills AA, Zheng B, Wang XJ, Vogel H, Roop DR, Bradley A. 1999. p63 is a p53 homologue required for limb and epidermal morphogenesis. *Nature* **398**: 708-713.

Moll UM, Slade N. 2004. p63 and p73: roles in development and tumor formation. *Molecular cancer research : MCR* **2**: 371-386.

Morton JP, Timpson P, Karim SA, Ridgway RA, Athineos D, Doyle B, Jamieson NB, Oien KA, Lowy AM, Brunton VG et al. 2010. Mutant p53 drives metastasis and overcomes growth arrest/senescence in pancreatic cancer. *Proceedings of the National Academy of Sciences of the United States of America* **107**: 246-251.

Muller PA, Trinidad AG, Caswell PT, Norman JC, Vousden KH. 2014. Mutant p53 regulates Dicer through p63-dependent and -independent mechanisms to promote an invasive phenotype. *The Journal of biological chemistry* **289**: 122-132.

Munoz U, Puche JE, Hannivoort R, Lang UE, Cohen-Naftaly M, Friedman SL. 2012. Hepatocyte growth factor enhances alternative splicing of the Kruppel-like factor 6 (KLF6) tumor suppressor to promote growth through SRSF1. *Molecular cancer research : MCR* **10**: 1216-1227.

Murakami H, Sanderson ND, Nagy P, Marino PA, Merlino G, Thorgeirsson SS. 1993. Transgenic mouse model for synergistic effects of nuclear oncogenes and growth factors in tumorigenesis: interaction of c-myc and transforming growth factor alpha in hepatic oncogenesis. *Cancer research* **53**: 1719-1723.

Murakami Y, Saigo K, Takashima H, Minami M, Okanoue T, Brechot C, Paterlini-Brechot P. 2005. Large scaled analysis of hepatitis B virus (HBV) DNA integration in HBV related hepatocellular carcinomas. *Gut* **54**: 1162-1168.

Murray-Zmijewski F, Lane DP, Bourdon JC. 2006. p53/p63/p73 isoforms: an orchestra of isoforms to harmonise cell differentiation and response to stress. *Cell death and differentiation* **13**: 962-972.

Nakagawa M, Koyanagi M, Tanabe K, Takahashi K, Ichisaka T, Aoi T, Okita K, Mochiduki Y, Takizawa N, Yamanaka S. 2008. Generation of induced pluripotent stem cells without Myc from mouse and human fibroblasts. *Nature biotechnology* **26**: 101-106.

Nakamoto Y, Guidotti LG, Kuhlen CV, Fowler P, Chisari FV. 1998. Immune pathogenesis of hepatocellular carcinoma. *The Journal of experimental medicine* **188**: 341-350.

Nakao K, Miyaaki H, Ichikawa T. 2014. Antitumor function of microRNA-122 against hepatocellular carcinoma. *Journal of gastroenterology*.

Narla G, DiFeo A, Fernandez Y, Dhanasekaran S, Huang F, Sangodkar J, Hod E, Leake D, Friedman SL, Hall SJ et al. 2008. KLF6-SV1 overexpression accelerates human and mouse prostate cancer progression and metastasis. *The Journal of clinical investigation* **118**: 2711-2721.

Narla G, Difeo A, Reeves HL, Schaid DJ, Hirshfeld J, Hod E, Katz A, Isaacs WB, Hebbring S, Komiya A et al. 2005. A germline DNA polymorphism enhances alternative splicing of the KLF6 tumor suppressor gene and is associated with increased prostate cancer risk. *Cancer research* **65**: 1213-1222.

Narla G, Heath KE, Reeves HL, Li D, Giono LE, Kimmelman AC, Glucksman MJ, Narla J, Eng FJ, Chan AM et al. 2001. KLF6, a candidate tumor suppressor gene mutated in prostate cancer. *Science* **294**: 2563-2566.

Narla G, Kremer-Tal S, Matsumoto N, Zhao X, Yao S, Kelley K, Tarocchi M, Friedman SL. 2007. In vivo regulation of p21 by the Kruppel-like factor 6 tumor-suppressor gene in mouse liver and human hepatocellular carcinoma. *Oncogene* **26**: 4428-4434.

Nassirpour R, Mehta PP, Yin MJ. 2013. miR-122 regulates tumorigenesis in hepatocellular carcinoma by targeting AKT3. *PloS one* **8**: e79655.

Newberne PM, Butler WH. 1969. Acute and chronic effects of aflatoxin on the liver of domestic and laboratory animals: a review. *Cancer research* **29**: 236-250.

Nguyen DX, Bos PD, Massague J. 2009. Metastasis: from dissemination to organ-specific colonization. *Nature reviews Cancer* **9**: 274-284.

Oda T, Tsuda H, Scarpa A, Sakamoto M, Hirohashi S. 1992. p53 gene mutation spectrum in hepatocellular carcinoma. *Cancer research* **52**: 6358-6364.

Okano J, Opitz OG, Nakagawa H, Jenkins TD, Friedman SL, Rustgi AK. 2000. The Kruppel-like transcriptional factors Zf9 and GKLF coactivate the human keratin 4 promoter and physically interact. *FEBS letters* **473**: 95-100.

Olive KP, Tuveson DA, Ruhe ZC, Yin B, Willis NA, Bronson RT, Crowley D, Jacks T. 2004. Mutant p53 gain of function in two mouse models of Li-Fraumeni syndrome. *Cell* **119**: 847-860.

Olive V, Jiang I, He L. 2010. mir-17-92, a cluster of miRNAs in the midst of the cancer network. *The international journal of biochemistry & cell biology* **42**: 1348-1354.

Olivier M, Hollstein M, Hainaut P. 2010. TP53 mutations in human cancers: origins, consequences, and clinical use. *Cold Spring Harbor perspectives in biology* **2**: a001008.

Oren M, Rotter V. 2010. Mutant p53 gain-of-function in cancer. *Cold Spring Harbor perspectives in biology* **2**: a001107.

Orlando A, Leandro G, Olivo M, Andriulli A, Cottone M. 2009. Radiofrequency thermal ablation vs. percutaneous ethanol injection for small hepatocellular carcinoma in cirrhosis: meta-analysis of randomized controlled trials. *The American journal of gastroenterology* **104**: 514-524.

Owsianka AM, Patel AH. 1999. Hepatitis C virus core protein interacts with a human DEAD box protein DDX3. *Virology* **257**: 330-340.

Ozturk M. 1991. p53 mutation in hepatocellular carcinoma after aflatoxin exposure. *Lancet* **338**: 1356-1359.

Palmer DH, Hussain SA, Johnson PJ. 2004. Systemic therapies for hepatocellular carcinoma. *Expert opinion on investigational drugs* **13**: 1555-1568.

Pan H, Liao SJ, Lai WY, Lu HC, Hsiao KM. 2002. Overexpression but lack of mutation and methylation of p73 in hepatocellular carcinoma. *Acta oncologica* **41**: 550-555.

Pan XC, Chen Z, Chen F, Chen XH, Jin HY, Xu XY. 2006. Inactivation of the tumor suppressor Kruppel-like factor 6 (KLF6) by mutation or decreased expression in hepatocellular carcinomas. *Journal of Zhejiang University Science B* **7**: 830-836.

Parada LA, Hallen M, Tranberg KG, Hagerstrand I, Bondeson L, Mitelman F, Johansson B. 1998. Frequent rearrangements of chromosomes 1, 7, and 8 in primary liver cancer. *Genes, chromosomes & cancer* **23**: 26-35.

Parsons CJ, Takashima M, Rippe RA. 2007. Molecular mechanisms of hepatic fibrogenesis. *Journal of gastroenterology and hepatology* **22 Suppl 1**: S79-84.

Peng SY, Lai PL, Hsu HC. 1993. Amplification of the c-myc gene in human hepatocellular carcinoma: biologic significance. *Journal of the Formosan Medical Association = Taiwan yi zhi* **92**: 866-870.

Persad R, Liu C, Wu TT, Houlihan PS, Hamilton SR, Diehl AM, Rashid A. 2004. Overexpression of caspase-3 in hepatocellular carcinomas. *Modern pathology : an official journal of the United States and Canadian Academy of Pathology, Inc* **17**: 861-867.

Petitjean A, Cavard C, Shi H, Tribollet V, Hainaut P, Caron de Fromentel C. 2005. The expression of TA and DeltaNp63 are regulated by different mechanisms in liver cells. *Oncogene* **24**: 512-519.

Poon RT, Fan ST, Lo CM, Liu CL, Ng IO, Wong J. 2000. Long-term prognosis after resection of hepatocellular carcinoma associated with hepatitis B-related cirrhosis. *Journal of clinical oncology : official journal of the American Society of Clinical Oncology* **18**: 1094-1101.

Poon RT, Fan ST, Lo CM, Liu CL, Wong J. 1999. Intrahepatic recurrence after curative resection of hepatocellular carcinoma: long-term results of treatment and prognostic factors. *Annals of surgery* **229**: 216-222.

Popescu NC, Goodison S. 2014. Deleted in Liver Cancer-1 (DLC1): An Emerging Metastasis Suppressor Gene. *Molecular diagnosis & therapy*.

Qin LX, Tang ZY, Ma ZC, Wu ZQ, Zhou XD, Ye QH, Ji Y, Huang LW, Jia HL, Sun HC et al. 2002. P53 immunohistochemical scoring: an independent prognostic marker for patients after hepatocellular carcinoma resection. *World journal of gastroenterology : WJG* **8**: 459-463.

Qiu RG, Abo A, McCormick F, Symons M. 1997. Cdc42 regulates anchorage-independent growth and is necessary for Ras transformation. *Molecular and cellular biology* **17**: 3449-3458.

Qiu RG, Chen J, Kirn D, McCormick F, Symons M. 1995a. An essential role for Rac in Ras transformation. *Nature* **374**: 457-459.

Qiu RG, Chen J, McCormick F, Symons M. 1995b. A role for Rho in Ras transformation. *Proceedings of the National Academy of Sciences of the United States of America* **92**: 11781-11785.

Quinn BA, Crane TL, Kocal TE, Best SJ, Cameron RG, Rushmore TH, Farber E, Hayes MA. 1990. Protective activity of different hepatic cytosolic glutathione S-transferases against DNA-binding metabolites of aflatoxin B1. *Toxicology and applied pharmacology* **105**: 351-363.

Ratziu V, Lalazar A, Wong L, Dang Q, Collins C, Shaulian E, Jensen S, Friedman SL. 1998. Zf9, a Kruppel-like transcription factor up-regulated in vivo during early hepatic fibrosis. *Proceedings of the National Academy of Sciences of the United States of America* **95**: 9500-9505.

Rehem RN, El-Shikh WM. 2011. Serum IGF-1, IGF-2 and IGFBP-3 as parameters in the assessment of liver dysfunction in patients with hepatic cirrhosis and in the diagnosis of hepatocellular carcinoma. *Hepato-gastroenterology* **58**: 949-954.

Roayaie S, Schwartz JD, Sung MW, Emre SH, Miller CM, Gondolesi GE, Krieger NR, Schwartz ME. 2004. Recurrence of hepatocellular carcinoma after liver transplant: patterns and prognosis. *Liver transplantation : official publication of the American Association for the Study of Liver Diseases and the International Liver Transplantation Society* **10**: 534-540.

Rodriguez E, Aburjania N, Priedigkeit NM, DiFeo A, Martignetti JA. 2010. Nucleo-cytoplasmic localization domains regulate Kruppel-like factor 6 (KLF6) protein stability and tumor suppressor function. *PloS one* **5**.

Roessler S, Jia HL, Budhu A, Forgues M, Ye QH, Lee JS, Thorgeirsson SS, Sun Z, Tang ZY, Qin LX et al. 2010. A unique metastasis gene signature enables prediction of tumor relapse in early-stage hepatocellular carcinoma patients. *Cancer research* **70**: 10202-10212.

Romano RA, Smalley K, Magraw C, Serna VA, Kurita T, Raghavan S, Sinha S. 2012. DeltaNp63 knockout mice reveal its indispensable role as a master regulator of epithelial development and differentiation. *Development* **139**: 772-782.

Rosenblatt AE, Garcia MI, Lyons L, Xie Y, Maiorino C, Desire L, Slingerland J, Burnstein KL. 2011. Inhibition of the Rho GTPase, Rac1, decreases estrogen receptor levels and is a novel therapeutic strategy in breast cancer. *Endocrine-related cancer* **18**: 207-219.

Rossman KL, Der CJ, Sondek J. 2005. GEF means go: turning on RHO GTPases with guanine nucleotide-exchange factors. *Nature reviews Molecular cell biology* **6**: 167-180.

Rubinstein M, Idelman G, Plymate SR, Narla G, Friedman SL, Werner H. 2004. Transcriptional activation of the insulin-like growth factor I receptor gene by the Kruppel-like factor 6 (KLF6) tumor suppressor protein: potential interactions between KLF6 and p53. *Endocrinology* **145**: 3769-3777.

Ruddell RG, Knight B, Tirnitz-Parker JE, Akhurst B, Summerville L, Subramaniam VN, Olynyk JK, Ramm GA. 2009. Lymphotoxin-beta receptor signaling regulates hepatic stellate cell function and wound healing in a murine model of chronic liver injury. *Hepatology* **49**: 227-239.

Sachdev P, Zeng L, Wang LH. 2002. Distinct role of phosphatidylinositol 3-kinase and Rho family GTPases in Vav3-induced cell transformation, cell motility, and morphological changes. *The Journal of biological chemistry* **277**: 17638-17648.

Sahai E, Marshall CJ. 2002. RHO-GTPases and cancer. *Nature reviews Cancer* **2**: 133-142.

Sandgren EP, Quaife CJ, Pinkert CA, Palmiter RD, Brinster RL. 1989. Oncogene-induced liver neoplasia in transgenic mice. *Oncogene* **4**: 715-724.

Sangodkar J, Dhawan NS, Melville H, Singh VJ, Yuan E, Rana H, Izadmehr S, Farrington C, Mazhar S, Katz S et al. 2012. Targeting the FOXO1/KLF6 axis regulates EGFR signaling and treatment response. *The Journal of clinical investigation* **122**: 2637-2651.

Sauzeau V, Sevilla MA, Rivas-Elena JV, de Alava E, Montero MJ, Lopez-Novoa JM, Bustelo XR. 2006. Vav3 proto-oncogene deficiency leads to sympathetic hyperactivity and cardiovascular dysfunction. *Nature medicine* **12**: 841-845.

Sayan AE, Sayan BS, Findikli N, Ozturk M. 2001. Acquired expression of transcriptionally active p73 in hepatocellular carcinoma cells. *Oncogene* **20**: 5111-5117.

Schaffhausen BS, Roberts TM. 2009. Lessons from polyoma middle T antigen on signaling and transformation: A DNA tumor virus contribution to the war on cancer. *Virology* **384**: 304-316.

Schilling T, Kairat A, Melino G, Krammer PH, Stremmel W, Oren M, Muller M. 2010. Interference with the p53 family network contributes to the gain of oncogenic function of mutant p53 in hepatocellular carcinoma. *Biochemical and biophysical research communications* **394**: 817-823.

Schmidt A, Hall A. 2002. Guanine nucleotide exchange factors for Rho GTPases: turning on the switch. *Genes & development* **16**: 1587-1609.

Scholzen T, Gerdes J. 2000. The Ki-67 protein: from the known and the unknown. *Journal of cellular physiology* **182**: 311-322.

Sebestyen MG, Budker VG, Budker T, Subbotin VM, Zhang G, Monahan SD, Lewis DL, Wong SC, Hagstrom JE, Wolff JA. 2006. Mechanism of plasmid delivery by hydrodynamic tail vein injection. I. Hepatocyte uptake of various molecules. *The journal of gene medicine* **8**: 852-873.

Sekine S, Ogawa R, McManus MT, Kanai Y, Hebrok M. 2009. Dicer is required for proper liver zonation. *The Journal of pathology* **219**: 365-372.

SenGupta DJ, Zhang B, Kraemer B, Pochart P, Fields S, Wickens M. 1996. A three-hybrid system to detect RNA-protein interactions in vivo. *Proceedings of the National Academy of Sciences of the United States of America* **93**: 8496-8501.

Sethi N, Dai X, Winter CG, Kang Y. 2011. Tumor-derived JAGGED1 promotes osteolytic bone metastasis of breast cancer by engaging notch signaling in bone cells. *Cancer cell* **19**: 192-205.

Shachaf CM, Kopelman AM, Arvanitis C, Karlsson A, Beer S, Mandl S, Bachmann MH, Borowsky AD, Ruebner B, Cardiff RD et al. 2004. MYC inactivation uncovers pluripotent differentiation and tumour dormancy in hepatocellular cancer. *Nature* **431**: 1112-1117.

Sharma P, Balan V, Hernandez JL, Harper AM, Edwards EB, Rodriguez-Luna H, Byrne T, Vargas HE, Mulligan D, Rakela J et al. 2004. Liver transplantation for hepatocellular carcinoma: the MELD impact. *Liver transplantation : official publication of the American Association for the Study of Liver Diseases and the International Liver Transplantation Society* **10**: 36-41.

Shih Ie M, Wang TL. 2007. Notch signaling, gamma-secretase inhibitors, and cancer therapy. *Cancer research* **67**: 1879-1882.

Shuno Y, Tsuno NH, Okaji Y, Tsuchiya T, Sakurai D, Nishikawa T, Yoshikawa N, Sasaki K, Hongo K, Tsurita G et al. 2010. Id1/Id3 knockdown inhibits metastatic potential of pancreatic cancer. *The Journal of surgical research* **161**: 76-82.

Siegel R, Naishadham D, Jemal A. 2013. Cancer statistics, 2013. *CA: a cancer journal for clinicians* **63**: 11-30.

Sigal A, Rotter V. 2000. Oncogenic mutations of the p53 tumor suppressor: the demons of the guardian of the genome. *Cancer research* **60**: 6788-6793.

Singer S, Ehemann V, Brauckhoff A, Keith M, Vreden S, Schirmacher P, Breuhahn K. 2007. Protumorigenic overexpression of stathmin/Op18 by gain-of-function mutation in p53 in human hepatocarcinogenesis. *Hepatology* **46**: 759-768.

Sirach E, Bureau C, Peron JM, Pradayrol L, Vinel JP, Buscail L, Cordelier P. 2007. KLF6 transcription factor protects hepatocellular carcinoma-derived cells from apoptosis. *Cell death and differentiation* **14**: 1202-1210.

Slavin DA, Koritschoner NP, Prieto CC, Lopez-Diaz FJ, Chatton B, Bocco JL. 2004. A new role for the Kruppel-like transcription factor KLF6 as an inhibitor of c-Jun proto-oncoprotein function. *Oncogene* **23**: 8196-8205.

Song J, Kim CJ, Cho YG, Kim SY, Nam SW, Lee SH, Yoo NJ, Lee JY, Park WS. 2006. Genetic and epigenetic alterations of the KLF6 gene in hepatocellular carcinoma. *Journal of gastroenterology and hepatology* **21**: 1286-1289.

Srivastava S, Wong KF, Ong CW, Huak CY, Yeoh KG, Teh M, Luk JM, Salto-Tellez M. 2012. A morpho-molecular prognostic model for hepatocellular carcinoma. *British journal of cancer* **107**: 334-339.

Srivastava S, Zou ZQ, Pirollo K, Blattner W, Chang EH. 1990. Germ-line transmission of a mutated p53 gene in a cancer-prone family with Li-Fraumeni syndrome. *Nature* **348**: 747-749.

Stern MC, Umbach DM, Yu MC, London SJ, Zhang ZQ, Taylor JA. 2001. Hepatitis B, aflatoxin B(1), and p53 codon 249 mutation in hepatocellular carcinomas from Guangxi, People's Republic of China, and a meta-analysis of existing studies. *Cancer epidemiology, biomarkers & prevention : a publication of the American Association for Cancer Research, cosponsored by the American Society of Preventive Oncology* **10**: 617-625.

Stiewe T, Tuve S, Peter M, Tannapfel A, Elmaagacli AH, Putzer BM. 2004. Quantitative TP73 transcript analysis in hepatocellular carcinomas. *Clinical cancer research : an official journal of the American Association for Cancer Research* **10**: 626-633.

Strano S, Fontemaggi G, Costanzo A, Rizzo MG, Monti O, Baccarini A, Del Sal G, Levrero M, Sacchi A, Oren M et al. 2002. Physical interaction with human tumor-derived p53 mutants inhibits p63 activities. *The Journal of biological chemistry* **277**: 18817-18826.

Stratton MR, Campbell PJ, Futreal PA. 2009. The cancer genome. *Nature* **458**: 719-724.

Su X, Chakravarti D, Cho MS, Liu L, Gi YJ, Lin YL, Leung ML, El-Naggar A, Creighton CJ, Suraokar MB et al. 2010. TAp63 suppresses metastasis through coordinate regulation of Dicer and miRNAs. *Nature* **467**: 986-990.

Su X, Paris M, Gi YJ, Tsai KY, Cho MS, Lin YL, Biernaskie JA, Sinha S, Prives C, Pevny LH et al. 2009. TAp63 prevents premature aging by promoting adult stem cell maintenance. *Cell stem cell* **5**: 64-75.

Suzuki T, Yamamoto T, Kurabayashi M, Nagai R, Yazaki Y, Horikoshi M. 1998. Isolation and initial characterization of GBF, a novel DNA-binding zinc finger protein that binds to the GC-rich binding sites of the HIV-1 promoter. *Journal of biochemistry* **124**: 389-395.

Takahashi K, Yamanaka S. 2006. Induction of pluripotent stem cells from mouse embryonic and adult fibroblast cultures by defined factors. *Cell* **126**: 663-676.

Takayama T, Makuuchi M, Hirohashi S, Sakamoto M, Yamamoto J, Shimada K, Kosuge T, Okada S, Takayasu K, Yamasaki S. 1998. Early hepatocellular carcinoma as an entity with a high rate of surgical cure. *Hepatology* **28**: 1241-1246.

Taketa K. 1990. Alpha-fetoprotein: reevaluation in hepatology. *Hepatology* **12**: 1420-1432.

Tan A, Yeh SH, Liu CJ, Cheung C, Chen PJ. 2008. Viral hepatocarcinogenesis: from infection to cancer. *Liver international : official journal of the International Association for the Study of the Liver* **28**: 175-188.

Tan B, Li Y, Zhao Q, Fan L, Wang D, Liu Y. 2013. Inhibition of gastric cancer cell growth and invasion through siRNA-mediated knockdown of guanine nucleotide exchange factor Vav3. *Tumour biology : the journal of the International Society for Oncodevelopmental Biology and Medicine*.

Tannapfel A, Busse C, Weinans L, Benicke M, Katalinic A, Geissler F, Hauss J, Wittekind C. 2001. INK4a-ARF alterations and p53 mutations in hepatocellular carcinomas. *Oncogene* **20**: 7104-7109.

Tannapfel A, Wasner M, Krause K, Geissler F, Katalinic A, Hauss J, Mossner J, Engeland K, Wittekind C. 1999. Expression of p73 and its relation to histopathology and prognosis in hepatocellular carcinoma. *Journal of the National Cancer Institute* **91**: 1154-1158.

Tarocchi M, Hannivoort R, Hoshida Y, Lee UE, Vetter D, Narla G, Villanueva A, Oren M, Llovet JM, Friedman SL. 2011. Carcinogen-induced hepatic tumors in KLF6+/- mice recapitulate aggressive human hepatocellular carcinoma associated with p53 pathway deregulation. *Hepatology* **54**: 522-531.

Thiery JP. 2002. Epithelial-mesenchymal transitions in tumour progression. *Nature reviews Cancer* **2**: 442-454.

Thongbai C, Sa-Nguanmoo P, Kranokpiruk P, Poovorawan K, Poovorawan Y, Tangkijvanich P. 2013. Hepatitis B Virus Genetic Variation and TP53 R249S Mutation in Patients with Hepatocellular Carcinoma in Thailand. *Asian Pacific journal of cancer prevention : APJCP* **14**: 3555-3559.

Tomasini R, Tsuchihara K, Wilhelm M, Fujitani M, Rufini A, Cheung CC, Khan F, Itie-Youten A, Wakeham A, Tsao MS et al. 2008. TAp73 knockout shows genomic instability with infertility and tumor suppressor functions. *Genes & development* **22**: 2677-2691.

Toumaniantz G, Ferland-McCollough D, Cario-Toumaniantz C, Pacaud P, Loirand G. 2010. The Rho protein exchange factor Vav3 regulates vascular smooth muscle cell proliferation and migration. *Cardiovascular research* **86**: 131-140.

Trevisani F, Frigerio M, Santi V, Grignaschi A, Bernardi M. 2010. Hepatocellular carcinoma in non-cirrhotic liver: a reappraisal. *Digestive and liver disease : official journal of the Italian Society of Gastroenterology and the Italian Association for the Study of the Liver* **42**: 341-347.

Tsai WC, Hsu SD, Hsu CS, Lai TC, Chen SJ, Shen R, Huang Y, Chen HC, Lee CH, Tsai TF et al. 2012. MicroRNA-122 plays a critical role in liver homeostasis and hepatocarcinogenesis. *The Journal of clinical investigation* **122**: 2884-2897.

Tsuchiya T, Okaji Y, Tsuno NH, Sakurai D, Tsuchiya N, Kawai K, Yazawa K, Asakage M, Yamada J, Yoneyama S et al. 2005. Targeting Id1 and Id3 inhibits peritoneal metastasis of gastric cancer. *Cancer science* **96**: 784-790.

Turati F, Edefonti V, Talamini R, Ferraroni M, Malvezzi M, Bravi F, Franceschi S, Montella M, Polesel J, Zucchetto A et al. 2012. Family history of liver cancer and hepatocellular carcinoma. *Hepatology* **55**: 1416-1425.

Ueda Y, Hijikata M, Takagi S, Chiba T, Shimotohno K. 1999. New p73 variants with altered C-terminal structures have varied transcriptional activities. *Oncogene* **18**: 4993-4998.

Ule J, Jensen KB, Ruggiu M, Mele A, Ule A, Darnell RB. 2003. CLIP identifies Nova-regulated RNA networks in the brain. *Science* **302**: 1212-1215.

Unger T, Nau MM, Segal S, Minna JD. 1992. p53: a transdominant regulator of transcription whose function is ablated by mutations occurring in human cancer. *The EMBO journal* **11**: 1383-1390.

Vauthey JN, Lauwers GY, Esnaola NF, Do KA, Belghiti J, Mirza N, Curley SA, Ellis LM, Regimbeau JM, Rashid A et al. 2002. Simplified staging for hepatocellular carcinoma. *Journal of clinical oncology : official journal of the American Society of Clinical Oncology* **20**: 1527-1536.

Verna L, Whysner J, Williams GM. 1996. N-nitrosodiethylamine mechanistic data and risk assessment: bioactivation, DNA-adduct formation, mutagenicity, and tumor initiation. *Pharmacology & therapeutics* **71**: 57-81.

Vesselinovitch SD, Mihailovich N, Rao KV. 1978. Morphology and metastatic nature of induced hepatic nodular lesions in C57BL x C3H F1 mice. *Cancer research* **38**: 2003-2010.

Vesselinovitch SD, Mihailovich N, Wogan GN, Lombard LS, Rao KV. 1972. Aflatoxin B 1 , a hepatocarcinogen in the infant mouse. *Cancer research* **32**: 2289-2291.

Vetter D, Cohen-Naftaly M, Villanueva A, Lee YA, Kocabayoglu P, Hannivoort R, Narla G, J ML, Thung SN, Friedman SL. 2012. Enhanced hepatocarcinogenesis in mouse models and human hepatocellular carcinoma by coordinate KLF6 depletion and increased messenger RNA splicing. *Hepatology* **56**: 1361-1370.

Villanueva A, Alsinet C, Yanger K, Hoshida Y, Zong Y, Toffanin S, Rodriguez-Carunchio L, Sole M, Thung S, Stanger BZ et al. 2012. Notch signaling is activated in human hepatocellular carcinoma and induces tumor formation in mice. *Gastroenterology* **143**: 1660-1669 e1667.

Villanueva A, Hoshida Y. 2011. Depicting the role of TP53 in hepatocellular carcinoma progression. *Journal of hepatology* **55**: 724-725.

Vousden KH, Lu X. 2002. Live or let die: the cell's response to p53. *Nature reviews Cancer* **2**: 594-604.

Wang S, Kang L, Chen X, Zhou H. 2010. Frequent down-regulation and deletion of KLF6 in primary hepatocellular carcinoma. *Journal of Huazhong University of Science and Technology Medical sciences = Hua zhong ke ji da xue xue bao Yi xue Ying De wen ban = Huazhong keji daxue xuebao Yixue Yingdewen ban* **30**: 470-476.

Wang W, Cheng B, Miao L, Mei Y, Wu M. 2013. Mutant p53-R273H gains new function in sustained activation of EGFR signaling via suppressing miR-27a expression. *Cell death & disease* **4**: e574.

Wang XW, Forrester K, Yeh H, Feitelson MA, Gu JR, Harris CC. 1994. Hepatitis B virus X protein inhibits p53 sequence-specific DNA binding, transcriptional activity, and association with transcription factor ERCC3. *Proceedings of the National Academy of Sciences of the United States of America* **91**: 2230-2234.

Warke VG, Nambiar MP, Krishnan S, Tenbrock K, Geller DA, Koritschoner NP, Atkins JL, Farber DL, Tsokos GC. 2003. Transcriptional activation of the human inducible nitric-oxide synthase promoter by Kruppel-like factor 6. *The Journal of biological chemistry* **278**: 14812-14819.

Weber A, Boege Y, Reisinger F, Heikenwalder M. 2011. Chronic liver inflammation and hepatocellular carcinoma: persistence matters. *Swiss medical weekly* **141**: w13197.

Welzel TM, Graubard BI, Quraishi S, Zeuzem S, Davila JA, El-Serag HB, McGlynn KA. 2013. Population-attributable fractions of risk factors for hepatocellular carcinoma in the United States. *The American journal of gastroenterology* **108**: 1314-1321.

Werner H, Karnieli E, Rauscher FJ, LeRoith D. 1996. Wild-type and mutant p53 differentially regulate transcription of the insulin-like growth factor I receptor gene. *Proceedings of the National Academy of Sciences of the United States of America* **93**: 8318-8323.

Westfall MD, Mays DJ, Sniezek JC, Pietenpol JA. 2003. The Delta Np63 alpha phosphoprotein binds the p21 and 14-3-3 sigma promoters in vivo and has transcriptional repressor activity that is reduced by Hay-Wells syndrome-derived mutations. *Molecular and cellular biology* **23**: 2264-2276.

Wijnhoven SW, Speksnijder EN, Liu X, Zwart E, vanOostrom CT, Beems RB, Hoogervorst EM, Schaap MM, Attardi LD, Jacks T et al. 2007. Dominant-negative but not gain-of-function effects of a p53.R270H mutation in mouse epithelium tissue after DNA damage. *Cancer research* **67**: 4648-4656.

Wilhelm MT, Rufini A, Wetzel MK, Tsuchihara K, Inoue S, Tomasini R, Itie-Youten A, Wakeham A, Arsenian-Henriksson M, Melino G et al. 2010. Isoform-specific p73 knockout mice reveal a novel role for delta Np73 in the DNA damage response pathway. *Genes & development* **24**: 549-560.

Wilhelm SM, Carter C, Tang L, Wilkie D, McNabola A, Rong H, Chen C, Zhang X, Vincent P, McHugh M et al. 2004. BAY 43-9006 exhibits broad spectrum oral antitumor activity and targets the RAF/MEK/ERK pathway and receptor tyrosine kinases involved in tumor progression and angiogenesis. *Cancer research* **64**: 7099-7109.

Wong IH, Lo YM, Zhang J, Liew CT, Ng MH, Wong N, Lai PB, Lau WY, Hjelm NM, Johnson PJ. 1999a. Detection of aberrant p16 methylation in the plasma and serum of liver cancer patients. *Cancer research* **59**: 71-73.

Wong N, Lai P, Lee SW, Fan S, Pang E, Liew CT, Sheng Z, Lau JW, Johnson PJ. 1999b. Assessment of genetic changes in hepatocellular carcinoma by comparative genomic hybridization analysis: relationship to disease stage, tumor size, and cirrhosis. *The American journal of pathology* **154**: 37-43.

Woo HG, Wang XW, Budhu A, Kim YH, Kwon SM, Tang ZY, Sun Z, Harris CC, Thorgeirsson SS. 2011. Association of TP53 mutations with stem cell-like gene expression and survival of patients with hepatocellular carcinoma. *Gastroenterology* **140**: 1063-1070.

Wurmbach E, Chen YB, Khitrov G, Zhang W, Roayaie S, Schwartz M, Fiel I, Thung S, Mazzaferro V, Bruix J et al. 2007. Genome-wide molecular profiles of HCV-induced dysplasia and hepatocellular carcinoma. *Hepatology* **45**: 938-947.

Yamashita K, Upadhyay S, Osada M, Hoque MO, Xiao Y, Mori M, Sato F, Meltzer SJ, Sidransky D. 2002. Pharmacologic unmasking of epigenetically silenced tumor suppressor genes in esophageal squamous cell carcinoma. *Cancer cell* **2**: 485-495.

Yang A, Kaghad M, Wang Y, Gillett E, Fleming MD, Dotsch V, Andrews NC, Caput D, McKeon F. 1998. p63, a p53 homolog at 3q27-29, encodes multiple products with transactivating, death-inducing, and dominant-negative activities. *Molecular cell* **2**: 305-316.

Yang A, Schweitzer R, Sun D, Kaghad M, Walker N, Bronson RT, Tabin C, Sharpe A, Caput D, Crum C et al. 1999. p63 is essential for regenerative proliferation in limb, craniofacial and epithelial development. *Nature* **398**: 714-718.

Yang A, Walker N, Bronson R, Kaghad M, Oosterwegel M, Bonnin J, Vagner C, Bonnet H, Dikkes P, Sharpe A et al. 2000. p73-deficient mice have neurological, pheromonal and inflammatory defects but lack spontaneous tumours. *Nature* **404**: 99-103.

Yang X, Klein R, Tian X, Cheng HT, Kopan R, Shen J. 2004. Notch activation induces apoptosis in neural progenitor cells through a p53-dependent pathway. *Developmental biology* **269**: 81-94.

Yea S, Narla G, Zhao X, Garg R, Tal-Kremer S, Hod E, Villanueva A, Loke J, Tarocchi M, Akita K et al. 2008. Ras promotes growth by alternative splicing-mediated inactivation of the KLF6 tumor suppressor in hepatocellular carcinoma. *Gastroenterology* **134**: 1521-1531.

Yuan RH, Jeng YM, Chen HL, Lai PL, Pan HW, Hsieh FJ, Lin CY, Lee PH, Hsu HC. 2006. Stathmin overexpression cooperates with p53 mutation and osteopontin overexpression, and is associated with tumour progression, early recurrence, and poor prognosis in hepatocellular carcinoma. *The Journal of pathology* **209**: 549-558.

Zender L, Spector MS, Xue W, Flemming P, Cordon-Cardo C, Silke J, Fan ST, Luk JM, Wigler M, Hannon GJ et al. 2006. Identification and validation of oncogenes in liver cancer using an integrative oncogenomic approach. *Cell* **125**: 1253-1267.

Zhang N, Bai H, David KK, Dong J, Zheng Y, Cai J, Giovannini M, Liu P, Anders RA, Pan D. 2010. The Merlin/NF2 tumor suppressor functions through the YAP oncoprotein to regulate tissue homeostasis in mammals. *Developmental cell* **19**: 27-38.

Zhang XY, Nie YQ, Du YL, Cao J, Shen B, Li YY. 2012a. MicroRNA-181a promotes gastric cancer by negatively regulating tumor suppressor KLF6. *Tumor Biol* **33**: 1589-1597.

Zhang Y, Li J, Cao L, Xu W, Yin Z. 2012b. Circulating tumor cells in hepatocellular carcinoma: detection techniques, clinical implications, and future perspectives. *Seminars in oncology* **39**: 449-460.

Zhang Y, Wang S, Li D, Zhnag J, Gu D, Zhu Y, He F. 2011. A systems biology-based classifier for hepatocellular carcinoma diagnosis. *PloS one* **6**: e22426.

Zhao X, Monson C, Gao C, Gouon-Evans V, Matsumoto N, Sadler KC, Friedman SL. 2010. Klf6/copeb is required for hepatic outgrowth in zebrafish and for hepatocyte specification in mouse ES cells. *Developmental biology* **344**: 79-93.

Zheng Q, Wang XJ. 2008. GOEAST: a web-based software toolkit for Gene Ontology enrichment analysis. *Nucleic acids research* **36**: W358-363.

Zhou D, Conrad C, Xia F, Park JS, Payer B, Yin Y, Lauwers GY, Thasler W, Lee JT, Avruch J et al. 2009. Mst1 and Mst2 maintain hepatocyte quiescence and suppress hepatocellular carcinoma development through inactivation of the Yap1 oncogene. *Cancer cell* **16**: 425-438.

Zhou X, Zimonjic DB, Park SW, Yang XY, Durkin ME, Popescu NC. 2008. DLC1 suppresses distant dissemination of human hepatocellular carcinoma cells in nude mice through reduction of RhoA GTPase activity, actin cytoskeletal disruption and down-regulation of genes involved in metastasis. *International journal of oncology* **32**: 1285-1291.

Zhu J, Jiang J, Zhou W, Chen X. 1998. The potential tumor suppressor p73 differentially regulates cellular p53 target genes. *Cancer research* **58**: 5061-5065.

Zins K, Lucas T, Reichl P, Abraham D, Aharinejad S. 2013. A Rac1/Cdc42 GTPase-specific small molecule inhibitor suppresses growth of primary human prostate cancer xenografts and prolongs survival in mice. *PloS one* **8**: e74924.